

Utah State University

DigitalCommons@USU

All Graduate Theses and Dissertations

Graduate Studies

5-2011

Ligand and Metal Effects of the Co-Release Reactivity of Metal Acireduction and Flavonolate Complexes

Katarzyna Grubel
Utah State University

Follow this and additional works at: <https://digitalcommons.usu.edu/etd>

 Part of the [Chemistry Commons](#)

Recommended Citation

Grubel, Katarzyna, "Ligand and Metal Effects of the Co-Release Reactivity of Metal Acireduction and Flavonolate Complexes" (2011). *All Graduate Theses and Dissertations*. 1031.
<https://digitalcommons.usu.edu/etd/1031>

This Dissertation is brought to you for free and open access by the Graduate Studies at DigitalCommons@USU. It has been accepted for inclusion in All Graduate Theses and Dissertations by an authorized administrator of DigitalCommons@USU. For more information, please contact digitalcommons@usu.edu.



LIGAND AND METAL EFFECTS ON THE CO-RELEASE REACTIVITY OF
METAL ACIREDUCTONE AND FLAVONOLATE COMPLEXES

by

Katarzyna Grubel

A dissertation submitted in partial fulfillment
of the requirements for the degree

of

DOCTOR OF PHILOSOPHY

in

Chemistry

Approved:

Lisa M. Berreau, Ph.D.
Major Professor

Alvan C. Hengge, Ph.D.
Committee Member

John L. Hubbard, Ph.D.
Committee Member

Marie K. Walsh, Ph.D.
Committee Member

Bradley S. Davidson, Ph.D.
Committee Member

Mark R. McLellan, Ph.D.
Vice President for Research and
Dean of the School of Graduate
Studies

UTAH STATE UNIVERSITY
Logan, Utah

2011

Copyright © Katarzyna Grubel 2011

All Rights Reserved

ABSTRACT

Ligand and Metal Effects on the CO-Release Reactivity of Metal Acireductone and
Flavonolate Complexes

by

Katarzyna Grubel, Doctor of Philosophy

Utah State University, 2011

Major Professor: Dr. Lisa M. Berreau
Department: Chemistry and Biochemistry

The research reported herein involves synthetic metal complexes of relevance to dioxygenase enzymes (Ni(II)-containing acireductone dioxygenase (Ni(II)-ARD) and quercetinase (2,4-flavonol dioxygenase) that promote oxidative carbon-carbon bond cleavage and CO release. The experiments focus on the elucidation of structure-reactivity relationships and evaluation of the conditions under which CO is generated.

It had been proposed that hydrogen bond donors in the secondary environment of the active site metal center in Ni(II)-ARD influence the coordination of the acireductone substrate on the nickel center. To evaluate this proposal, we investigated the Ni(II) coordination chemistry of an acireductone-type enolate anion using a supporting chelate ligand having two internal hydrogen bond-donors. The resulting complex exhibited differences in terms of the organic product distribution in a CO release reaction resulting from oxidative C-C bond cleavage of the enolate ligand relative to this reported for the

hydrophobic, 6-Ph₂TPA-supported (6-Ph₂TPA = N,N-bis((6-phenyl-2-pyridyl)methyl)-N-((2-pyridyl)methyl)amine) analogue.

In another study, we found that changes in the supporting chelate ligand or metal center influenced the coordination chemistry of the acireductone-type enolate anion. This chemistry highlighted the propensity of the enolate to undergo isomerization without CO release in the presence of water. Rigorously excluding water enabled the isolation of a Ni(II) enolate complex of the 6-PhTPA ligand and examination of its oxidative CO release chemistry, as well as the spectroscopic characterization of the first Co(II) complex of an acireductone-type enolate.

To elucidate factors influencing the CO-release reactivity of metal-flavonoid complexes, some of which have relevance to quercentinase enzymes, we synthesized and characterized the first series of structurally-related metal-flavonolate complexes [(6-Ph₂TPA)M(3-Hfl)]X (M = Mn(II), Co(II), Ni(II), Cu(II), Zn(II), Cd(II), Hg(II); X = OTf or ClO₄⁻). Exposure of these complexes to UV light initiated photooxidative carbon-carbon bond cleavage and CO release in a metal-dependent manner, with closed-shell *d*¹⁰ metals giving rise to the highest rate of CO release. These studies suggest that metal flavonolate species may be useful as a new type of photo-induced CO release molecules (CORMs). Such species are of current interest for possible therapeutic applications.

ACKNOWLEDGMENTS

I would like to thank all the people who have contributed to this dissertation, and without whom the research outlined in this document would be impossible.

- » I extend special thanks to my advisor (Boss and PI), Professor Lisa Berreau, to whom I owe my deepest gratitude for everything she has taught me, and for all the things she has ever done for me.
- » I thank my parents, Walentyna and Jerzy, without whom I would not exist.
- » I would also like to thank my friends, who always stood by me: Gosia Podstawska, Iza Lalik, Justyna Majewska, Kasia Rudzka, James Danford, Karamatullah Danyal, Caleb Allpress, Mark and Stefanie Haney, Gosia and Piotr Dobrowolscy...
- » ...and everybody whom I met on my life's path and who helped to shape the person I am now.

I dedicate this dissertation to Edward and Ludwika Grubel

CONTENTS

	Page
ABSTRACT.....	iii
ACKNOWLEDGMENTS.....	v
LIST OF TABLES.....	vii
LIST OF FIGURES.....	ix
LIST OF SCHEMES.....	xiii
CHAPTER	
1. CO RELEASE IN BIOLOGICAL AND SYNTHETIC SYSTEMS....	1
2. O ₂ -DEPENDENT ALIPHATIC CARBON-CARBON BOND CLEAVAGE REACTIVITY IN A Ni(II) ENOLATE COMPLEX HAVING A HYDROGEN BOND DONOR MICROENVIRONMENT; COMPARISON WITH A HYDROPHOBIC ANALOG.....	25
3. INFLUENCE OF WATER ON THE FORMATION OF O ₂ - REACTIVE DIVALENT METAL ENOLATE COMPLEXES OF RELEVANCE TO ACIREDUCTONE DIOXYGENASES.....	62
4. SYNTHESIS, CHARACTERIZATION, AND LIGAND EXCHANGE REACTIVITY OF A SERIES OF FIRST ROW DIVALENT METAL 3-HYDROXYFLAVONOLATE COMPLEXES.....	102
5. PHOTOCHEMICALLY-INDUCED DIOXYGENASE-TYPE CO- RELEASE OF GROUP 12 FLAVONOLATE COMPLEXES.....	153
6. PHOTOCHEMICAL CO RELEASE REACTIVITY OF OPEN- SHELL 3 <i>d</i> DIVALENT FLAVONOLATE COMPLEXES.....	179
7. SUMMARY.....	197
APPENDICES.....	200

CURRICULUM VITAE..... 214

LIST OF TABLES

Table		Page
1-1.	Selected Physicochemical Properties of Carbon Monoxide.....	1
2-1.	Summary of X-ray Data Collection and Refinement.....	43
2-2.	Selected Bond Distances (Å) and Angles (°).....	44
2-3.	Structural Properties of bnpapa-ligated Mononuclear Ni(II) Complexes.....	53
2-4.	Structural Properties of 6-Ph ₂ TPA-ligated Mononuclear Ni(II) Complexes.....	53
3-1.	¹ H NMR Chemical Shifts for 3-6 in CD ₃ CN at 298 K.....	71
3-2.	Summary of X-ray Data Collection and Refinement.....	73
3-3.	Selected Bond Lengths (Å) and Angles (°).....	74
3-4.	¹ H NMR Chemical Shifts for 8-10 in CD ₃ CN at 298 K.....	80
4-1.	Summary of ¹ H NMR of 7 in CD ₃ CN.....	114
4-2.	Summary of X-ray Data Collection and Refinement.....	123
4-3.	Selected Bond Distances (Å) for Complexes 1-5-ClO₄	124
4-4.	Selected Bond Angles (deg) for Complexes 1-5-ClO₄	124
4-5.	Analytical, Spectroscopic, Magnetic, and Cyclic Voltammetry Data for 1-5-OTf	128
4-6.	Summary of X-ray Data Collection and Refinement for 6·2.5CH₃CN . ..	142
4-7.	Selected Bond Distances (Å) for 6·2.5CH₃CN	143
4-8.	Selected Bond Angles (deg) for 6·2.5CH₃CN	143
5-1.	Summary of X-ray Data Collection and Refinement for 2-5	172
5-2.	Selected Bond Distances (Å) for Complexes 2-5	173

5-3.	Selected Bond Angles (deg) for Complexes 2-5	173
6-1.	Summary of X-ray Data Collection and Parameters for 9	185
6-2.	Selected Bond Distances (Å) and Angles (°) for 9	186

LIST OF FIGURES

Figure		Page
1-1.	Proposed ES adducts in the reactions catalyzed by acireductone dioxygenase.....	7
1-2.	Examples of known CO-releasing molecules.....	9
1-3.	Relevant acireductones.....	11
1-4.	6-NA-6-Ph ₂ TPA ligand (left) and core of 4 in which the supporting ligand has been truncated (right).....	14
1-5.	ORTEP representations of 5 . View from the top (left), one layer of the cluster (center), and side view with truncated acireductone ligand (right).	14
1-6.	Examples of supporting ligands used in model studies of 2,4- <i>quercetin</i> dioxygenase.....	16
2-1.	Supporting chelate ligands used to isolate Ni(II) enediolate (top) and enolate (bottom) complexes of relevance to Ni(II)-ARD.....	29
2-2.	Thermal ellipsoid drawings of the cationic portions of 16 and 17	41
2-3.	Thermal ellipsoid drawings of the cationic portions of 18 and 19	42
2-4.	Onsager plots of the solution conductivity properties of 9 , 16-19 , and the 1:1 standard Me ₄ NClO ₄ in CH ₃ CN at 22(1) °C.....	45
2-5.	¹ H NMR spectral features of (a) 14 , (b) 16 , and (c) 17 in the region of 20-80 ppm. Spectra obtained in CD ₃ CN at 22(1) °C.....	46
2-6.	Positions of deuteration in <i>bnpapa</i> ligand used for ² H NMR investigations.....	47
2-7.	¹ H NMR spectral features of (a) 18 and (b) 19 , in the region of 20-80 ppm. Spectra obtained in CD ₃ CN at 22(1) °C.....	48
2-8.	(a) Proposed structure of [(<i>bnpapa</i>)Ni(PhC(O)C(OH)C(O)Ph)]ClO ₄ (14). (b) Structure of [(6-Ph ₂ TPA)Ni(PhC(O)C(OH)C(O)Ph)]ClO ₄ (2) as determined by X-ray crystallography.....	49

3-1.	A region of the ^1H NMR spectra for (a) the reaction mixture produced upon treatment of 6-PhTPA with an equimolar amount of $\text{Ni(II)(ClO}_4)_2 \cdot 6\text{H}_2\text{O}$ and slight stoichiometric excesses of $\text{Me}_4\text{NOH} \cdot 5\text{H}_2\text{O}$ and 2-hydroxy-1,3-diphenylpropan-1,3-dione in CH_3CN (~3000 ppm H_2O); (b) [(6-PhTPA)Ni(PhC(O)C(OH)C(O)Ph)] ClO_4 (3); (c) [(6-PhTPA)Ni(PhC(O)CHC(O)Ph)] ClO_4 (4); (d) [(6-PhTPA)Ni(CH_3CN)(CH_3OH)](ClO_4) $_2$ (5); (e) [(6-PhTPA)Ni(O_2CPh)] ClO_4 (6).....	67
3-2.	Thermal ellipsoid drawing of the cationic portion of 3	69
3-3.	Thermal ellipsoid drawings of the cationic portions of 4 (top) and 5 (bottom).....	70
3-4.	Regions of the ^1H NMR spectra of (a) the reaction mixture produced upon treatment of 6-Ph $_2$ TPA with an equimolar amount of $\text{Co(II)(ClO}_4)_2 \cdot 6\text{H}_2\text{O}$ and slight stoichiometric excesses of $\text{Me}_4\text{NOH} \cdot 5\text{H}_2\text{O}$ and 2-hydroxy-1,3-diphenylpropan-1,3-dione in CH_3CN (~3000 ppm H_2O); (b) the reaction mixture generated using conditions identical to those employed for the preparation of 3 (predrying of base and solvent); (c) the reaction mixture produced upon predrying of base and solvent and shorter reaction time; (d) [(6-Ph $_2$ TPA)Co(PhC(O)CHC(O)Ph)] ClO_4 (8); (e) [(6-Ph $_2$ TPA)Co(CH_3CN)](ClO_4) $_2 \cdot \text{ClO}_4 \cdot \text{CH}_3\text{CN}$ (9); (f) [(6-Ph $_2$ TPA)Co(O_2CPh)] ClO_4 (10).....	77
3-5.	Thermal ellipsoid drawings of the cationic portions of 8 and 10	78
3-6.	Labeling scheme for the 6-Ph $_2$ TPA ligand.....	81
4-1.	Thermal ellipsoid drawings (50% probability) of the cationic portions of 1-ClO$_4$ (top) and 3-ClO$_4$ (bottom).....	121
4-2.	Thermal ellipsoid drawing (50% probability) of the cationic portion of one of the two cations present in the asymmetric unit of 2-ClO$_4$·2CH$_3$CN	122
4-3.	Thermal ellipsoid drawings (50% probability) of the cationic portions of 4-ClO$_4$·Et$_2$O (top) and 5-ClO$_4$·2CH$_2$Cl$_2$ (bottom).....	125
4-4.	EPR spectra of 1-OTf and 4-OTf	131
4-5.	^1H NMR spectra of 2-OTf (top) and 3-OTf (bottom) in CD_3CN at ambient temperature.....	132

4-6.	Cyclic voltammogram for the Cu(II) Complex 4-OTf	133
4-7.	Thermal ellipsoid drawings (50% probability) of the cationic portions of 6·2.5CH₃CN	138
4-8.	¹ H NMR spectrum of [(6-Ph ₂ TPA)Fe(3-Hfl)]ClO ₄ (8) in CD ₃ CN at ambient temperature.....	140
4-9.	UV-vis absorption features of [(6-Ph ₂ TPAFe(3-Hfl)) ₂ (μ-O)](ClO ₄) ₂ (6) and [(6-Ph ₂ TPA)Fe(3-Hfl)]ClO ₄ (8).....	144
4-10.	¹ H NMR spectrum of 6 in CD ₃ CN.....	145
5-1.	Top: Structure of quercetin (including numbering of C-C bond that undergoes oxidative cleavage) and the reaction catalyzed by quercetinase enzymes. Bottom: Structure of 3-hydroxyflavonol (3-Hfl) and labeling of rings.....	154
5-2.	Thermal ellipsoid drawings of the cationic portions of 2 and 3	156
5-3.	¹ H NMR spectra of [(6-Ph ₂ TPA)Zn(3-Hfl)]ClO ₄ (1 , top), [(6-Ph ₂ TPA)Cd(3-Hfl)]ClO ₄ (2 , middle), and [(6-Ph ₂ TPA)Hg(3-Hfl)]ClO ₄ (3 , bottom).....	157
5-4.	Absorption and emission spectra of 1	158
5-5.	Absorption and emission spectra of 2	159
5-6.	Absorption and emission spectra of 3	159
5-7.	¹³ C{ ¹ H} NMR chemical shift assignments (in ppm) for 2	161
5-8.	¹³ C{ ¹ H} NMR chemical shift assignments (in ppm) for 5	162
5-9.	¹³ C{ ¹ H} NMR chemical shift assignments (in ppm) for [(6-Ph ₂ TPA)Cd(CH ₃ CN)](ClO ₄) ₂ (7).....	163
5-10.	¹ H NMR spectra of [(6-Ph ₂ TPA)Zn(<i>O</i> -bs)]ClO ₄ (4 , top), [(6-Ph ₂ TPA)Cd(<i>O</i> -bs)]ClO ₄ (5 , middle), and [(6-Ph ₂ TPA)Hg(<i>O</i> -bs)]ClO ₄ (6 , bottom).....	163
6-1.	Top: Structure of 3-hydroxyflavonol. Bottom: Structure of quercetin and reaction catalyzed by quercetinase enzymes.....	180
6-2.	Structural features of 1-7	181

6-3.	Absorption and emission spectra of 1	183
6-4	Thermal ellipsoid drawing of the cationic portion of 9 · 0.5CH₃CN	184
6-5.	Features of the ¹ H NMR spectra of [(6-Ph ₂ TPA)Co(3-Hfl)]ClO ₄ (2 , top), [(6-Ph ₂ TPA)Co(<i>O</i> -bs)]ClO ₄ (9 , middle), and 9 upon treatment with one equivalent of 3-Hfl in CD ₃ CN (bottom).....	187
6-6.	Features of the ¹ H NMR spectra of [(6-Ph ₂ TPA)Ni(3-Hfl)]ClO ₄ (3 , top), [(6-Ph ₂ TPA)Ni(<i>O</i> -bs)]ClO ₄ (10 , middle), and 10 upon treatment with one equivalent of 3-Hfl in CD ₃ CN (bottom).....	187
6-7.	Features of the UV-vis spectra of 1 , 8 , and the reaction of 8 with one equivalent of 3-Hfl in CH ₃ CN.....	188
6-8.	Features of the UV-vis spectra of 2 , 9 , and the reaction of 9 with one equivalent of 3-Hfl in CH ₃ CN.....	189
6-9.	Features of the UV-vis spectra of 3 , 10 , and the reaction of 10 with one equivalent of 3-Hfl in CH ₃ CN.....	189
6-10.	Features of the UV-vis spectra of 4 , 11 , and the reaction of 11 with one equivalent of 3-Hfl in CH ₃ CN.....	190

LIST OF SCHEMES

Scheme	Page
1-1. Degradation of Heme Catalyzed by Heme Oxygenase Enzymes.....	5
1-2. Methionine Salvage Pathway.....	6
1-3. Degradation of Quercetin to a 2-protocatechuoylphloroglucinol Carboxylic Acid.....	8
1-4. O ₂ -dependent aliphatic C-C bond cleavage of the enolate catalyzed by complex 1	11
1-5. Proposed oxidation of model acireductone starting from 1	12
1-6. O ₂ -dependent Aliphatic C-C Bond Cleavage of the Enolate Catalyzed by Complex 4	14
2-1. Proposed Coordination Modes of the Acireductone Molecule.....	27
2-2. A Shift from Bidentate to Monodentate of the Carboxylate Anions in the Presence of Water as a Function of the Hydrophobicity of the Supporting Ligand.....	30
2-3. Major Products Identified in Reaction of 14 and 2 with O ₂	50
2-4. Possible Reaction Pathways for Oxidative Carbon-carbon Bond Cleavage in the Ni(II) Enolate Complexes 2 and 14	56
3-1. Top: Reaction Catalyzed by Ni(II)-ARD. Middle: Native and Alternative Substrates for Ni(II)-ARD; C(1)-phenyl-containing Model Substrate. Bottom: Structural Drawings of 1 and 2	64
3-2. (a) Previously Reported Synthetic Route for the Preparation of 1 . (b) Synthetic Routes for the Preparation of 3	68
3-3. Proposed Pathway of Isomerization of 1,3-diphenylpropane-1,3-dione to Generate 2-oxo-2-phenylethylbenzoate.....	68
4-1. Degradation of Quercetin.....	104
4-2. Synthetic Routes for Preparation of the 6-Ph ₂ TPA Supported Flavonolate Complexes.....	120

4-3.	Proposed Reaction Pathway for Ligand Exchange in the Reaction of 1-OTf with Divalent Metal Perchlorate Salts.....	136
4-4.	A Summary of the Iron Coordination Chemistry.....	144

CHAPTER 1

CO RELEASE IN BIOLOGICAL AND SYNTHETIC SYSTEMS

Physicochemical Properties of Carbon Monoxide

Carbon monoxide (CO) is an air-stable, diatomic molecule with molar mass 28.01 g/mol and density 1.145 g/cm³ at 298 K and 1 atm.¹ The molecule has ten valence electrons and, since all of them are paired-up, a singlet ground state. It contains a triple bond with length of 1.128 Å and dissociation energy 1077 kJ/mol at 298 K^{1,2}, which makes it one of the strongest bonds known. The bond is slightly polarized (0.122 D),³ allowing carbon monoxide to be used as a ligand toward metal centers where it acts as both σ -donor and π -acceptor. Selected properties of CO are presented in Table 1-1.

Table 1-1. Selected Physicochemical Properties of Carbon Monoxide.¹

Property	Value
Molecular Weight	28.01 g/mol
Boiling Point	-191.6 °C
Melting Point	-205.0 °C
Autoignition Point	606.0 °C
Density	1.250 g/L at 0 °C, 1 atm 1.145 g/L at 25 °C, 1 atm
Density (Vapor)	0.968 (air = 1)
Solubility in H ₂ O	3.54 ml/100 ml at 0 °C, 1 atm 2.14 ml/100 ml at 25 °C, 1 atm 1.83 ml/100 ml 37 °C, 1 atm
Flammable Limits in Air	12-75 vol. %

A Brief History of Carbon Monoxide

Carbon monoxide (CO) is proposed to be one of the most important components of the *primordial soup* and therefore contributed to the evolution of life⁴ and the Universe in general.^{4c} However, due to its colorless and odorless nature, as well as a strong association with blood components, for millennia carbon monoxide was regarded as a poison and a *silent killer*.⁵⁻¹⁰ The oldest reference to its lethal nature can be found in the works of Aristotle (384-322 B. C.), where he described how the inhalation of coal fumes, in which carbon monoxide is the main component, led to poisoning and death.⁵ Also, a case study by Lascaratos and Marcetos showed that in 363 and 364 A.D. two Byzantine emperors, Julian the Apostate and his successor Jovian, were poisoned by inhalation of coal fumes.⁶ Throughout the ages, carbon monoxide, even though its mode of action was not known, was recognized as a harmful and deadly agent. However, it was not until 1794 in the *General Prussian State Laws* that the first rules for proper protection against the coal fumes were passed.⁵

The first preparation of pure CO gas is attributed to de Lassone, who accomplished it in 1776.^{5,7} Over the next few years, the properties and structure of CO were established and described. In the mid 19th century, some aspects of the action of carbon monoxide on the human body were elucidated first by Bernard, and then by Hoppe-Seyler.⁵ The 20th century brought about the introduction of *illuminating gas* (a mixture of combustible gases, mainly methane and hydrogen with smaller amounts of carbon monoxide, propane, butane, acetylene, ethylene, or natural gas) for industrial and domestic purposes, and led to an increased risk of CO poisoning, but also to a better

understanding of carbon monoxide toxicity.⁵ In 1895, Haldane described how the binding of carbon monoxide to hemoglobin^{8a} decreased its capacity for transporting oxygen.^{8b,c} Additionally, it had been known since 1868 that CO poisoning could be alleviated by inhalation of oxygen under atmospheric pressure.⁵ Therefore, in 1960 a Hyperbaric Oxygenation (HBO) therapy for CO-poisoned patients was introduced.⁹ Even though more recently there have been questions raised about this treatment,¹⁰ to date, the HBO procedure remains the most effective treatment for the carbon monoxide poisoning.¹¹

Considering the acute toxicity of carbon monoxide, it may come as a surprise that this molecule is produced endogenously in humans. The first mention of the presence of CO in human blood dates back to Nicloux's report from 1898.⁵ Nearly a century later, in 1991, Marks postulated that carbon monoxide is not only a poison and a waste product of heme degradation, but may actually possess a physiological role.¹² Almost a decade later, it was shown that CO exhibits powerful cytoprotective,^{13a} anti-inflammatory,^{13b} and antiapoptotic^{13c} properties. However, even before those beneficial effects of CO were experimentally demonstrated, in the early 1990's it was proposed that CO could be a neural transmitter and regulate cyclic guanylyl monophosphate (cGMP) in a way similar to that of nitric oxide (NO).¹⁴ Another significant discovery was made in 2001 when it was shown that the administration of exogenous carbon monoxide (1% vol. in air) repressed heart graft rejection in a mouse-to-rat transplant.¹⁵ These interesting findings opened up a completely new field and prompted scientists to investigate both natural and synthetic systems as possible therapeutic agents for CO release. Specific approaches currently under investigation toward delivering CO include: (i) inhalation of CO gas, (ii)

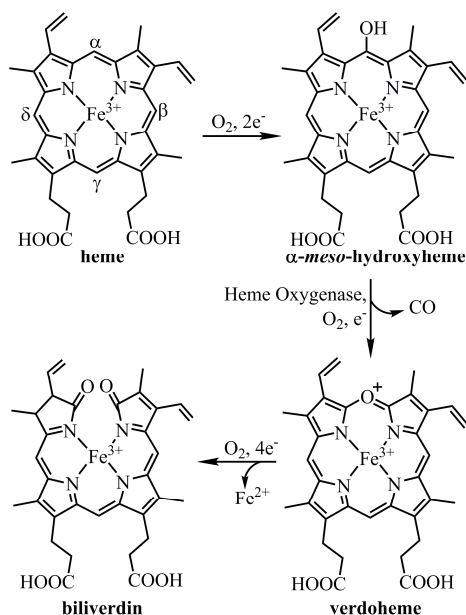
up- or down-regulation of the CO-producing enzymes responsible for heme catabolism, and (iii) application of synthetic CO-releasing molecules.¹⁶

Enzymatic Carbon Monoxide Release

In nature, carbon monoxide release from an organic molecule is catalyzed by three types of enzymes: heme oxygenases (HOs) in humans, and acireductone dioxygenase (ARD) and 2,4-querctin dioxygenase (querctinase) in bacteria and fungi.

Endogenous CO Production by Heme Oxygenase

Although in the human body small amounts of CO may be produced as a by-product of the cytochrome P-450 cycle and lipid peroxidation, the main source of endogenous CO production comes from heme degradation catalyzed by heme oxygenase enzymes (Scheme 1-1).^{5,7,12-25} Heme oxygenases (HOs) are found in three isoforms: (i) inducible HO-1 expressed in response to cellular stress, (ii) HO-2, which is controlled by post-translational modifications, and (iii) a recently discovered HO-3 of yet unknown purpose.¹⁷ The mechanism of the degradation of heme involves three consecutive steps (Scheme 1-1): (i) hydroxylation of an α -carbon of the porphyrin, (ii) conversion of the Fe(III)- α -meso-heme produced in the first step into Fe(II)-verdoheme and CO, and (iii) cleavage of the Fe(II)-verdoheme ring and formation of biliverdin and free Fe(II) ion.^{16b,c,18} Heme degradation catalyzed by HOs was discovered in 1968 by Tenhunen and Schmidt.¹⁹ Since then, it has been shown that the production of carbon monoxide from heme degradation might be influenced by many factors, including multiple hematological diseases such as, but not restricted to, anemia, sickle cell disease, and cystic fibrosis. In a

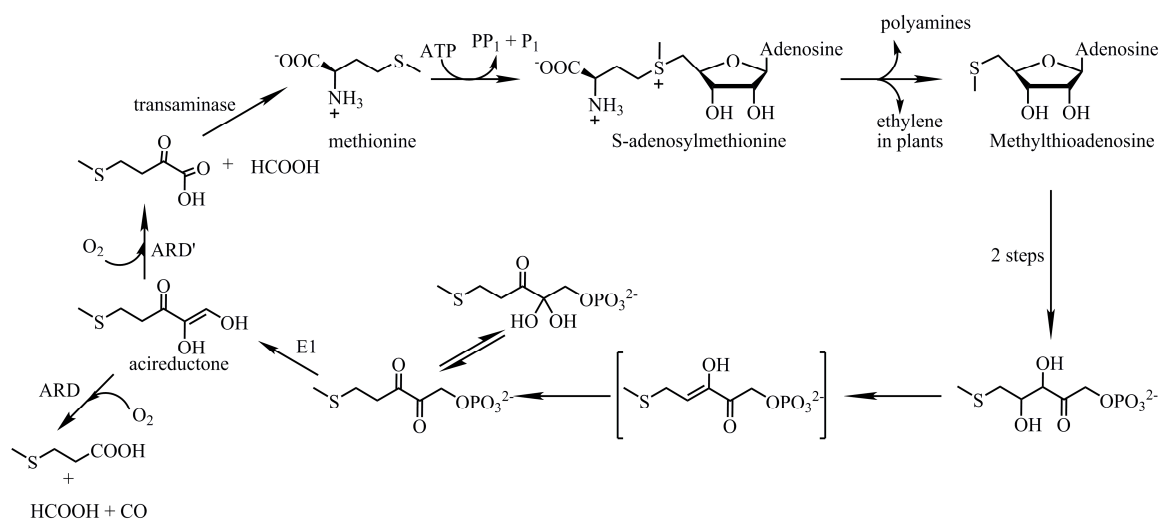


Scheme 1-1.

healthy individual, the rate of CO production oscillates around 18.8 $\mu\text{mol/h}$ and its average concentration in tissues is in the nanomolar range.²⁰ During heme degradation, HOs produce one equivalent of carbon monoxide per each heme molecule. The main site of CO production is the liver, where the majority of heme catabolism takes place.^{20,21}

CO Release Catalyzed by Acireductone Dioxygenase

Acireductone dioxygenase (ARD) is a member of the cupin superfamily of proteins and is found at the only branch point in the methionine salvage pathway in bacteria (Scheme 1-2). To our knowledge, it is the only enzyme known wherein the nature of the products formed depends exclusively on the identity of the metal ion present in the active site.²²⁻²⁵ The Fe(II)-containing form catalyzes the on-pathway reaction converting the 1,2-dihydroxy-3-oxo-5-(methylthio)pent-1-ene (acireductone) to 4-methylthio-2-



Scheme 1-2.

ketobutyrate and formic acid (Scheme 1-2). It should be noted that this is the same reaction that occurs in the absence of the ARD enzyme.²⁶ The Ni(II)-containing ARD enzyme catalyzes an off-pathway reaction, yielding CO, formic acid, and 3-(methylthio)propionic acid (Scheme 1-2).²²⁻²⁶ Thus, the nature of the metal center is important to inducing carbon monoxide release in this system. The difference in the reactivity of the enzymes is proposed to stem from different coordination modes of the substrate to the metal center (Figure 1-1), resulting in the activation of different C-C bonds for oxidative cleavage reactions.^{22,24} Interestingly, in 1999 Dai *et al.* demonstrated that the substitution of a Ni(II) by Co(II) in the active site of the ARD also results in an enzyme that catalyzes the CO-producing reaction.²⁵ In terms of the influence of active site residues, it has been proposed that the presence of a hydrogen-bonding arginine residue(s) in the secondary environment helps to position and stabilize the metal-bound enediolate in the active site of Ni(II)-ARD.²⁴

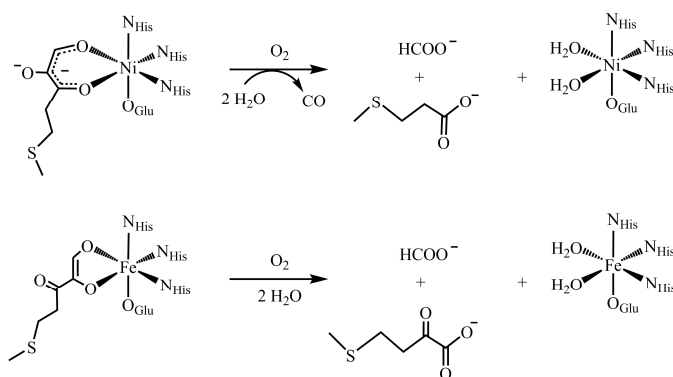
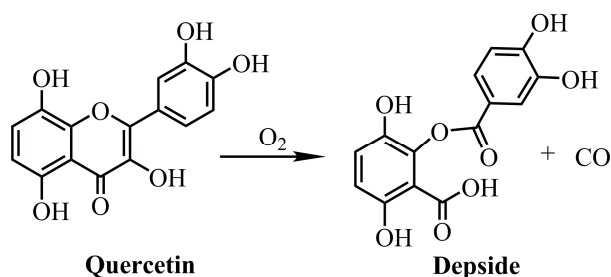


Figure 1-1. Proposed ES adducts in the reactions catalyzed by acireductone dioxygenase.

CO Release Catalyzed by 2,4-Quercetin Dioxygenase

Quercetin is a flavonol which is widely distributed in plants. Because it exhibits antibacterial²⁷ and antifungal²⁸ properties, both bacteria and fungi have developed a defense mechanism in the form of an enzyme, quercetin dioxygenase, which breaks down this molecule. Degradation of quercetin to a 2-protocatechuoylphloroglucinol carboxylic acid molecule (*O*-benzoylsalicylic acid, depside) was described as early as in 1958.²⁹ Two years later, CO release during the same reaction was reported.³⁰

Quercetin dioxygenase catalyzes the oxidative cleavage of a C=C bond (Scheme 1-3).³¹ Like the ARD enzyme, 2,4-quercetin dioxygenase belongs to the cupin superfamily of proteins.³² In 1971, it was shown that the fungal quercetinase contains a mononuclear Cu(II) in its active site.³³ The enzyme produced by bacteria, e.g. *Bacillus subtilis* and *Streptomyces* sp. FLA, is instead able to incorporate several different divalent metals while retaining at least partial activity.^{34,35} The most active forms of the quercetinase enzyme were obtained during the reconstitution of the *apo* form of the enzyme from the *Streptomyces* sp. FLA with Ni(II) or Co(II).³⁵ However, it is not known



Scheme 1-3.

how the different metal ions influence the enzymatic CO production in this system and/or whether changes in the metal center influence the chemistry other than fine tuning of the redox potential of the enzymatic active site.

Carbon Monoxide Release in Synthetic Systems

Carbon Monoxide-Releasing Molecules (CORMs)

In his initial paper from 2002, Motterlini laid the groundwork for the development of a new class of pharmaceuticals: carbon monoxide-releasing molecules (CORMs).³⁶ Since this report, the field has been developing rapidly and in as little as nine years many patents involving CORMs have been filed.^{16a} So far, they mainly involve metal-carbonyl species (Figure 1-2),³⁷ although some organic CORMs such as borates,^{37c} aldehydes, esters, imines, etc.^{16a} have also been proposed. Interestingly, in 2002, a patent describing CO release from methylene chloride was filed.^{16a} Nonetheless, none of those molecules offers the much-needed control over the CO dosage supplied to a desired target, as majority of CORMs release CO immediately upon dissolution.^{37j} Additionally, the metal-containing CORMs reported to date contain heavy metals. Moreover, the definite amount

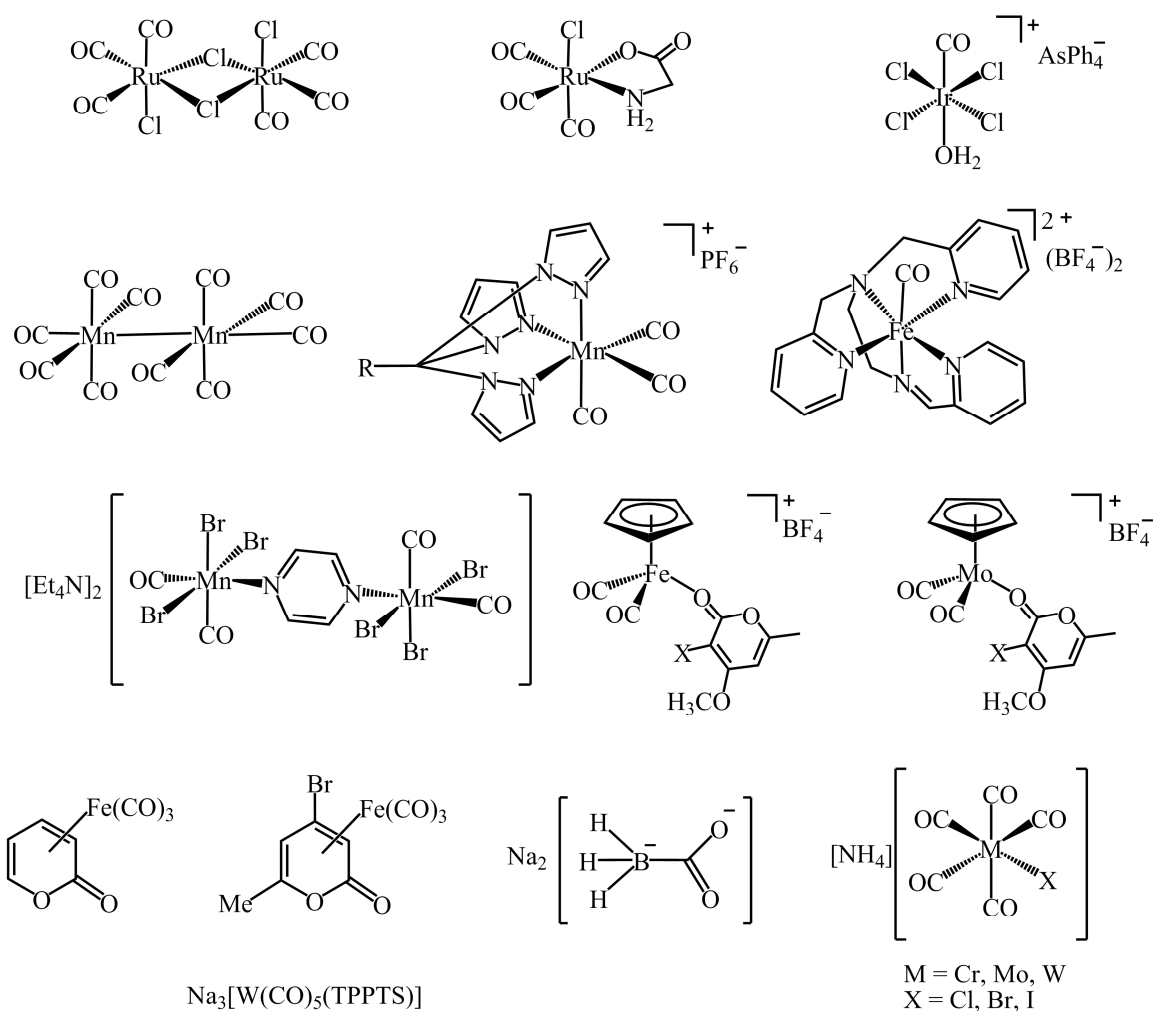


Figure 1-2. Examples of known CO-releasing molecules.

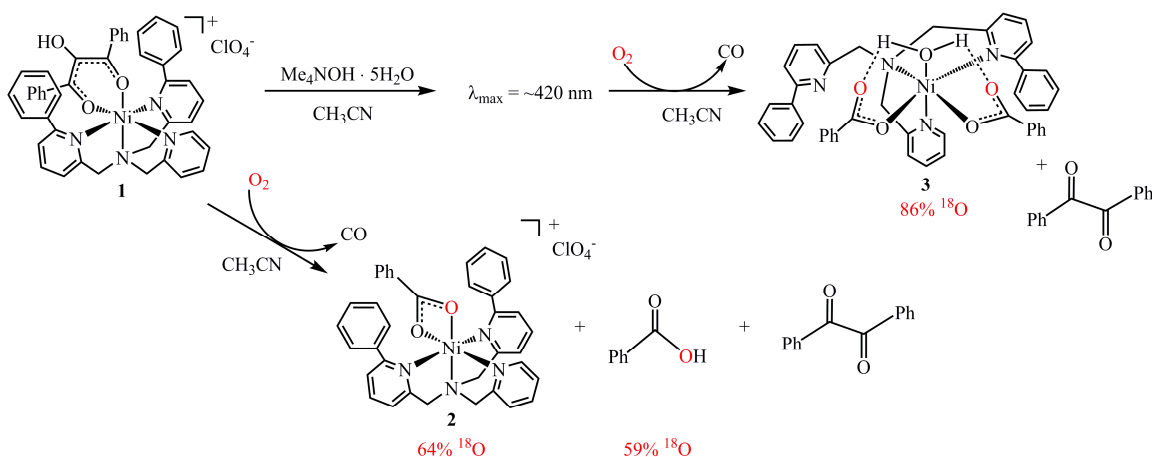
of CO gas released from those systems cannot be accurately controlled. For example, even though the most widely used CORM-3 ($[\text{RuCl}(\text{gly})(\text{CO})_3]$) releases precisely one CO molecule in 37 °C in water, its half life in human plasma is only 3.6 minutes, making CO delivery very unspecific.^{37b} The majority of currently known CORMs suffer from similar setbacks.^{37j}

A promising way to control carbon monoxide release is sensitization of CORMs toward light. It is known that photodynamic therapy allows for precise control over location, dosage, and timing of the therapeutical agent.³⁸ In this regard, several photo-activated CORMs have been reported.^{37f,g,i,38} Such compounds are stable in the dark and release CO upon irradiation with light. A challenge in the development of new photoswitchable CORMs is the adjustment of the irradiation wavelength toward longer values (far visible and near IR wavelengths; > 600 nm).³⁹

Most recently, new ways of controlled CO release and delivery from CORMs, such as CO-releasing micelles⁴⁰ and enzyme-triggered CORMs (ET-CORM), have been proposed.⁴¹ These new systems are designed to avoid the inherent toxicity of heavy metals as well as the use of high frequency irradiation.

CO Release in Model Systems of Ni(II)-Containing Acireductone Dioxygenase

The first synthetic model of the active site of Ni(II)-containing ARD was reported in 2005 by the Berreau group.^{42a} A mononuclear Ni(II)-enolate complex supported by a hydrophobic 6-Ph₂TPA ligand was synthesized and isolated (**1**, Scheme 1-4). Because no procedure for synthesis of the natural substrate was known, a model (Figure 1-3) of the native substrate was used. This compound is not a substrate for the acireductone dioxygenase enzyme due to the presence of a phenyl substituent on the C(1) carbon. Complex **1** was shown to undergo an O₂-dependent aliphatic C-C bond cleavage of the enolate to yield either a monobenzoate complex (**2**, Scheme 1-4), or a dibenzoate complex (**3**, Scheme 1-4), depending on the protonation level of the metal-bound acireductone.^{42,43}



In both cases it was noted that during the reaction the organic by-product benzil was being formed along with CO. To elucidate the possible pathways leading to formation of observed products, mechanistic studies were undertaken. As a result of these investigations, it was concluded that the oxidative C-C bond cleavage using the phenyl-containing model acireductone proceeds through diphenyl triketone and hydroperoxide as intermediates. Additionally, DFT calculations showed that the monoanionic form of acireductone analogue is predisposed to extrude CO during the oxidative C-C bond

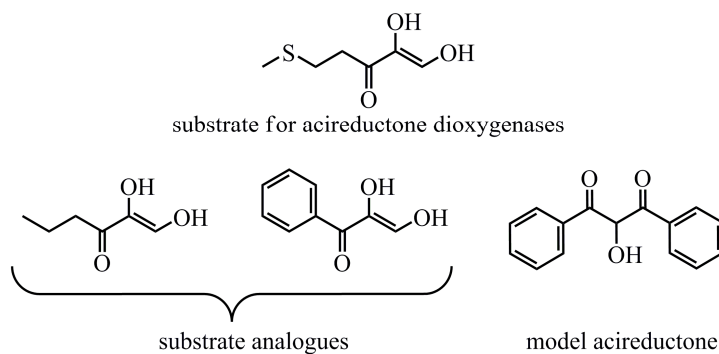
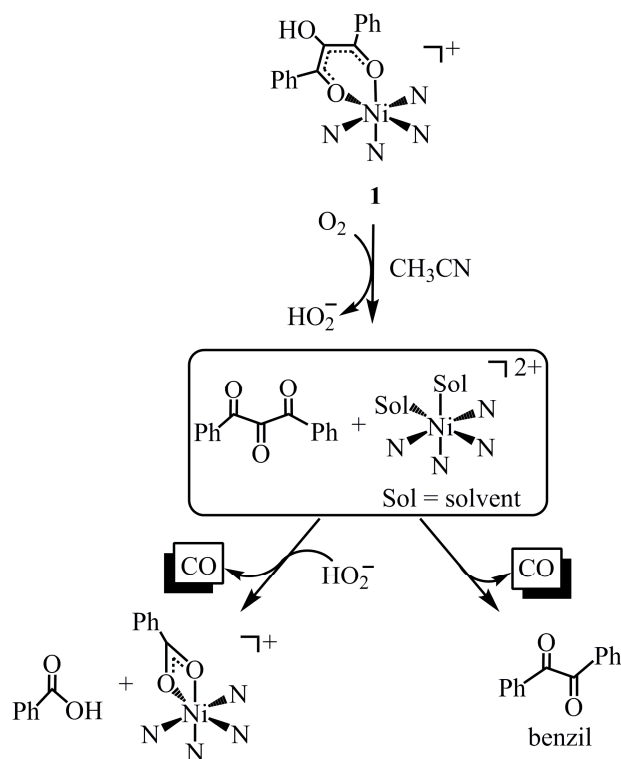


Figure 1-3. Relevant acireductones.

cleavage (Scheme 1-5). This predisposition is a direct result of a presence of the phenyl substituent on carbon C(1) of the acireductone.^{42b}



Scheme 1-5. Proposed oxidation of model acireductone starting from **1**. For clarity, the supporting 6-Ph₂TPA ligand has been truncated.

As mentioned in the description of the enzymatic CO release in the Ni(II)-ARD system, the secondary environment of the active site in the ARD enzyme contains at least one arginine residue.²⁴ It was proposed that this amino acid may play a crucial role in stabilizing the doubly deprotonated substrate on the metal center through the formation of hydrogen bonds.^{22,24} To evaluate this possibility, a new ligand, 6-NA-6-Ph₂TPA, containing one hydrogen bond donor arm was synthesized and used to investigate how

secondary hydrogen bonds influence the coordination of an acireductone-type ligand. Using the 6-NA-6-Ph₂TPA ligand, a trinuclear Ni(II) enediolate complex was isolated and characterized (**4**, Figure 1-4).⁴⁴ Notably, the acireductone analog exhibits a different coordination mode in this complex, forming two five-membered rings that bridge two Ni(II) centers. Complex **4** undergoes reaction with O₂ to generate two equivalents of a Ni(II) benzoate complex, CO, benzyl, and a Ni benzoate salt (Scheme 1-6). It is noteworthy that ¹⁸O labeling experiments involving either **1** in the presence of one equivalent of base (Scheme 1-4 (top)) or **4** (Scheme 1-6) resulted in identical incorporation of labeled oxygen into the benzoate complexes (86% via inspection by mass spectrometry).⁴⁴ This result is not surprising since it was implied that a putative, dianionic species was formed in the pathway shown across the top of Scheme 1-4.⁴³ In 2010 the isolation, characterization, and reactivity of this proposed intermediate was further investigated.⁴⁵ It was shown that the treatment of **1** with one equivalent of base results in displacement of the supporting ligand 6-Ph₂TPA and formation of the hexanickel cluster (**5**, Figure 1-5) with $\lambda_{\text{max}} = \sim 420$ nm (Scheme 1-4). Because isolation of the bulk material from the reaction mixture proved impossible, an alternative synthetic route for obtaining the cluster was employed. This independently synthesized species was then exposed to O₂ in the presence of 1/6 equivalent of 6-Ph₂TPA, yielding a product distribution identical with the oxidation reaction starting from **1** and one equivalent of base (Scheme 1-4 (top)). Additionally, ¹⁸O labeling studies of the oxidation reaction starting from **5** resulted in the level of isotope incorporation (83%-86%), which matched well with the reaction starting from **1** in presence of one equivalent of base (86%).

As outlined above, introduction of one hydrogen bond donating arm to the supporting ligand enabled stabilization of an enediolate species in a multinuclear structure.⁴³ Hypothesizing that the introduction of multiple hydrogen-bonding appendages to the chelate ligand might enable stabilization of a mononuclear species with doubly deprotonated model acireductone, such studies were initiated and their results are offered in Chapter 2.

To further elucidate factors influencing the formation of the acireductone-type enolate complexes, additional studies involving changes in the metal center, Ni(II) to Co(II), and supporting chelate ligand, 6-Ph₂TPA to 6-PhTPA, were performed. The outcome of these investigations provided better insight into the challenges encountered in acireductone coordination chemistry. This issue is further discussed in Chapter 3.

CO Release in Model Systems of 2,4-Quercetin Dioxygenase

Initial models of the quercetinase enzymes were reported in 1979 and involved simple, base catalyzed oxygenation of quercetin or other flavonols.⁴⁶ However, the first structure of a metal-containing complex to mimic the enzyme active site was reported more than a decade later in 1990.⁴⁷ Since at that time only the copper-containing fungal quercetinase was known, the complexes contained exclusively Cu(I) or Cu(II) as the metal ion. These complexes involved homoleptic flavonolate coordination,⁴⁸ or copper centers supported by a monodentate phosphine ligand.⁴⁷ However, there have now been at least 11 different ligands (see examples in Figure 1-6) and over eight quercetin analogues used for this purpose.^{49b} Multiple Cu-flavonolate species have been prepared and shown to release CO in DMF when heated.⁴⁹

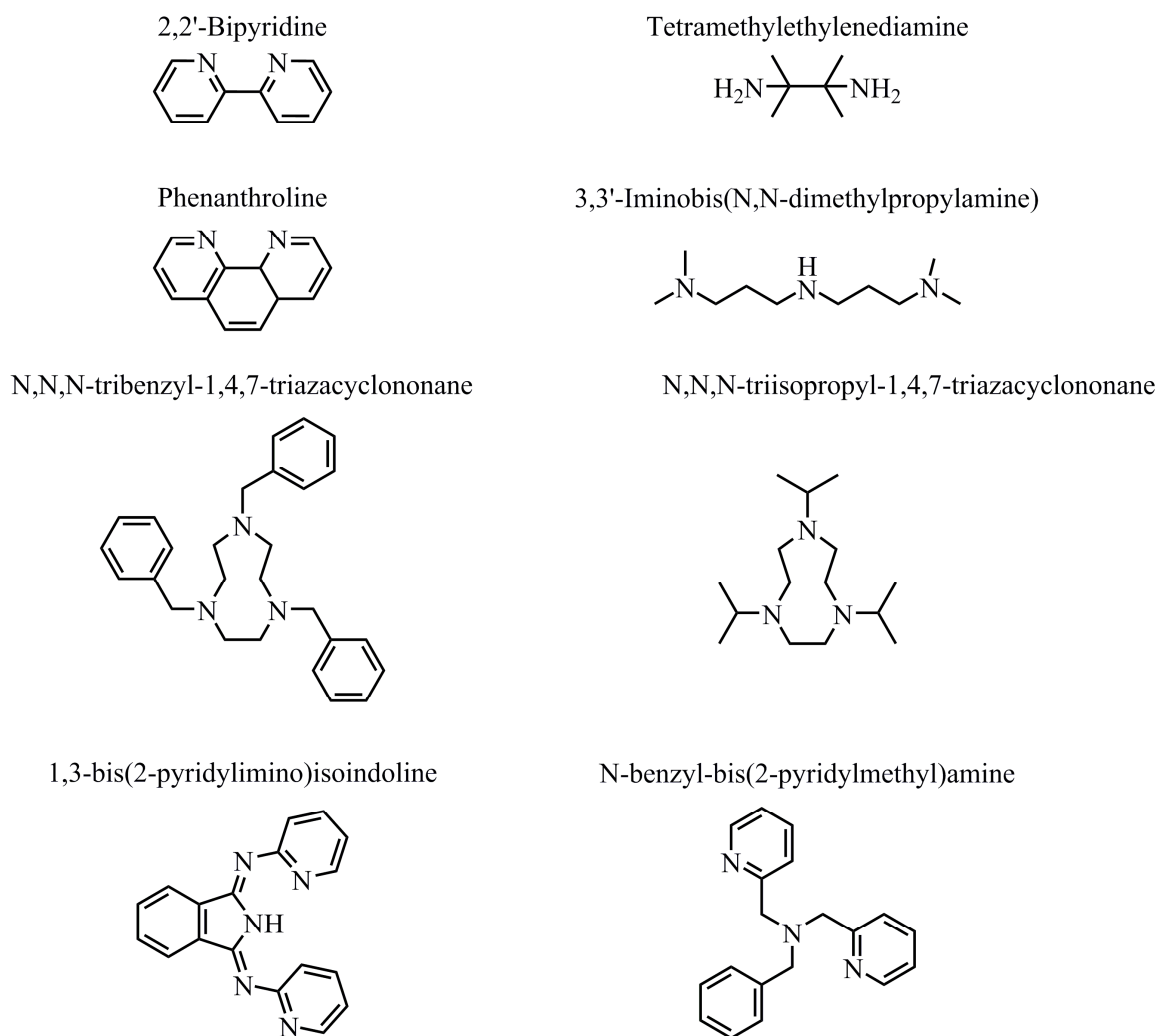


Figure 1-6. Examples of supporting ligands used in model studies of 2,4-querctin dioxygenase.

Although a cobalt complex-promoted oxidation of quercetin was reported as early as 1974,⁵⁰ the first cobalt(III)-coordinated flavonolate structure was solved in 1992.⁵¹ Further studies of metal-flavonolate complexes provided structures of Fe(III)-,⁵¹ Mn(II)-,^{52b} Ni(II)-,⁵³ and Zn(II)-containing⁵⁴ compounds. Nonetheless, despite a growing structural database for metal flavonolate complexes, each complex contained a different

supporting ligand and/or a different oxidation state of the metal ion. As a result, it was impossible to assess the influence of the metal ion on the oxidative C-C bond cleavage of the metal-bound flavonolate moiety. To address this deficiency, the Berreau group has developed the very first series of a model 3-hydroxyflavonolate anion coordinated on divalent metal centers supported by the same, hydrophobic 6-Ph₂TPA ligand. This allowed for direct comparison of the influence of the metal ion on both the coordination mode and spectroscopic features of the metal-bound flavonolate. This comparison is further discussed in Chapter 4. Having synthesized and characterized the aforementioned family of flavonolate complexes, we were positioned to investigate the O₂-dependent reactivity and CO release reactivity of these complexes under various conditions. Results of these investigations are further explored in Chapters 5 and 6.

Conclusions

Carbon monoxide is a small molecule with increasing significance to human health. Because of its growing importance, it is imperative to understand the factors controlling its release in enzymatic systems, as well as its release from synthetic complexes. In the Berreau group, we are interested in elucidating factors influencing CO release in synthetic systems of relevance to CO producing enzymes. In the subsequent chapters of this dissertation the influence of both chelate ligand and metal ion on CO production in synthetic systems of relevance to acireductone dioxygenase and 2,4-flavonol dioxygenase is presented.

References

1. (a) *CRC Handbook of Chemistry and Physics*, 91st ed.; Internet Version 2011; (b) <http://encyclopedia.airliquide.com/>
2. B. de B. Darwent *Bond Dissociation Energies in Simple Molecules*, NSRDS-NBS 31, National Bureau of Standards, Washington D.C., 1970.
3. Scuseria, G. E.; Miller, M. D.; Jensen, F.; Gertsen, J. *J. Chem. Phys.* **1991**, *94*, 6660-6664.
4. (a) Schlesinger, G.; Miller, S. L. *J. Mol. Evol.* **1983**, *19*, 376-382. (b) Miyakawa, S.; Yamanashi, H.; Kobayashi, K.; Cleaves, H. J.; Miller, S. L. *PNAS* **2002**, *99*, 14628-14631 and references cited therein. (c) Ferry, J. G. *Ann. Microbiol.* **2010**, *60*, 1-12; (d) Kundell, F. A. *Orig. Life Evol. Biosph.* **2011**, *41*, 175-198; (e) Ehrenfreund, P.; Spaans, M.; Holm, N. G. *Phil. Trans. R. Soc. A* **2011**, *369*, 538-554; (f) Apfel, U.-P.; Weigand, W. *Angew. Chem. Int. Ed.* **2011**, *50*, 2-5.
5. Penney, D. G. *Carbon Monoxide Toxicity* CRC Press LLC, Boca Raton 2000.
6. Lascaratos, J. G.; Marketos, S. G. *Clinic. Toxicol.* **1998**, *1-2*, 103-107.
7. Prockop, L. D.; Chichkova, R. I. *J. Neur. Sci.* **2007**, *262*, 122-130.
8. (a) Haldane, J. B. *J. Physiol.* **1895**, *18*, 430-462; (b) Douglas, C. G.; Hadane, J. S.; Haldane, J. B. *J. Physiol.* **1912**, *44*, 275-304; (c) Haldane, J. B. *Biochem. J.* **1927**, *21*, 1068-1075.
9. Smith, G.; Sharp, G. R. *Lancet* **1960**, *276*, 905-906.
10. Annane, D.; Chadda, K.; Gajdos, P.; Jars-Guinestre, M.-C.; Chevret, S.; Raphael, J.-C. *Intensive Care Med.* **2010**, *37*, 486-492.

11. (a) Olson, K.; Smollin, C. *Clin. Evid.* **2010**, *10*, 2103-2109; (b) Birmingham, C. M.; Hoffman, R. S.; *Intensive Care Med.* **2011**, Online FirstTM.
12. Marks, G. S.; Brien, J. F.; Nakatsu, K.; McLaughlin, B. E. *Trends Pharmacol. Sci.* **1991**, *12*, 185-188.
13. (a) Otterbein, L. E.; Mantell, L. L.; Choi, A. M. *Am. J. Physiol.* **1999**, *276*, L688-L694; (b). Otterbein, L. E.; Bach, F. H.; Alam, J.; Soares, M. P.; Tao, H. L.; Wysk, M.; Davis, R.; Flavell, R.; Choi, A. M. K. *Nat. Med.* **2000**, *6*, 422-428; (c) Brouard, S.; Otterbein, L. E.; Anrather, J.; Tobiasch, E.; Bach, F. H.; Choi, A. M. K.; Soares, M. P. *J. Exp. Med.* **2000**, *192*, 1015- 1025.
14. (a) Verma, A.; Hirsch, D. J.; Glatt, C. E.; Ronnett, G. V.; Snyder, S. H. *Science* **1993**, *259*, 381-384; (b) Maines, M. D. *Mol. Cell. Neurosci.* **1993**, *4*, 389-397; (c) Ingi, T.; Cheng, J.; Ronnett, G. V. *Neuron* **1996**, *16*, 835-842.
15. Sato, K.; Balla, J.; Otterbein, L.; Smith, R. N.; Brouard, S.; Lin, Y.; Csizmadia, E.; Sevigny, J.; Robson, S. C.; Vercellotti, G.; Choi, A. M.; Bach, F. H.; Soares, M. P. *J. Immunol.* **2001**, *166*, 4185-4194.
16. (a) Bannenberg G. L.; Vieira, H. L. A. *Expert Opin. Ther. Patents* **2009**, *19*, 663-682; (b) Mann, B. E. *Topics Organomet. Chem.* **2010**, *32*, 247-285; (c) Motterlini, R.; Otterbein, L. E. *Nature Rev. Drug Discovery* **2010**, *9*, 728-743.
17. Ryter, S.; Alam, S. W.; Choi, J. A. M. K. *Physiol. Rev.* **2006**, *86*, 583-650.
18. Matsui, T.; Unno, M.; Ikeda-Saito, M. *Acc. Chem. Res.* **2009**, *43*, 240-247 and references cited therein.

19. Tenhunen, R.; Marver, H. S.; Schmidt, R. *Proc. Natl. Acad. Sci. USA* **1968**, *61*, 748-755.
20. Owens, E. O. *Clin. Biochem.* **2010**, *43*, 1183-1188.
21. Berk, P. D.; Blaschke, T. F.; Scharschmidt, B. F.; Waggoner, J. G.; Berlin, N. I. *J. Lab. Clin. Med.* **1976**, *87*, 767-780.
22. Pochapsky, T. C.; Ju, T.; Dang, R.; Beaulieu, R.; Pagani, G. M.; OuYang, B. In *Metal Ions in Life Sciences*; Sigel, A.; Sigel, H.; Sigel, R. K. O., Eds. Wiley-VCH: Weinheim, Germany, 2007, 473-498.
23. Wray, J. W.; Abeles, R. H. *J. Biol. Chem.* **1995**, *270*, 3147-3153.
24. Ju, T. T.; Goldsmith, R. B.; Chai, S. C.; Maroney, M. J.; Pochapsky, S. S.; Pochapsky, T. C. *J. Mol. Biol.* **2006**, *363*, 523-534.
25. Dai, Y.; Wensink, P. C.; Abeles, R. H. *J. Biol. Chem.* **1999**, *274*, 1193-1195.
26. Wray, J. W.; Abeles, R. H. *J. Biol. Chem.* **1993**, *268*, 21466-21469.
27. (a) Alcubilla, M.; Diaz-Palacio, M. P.; Kreutzer, K.; Laatsch, W.; Rehfuess, K. E.; Wenzel, G. *Eur. J. Forest Pathol.* **1971**, *1*, 100-114; (b) Nemeč, S. *Mycopathologia*, **1976**, *59*, 37-40.
28. Naghski, J.; Copley, M. J.; Couch, J. F. *Science* **1947**, *105*, 125-126.
29. (a) El Khadem, H. *J. Chem. Soc.* **1958**, 3320-3323; (b) Westlake, D. W. S.; Talbot, G.; Blakley, E. R.; Simpson F. J. *Can. J. Microbiol.* **1958**, *5*, 621-629.
30. Simpson F. J.; Talbot, G.; Westlake, D. W. S. *Biochem. Biophys. Res. Commun.* **1960**, *2*, 15-18.

31. Oka, T.; Simpson, F. J.; Krishnamurty, H. G. *Can. J. Microbiol.* **1972**, *18*, 493-508.
32. Fusetti, F.; Schröter, K. H.; Steiner, R. A.; van Noort, P. I.; Pijning, T.; Rozeboom, H. J.; Kalk, K. H.; Egmond M. R.; Dijkstra, B. W. *Structure* **2002**, *10*, 259-268.
33. Oka, T.; Simpson, F. J. *Biochem. Biophys. Res. Commun.* **1971**, *43*, 1-5.
34. Schaab, M. R.; Barney, B. M.; Francisco, W. A. *Biochemistry*, **2006**, *45*, 1009-1016.
35. Merkens, H.; Kappl, R.; Jakob, R. P.; Schmid, F. X.; Fetzner, S. *Biochemistry*, **2008**, *47*, 12185-12196.
36. Motterlini, R.; Clark, J. E.; Foresti, R.; Sarathchandra, P.; Mann, B. E.; Green, C. *J. Circ. Res.* **2002**, *90*, e17-e24.
37. (a) Clark, J. E.; Naughton, P.; Shurey, S.; Green, C.J.; Johnson, T. R.; Mann, B. E.; Foresti, R.; Motterlini, R. *Circ Res* **2003**, *93*, e2-e8; (b) Motterlini, R.; Mann, B. E.; Johnson, T. R.; Clark, J. E.; Foresti, R.; Green, C. *J. Curr. Pharm. Des.* **2003**, *9*, 2525-2539; (c) Motterlini, R.; Sawle, P.; Hammad, J.; Bains, S. K.; Alberto, R.; Foresti, R.; Green, C. *J. FASEB J.* **2005**, *19*, 284-286; (d) Fairlamb, I. J. S.; Duhme-Klair, A. K.; Lynam, J. M.; Moulton, B. E.; O'Brien, C. T.; Sawle, P.; Hammad, J.; Motterlini, R. *Bioorg. Med. Chem. Lett.* **2006**, *16*, 995-998; (e) Fairlamb, I. J. S.; Lynam, J.M.; Moulton, B. E.; Taylor, I. E.; Duhme-Klair, A. K.; Sawle, P.; Motterlini, R. *Dalton Trans.* **2007**, 3603-3605; (f) Niesel, J.; Pinto, A.; Peindy N'Dongo, H.W.; Merz, K.; Ott, I.; Gust, R.; Schatzschneider, U. *Chem.*

- Commun.* **2008**, 1798-1800; (g) Pfeiffer, H.; Rojas, A.; Niesel, J.; Schatzschneider, U. *Dalton Trans.* **2009**, 4292-4298; (h) Zhang, W.-Q.; Atkin, A. J.; Thatcher, R. J.; Whitwood, A. C.; Fairlamb, I. J. S.; Lynam, J. M. *Dalton Trans.* **2009**, 4351-4358; (i) Rimmer, R. D.; Richter, H.; Ford, P.C. *Inorg. Chem.* **2010**, *49*, 1180-1185; (j) Bikiel, D. E.; González Solveyra, E.; Di Salvo, F.; Milagre, H. M. S.; Eberlin, M. N.; Corrêa, R. S.; Ellena, J.; Estrin, D. A.; Doctorovich, F. *Inorg. Chem.* **2011**, *50*, 2334-2345; (k) Gonzales, M. A.; Fry, N. L.; Burt, R.; Davda, R.; Hobbs, A.; Mascharak, P. K. *Inorg. Chem.* **2011**, *50*, 3127-3134; (l) Dördelmann, G.; Pfeifer, H.; Brikner, A.; Schatzschneider, U. *Inorg. Chem.* **2011**, *50*, 4362-4367; (m) Jackson, C. S.; Schmitt, S.; Ping Dou, Q.; Kodanko, J. J. *Inorg. Chem.* **2011**, *50*, 5336-5338.
38. (a) Crespy, D.; Landfester, K.; Schubert, U. S.; Schiller, A. *Chem. Commun.* **2010**, *46*, 6651-6662; (b) Schatzschneider, U. *Eur. J. Inorg. Chem.* **2010**, 1457-1461 and references cited therein.
39. Ford, P. *Acc. Chem. Res.* **2008**, *41*, 190-200.
40. Hasegawa, U.; van der Vlies, A. J.; Simeoni, E.; Wandrey, C.; Hubbell, J. A. *J. Am. Chem. Soc.* **2010**, *132*, 18273-18280.
41. Romansi, S.; Kraus, B.; Schatzschneider, U.; Neudörf, J.-M.; Amslinger, S.; Schmalz, H.-G. *Angew. Chem. Int. Ed.* **2011**, *50*, 1-6.
42. (a) Szajna, E.; Arif, A. M.; Berreau, L. M. *J. Am. Chem. Soc.* **2005**, *127*, 17186-17187; (b) Berreau, L. M.; Borowski, T.; Grubel, K.; Allpress, C. J.; Wikstrom, J.

- P.; Germain, M. E.; Rybak-Akimova, E. V.; Tierney, D. L. *Inorg. Chem.* **2011**, *50*, 1047-1057.
43. Szajna-Fuller, E.; Rudzka, K.; Arif, A. M.; Berreau, L. M. *Inorg. Chem.* **2007**, *46*, 5499-5507.
44. Rudzka, K.; Arif, A. M.; Berreau, L. M. *Inorg. Chem.* **2008**, *47*, 10832-10840.
45. Rudzka, K.; Grubel, K.; Arif, A. M.; Berreau, L. M. *Inorg. Chem.* **2010**, *49*, 7623–7625
46. Nishinaga, A.; Tojo, T.; Tomita, H.; Matsuura, T. *J. Chem. Soc. Perkin Trans.* **1979**, 2511-2516.
47. Speier, G.; Fülöp, V.; Párkányi, L. *J. Chem. Soc. Chem. Commun.* **1990**, 512-513.
48. Balogh-Hergovich, É.; Speier, G.; Argay, G. *J. Chem. Soc. Chem. Commun.* **1991**, *8*, 551-552.
49. (a) Kaizer, J.; Balogh-Hergovich, É.; Czaun, M.; Csay, T.; Speier, G. *Coord. Chem. Rev.* **2006**, *250*, 2222-2233; (b) Pap, J. S.; Kaizer, J. Speier, G. *Coord. Chem. Rev.* **2010**, *254*, 781-793.
50. Nishinaga, A.; Tojo, T.; Matsuura, T. *J. Chem. Soc. Chem. Commun.* **1974**, 896-897.
51. Hiller, W.; Nishinaga, A.; Rieker, A. *Z. Naturforsch. B: Chem. Sci.* **1992**, *47*, 1185-1188.
52. (a) El Amrani, F. B. A.; Perrelló, L.; Real, J. A.; Gozález-Álvarez, M.; Alzuet, G.; Borrás, J.; Garcia-Granda, S.; Montejo-Bernardo, J. *J. Inorg. Biochem.* **2006**, *100*,

- 1208-1218; (b) Kaizer, J.; Baráth, G.; Pap, J.; Speier, G.; Giorgi, M.; Réglie, M. *Chem. Commun.* **2007**, 5235-5237.
53. Farina, Y.; Yamin, B. M.; Fun, H-K.; Yip, B-C.; Teoh, S-G. *Acta Cryst.* **1995**, *C51*, 1537-1540.
54. Annan, T.A.; Peppe, C.; Tuck, D.G. *Can. J. Chem.* **1990**, *68*, 423-430; Balogh-Hergovich, É.; Kaizer, J.; Speier, G.; Huttner, G.; Rutsch, P. *Acta Crystallogr., Sect. C: Cryst. Struct. Commun.* **1999**, *55*, 557-558; Kaizer, J.; Kupán, A.; Pap, J.; Speier, G.; Réglie, M.; Michel, G. *Z. Kristallogr.-New Cryst. Struct.* **2000**, *215*, 571-572.

CHAPTER 2

O₂-DEPENDENT ALIPHATIC CARBON-CARBON BOND CLEAVAGE
REACTIVITY IN A Ni(II) ENOLATE COMPLEX HAVING A HYDROGEN BOND
DONOR MICROENVIRONMENT; COMPARISON WITH A HYDROPHOBIC
ANALOG¹

Abstract

A mononuclear Ni(II) complex having an acireductone type ligand, and supported by the bnpapa (N,N-bis((6-neopentylamino-2-pyridyl)methyl-N-((2-pyridyl)methyl)amine ligand, [(bnpapa)Ni(PhC(O)C(OH)C(O)Ph)]ClO₄ (**14**), has been prepared and characterized by elemental analysis, ¹H NMR, FTIR, and UV-vis. To gain insight into the ¹H NMR features of **14**, the air stable analog complexes [(bnpapa)Ni(CH₃C(O)CHC(O)CH₃)]ClO₄ (**16**) and [(bnpapa)Ni(ONHC(O)CH₃)]ClO₄ (**17**) were prepared and characterized by X-ray crystallography, ¹H NMR, FTIR, UV-vis, mass spectrometry, and solution conductivity measurements. Compounds **16** and **17** are 1:1 electrolyte species in CH₃CN. ¹H and ²H NMR studies of **14**, **16**, and **17** and deuterated analogs revealed that the complexes having six-membered chelate rings for the exogenous ligand (**14** and **16**) do not have a plane of symmetry within the solvated cation

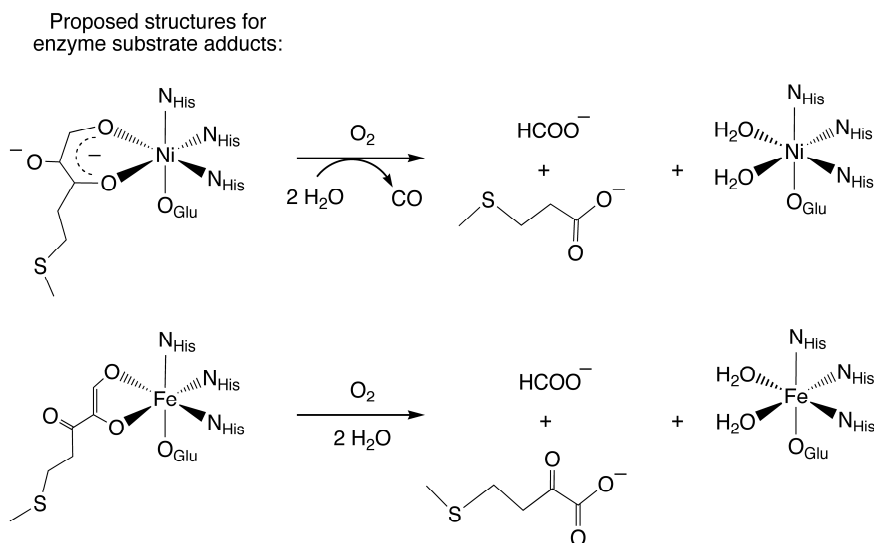
¹Coauthored by Katarzyna Grubel, Amy L. Fuller, Bonnie M. Chambers, Atta M. Arif, and Lisa M. Berreau. Reproduced with permission from *Inorganic Chemistry* **2010**, *49*, 1071-1081. Copyright 2010 American Chemical Society.

and thus exhibit more complicated ^1H NMR spectra. Compound **17**, as well as other simple Ni(II) complexes of the bnpapa ligand (e.g. $[(\text{bnpapa})\text{Ni}(\text{ClO}_4)(\text{CH}_3\text{CN})]\text{ClO}_4$ (**18**) and $[(\text{bnpapaNi})_2(\mu\text{-Cl})_2](\text{ClO}_4)_2$ (**19**)), exhibit ^1H NMR spectra consistent with the presence of a plane of symmetry within the cation. Treatment of $[(\text{bnpapa})\text{Ni}(\text{PhC}(\text{O})\text{C}(\text{OH})\text{C}(\text{O})\text{Ph})]\text{ClO}_4$ (**14**) with O_2 results in aliphatic carbon-carbon bond cleavage within the acireductone-type ligand and the formation of $[(\text{bnpapa})\text{Ni}(\text{O}_2\text{CPh})]\text{ClO}_4$ (**9**), benzoic acid, benzil, and CO. Use of $^{18}\text{O}_2$ in the reaction gives high levels of incorporation (>80%) of one labeled oxygen atom into **9** and benzoic acid. The product mixture and level of ^{18}O incorporation in this reaction is different than that exhibited by the analog supported the hydrophobic 6-Ph₂TPA ligand, $[(6\text{-Ph}_2\text{TPA})\text{Ni}(\text{PhC}(\text{O})\text{C}(\text{OH})\text{C}(\text{O})\text{Ph})]\text{ClO}_4$ (**2**). We propose that this difference is due to variations in the reactivity of bnpapa- and 6-Ph₂TPA-ligated Ni(II) complexes with triketone and/or peroxide species produced in the reaction pathway.

Introduction

Interest in how the secondary environment of a metal center influences the reactivity of metal-bound ligands stems from the possible roles of secondary interactions in metal-catalyzed reactions in biological systems.¹ In the acireductone dioxygenases Ni(II)-ARD and Fe(II)-ARD, which contain the same protein component, it is proposed that differences in the secondary environment surrounding the divalent metal center influence the coordination mode of the acireductone substrate and the regioselectivity of the oxidative carbon-carbon bond cleavage reaction.¹ Specifically, in Ni(II)-ARD the

positioning of a tryptophan side chain (W162) is suggested to promote the formation of a six-membered chelate ring in the enzyme substrate adduct (Scheme 2-1(top)).² Reaction of this adduct with O_2 results in oxidative cleavage of the C(1)-C(2) and C(2)-C(3) bonds and the formation of CO and carboxylate products. For Fe(II)-ARD, a more open active site is suggested to enable the formation of a five-membered chelate enediolate structure, within which only C(1)-C(2) bond cleavage occurs upon reaction with O_2 (Scheme 2-1(bottom)). For both Ni(II)-ARD and Fe(II)-ARD secondary hydrogen bonding interactions involving an arginine residue are suggested to stabilize enolate/enediolate coordination.



Scheme 2-1.

Interest in reactions of relevance to Ni(II)-ARD also stems from the fact that carbon monoxide is a molecule of current interest in biological systems. In humans, CO is

primarily produced via the oxidative breakdown of heme catalyzed by heme oxygenases.³ While carbon monoxide is typically viewed as a toxic gas, recent studies have shown that this small molecule can have beneficial health effects. The signaling mechanism of CO is similar to that of NO in that it activates soluble guanylyl cyclase to produce cyclic guanylyl monophosphate (cGMP).³ This compound is involved in pathways pertinent to smooth muscle relaxation, platelet inhibition, and cell growth and differentiation. As these factors are related to several diseases, recent studies have focused on efforts toward the development of CO-releasing compounds for use as therapeutic agents.⁴ The majority of the chemical compounds tested so far have been transition metal carbonyl species,⁵ although a main group CO-releasing compound ($\text{Na}_2[\text{H}_3\text{BCO}_2]$) has been recently reported.⁴ We are interested in the CO release properties of acireductones and flavonolates, both of which possess three consecutive carbon centers having an oxygen substituent. In fungal and bacterial systems, quercetin dioxygenases catalyze CO release from a metal-coordinated flavonolate in a 2,4-dioxygenolytic ring cleavage reaction.⁶⁻¹⁴ In a broad sense, we are interested in understanding in detail the chemical factors that modulate the CO-release reactivity of metal-coordinated acireductone and flavonolate species, with a long-term goal of producing new types of CO-releasing compounds containing these novel structural motifs.

Our laboratory has reported the only examples to date of synthetic complexes of relevance to substrate- and product carboxylate-bound forms of Ni(II)-ARD.¹⁵⁻¹⁸ We recently reported that use of a chelate ligand having a mixed hydrophobic/hydrogen bond donor secondary environment produced the first example of a Ni(II) enediolate complex

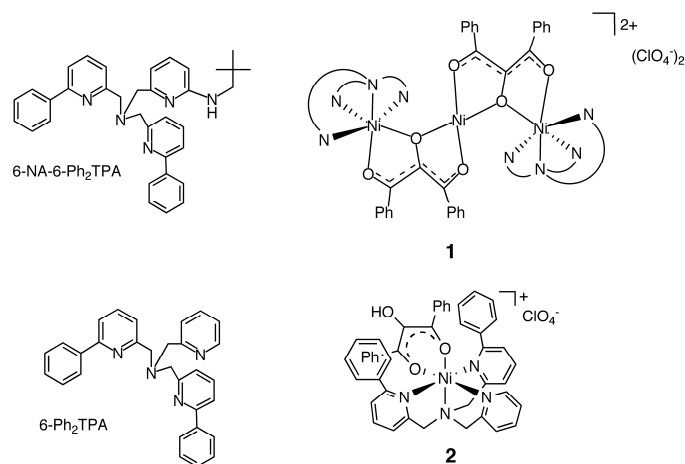
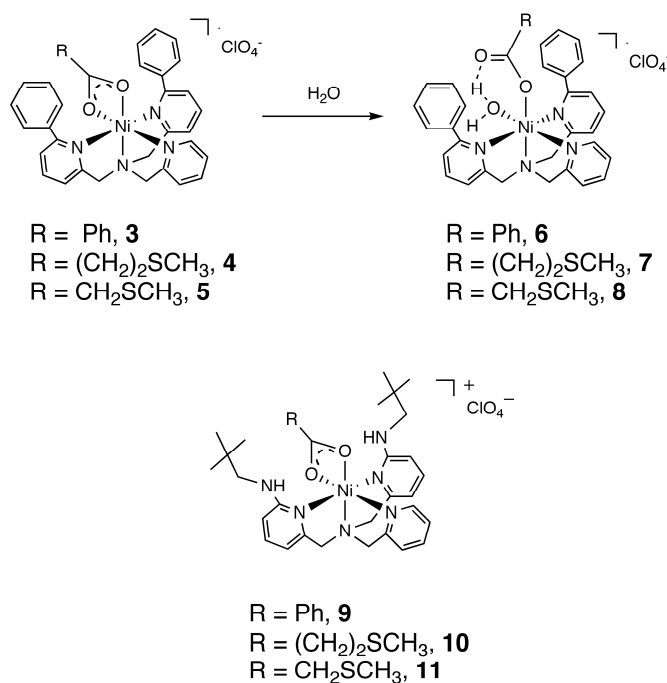


Figure 2-1. Supporting chelate ligands used to isolate Ni(II) enediolate (top) and enolate (bottom) complexes of relevance to Ni(II)-ARD.

of an acireductone-type ligand (**1**, Figure 2-1(top)).¹⁸ Somewhat surprisingly, this complex was originally generated under similar conditions to those used to produce the mononuclear Ni(II) enolate complex [(6-Ph₂TPA)Ni(PhC(O)C(OH)C(O)Ph)]ClO₄ (**2**, Figure 2-1(bottom)). These combined results indicate that the presence of a hydrogen bond donor in the secondary environment influences the coordination chemistry of an acireductone-type ligand.

In terms of carboxylate chemistry, we discovered that the secondary environment of the chelate ligand affects the coordination chemistry of Ni(II)-carboxylate species that are generated in O₂-dependent ARD-type reactions. As shown in Scheme 2-2 (top), a Ni(II)-carboxylate ligand in a hydrophobic microenvironment undergoes a shift from bidentate to monodentate in the presence of water (conversion of compounds **3-5** to **6-8**).¹⁷ No evidence was found for this type of carboxylate shift chemistry in bnpapa-ligated Ni(II) carboxylate complexes (**9-11**, Scheme 2-2 (bottom)). In these analogs, the



Scheme 2-2.

hydrogen bond donor appendages interact with one oxygen atom of the bidentate carboxylate. In a Ni(II) benzoate complex supported by a chelate ligand containing both hydrophobic phenyl appendages and a hydrogen bond donor, [(6-NA-6-Ph₂TPA)Ni(O₂CPh)(H₂O)]ClO₄ (**12**), a bidentate coordinated carboxylate ligand was also identified.¹⁸

From our initial studies, it is clear that the ligand environment of a Ni(II) center influences the chemistry of an acireductone-type ligand. In the studies outlined herein, we have further evaluated the influence of the chelate ligand environment by preparing and characterizing the enolate complex [(bnpapa)Ni(PhC(O)C(OH)C(O)Ph)]ClO₄ (**14**) as an analog to the 6-Ph₂TPA-supported **2** (Figure 2-1). Complex **14** has been characterized by elemental analysis, ¹H NMR, FTIR, and UV-vis. Comparative O₂ reactivity studies for **2**

and **14** have been performed under conditions wherein the inorganic and organic byproducts were identified. Interestingly, these reactions differ in the specific mixture of products that is generated and in the level of ^{18}O incorporation in the benzoate/benzoic acid products. We propose that these differences are due to variations in the reactivity of bnpapa- and 6-Ph₂TPA ligated Ni(II) complexes with triketone and peroxide/hydroperoxide species produced in the reaction pathway.

In the course of this research, as a means of gaining additional insight in the spectroscopic and solution properties of [(bnpapa)Ni(PhC(O)C(OH)C(O)Ph)]ClO₄ (**14**), we have also prepared and characterized mononuclear bnpapa-supported Ni(II) acetoacetonato and hydroxamato complexes, as well as perchlorate and chloro derivatives. Preparation of this family of complexes has enabled a structural comparison with a similar family of 6-Ph₂TPA-supported mononuclear Ni(II) complexes. This comparison has provided insight into the structural factors that may be responsible for the differences in O₂ reactivity between [(bnpapa)Ni(PhC(O)C(OH)C(O)Ph)]ClO₄ (**14**) and [(6-Ph₂TPA)Ni(PhC(O)C(OH)C(O)Ph)]ClO₄ (**2**) as noted above.

Experimental

General Methods. All reagents and solvents were obtained from commercial sources and were used as received unless otherwise noted. Solvents were dried according to published procedures and were distilled under N₂ prior to use.¹⁹ Air sensitive reactions were performed in the MBraun Unilab glovebox or a Vacuum Atmospheres MO-20 glovebox under a N₂ atmosphere. The ligand bnpapa and the Ni(II) complex [(6-

$\text{Ph}_2\text{TPA})\text{Ni}(\text{PhC}(\text{O})\text{C}(\text{OH})\text{C}(\text{O})\text{Ph})\text{]ClO}_4$ (**2**) were prepared according to literature procedures.^{15,17}

Physical Methods. ^1H NMR spectra of Ni(II) complexes were obtained using a Bruker ARX-400 spectrometer as previously described.²⁰ Chemical shifts (in ppm) are referenced to the residual solvent peak(s) in CHD_2CN (1H, 1.94 (quintet) ppm). UV-vis spectra were collected on a HP8453A spectrometer at ambient temperature. FTIR spectra were recorded on a Shimadzu FTIR-8400 spectrometer as KBr pellets. Conductance measurements were made at 22(1) °C using an YSI model 31A conductivity bridge with a cell having a cell constant of 1.0 cm^{-1} and using Me_4NClO_4 as a 1:1 electrolyte standard. Preparation of the acetonitrile and standard solutions for conductance measurements and subsequent data analysis were performed as previously described.²¹ Mass spectrometry data was obtained at the Mass Spectrometry Facility, Department of Chemistry, University of California, Riverside. Elemental analyses were performed by Atlantic Microlabs, Inc., Norcross, Georgia, or Canadian Microanalytical Service, Inc., British Columbia.

***Caution!** Perchlorate salts of metal complexes with organic ligands are potentially explosive. Only small amounts of material should be prepared, and these should be handled with great care.*²²

$[(\text{bnpapa})\text{Ni}(\text{PhC}(\text{O})\text{C}(\text{OH})\text{C}(\text{O})\text{Ph})\text{]ClO}_4$ (14**).** Under a N_2 atmosphere, equimolar amounts of bnpapa (0.273 mmol) and $\text{Ni}(\text{ClO}_4)_2 \cdot 6\text{H}_2\text{O}$ (0.273 mmol) were

mixed in acetonitrile and stirred until the ligand had fully dissolved. $\text{Me}_4\text{NOH}\cdot 5\text{H}_2\text{O}$ (0.301 mmol) was then added to the mixture, which was stirred for additional 15 minutes, resulting in a dark green solution. The solution was added to solid 2-hydroxy-1,3-diphenylpropan-1,3-dione²³ (0.301 mmol) and the mixture was stirred for 4 h, yielding a very dark orange/red solution. The solvent was then removed under reduced pressure. The solid was dissolved in CH_2Cl_2 and the solution was filtered through a celite plug. The filtrate was concentrated and brought to dryness under vacuum, leaving a dark orange/red solid, which was washed with Et_2O and dried under vacuum. Yield: 83%. Anal. Calcd for $\text{C}_{43}\text{H}_{51}\text{N}_6\text{O}_7\text{ClNi}$: C, 60.19; H, 5.99; N, 9.79. Found: C, 60.52; H, 5.88; N, 9.57. UV-vis [CH_3CN , nm (ϵ , $\text{M}^{-1}\text{cm}^{-1}$)] 393(10,000); FTIR: (KBr, cm^{-1}) 3420 (br s, ν_{NH}), 1094 (ν_{ClO_4}), 621 (ν_{ClO_4}).

[(bnpapa)Ni(CH₃C(O)CHC(O)CH₃)]ClO₄ (16). A solution of $\text{Ni}(\text{ClO}_4)_2\cdot 6\text{H}_2\text{O}$ (0.15 mmol) in CH_3CN (~1 mL) was added to solid bnpapa (0.15 mmol). The resulting mixture was stirred for 20 min at room temperature. The solution was then transferred to a vial containing $\text{Me}_4\text{NOH}\cdot 5\text{H}_2\text{O}$ (0.15 mmol). To this mixture 2,4-pentanedione (0.15 mmol) was added and the resulting solution was stirred overnight. The solvent was then removed under reduced pressure. The remaining solid was dissolved in CH_2Cl_2 (~5 mL) and the solution was filtered through a celite/glass wool plug. Pentane diffusion into CH_2Cl_2 yielded purple crystals suitable for X-ray crystallography. The crystals were crushed and dried under vacuum prior to elemental analysis. Yield: 46%. Anal. Calcd for $\text{C}_{33}\text{H}_{47}\text{ClN}_6\text{NiO}_6$: C, 55.21; H, 6.60; N, 11.71. Found: C, 55.28; H, 6.55; N, 11.70. FTIR (KBr, cm^{-1}) ~3300 (s, ν_{NH}), 1089 (ν_{ClO_4}), 622 (ν_{ClO_4}). UV-vis [CH_3CN , nm (ϵ , $\text{M}^{-1}\text{cm}^{-1}$)]

244(31600), 305(17800), 543(sh), 966(19); FAB-MS [m/z (relative intensity)]: 617 ($[M - ClO_4]^+$, 100%).

[(bnpapa)Ni(ONHC(O)CH₃)]ClO₄ (17). A solution of Ni(ClO₄)₂·6H₂O (0.11 mmol) in CH₃CN (~1 mL) was added to solid bnpapa (0.11 mmol). The resulting mixture was stirred for 5 min at the room temperature. The solution was then transferred to a vial containing Me₄NOH·5H₂O (0.12 mmol) and acetohydroxamic acid (0.12 mmol), and the resulting solution was stirred for 1 h. The solvent was then removed under reduced pressure. The remaining solid was dissolved in CH₂Cl₂ (~5 mL) and the solution was filtered through a celite/glass wool plug. Diffusion of diethyl ether into a CH₂Cl₂/MeOH/*i*PrOH (1:0.5:1) solution of the compound yielded purple crystals suitable for single crystal X-ray crystallography. These crystals were crushed and dried under vacuum prior to elemental analysis. Yield: 60%. Anal. Calcd for C₃₀H₄₄N₇NiO₆Cl·0.25AHA·0.35CH₂Cl₂: C, 51.93; H, 6.34; N, 13.12. Found: C, 51.55; H, 6.41; N, 13.63. The presence of acetohydroxamic acid (AHA) in the crystalline sample was confirmed by X-ray crystallography. The presence of CH₂Cl₂ in the elemental analysis sample was confirmed by ¹H NMR. FTIR (KBr, cm⁻¹) ~3288 (s, ν_{NH}), 1103 (ν_{ClO₄}), 621 (ν_{ClO₄}); UV-vis [CH₃CN, nm (ε, M⁻¹cm⁻¹)] 247(25800), 325(10400), 548(sh), 977(32); ESI/APCI-MS [m/z (relative intensity)]: 592.2914 ($[M - ClO_4]^+$, 100%).

[(bnpapa)Ni(ClO₄)(CH₃CN)]ClO₄ (18). A solution of Ni(ClO₄)₂·6H₂O (0.07 mmol) in CH₃CN (~1 mL) was added to solid bnpapa (0.07 mmol). The resulting mixture was stirred for 20 min at room temperature. The solvent was then removed under reduced pressure and the residue was dissolved in CH₂Cl₂. Pentane diffusion yielded purple

crystals suitable for X-ray crystallography. The crystals were crushed and dried under vacuum prior to elemental analysis. Yield: 54%. Anal. Calcd for $C_{30}H_{43}Cl_2N_7NiO_8 \cdot 1/2CH_2Cl_2$: C, 45.69; H, 5.53; N, 12.23. Found: C, 45.32; H, 5.60; N, 12.09. UV-vis [CH_3CN , nm (ϵ , $M^{-1}cm^{-1}$)] 318(10300), 553(15), 931(17); FTIR (KBr, cm^{-1}) \sim 3400 (s, ν_{NH}), 1103 (ν_{ClO_4}), 624 (ν_{ClO_4}); FAB-MS [m/z (relative intensity)]: 617 ($[M - ClO_4 - CH_3CN]^+$, 100%).

$[(bnpapaNi)_2(\mu-Cl)_2](ClO_4)_2$ (19). A solution of $Ni(ClO_4)_2 \cdot 6H_2O$ (0.14 mmol) in MeOH (\sim 1 mL) was added to a solution of bnpapa (0.14 mmol) in MeOH (\sim 1 mL). The resulting mixture was stirred for 20 min at room temperature. The solution was then transferred to a vial containing $Me_4NCl \cdot 5H_2O$ (0.14 mmol) and the resulting mixture was stirred for 1 h. The solvent was then removed under reduced pressure. The remaining solid was dissolved in CH_2Cl_2 (\sim 5 mL), and the solution was filtered through a celite/glass wool plug. Diffusion of diethyl ether into a CH_2Cl_2 solution of the compound yielded green crystals suitable for X-ray crystallography. The crystals were crushed and dried under vacuum prior to elemental analysis. Yield: 33%. Anal. Calcd for $C_{28}H_{40}Cl_2N_6NiO_4$: C, 51.40; H, 6.16; N, 12.84. Found: C, 51.15; H, 6.29; N, 12.88. FTIR (KBr, cm^{-1}) \sim 3340 (s, ν_{NH}), 1095 (ν_{ClO_4}), 621 (ν_{ClO_4}); UV-vis [CH_3CN , nm (ϵ , $M^{-1}cm^{-1}$)] 325(15900), 600(31), 1032(33); ESI/APCI-MS [m/z (relative intensity)]: 553.2348 ($[M - 2ClO_4]^{2+}$, 100%).

O_2 Reactivity of 14: Product Isolation and ^{18}O Labeling Studies. Complex 14 (0.101 mmol) was dissolved in 10 mL of acetonitrile and O_2 was bubbled through the solution for \sim 1 min. The reaction was then left stirring overnight at ambient temperature.

Over the course of this time, the color changed from deep orange/red to pale yellow. CO production was verified by the PdCl₂ method.²⁴ The solvent was removed under reduced pressure and the resulting solid was dissolved in hexanes:ethyl acetate (4:1) and the solution was passed through a silica plug. This produced a yellow filtrate containing the organic products from the reaction. Ni(II) complexes that adhered to the silica gel were then eluted using acetonitrile, followed by methanol. As determined by TLC, ¹H NMR, and GC-MS, the organic fraction contained primarily benzoic acid (11 mg overall yield – 91% based on production of one equivalent of free benzoic acid per enolate ligand; sample is 88-90% benzoic acid based on ¹H NMR), with a small amount of benzil (PhC(O)C(O)Ph; 10-12%) and a trace amount of the ester PhC(O)OCH₂C(O)Ph present. The ester was identified via independent synthesis.²⁵ This compound is an isomer of 2-hydroxy-1,3-diphenylpropan-1,3-dione,²³ and the reaction leading to ester formation will be discussed in detail elsewhere. In each reaction, two Ni(II) complexes were eluted from the column, [(bnpapa)Ni(O₂CPh)]ClO₄ (**9**) and [(bnpapa)Ni(PhC(O)C(O)CHC(O)Ph)]ClO₄ (**15**), the latter of which was present in a very low amount (<5%) and was identified via mass spectrometry (ESI-MS [*m/z* (relative intensity)]: 769.3376 (M – ClO₄)⁺, 100%). The formation of **15** is related to the trace ester formation in the reaction and will be discussed in detail elsewhere. The yield of the metal complexes was ~88% by mass following the column (based on stoichiometric formation of [(bnpapa)Ni(O₂CPh)]ClO₄ (**9**)). Thus, from this data, the formation of [(bnpapa)Ni(O₂CPh)]ClO₄ (**9**) was judged as quantitative. Use of ¹⁸O₂ in the reaction of **14** with O₂ produces benzoic acid with 81% incorporation of one labeled oxygen atom.

No ^{18}O incorporation was found in benzil or the ester $\text{PhC}(\text{O})\text{OCH}_2\text{C}(\text{O})\text{Ph}$, as determined by GC-MS. Mass spectral analysis of the metal complexes indicated 87% ^{18}O incorporation into one oxygen atom of the benzoate ligand of **9**. No ^{18}O incorporation was found in **15**.

Reanalysis of O_2 reactivity of $[(6\text{-Ph}_2\text{TPA})\text{Ni}(\text{PhC}(\text{O})\text{C}(\text{OH})\text{C}(\text{O})\text{Ph})]\text{ClO}_4$ (2**).** Compound **2** was treated with an excess of O_2 in a reaction very similar to that outlined above using **14**. An identical work-up procedure was also performed. The organic products generated were benzoic acid and benzil in a reproducible ~75:25 ratio. A trace amount of the ester $\text{PhC}(\text{O})\text{OCH}_2\text{C}(\text{O})\text{Ph}$ is also generated, as determined by GC-MS and ^1H NMR. The total yield of organic products was ~96% based on the proposed formation of one equivalent of free benzoic acid per enolate ligand of **2**. As previously reported, the Ni(II) complex, $[(6\text{-Ph}_2\text{TPA})\text{Ni}(\text{O}_2\text{Ph})]\text{ClO}_4$ (**3**) is produced in this reaction.¹⁶ A trace amount of the enolate complex $[(6\text{-Ph}_2\text{TPA})\text{Ni}(\text{PhC}(\text{O})\text{C}(\text{O})\text{CHC}(\text{O})\text{Ph})]\text{ClO}_4$ ¹⁶ is also generated. The reaction leading to the formation this complex will be discussed in detail elsewhere. The total mass of complexes isolated suggests a ~70% yield based on the stoichiometric formation of **3**. However, a control experiment using $[(6\text{-Ph}_2\text{TPA})\text{Ni}(\text{O}_2\text{Ph})]\text{ClO}_4$ (**3**) indicated that ~30% of the material is lost in the column purification process used to isolate the metal complexes from the reaction mixture. Thus, the formation of **3** is nearly quantitative in the O_2 reaction of **2**. Use of $^{18}\text{O}_2$ in the reaction produced free benzoic acid with 59% ^{18}O incorporation in one oxygen atom position, and the benzoate complex **3** having 64%

incorporation in one oxygen atom. The level of isotope incorporation into **3** is slightly higher than that previously reported (~50%) based on multiple ^{18}O reactions.¹⁶

$^{18}\text{O}_2$ reactivity of $[\text{Me}_4\text{N}][\text{PhC}(\text{O})\text{C}(\text{OH})\text{C}(\text{O})\text{Ph}]$. We have previously reported that treatment of the salt $[\text{Me}_4\text{N}][\text{PhC}(\text{O})\text{C}(\text{OH})\text{C}(\text{O})\text{Ph}]$ with O_2 results in the formation of tetramethylammonium benzoate, benzoic acid, and CO .¹⁶ We have repeated this reaction using $^{18}\text{O}_2$ and have found by mass spectrometry that the benzoate/benzoic acid contains ~65% ^{18}O incorporation when generated from $\text{Me}_4\text{NOH}\cdot 5\text{H}_2\text{O}$ and $\text{PhC}(\text{O})\text{C}(\text{OH})\text{C}(\text{O})\text{Ph}$ in dry CH_3CN . Pre-drying of the $\text{Me}_4\text{NOH}\cdot 5\text{H}_2\text{O}$ under vacuum for 24 h prior to use in the reaction produced a slightly higher level of ^{18}O incorporation (72%) in the benzoate/benzoic acid product.

X-ray Crystallography. A single crystal of each compound **16**, **17-1/4AHA** (AHA = acetohydroxamic acid), **18-CH₂Cl₂**, and **19-2CH₂Cl₂** was mounted on a glass fiber with traces of viscous oil and then transferred to a Nonius KappaCCD diffractometer equipped with Mo $\text{K}\alpha$ radiation ($\lambda = 0.71073 \text{ \AA}$) for data collection. For unit cell determination, ten frames of data were collected at 103(1) K or 150(1) K with an oscillation range of 1 deg/frame and an exposure time of 20 sec/frame. Final cell constants were determined from a set of strong reflections from the actual data collection. All reflections were indexed, integrated, and corrected for Lorentz polarization and absorption effects using DENZO-SMN and SCALEPAC.²⁶ The structures were solved by a combination of direct and heavy-atom methods using SIR 97. All of the non-hydrogen atoms were refined with anisotropic displacement coefficients. Unless otherwise stated, all hydrogen atoms were assigned isotropic displacement coefficients $U(\text{H}) = 1.2U(\text{C})$ or

1.5U(C_{methyl}), and their coordinates were allowed to ride on their respective carbons using SHELXL97.²⁷ Complex **16** crystallizes in the space group *P*-1, with two carbon atoms of one neopentyl group exhibiting disorder over two positions. Complex **17·1/4AHA** crystallizes in the space group *C*₂/*c* with three oxygen atoms of the perchlorate anion and the carbon atoms of one neopentyl group exhibiting disorder. Complex **18·CH₂Cl₂** crystallizes in the space group *P*2₁/*c*. The CH₂Cl₂ solvate molecule exhibits disorder. Complex **19·2CH₂Cl₂** crystallizes in the space group *P*2₁/*n*, with one CH₂Cl₂ exhibiting disorder in the position of one chlorine atom.

Results

Preparation and Characterization of

[(bnpapa)Ni(PhC(O)C(OH)C(O)Ph)]ClO₄ (14). Treatment of the bnpapa chelate ligand with equimolar amounts of Ni(ClO₄)₂·6H₂O, Me₄NOH·5H₂O, and 2-hydroxy-1,3-diphenylpropan-1,3-dione in CH₃CN, followed by work up using CH₂Cl₂, yielded a deep orange/red solid. Unfortunately, repeated attempts to produce crystals of this complex suitable for single crystal X-ray crystallography were unsuccessful. Instead, the orange/red solid was characterized by elemental analysis, UV-vis, FTIR, and ¹H NMR. The elemental analysis data is consistent with the proposed formulation. The π→π* transition of the coordinated enolate ligand of **14** is found at 393 nm (ε ~ 10,000 M⁻¹cm⁻¹). The wavelength and intensity of this absorption feature is generally similar to that reported for [(6-Ph₂TPA)Ni((PhC(O)C(OH)C(O)Ph)]ClO₄ (**2**; λ_{max} = 399 nm (ε ~ 6,800 M⁻¹cm⁻¹)).¹⁶ A broad absorption feature at ~3420 cm⁻¹ in the infrared spectrum of **14** is

consistent with hydrogen bonding interactions involving the neopentylamine groups of the bnpapa chelate ligand. Based on structural studies of air stable analogs (*vide infra*), we propose that this hydrogen bonding involves an oxygen atom of the chelating enolate ligand that is positioned *trans* to the tertiary amine nitrogen donor of the chelate ligand.

Air Stable Analogs. To aid in the interpretation of the ^1H NMR spectroscopic features of **14**, air stable analog complexes containing a bidentate acetoacetonato ($[(\text{bnpapa})\text{Ni}(\text{CH}_3\text{C}(\text{O})\text{CHC}(\text{O})\text{CH}_3)]\text{ClO}_4$ (**16**)) or hydroxamato ($[(\text{bnpapa})\text{Ni}(\text{CH}_3\text{C}(\text{O})\text{NHO})]\text{ClO}_4$ (**17**)) ligand were prepared and comprehensively characterized. For solution conductivity and spectroscopic studies, the perchlorate complex $[(\text{bnpapa})\text{Ni}(\text{ClO}_4)(\text{CH}_3\text{CN})]\text{ClO}_4$ (**18**) and chloride complex $[(\text{bnpapaNi})_2(\mu\text{-Cl})_2](\text{ClO}_4)_2$ (**19**) were also prepared and characterized.

X-ray Crystallography. The cationic portions of **16** and **17** are shown in Figure 2-2, and those of **18** and **19** are shown in Figure 2-3. Details of the data collection and refinement are given in Table 2-1. Selected bond distances and angles are given in Table 2-2. The mononuclear **16** and **17** each contain a pseudo-octahedral Ni(II) center with the oxygen donor atoms of the chelate ligand positioned *trans* to N(3) and N(6). The respective Ni-O/N bonds of the primary coordination sphere are similar in these complexes, with the most noticeable difference in bond lengths being that the Ni-N interactions involving the neopentylamine-appended pyridyl donors are ~ 0.02 Å longer in **16** than those found in the hydroxamato complex (**17**). In terms of bond angles, a more acute O(1)-Ni(1)-O(2) angle in **17** ($81.86(10)^\circ$) than that found in **16** ($94.98(3)^\circ$) is due to the difference in chelate ring size of the bidentate *O,O*-donor ligands. In both complexes,

an oxygen atom of the bidentate chelate ligand accepts two hydrogen bonds from the neopentyl amine groups of the supporting chelate ligand. These interactions are characterized by N(H)...O distances of 2.8-2.9 Å.

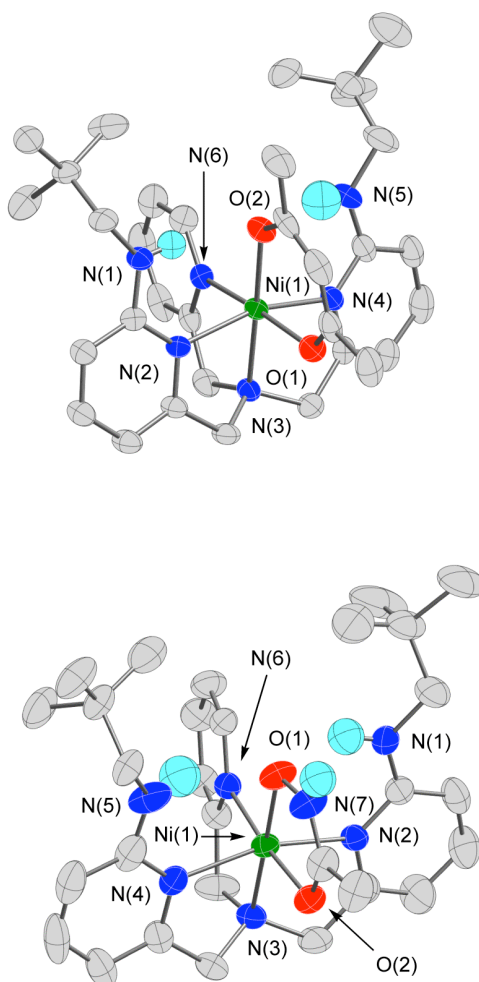


Figure 2-2. Thermal ellipsoid drawings of the cationic portions of **16** and **17**. All ellipsoids are drawn at the 50% probability level. Hydrogen atoms, other than the neopentyl amine N-H hydrogen atoms, and the hydroxyamate N-H hydrogen in **17**, have been omitted for clarity.

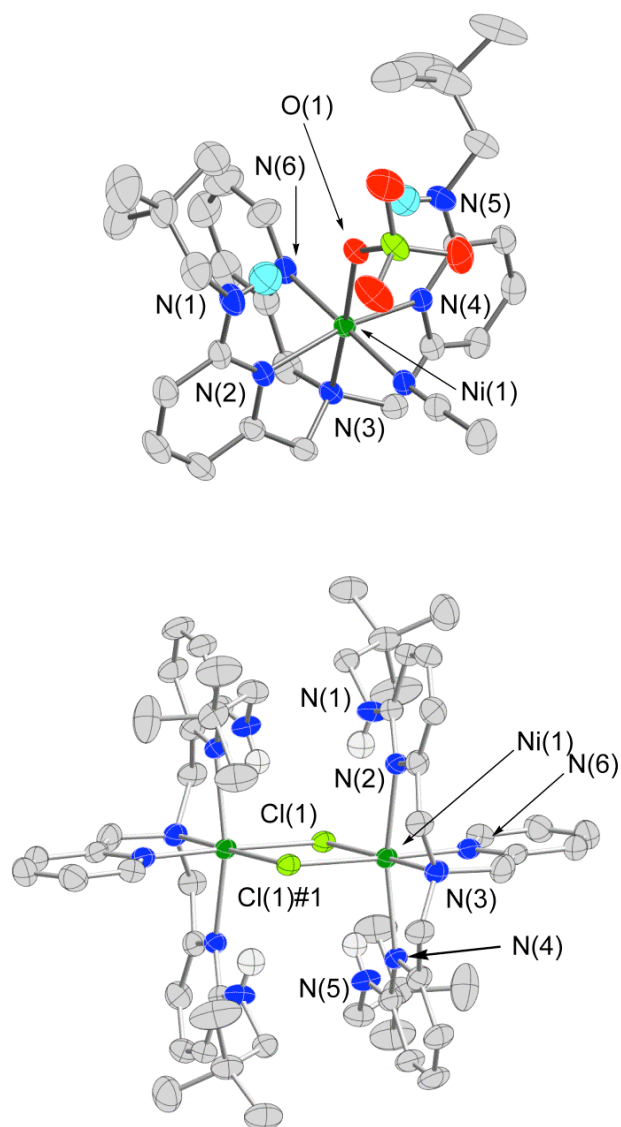


Figure 2-3. Thermal ellipsoid drawings of the cationic portions of **18** and **19**. All ellipsoids are drawn at the 50% probability level. Hydrogen atoms other than the neopentyl amine N-H hydrogen atoms have been omitted for clarity.

Table 2-1. Summary of X-ray Data Collection and Refinement.^a

	16	17-1/4AHA	18-CH₂Cl₂	19-2CH₂Cl₂
Empirical formula	C ₃₃ H ₄₇ ClN ₆ NiO ₆	C _{30.50} H _{45.25} ClN _{7.25} NiO _{6.5}	C ₃₁ H ₄₅ Cl ₄ N ₇ NiO ₈	C ₅₈ H ₈₄ Cl ₈ N ₁₂ Ni ₂ O ₈
<i>M_r</i>	717.93	711.25	844.25	1478.39
Crystal system	triclinic	monoclinic	monoclinic	monoclinic
Space group	<i>P</i> -1	<i>C</i> 2/ <i>c</i>	<i>P</i> 2 ₁ / <i>c</i>	<i>P</i> 2 ₁ / <i>n</i>
<i>a</i> / Å	8.9810(2)	32.3396(8)	8.8221(2)	10.9123(2)
<i>b</i> / Å	10.9647(2)	11.4649(3)	20.0037(4)	18.9857(3)
<i>c</i> / Å	18.2657(4)	19.4692(3)	21.7170(4)	16.9677(3)
α /°	102.6548(12)	90	90	90
β /°	96.3498(11)	93.1236(14)	91.7754(11)	96.6495(10)
γ /°	93.1764(13)	90	90	90
<i>V</i> / Å ³	1738.34(6)	7207.9(3)	3830.66(14)	3491.68(10)
<i>Z</i>	2	8	4	2
<i>D_c</i> / Mg m ⁻³	1.372	1.312	1.464	1.406
<i>T</i> / K	150(1)	103(1)	150(1)	150(1)
Crystal size/ mm	0.38 × 0.30 × 0.28	0.20 x 0.20 x 0.15	0.38 × 0.38 × 0.33	0.38 × 0.30 × 0.25
μ / (mm ⁻¹)	0.687	0.644	0.842	0.904
2 θ max (°)	55.00	55.04	54.96	54.96
Completeness to θ (%)	97.9	99.5	99.2	99.8
Reflections collected	12170	15128	14723	15105
Independent reflections	7825	8259	8717	7984
<i>R</i> _{int}	0.0219	0.0401	0.0255	0.0200
Variable parameters	577	486	469	422
<i>R</i> 1 / <i>wR</i> 2 <i>b</i>	0.0491/0.1289	0.0620/0.1452	0.0636/0.1571	0.0432/0.1038
Goodness-of-fit (<i>F</i> ²)	1.043	1.040	1.042	1.081
$\Delta\rho$ max/min / e Å ⁻³	0.758/-0.778	0.790/-0.626	0.783/-1.250	0.499/-0.530

^aDiffractometer: Nonius KappaCCD; Radiation used: Mo K α (λ = 0.71073 Å). *bR*1 = $\sum ||F_o| - |F_c| || / \sum |F_o|$; *wR*2 = $[\sum [w(F_o^2 - F_c^2)^2] / [\sum (F_o^2)^2]]^{1/2}$, where $w = 1/[\sigma^2(F_o^2) + (aP)^2 + bP]$.

Table 2-2. Selected Bond Distances (Å) and Angles (°).

	16	17-1/4AHA	18-CH₂Cl₂	19-2CH₂Cl₂
Ni(1)-O(1)	2.0162(18)	2.018(2)	2.177(2)	
Ni(1)-O(2)	2.0183(17)	2.058(2)		
Ni(1)-N(2)	2.1509(19)	2.137(3)	2.151(3)	2.1998(19)
Ni(1)-N(3)	2.0762(19)	2.076(3)	2.055(3)	2.0648(19)
Ni(1)-N(4)	2.154(2)	2.134(3)	2.164(3)	2.2267(19)
Ni(1)-N(6)	2.061(2)	2.048(3)	2.042(3)	2.038(2)
Ni(1)-N(7)			2.049(3)	
Ni(1)-Cl(1)				2.4284(6)
Ni(1)-Cl(1)#1				2.4485(6)
O(1)-Ni(1)-O(2)	90.94(8)	81.86(10)		
O(1)-Ni(1)-N(6)	172.86(8)	94.53(10)	90.23(12)	
O(2)-Ni(1)-N(6)	95.76(8)	174.68(10)		
O(1)-Ni(1)-N(3)	89.89(8)	178.78(10)	176.14(10)	
O(2)-Ni(1)-N(3)	178.63(7)	99.35(11)		
N(6)-Ni(1)-N(3)	83.46(8)	84.26(11)	85.97(13)	85.13(8)
O(1)-Ni(1)-N(2)	91.27(7)	99.44(11)	99.80(10)	
O(2)-Ni(1)-N(2)	99.02(7)	89.69(10)		
N(6)-Ni(1)-N(2)	90.13(7)	87.04(11)	88.72(11)	88.00(7)
N(3)-Ni(1)-N(2)	79.86(7)	80.67(11)	80.84(11)	79.27(7)
O(1)-Ni(1)-N(4)	88.86(8)	100.25(12)	98.42(10)	
O(2)-Ni(1)-N(4)	99.99(8)	91.27(10)		
N(6)-Ni(1)-N(4)	87.55(8)	93.24(11)	89.12(11)	90.16(7)
N(3)-Ni(1)-N(4)	81.12(8)	79.68(11)	80.84(11)	79.58(7)
N(2)-Ni(1)-N(4)	160.98(8)	160.22(11)	161.66(11)	
N(6)-Ni(1)-N(7)			179.59(13)	
N(7)-Ni(1)-N(3)			94.09(12)	
N(7)-Ni(1)-N(2)			90.89(11)	
N(7)-Ni(1)-N(4)			91.29(11)	
N(7)-Ni(1)-O(1)			89.71(11)	
N(6)-Ni(1)-Cl(1)				97.34(6)
N(3)-Ni(1)-Cl(1)				177.53(6)
N(2)-Ni(1)-Cl(1)				100.65(5)
N(4)-Ni(1)-Cl(1)				100.48(5)

Table 2-2. continued

N(6)-Ni(1)-Cl(1)#1	177.63(6)
N(3)-Ni(1)-Cl(1)#1	93.76(6)
N(2)-Ni(1)-Cl(1)#1	89.74(5)
N(4)-Ni(1)-Cl(1)#1	91.70(5)
Cl(1)-Ni(1)-Cl(1)#1	83.77(2)
Ni(1)-Cl(1)-Ni(1)#1	96.23(2)

Solution Conductivity Properties. The acetoacetonato complex **16** and the hydroxamato complex **17** both are 1:1 electrolytes in CH₃CN, as determined by variable concentration conductance measurements.²¹ Onsager plots for these complexes (Figure 2-4) exhibit slopes similar to the 1:1 standard Me₄NClO₄, and a notably different slope than that exhibited by [(bnpapa)Ni(ClO₄)(CH₃CN)](ClO₄)₂ (**18** (Figure 2-3(top)) or [(bnpapaNi)₂(μ-Cl)₂](ClO₄)₂ (**19**, Figure 2-3(bottom)), both of which are 1:2 electrolyte species in CH₃CN.

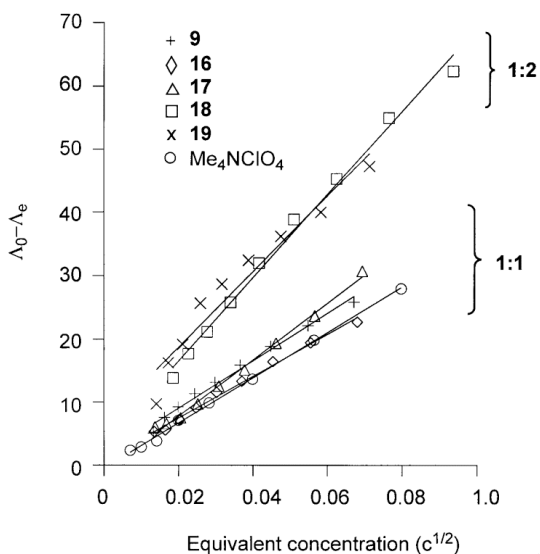


Figure 2-4. Onsager plots of the solution conductivity properties of **9**, **16-19**, and the 1:1 standard Me₄NClO₄ in CH₃CN at 22(1) °C.

^1H NMR Spectra. The ^1H NMR features of analytically pure $[(\text{bnpapa})\text{Ni}(\text{CH}_3\text{C}(\text{O})\text{CHC}(\text{O})\text{CH}_3)]\text{ClO}_4$ (**16**) and $[(\text{bnpapa})\text{Ni}(\text{ONHC}(\text{O})\text{CH}_3)]\text{ClO}_4$ (**17**) in CD_3CN at $22(1)^\circ\text{C}$ in the region of 20-80 ppm are shown in Figure 2-5(b) and (c). These are compared to the ^1H NMR spectral features of the O_2 -sensitive enolate complex $[(\text{bnpapa})\text{Ni}(\text{PhC}(\text{O})\text{C}(\text{OH})\text{C}(\text{O})\text{Ph})]\text{ClO}_4$ (**14**, Figure 2-5(a)). The resonances in the 20-80 ppm region include those of pyridyl β -H ring protons and a portion of the benzylic proton resonances.²⁰ The ^1H NMR spectra of **14** and **16** (Figure 2-5(a) and (b)) are similar, both having a more complicated appearance than that of the hydroxamato compound **17**. Based on the conductivity data presented above for the air stable **16** and **17**, which are both 1:1 electrolyte species in acetonitrile, the greater complexity of the ^1H NMR spectrum of **16**, relative to the spectral features of **17**, is not due to the formation of multinuclear species in solution. ^2H NMR studies of analogs of **14**, **16**, and **17** supported by a version of the bnpapa chelate ligand (Figure 2-6) having deuterium atoms at the

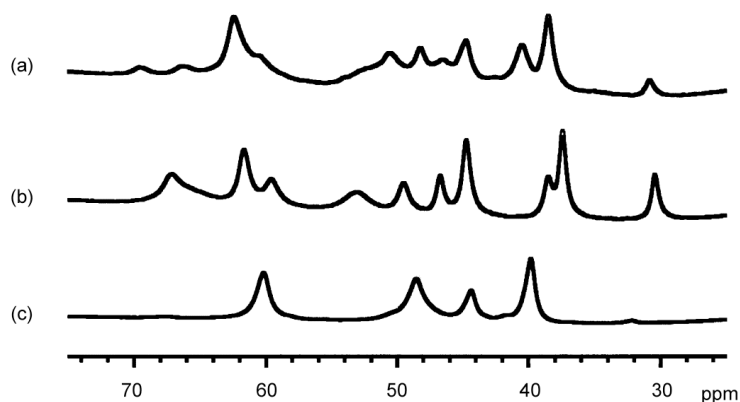


Figure 2-5. ^1H NMR spectral features of (a) **14**, (b) **16**, and (c) **17** in the region of 20-80 ppm. Spectra obtained in CD_3CN at $22(1)^\circ\text{C}$.

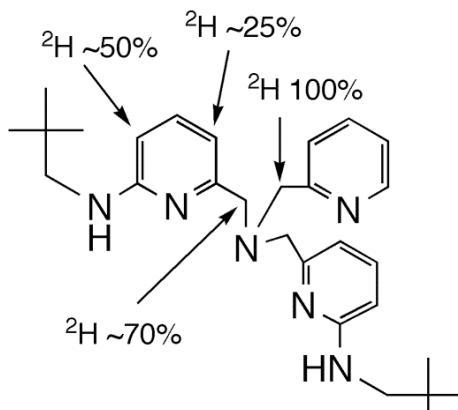


Figure 2-6. Positions of deuteration in bnpapa ligand used for ^2H NMR investigations. The ^2H substitution is present in both neopentyl-appended pyridyl donors.

benzylic positions, as well as partial deuteration of the β -H positions of the neopentylamine-appended pyridyl rings, indicated the presence of three unique benzylic proton resonances for **14** and **16** in the region of 165-175 ppm. This is consistent with no plane of symmetry within the cation.²⁰ However, **17** exhibits only one benzylic proton resonance in the same region, which is consistent with the presence of a plane of symmetry containing the unsubstituted pyridyl donor and the hydroxamato ligand. The factors that govern the subtle differences in solution structure of the cationic portions of **14**, **16**, and **17** are not entirely clear, but appear to relate to the chelate ring size of the *O,O*-donor ligand coordinated to the Ni(II) center. Specifically, the compounds having a six-membered chelate *O,O*-donor lack a plane of symmetry in the solution form of the cation. We note that the 1:2 electrolyte compounds [(bnpapa)Ni(ClO₄)(CH₃CN)](ClO₄)₂ (**18**) or [(bnpapaNi)₂(μ -Cl)₂](ClO₄)₂ (**19**) both exhibit ^1H NMR spectra similar to **17** wherein an effective plane of symmetry renders the two neopentylamine-appended

pyridyl donors equivalent in solution (Figure 2-7). Ni(II) carboxylate complexes of the general formula $[(\text{bnpapa})\text{Ni}(\text{O}_2\text{CR})]\text{ClO}_4$ ($\text{R} = \text{Ph}$, $(\text{CH}_2)_2\text{SCH}_3$, and H) also exhibit ^1H NMR spectra that are generally similar to the spectrum found for the hydroxamato complex **17**.¹⁷ In terms of comparing chelate ligand environments, the mononuclear Ni(II) complexes $[(6\text{-Ph}_2\text{TPA})\text{Ni}(\text{PhC}(\text{O})\text{C}(\text{OH})\text{C}(\text{O})\text{Ph})]\text{ClO}_4$ (**2**) and $[(6\text{-Ph}_2\text{TPA})\text{Ni}(\text{RC}(\text{O})\text{CHC}(\text{O})\text{R})]\text{ClO}_4$ ($\text{R} = \text{Ph}$, CH_3) exhibit spectra which indicate the presence of a plane of symmetry within the cation.^{15,16} Thus, the bnpapa-ligated Ni(II) six-membered ring enolate complexes **14** and **16** exhibit unique solution ^1H NMR properties relative to their hydrophobic analogs. Based on the structural and solution features of the air stable acetoacetonato complex **16**, and the similarity of the ^1H NMR spectrum of this complex to the spectrum of $[(\text{bnpapa})\text{Ni}(\text{PhC}(\text{O})\text{C}(\text{OH})\text{C}(\text{O})\text{Ph})]\text{ClO}_4$ (**14**), we propose that the O_2 -reactive enolate complex **14** has a structure that is similar to the analog supported by 6- Ph_2TPA (Figure 2-8), but is distorted such that no plane of symmetry relates the neopentylamine pyridyl donors in the solution form of the cation.

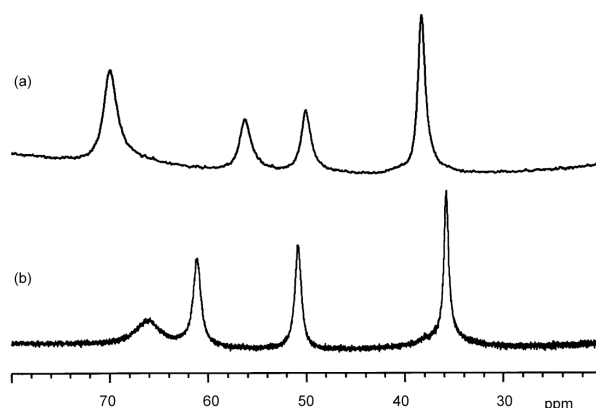


Figure 2-7. ^1H NMR spectral features of (a) **18** and (b) **19**, in the region of 20-80 ppm. Spectra obtained in CD_3CN at $22(1)^\circ\text{C}$.

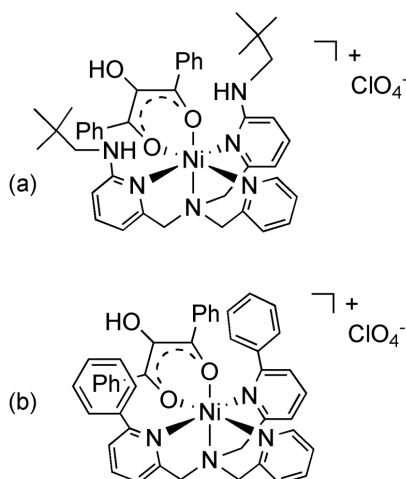
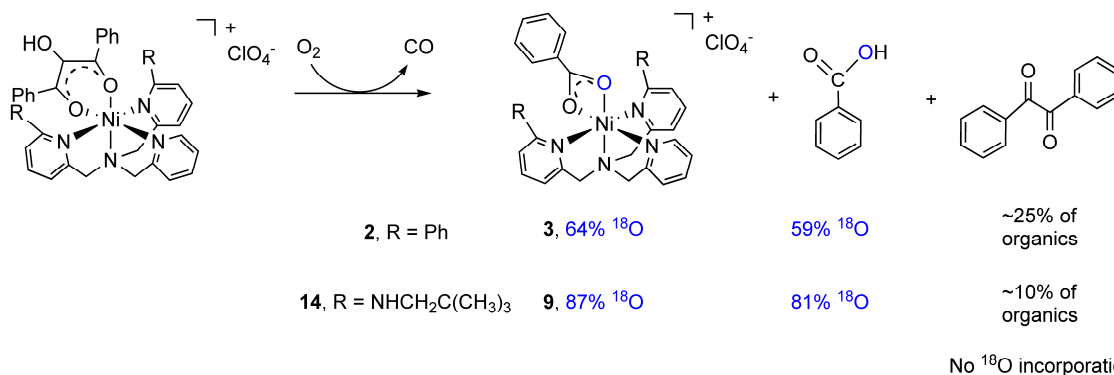


Figure 2-8. (a) Proposed structure of $[(\text{bnpapa})\text{Ni}(\text{PhC}(\text{O})\text{C}(\text{OH})\text{C}(\text{O})\text{Ph})]\text{ClO}_4$ (**14**). (b) Structure of $[(6\text{-Ph}_2\text{TPA})\text{Ni}(\text{PhC}(\text{O})\text{C}(\text{OH})\text{C}(\text{O})\text{Ph})]\text{ClO}_4$ (**2**) as determined by X-ray crystallography.³

Reaction of 14 with O₂. Exposure of a CH₃CN solution of **14** to O₂ results in an immediate color change from deep orange/red to yellow. CO production in this reaction was identified qualitatively using the PdCl₂ method.²⁴ The inorganic and organic products of the reaction were separated by column chromatography and identified (Scheme 2-3). One equivalent of benzoic acid is generated along with a small amount of benzil (PhC(O)C(O)Ph; ratio of benzoic acid to benzil is ~90:10) and a trace amount of the ester PhC(O)OCH₂C(O)Ph, the latter of which was identified via independent synthesis.²⁵ The reaction leading to ester formation will be described elsewhere. The monobenzoate complex $[(\text{bnpapa})\text{Ni}(\text{O}_2\text{CPh})]\text{ClO}_4$ (**9**) is produced in nearly quantitative yield in the



Scheme 2-3. Major products identified in reaction of **14** and **2** with O_2 ; results of reactions performed using $^{18}\text{O}_2$.

reaction leading to ester formation will be described elsewhere. The monobenzoate complex $[(\text{bnpapa})\text{Ni}(\text{O}_2\text{CPh})]\text{ClO}_4$ (**9**) is produced in nearly quantitative yield in the reaction, with a trace amount of a second Ni(II) complex, $[(\text{bnpapa})\text{Ni}(\text{PhC}(\text{O})\text{C}(\text{O})\text{CHC}(\text{O})\text{Ph})]\text{ClO}_4$ (**15**), being identified by mass spectrometry. The production of **15** is related to the presence of the ester $\text{PhC}(\text{O})\text{OCH}_2\text{C}(\text{O})\text{Ph}$ in the reaction and will be discussed elsewhere. Use of $^{18}\text{O}_2$ in the reaction with **14** produces benzoic acid with 81% ^{18}O incorporation in one oxygen atom position. No ^{18}O incorporation was found in benzil or the ester $\text{PhC}(\text{O})\text{OCH}_2\text{C}(\text{O})\text{Ph}$, as determined by GC-MS. Mass spectral analysis of the Ni(II) products indicated that the benzoate complex **9** had 87% ^{18}O incorporation in one oxygen atom of the benzoate ligand. No ^{18}O incorporation was found in **15**. We note that the level of ^{18}O incorporation for the reaction involving **14** is slightly higher than that reported for the Ni(II)-ARD enzymatic reaction (77.5%).²⁸

The work-up procedure used to isolate the organic and inorganic products of the reaction of **14** with O₂ is slightly different in terms of solvents used from the procedure that we previously reported for identification of the products of the reaction of [(6-Ph₂TPA)Ni(PhC(O)C(OH)C(O)Ph)]ClO₄ (**2**) with O₂.¹⁶ The new conditions are more amenable to the isolation of free benzoic acid in the reaction mixture. Therefore, the reaction involving **2** was repeated under conditions identical with those employed for [(bnpapa)Ni(PhC(O)C(OH)C(O)Ph)]ClO₄ (**14**), with the results shown in Scheme 2-3. CO production was again identified qualitatively using the PdCl₂ method.²⁴ In this reaction a ~75:25 mixture of benzoic acid and benzil is produced, along with a trace amount of the ester PhC(O)OCH₂C(O)Ph. The Ni(II)-containing products are [(6-Ph₂TPA)Ni(O₂CPh)]ClO₄ (**3**) and a trace amount of [(6-Ph₂TPA)Ni(PhC(O)C(O)CHC(O)Ph)]ClO₄ (**20**).^{16,17} Use of ¹⁸O₂ in the reaction with **2** yielded benzoic acid with 59% ¹⁸O incorporation in one oxygen atom position, and the benzoate complex **3** having 64% incorporation in one oxygen atom. We note that the level of isotope incorporation in **3** is slightly higher than previously reported (~50%), but is similar to that found for the O₂ reaction of the salt [Me₄N][PhC(O)C(OH)C(O)Ph], which decomposes upon reaction with ¹⁸O₂ to give [Me₄N][O₂CPh] and benzoic acid (~65% incorporation of one ¹⁸O into carboxylate group) and CO. Thus, the reaction involving **2** gives a mixture of organic products (benzoic acid and benzil), but with a similar level of ¹⁸O incorporation to that found for the O₂ reaction of [Me₄N][PhC(O)C(OH)C(O)Ph].

Overall, the studies outlined above revealed two interesting differences in the O₂ reactivity of [(bnpapa)Ni(PhC(O)C(OH)C(O)Ph)]ClO₄ (**14**) and [(6-Ph₂TPA)Ni(PhC(O)C(OH)C(O)Ph)]ClO₄ (**2**). First, the O₂ reaction involving the bnpapa-ligated complex **14** produces less of the side product benzil. Second, the reaction involving **14** has a higher level of ¹⁸O incorporation in the benzoic acid/benzoate products. These combined results provide evidence that the chelate ligand environment is influencing the aliphatic carbon-carbon bond cleavage reaction pathway.

Comparison of the Secondary Environments of bnpapa- and 6-Ph₂TPA-ligated Ni(II) Complexes. To date, we have structurally characterized four bnpapa- and thirteen 6-Ph₂TPA-ligated mononuclear Ni(II) complexes. Shown in Tables 2-3 and 2-4 are bond distances and angles involving the neopentyl-appended pyridyl donors in the bnpapa complexes and the phenyl-appended pyridyl donors in the 6-Ph₂TPA derivatives. Several conclusions can be drawn from comparison of the microenvironments in these two families of complexes. First, the neopentylamine amine-appended pyridyl donors in the bnpapa ligand, which have a substituent that is more electron donating and less sterically demanding relative to the phenyl substituents of the 6-Ph₂TPA ligand, have slightly shorter Ni-N distances (overall average of bnpapa complexes 2.14 Å; 6-Ph₂TPA complexes 2.22 Å). There is also a more linear N-Ni-N bond angle (overall average of bnpapa complexes 161°; 6-Ph₂TPA complexes 154°) between the substituted pyridyl groups. Second, the phenyl-appended pyridyl donors of 6-Ph₂TPA exhibit more variation in terms of Ni-N distances (~0.12 Å) in response to the presence of different exogenous ligands. This is not surprising in that aryl-appended pyridyl donors of chelate ligands

have been shown to fully dissociate from a metal center in response to exogenous ligand coordination.²⁹ Third, the microenvironment of bnpapa-ligated complexes is more compact, as determined by comparison of the distance between the two neopentylamine nitrogen atoms (~5.6 Å) versus that of the ipso carbons of the phenyl appendages of 6-Ph₂TPA (~6.4 Å).

Table 2-3. Structural Properties of bnpapa-ligated Mononuclear Ni(II) Complexes.

Complex	N(2)-Ni-N(4) (°) ^a	Ni-N(2), Ni-N(4) (Å) ^a	N(H)...N(H) (Å)	Ref.
[(bnpapa)Ni(ClO ₄)(CH ₃ CN)]ClO ₄	161.66(11)	2.151(3), 2.164(3)	5.7	this work
[(bnpapa)Ni(OHNC(O)CH ₃)]ClO ₄	160.22(11)	2.137(3), 2.134(3)	5.5	this work
[(bnpapa)Ni(CH ₃ C(O)CHC(O)CH ₃)]ClO ₄	160.98(8)	2.1509(19), 2.154(2)	5.6	this work
[(bnpapa)Ni(O ₂ Ph)]ClO ₄ ^b	161.78(12)	2.125(3), 2.136(3)	5.6	17

^aN(2) and N(4) are the neopentylamine-appended pyridyl donors of the bnpapa ligand. ^bData reported for one of two crystalline forms of the complex that were previously reported.

Table 2-4. Structural Properties of 6-Ph₂TPA-ligated Mononuclear Ni(II) Complexes.

Complex	N(3)-Ni-N(4) (°) ^a	Ni-N(3), Ni-N(4) (Å) ^a	C(Ph)...C(Ph) (Å) ^b	Ref.
[(6-Ph ₂ TPA)Ni(CH ₃ CN)(CH ₃ OH)](ClO ₄) ₂	158.59(16)	2.218(5), 2.200(5)	6.3	20
[(6-Ph ₂ TPA)Ni(OHNC(O)CH ₃)]ClO ₄	147.19(7)	2.229(2), 2.263(2)	6.4	20
[(6-Ph ₂ TPA)Ni(CH ₃ C(O)CHC(O)CH ₃)]ClO ₄	150.41(8)	2.217(2), 2.221(2)	6.4	16
[(6-Ph ₂ TPA)Ni(PhC(O)C(O)CHC(O)Ph)]ClO ₄	158.40(11)	2.209(3), 2.333(3)	6.5	16
[(6-Ph ₂ TPA)Ni(PhC(O)C(OH)C(O)Ph)]ClO ₄	157.04(8)	2.271(2), 2.323(2)	6.6	15
[(6-Ph ₂ TPA)NiCl(CH ₃ CN)]ClO ₄	157.67(10)	2.081(3), 2.213(2)	6.4	20
[(6-Ph ₂ TPA)Ni(O ₂ CPh)]ClO ₄	149.83(6)	2.1458(16), 2.234(16)	6.2	16
[(6-Ph ₂ TPA)Ni(O ₂ CPh)(H ₂ O)]ClO ₄	158.28(10)	2.216(2), 2.241(2)	6.4	17
[(6-Ph ₂ TPA)Ni(O ₂ C(CH ₂) ₂ SCH ₃)]ClO ₄	141.57(10)	2.233(3), 2.193(3)	6.3	17
[6-Ph ₂ TPA)Ni(O ₂ (CH ₂) ₂ SCH ₃)(H ₂ O)]ClO ₄	159.33(12)	2.240(3), 2.186(3)	6.3	17
[(6-Ph ₂ TPA)Ni(O ₂ CCH ₂ SCH ₃)]ClO ₄	148.73(8)	2.198(2), 2.165(2)	6.3	17
[(6-Ph ₂ TPA)Ni(O ₂ CCH ₂ SCH ₃)(H ₂ O)]ClO ₄	150.97(7)	2.1884(17), 2.2050(17)	6.4	17
[(6-Ph ₂ TPA)Ni(O ₂ CH)(H ₂ O)]ClO ₄	158.42(11)	2.194(3), 2.218(3)	6.3	17

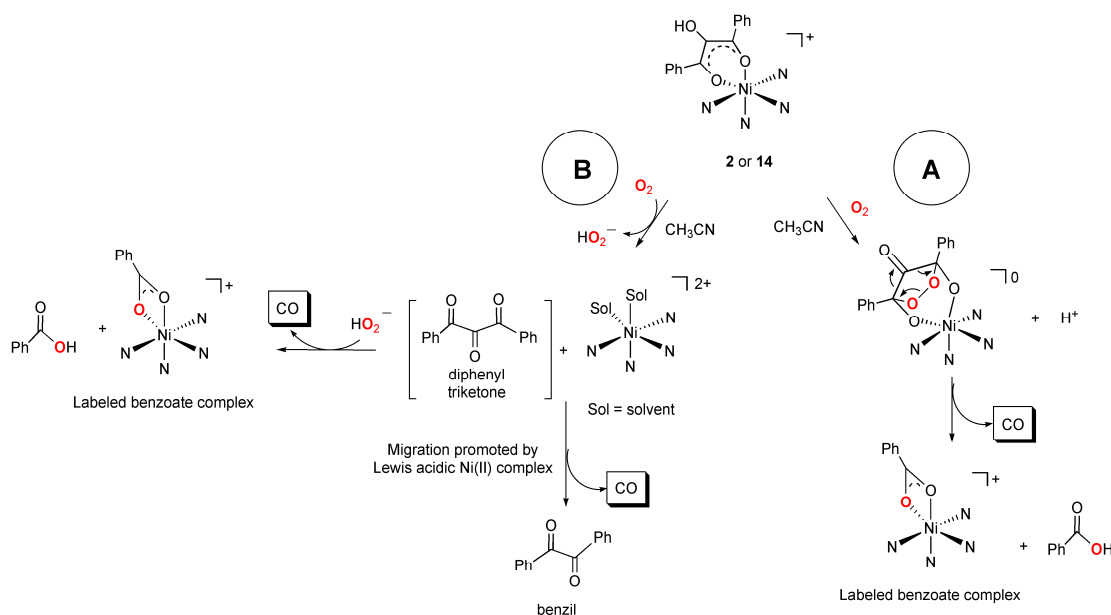
^aN(3) and N(4) are the phenyl-appended pyridyl donors of the 6-Ph₂TPA ligand. ^b*Ipsa* carbon atoms of phenyl appendages.

Discussion

As shown in Scheme 2-1, a key issue in the chemistry of acireductone dioxygenases is how the coordination mode of the acireductone substrate may influence the reaction with O₂. Pochapsky and coworkers have suggested, on the basis of NMR experiments, that differences in the secondary environment in Ni(II)- versus Fe(II)-containing ARD enzyme may be responsible for inducing different coordination modes of the acireductone substrate.¹ Specifically, in Ni(II)-ARD the side chain of the tryptophan residue is positioned such that the binding pocket for the acireductone is smaller than that found in Fe(II)-ARD. This is proposed to induce the formation of a six-membered chelate ring structure, which leads to 1,3-dioxygenolytic bond cleavage and CO production. We note that in both Ni(II)- and Fe(II)-containing acireductone dioxygenases an arginine residue is positioned within the active site, likely within hydrogen-bonding distance of the coordinated acireductone.¹

As an approach toward evaluating the influence of the secondary environment on the chemistry of Ni(II) complexes having an acireductone-type ligand, we have prepared and characterized [(6-Ph₂TPA)Ni(PhC(O)C(OH)C(O)Ph)]ClO₄ (**2**), which has a hydrophobic microenvironment, and [(bnpapa)Ni(PhC(O)C(OH)C(O)Ph)]ClO₄ (**14**), which contains a hydrogen-bond donor secondary environment. Based on the results of analytical and spectroscopic studies, we propose that the coordination mode of the acireductone-type ligand in these complexes is similar, with each having a six-membered chelate ring. However, the solutions structures of **2** and **14** differ in terms of the presence of a plane of symmetry that relates the modified pyridyl donors, with the hydrogen bond

donor pocket lacking such symmetry. Treatment of each complex with O₂ results in CO production and aliphatic carbon-carbon bond cleavage, with the major products in each reaction being a mononuclear Ni(II) benzoate complex, benzoic acid, and CO. In both reactions, the formation of the side product benzil was also identified. The yield of this byproduct is higher in the reaction involving [(6-Ph₂TPA)Ni(PhC(O)C(OH)C(O)Ph)]ClO₄ (**2**). Notably, this reaction exhibits a level of ¹⁸O incorporation in the benzoate/benzoic acid products that is ~20% lower than the reaction involving **14**. A possible rationale for the differences in product distribution and ¹⁸O incorporation between the reactions involving **2** and **14** could be that differing pathways for carbon-carbon bond cleavage may be operative as outlined in Scheme 2-4. Pathway A involves a cyclic peroxide resulting from two-electron oxidation of the coordinated acireductone analog. Carbon-carbon bond cleavage in this type of structure would produce two equivalents of benzoate/benzoic acid, with each product having one labeled oxygen atom if the reaction were performed using ¹⁸O₂. The production of benzoic acid in high yield in the reaction involving [(bnpapa)Ni(PhC(O)C(OH)C(O)Ph)]ClO₄ (**14**), and the observed high level of ¹⁸O incorporation, suggests that this pathway could possibly be operative for this reaction. However, the production of a small amount of benzil in the reaction involving **14** suggests that another type of reactivity is also occurring. For both complexes, we propose that benzil is generated via a pathway B type reaction sequence (Scheme 2-4). Specifically, two electron oxidation of the coordinated acireductone type ligand could produce 1,3-diphenyltriketone and a solvated Ni(II) complex of the chelate ligand. It has



Scheme 2-4. Possible reaction pathways for oxidative carbon-carbon bond cleavage in the Ni(II) enolate complexes **2** and **14**. The supporting chelate ligands have been omitted for clarity.

been previously shown that 1,3-diphenyltriketone will undergo phenyl or benzyl migration in the presence of a Lewis acids such as AlCl_3 to give benzil and carbon monoxide.³⁰ If this type of reaction pathway is occurring with the complexes described herein, the secondary environment of the $[(\text{bnpapa})\text{Ni}(\text{sol})_2]^{2+}$ and $[(6\text{-Ph}_2\text{TPA})\text{Ni}(\text{sol})_2]^{2+}$ cations (sol = solvent; e.g. CH_3CN) could influence interactions between the Ni(II) center and the 1,3-diphenyltriketone. For example, the larger pocket for the 6- Ph_2TPA -ligated Ni(II) center could be a key factor in promoting Lewis acid activation of a carbonyl moiety of the triketone, which is necessary for the migration reaction leading to benzil production.³⁰ This is a possible rationale for the higher amount of benzil produced in the reaction involving **2**. In terms of the lower level of ^{18}O incorporation found this reaction,

triketones are known to hydrate easily at the central carbonyl, and this may be a pathway for the introduction of unlabeled oxygen atoms into the benzoate/benzoic acid products.³¹ The observation that the salt $[\text{Me}_4\text{N}][\text{PhC}(\text{O})\text{CH}(\text{OH})\text{C}(\text{O})\text{Ph}]$ undergoes reaction with $^{18}\text{O}_2$ to produce a similar level of ^{18}O incorporation (~65%) in the benzoic acid product as is found for the reaction involving **2** suggests that both may proceed via a similar reaction pathway. ^{18}O incorporation into the carbon-carbon bond cleavage products could occur via reaction of the free triketone with hydroperoxide to form a five-membered cyclic peroxide species from which carbon-carbon bond cleavage could occur. Pochapsky has previously shown that treatment of 2,3,4-pentanetrione with H_2O_2 results in the formation of CO and two equivalents acetic acid.³² No isotope labeling studies were reported for this reaction.

The higher level of ^{18}O incorporation in the benzoate/benzoic acid products of the reaction involving **14** is interesting. Based on the results of our current experiments, it is unclear whether exclusively pathway B chemistry is occurring in the O_2 reactions of **14** and **2**, or whether a portion of the labeled product is generated via pathway A type reactivity. If exclusively pathway B chemistry is operative, an important distinction between the two supporting chelate ligand systems is that the bnpapa-ligated Ni(II) center may coordinate the hydroperoxide anion within the hydrogen bond donor pocket. The bnpapa chelate ligand has been previously used to stabilize mononuclear Zn(II) and Cu(II) hydroperoxide complexes.^{33,34} To date, similar complexes have not been reported using the 6-Ph₂TPA ligand. Thus, differences in the anion coordination properties

between the bnpapa and 6-Ph₂TPA-supported complexes could contribute to the observed differences in reactivity between **2** and **14**.

The results of this investigation have enabled the formulation of hypotheses regarding the reaction pathways of **2** and **14** with O₂ (Scheme 2-4) that can now be tested in individual control reactions. For example, we are now performing experiments to examine the reactivity of [(6-Ph₂TPA)Ni(CH₃CN)(CH₃OH)](ClO₄)₂³⁵ and [(bnpapa)Ni(ClO₄)(CH₃CN)]ClO₄ (**18**) with 1,3-diphenyltriketone and H₂O₂ to evaluate the efficacy of pathway B chemistry leading to the observed products. Additionally, we are pursuing kinetic studies of the reactions of complexes **2** and **14** with O₂, as well as examining the reactivity of [Me₄N][PhC(O)C(OH)C(O)Ph] with O₂ via computational methods to assess its reactivity relative to that found in the native C(1)-H acireductone substrate processed by the acireductone dioxygenases.³⁶

Conclusions

Using the hydrogen-bond donor ligand bnpapa, a mononuclear Ni(II) complex of the formula [(bnpapa)Ni(PhC(O)C(OH)C(O)Ph)]ClO₄ (**14**) has been isolated and characterized. Based on comparison of the spectroscopic features of this complex to those of air stable analogs, the structure of **14** is proposed to be generally similar to that previously reported for [(6-Ph₂TPA)Ni(PhC(O)C(OH)C(O)Ph)]ClO₄ (**2**). Notably, complexes **2** and **14** exhibit differences in their O₂-dependent aliphatic carbon-carbon bond cleavage reactivity in terms of the product mixture generated and the level of ¹⁸O incorporation in the benzoate/benzoic acid products. Two possible reaction pathways leading to ¹⁸O incorporation into the benzoate/benzoic acid products are proposed, with

one pathway involving the formation of a triketone and hydroperoxide anion. Comparison of the chemical features of several bnpapa- and 6-Ph₂TPA-ligated complexes suggests that differences in the pocket size and anion binding properties for these two ligand types may be key factors in producing the observed differences in reaction products.

References

1. Pochapsky, T. C.; Ju, T.; Dang, R.; Beaulieu, R.; Pagani, G. M.; OuYang, B. In *Metal Ions in Life Sciences*; Sigel, A., Sigel, H., Sigel, R. K. O., Eds.; Wiley-VCH: Weinheim, Germany, 2007; pp 473-498.
2. Ju, T.; Goldsmith, R. B.; Chai, S. C.; Maroney, M. J.; Pochapsky, S. S.; Pochapsky, T. C. *J. Mol. Biol.* **2006**, *393*, 823-834.
3. Mann, B. E.; Motterlini, R. *Chem. Commun.* **2007**, 4197-4208.
4. Motterlini, R.; Sawle, P.; Hammad, J.; Bains, S.; Alberto, R. Foresti, R.; Green, C. J. *FASEB J.* **2005**, *19*, 284-286.
5. Zhang, W-Q.; Atkin, A. J.; Thatcher, R. J.; Whitwood, A. C.; Fairlamb, I. J. S.; Lynam, J. M. *Dalton Trans.* **2009**, 4351-4358 and references cited therein.
6. Oka, T.; Simpson, F. J. *Biochem. Biophys. Res. Commun.* **1971**, *43*, 1-5.
7. Oka, T.; Simpson, F. J.; Krishnamurty, H. G. *Can. J. Microbiol.* **1972**, *18*, 493-508.
8. Hund, H. K.; Breuer, J.; Lingens, F.; Huttermann, J.; Kappl, R.; Fetzner, S. *Eur. J. Biochem.* **1999**, *263*, 871-878.
9. Tranchimand, S.; Ertel, G.; Gaydou, V.; Gaudin, C.; Tron, T.; Iacazio, G. *Biochimie* **2008**, *90*, 781-789.

10. Kooter, I. M.; Steiner, R. A.; Dijkstra, B. W.; van Noort, P. I.; Egmond, M. R.; Huber, M. *Eur. J. Biochem.* **2002**, *269*, 2971-2979.
11. Fusetti, F.; Schroter, K. H.; Steiner, R. A.; van Noort, P. I. *Structure* **2002**, *10*, 259-268.
12. Gopal, B.; Madan, L. L.; Betz, S. F.; Kossiakoff, A. A. *Biochemistry* **2005**, *44*, 193-201.
13. Schaab, M. R.; Barney, B. M.; Francisco, W. A. *Biochemistry* **2006**, *45*, 1035-1042.
14. Merkens, H.; Kappl, R.; Jakob, R. P.; Schmid, F. X.; Fetzner, S. *Biochemistry* **2008**, *47*, 12185-12196.
15. Szajna, E.; Arif, A. M.; Berreau, L. M. *J. Am. Chem. Soc.* **2005**, *127*, 17186-17187.
16. Szajna-Fuller, E.; Rudzka, K.; Arif, A. M.; Berreau, L. M. *Inorg. Chem.* **2007**, *46*, 5499-5507.
17. Szajna-Fuller, E.; Chambers, B. M.; Arif, A. M.; Berreau, L. M. *Inorg. Chem.* **2007**, *46*, 5486-5498.
18. Rudzka, K.; Arif, A. M.; Berreau, L. M. *Inorg. Chem.* **2008**, *47*, 10832-10840.
19. Armarego, W. L. F; Perrin, D. D. *Purification of Laboratory Chemicals*, 4th ed.; Butterworth-Heinemann: Boston, MA, 1996.
20. Szajna, E.; Dobrowolski, P. D.; Fuller, A. L.; Berreau, L. M. *Inorg. Chem.* **2004**, *43*, 3988-3997.

21. Allred, R. A.; McAlexander, L. H.; Arif, A. M.; Berreau, L. M. *Inorg. Chem.* **2002**, *41*, 6790-6801.
22. Wolsey, W. C. *J. Chem. Educ.* **1973**, *50*, A335-A337.
23. Plietker, B. *J. Org. Chem.* **2004**, *69*, 8287-8296.
24. Allen, T. H.; Root, W. S. *J. Biol. Chem.* **1955**, *216*, 309-317.
25. (a) Ming, L.; Guilong, Z.; Lirong, W.; Huazheng, Y. *Synth. Comm.* **2005**, *35*, 493-501. (b) Liu, Z.; Chen, Z-C.; Zheng, Q-G. *Synthesis* **2004**, 33-36.
26. Otwinowski, Z.; Minor, M. *Methods Enzymol.* **1997**, *276*, 307-326.
27. Sheldrick, G. M. SHELXL-97, Program for the Refinement of Crystal Structures; University of Göttingen: Göttingen, Germany, 1997.
28. Wray, J. W.; Abeles, R. H. *J. Biol. Chem.* **1995**, *270*, 3147-3153.
29. Berreau, L. M. *Comm. Inorg. Chem.* **2007**, *28*, 123-171.
30. Roberts, J. D.; Smith, D. R.; Lee, C. C. *J. Am. Chem. Soc.* **1951**, *73*, 618-625.
31. Rubin, M. B.; Gleiter, R. *Chem. Rev.* **2000**, *100*, 1121-1164.
32. Dai, Y.; Pochapsky, T. C.; Abeles, R. H. *Biochemistry* **2001**, *40*, 6379-6387.
33. Wada, A.; Yamaguchi, S.; Jitsukawa, K.; Masuda, H. *Angew. Chem. Int. Ed.* **2005**, 5698-5701.
34. Fujii, T.; Yamaguchi, S.; Hirota, S.; Masuda, H. *Dalton Trans.* **2008**, 164-170.
35. Makowska-Grzyska, M. M.; Szajna, E.; Shipley, C.; Arif, A. M.; Mitchell, M. H.; Halfen, J. A.; Berreau, L. M. *Inorg. Chem.* **2003**, *42*, 7472-7488.
36. Borowski, T.; Bassan, A.; Siegbahn, P.E.M. *J. Mol. Struct. THEOCHEM* **2006**, *772*, 89-92.

CHAPTER 3

INFLUENCE OF WATER ON THE FORMATION OF O₂-REACTIVE DIVALENT
METAL ENOLATE COMPLEXES OF RELEVANCE TO ACIREDUCTONE
DIOXYGENASES¹**Abstract**

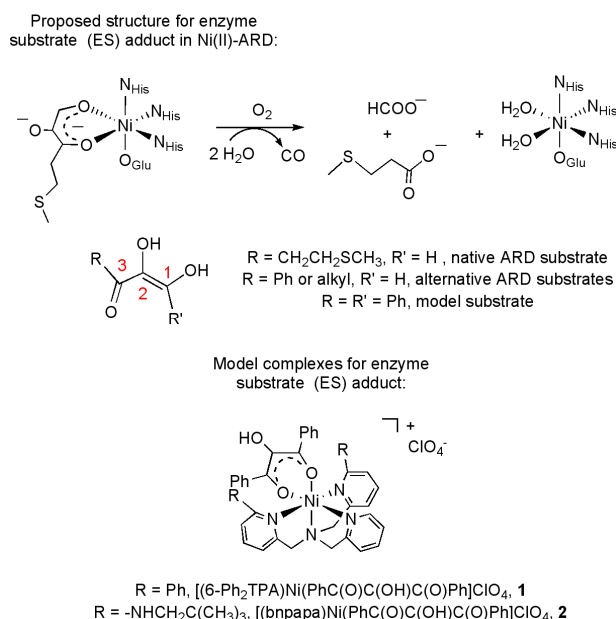
Reaction conditions were evaluated for the preparation of [(6-PhTPA)Ni(PhC(O)C(OH)C(O)Ph)]ClO₄ (**3**) and [(6-Ph₂TPA)Co(PhC(O)C(OH)C(O)Ph)]ClO₄ (**7**), two complexes of structural relevance to the enzyme/substrate (ES) adduct in Ni(II)- and Co(II)-containing forms of acireductone dioxygenase. The presence of water in reactions directed at the preparation of **3** and **7** was found to result in isomerization of the enolate precursor 2-hydroxy-1,3-diphenylpropane-1,3-dione to give the ester 2-oxo-2-phenylethylbenzoate. Performing synthetic procedures under dryer conditions reduced the amount of ester production and enabled the isolation of **3** in high yield. This complex was comprehensively characterized, including by X-ray crystallography. Using similar conditions for the 6-Ph₂TPACo-containing system, the amount of ester generated was only modestly affected, but the formation of a benzoate complex ([[(6-Ph₂TPA)Co(O₂CPh)]ClO₄, **10**) resulting from ester hydrolysis was

¹Coauthored by Katarzyna Grubel, Gajendrasingh K. Ingle, Amy L. Fuller, Atta M. Arif, and Lisa M. Berreau. Reproduced with permission from Dalton Transactions **2011**, 49, 1071-1081. Copyright 2011 The Royal Society of Chemistry.

prevented. The best preparation of **7** was found to involve dry conditions and short reaction times. The difference in water-dependent chemistry encountered in the (6-PhTPA)Ni- and (6-Ph₂TPA)Co-containing systems appears to relate to differences in the M-OH/H₂O chemistry of the metal/ligand combinations. The approach outlined herein toward determining appropriate reaction conditions for the preparation of **3** and **7** involved the preparation and characterization of several air-stable (6-PhTPA)Ni- and (6-Ph₂TPA)Co-containing analogue complexes having enolate, solvent, and benzoate ligands. These complexes were used as paramagnetic ¹H NMR standards for evaluation of reaction mixtures containing **3** and **7**.

Introduction

Acireductone dioxygenases (ARDs) catalyze dioxygenase-type oxidative reactions involving the cleavage of one or more aliphatic carbon-carbon bonds in an intermediate generated in the methionine salvage pathway.¹ With Ni(II) or Co(II) as the active site metal ion (Ni(II)-ARD or Co(II)-ARD), the cleavage reaction results in the formation of carboxylic acid products and CO (Scheme 3-1, top).¹ This reaction is proposed to proceed from an enzyme/substrate (ES) adduct having a coordinated enediolate moiety. To date, our laboratory has produced the only synthetic complexes of structural relevance to the ES adduct in Ni(II)-ARD using a C(1)-Ph containing analog of the native acireductone substrate (Scheme 3-1, middle).² These complexes, [(6-Ph₂TPA)Ni(PhC(O)C(OH)C(O)Ph)]ClO₄ (**1**) and [(bnpapa)Ni(PhC(O)C(OH)C(O)Ph)]ClO₄ (**2**) (Scheme 3-1, bottom), undergo reaction with O₂ to produce CO and carboxylate/carboxylic acid products in a reaction similar to



Scheme 3-1. Top: Reaction catalyzed by Ni(II)-ARD. Middle: Native and alternative substrates for Ni(II)-ARD; C(1)-phenyl-containing model substrate. Bottom: Structural drawings of **1** and **2**.

the Ni(II)-ARD enzymatic reaction.² However, the formation of a small amount of another organic product, benzil ($\text{PhC}(\text{O})\text{C}(\text{O})\text{Ph}$), in the reactions involving **1** and **2**, suggested the possibility of a “hydroperoxide” pathway for oxidative carbon-carbon bond cleavage reactivity involving triketone and OOH^- intermediates. This proposed pathway is supported by recent computational and mechanistic studies for the oxidative carbon-carbon bond cleavage reaction involving **1**.³ This mechanism differs from a radical pathway⁴ available for carbon-carbon bond cleavage in the native substrate for the enzyme and is consequence of the phenyl substituent at the C(1)-carbon. Thus, while our previous studies show that the C(1)-phenyl-containing acireductone analog introduces mechanistic differences in terms of its oxidative cleavage reactivity, it is a convenient

species for exploring bioinspired coordination chemistry of an acireductone-type molecule. We note that prior to our preparation and characterization of **1**, only a single complex having an acireductone type ligand had been previously characterized by X-ray crystallography.⁵ This complex, $[\text{Ru}(\text{bipy})_2(\mu\text{-C}_4\text{H}_4\text{O}_3)\text{Ru}(\text{bipy})_2](\text{PF}_6)_2$, was generated as a byproduct in an ethylene glycol-containing reaction mixture and no further chemistry of the complex was reported. The $[\text{C}_4\text{H}_4\text{O}_3]^{2-}$ acireductone-type ligand bridges the two ruthenium centers via two five-membered chelate rings. We have reported a similar coordination motif for the dianionic form of the C(1)-phenyl-containing acireductone analog in Ni(II) trinuclear and cluster complexes.^{6,7}

In further exploration of the coordination chemistry of the $[\text{PhC}(\text{O})\text{C}(\text{OH})\text{C}(\text{O})\text{Ph}]^-$ anion, we describe herein our efforts to prepare analogs of **1** containing a sterically less-demanding supporting chelating ligand, 6-PhTPA,⁸ or a different metal ion, Co(II). Notably, we have found that the preparation of $[(6\text{-PhTPA})\text{Ni}(\text{PhC}(\text{O})\text{C}(\text{OH})\text{C}(\text{O})\text{Ph})]\text{ClO}_4$ (**3**) and $[(6\text{-Ph}_2\text{TPA})\text{Co}(\text{PhC}(\text{O})\text{C}(\text{OH})\text{C}(\text{O})\text{Ph})]\text{ClO}_4$ (**7**) is complicated by water-dependent isomerization chemistry involving the C(1)-phenyl-containing acireductone analog which results in the formation of an ester. While we were able to modify the reaction conditions to successfully isolate and characterize **3**, the Co(II) chemistry is more complicated and includes ester hydrolysis reactivity. Our approach toward identifying the best conditions under which to generate **7** involved the preparation and characterization of three new 6-Ph₂TPA-supported Co(II) complexes that were used as paramagnetic ¹H NMR standards. Overall, these studies demonstrate that the conditions required for the preparation of

metal enolate complexes of relevance to the ES adduct in acireductone dioxygenases depend on several factors, including the presence of water in the reaction mixture.

Results and Discussion

Isomerization reactivity of a C(1)-phenyl containing acireductone analog and the preparation of [(6-PhTPA)Ni(PhC(O)C(OH)C(O)Ph)]ClO₄ (3**).** In our initial attempts to prepare the 6-PhTPA-supported Ni(II) complex **3**, we used reaction conditions identical to those which had enabled us to isolate the O₂-reactive [(6-Ph₂TPA)Ni(PhC(O)C(OH)C(O)Ph)]ClO₄ (**1**) in high yield (>90%).^{2a} These conditions are referred to herein as the “wet” conditions. Karl-Fischer titration of the CaH₂-dried acetonitrile typically used in this type of reaction indicated a concentration of [H₂O] ~3000 ppm. For the preparation of **3**, these conditions proved problematic, as a mixture of Ni(II) complexes was generated, as determined by ¹H NMR (Figure 3-1(a)), along with a significant amount of an isomerization product, 2-oxo-2-phenylethyl benzoate⁹ (~46% isolated yield based on dione; Scheme 3-2(b)). This ester, 2-oxo-2-phenylethyl benzoate, has been previously reported to form upon treatment of 2-hydroxy-1,3-diphenylpropane-1,3-dione with sodium bicarbonate in H₂O/methanol.¹⁰ In this prior report, a reaction pathway was proposed wherein the deprotonated keto form undergoes intramolecular attack of the C(2)-O⁻ moiety on an adjacent carbonyl (Scheme 3-3). This results in the formation of a new C-O bond and the cleavage of a C-C bond involving the C(2) center. We had not previously identified this rearrangement chemistry in preparing **1**. However, we have now reexamined the organic products remaining following the isolation of **1** and have found that some ester is generated in this reaction, but it is only approximately half

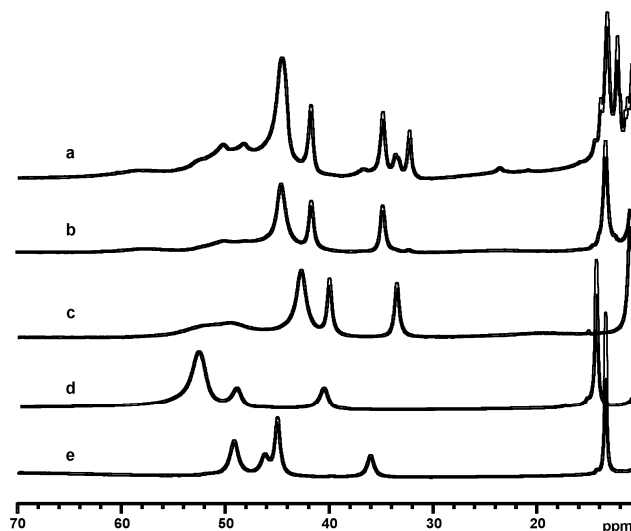
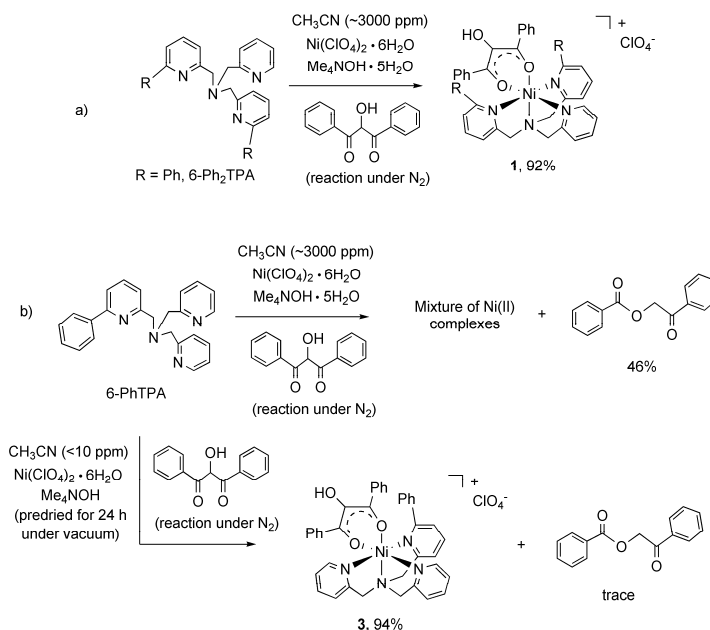
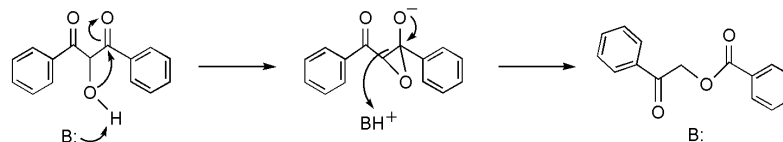


Figure 3-1. A region of the ^1H NMR spectra for (a) the reaction mixture produced upon treatment of 6-PhTPA with an equimolar amount of $\text{Ni}(\text{II})(\text{ClO}_4)_2 \cdot 6\text{H}_2\text{O}$ and slight stoichiometric excesses of $\text{Me}_4\text{NOH} \cdot 5\text{H}_2\text{O}$ and 2-hydroxy-1,3-diphenylpropan-1,3-dione in CH_3CN (~ 3000 ppm H_2O); (b) $[(6\text{-PhTPA})\text{Ni}(\text{PhC}(\text{O})\text{C}(\text{OH})\text{C}(\text{O})\text{Ph})]\text{ClO}_4$ (**3**); (c) $[(6\text{-PhTPA})\text{Ni}(\text{PhC}(\text{O})\text{CHC}(\text{O})\text{Ph})]\text{ClO}_4$ (**4**); (d) $[(6\text{-PhTPA})\text{Ni}(\text{CH}_3\text{CN})(\text{CH}_3\text{OH})](\text{ClO}_4)_2$ (**5**); (e) $[(6\text{-PhTPA})\text{Ni}(\text{O}_2\text{CPh})]\text{ClO}_4$ (**6**). Spectra b-e are for analytically pure compounds. The ^1H NMR spectra were collected in CD_3CN at ambient temperature and were referenced to the ^1H NMR signal of CD_2HCN (1.94 ppm).

of what is found in the 6-PhTPA system. We propose that this difference in ester formation for the 6-Ph₂TPA and 6-PhTPA systems might involve differences in interactions of the Ni(II) center in each complex with the reactants due to the modulation of the hydrophobic microenvironment by the differing chelate ligands. Specifically, factors such as the greater possible propensity of the 6-PhTPA complex to form dimeric structures, as well as electronic effects at the metal, and differing anion association constants, may be responsible for the observed differences in reactivity. Notably, we discovered that reducing the amount of water in the reaction mixture involving the 6-



Scheme 3-2. (a) Previously reported synthetic route for the preparation of **1**. (b) Synthetic routes for the preparation of **3**.



Scheme 3-3. Proposed pathway of isomerization of 1,3-diphenylpropane-1,3-dione to generate 2-oxo-2-phenylethylbenzoate.¹⁰

PhTPA-supported Ni(II) complex via predrying of the base and use of extra dry CH_3CN (<10 ppm H_2O) enables the isolation of **2** in high yield (94%, Scheme 3-2(b)). Additionally, only a trace amount of ester was detected in this reaction mixture. These combined results indicate that water plays a key role in this system in promoting the isomerization reactivity that results in ester formation, and that a lower amount of ester formation correlates with a higher yield of the desired enolate complex **3**. Complex **3**

(Figure 3-2) has a six-coordinate Ni(II) center with the longest Ni-N interaction being for the phenyl-substituted pyridyl donor (Ni(1)-N(4), 2.202(4) Å). This distance is slightly shorter than that found for the Ni-NPhPy bonds in **1** (Ni(1)-N(3) 2.271(2) Å, Ni(1)-N(4) 2.323(2) Å),^{2a} presumably due to reduced steric hindrance as a second phenyl-appended pyridyl donor is not present in **3**. The remaining bond distances/angles in this complex are similar to those found in **1**. The spectroscopic properties of **3** are also generally similar to those found for **1**. For example, both complexes form orange-brown solutions with λ_{max} at 393 (6800 M⁻¹cm⁻¹) and 399 (10300 M⁻¹cm⁻¹) nm, respectively.^{2b} The ¹H NMR features of **3** in the region of 70-10 ppm are shown in Figure 3-1(b) and collected in Table 3-1.

Prior ¹H NMR studies of 6-Ph₂TPA-ligated Ni(II) complexes have identified this region as containing pyridyl ring proton resonances that are sensitive to changes in ligation at the Ni(II) center.^{11,12} In order to perform spectral comparisons for 6-PhTPA-supported Ni(II) complexes, the air stable dibenzoylmethane-derived enolate complex

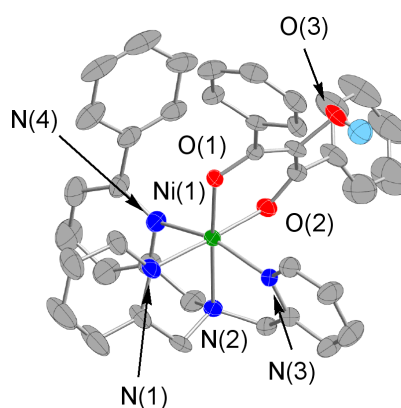


Figure 3-2. Thermal ellipsoid drawing of the cationic portion of **3**. Ellipsoids are drawn at the 50% probability level. Hydrogen atoms except the hydroxyl proton of the enolate ligand are not shown for clarity.

$[(6\text{-PhTPA})\text{Ni}(\text{PhC}(\text{O})\text{CHC}(\text{O})\text{Ph})]\text{ClO}_4$ (**4**, Figure 3-3(top)), the solvent-bound complex $(6\text{-PhTPA})\text{Ni}(\text{CH}_3\text{CN})(\text{CH}_3\text{OH})](\text{ClO}_4)_2$ (**5**, Figure 3-3(bottom)), and the benzoate complex $[(6\text{-PhTPA})\text{Ni}(\text{O}_2\text{CPh})]\text{ClO}_4$ (**6**) were prepared and characterized.

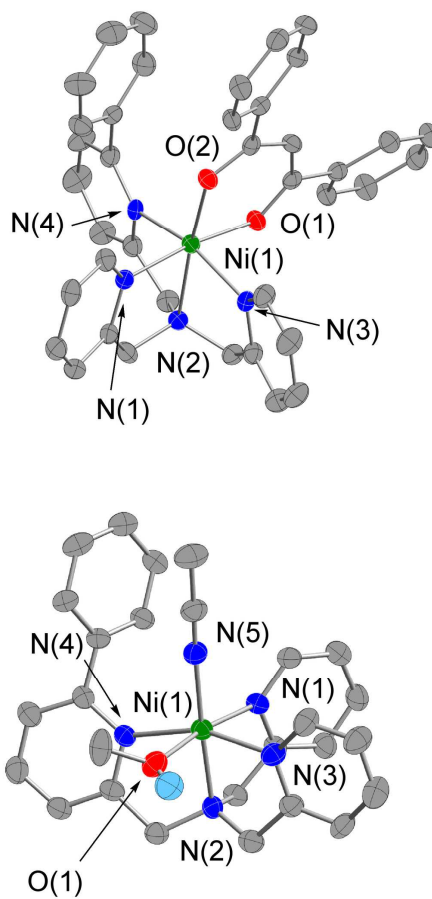


Figure 3-3. Thermal ellipsoid drawings of the cationic portions of **4** (top) and **5** (bottom). Ellipsoids are plotted at the 50% probability level. Hydrogen atoms, except the methanol proton of the coordinated methanol ligand in **5**, are not shown for clarity.

Table 3-1. ^1H NMR chemical shifts for **3-6** in CD_3CN at 298 K.

assignment	shift (ppm) ^a	$\Delta\nu_{1/2}(\text{Hz})^b$	rel area
[(6-PhTPA)Ni(PhC(O)C(OH)C(O)Ph)]ClO ₄ (3)			
α	150.0	<i>c</i>	<i>c</i>
β	41.6, 34.8	183, 172	1, 1
β'	44.5, 13.3	450, 179	2, 2
γ	<i>c</i>	<i>c</i>	<i>c</i>
γ'	10.6	91.6	<i>c</i>
CH ₂	57.7, 23.3, <i>c</i>	<i>c, c, c</i>	<i>c, c, c</i>
[(6-PhTPA)Ni(PhC(O)CHC(O)Ph)]ClO ₄ (4)			
α	148.6	<i>c</i>	<i>c</i>
β	43.8, <i>c</i>	355	<i>c, c</i>
β'	41.1, 34.8	183, 214	1, 1
γ	13.2	175	2
γ'	<i>c</i>	<i>c</i>	<i>c</i>
CH ₂	138.2, 51.0, 50.5	<i>c, c, c</i>	<i>c, c, c</i>
CH (dbm)	-13.1	256	1
[(6-PhTPA)Ni(CH ₃ CN)(CH ₃ OH)](ClO ₄) ₂ (5)			
α	150.0	<i>c</i>	<i>c</i>
β	52.8, <i>c</i>	543, <i>c</i>	<i>c, c</i>
β'	49.2, 40.8	484, 324	<i>c, 1</i>
γ	14.6	126	<i>c</i>
γ'	10.1	107	<i>c</i>
[(6-PhTPA)Ni(O ₂ CPh)]ClO ₄ (6)			
α	150.9	2922	1
β	46.3, 36.2	<i>c, 328</i>	<i>c, 1</i>
β'	49.3, 45.1	362, 244	2, <i>c</i>
γ	13.5	72	2
γ'	10.0	84	1
CH ₂	77.5, <i>c, c</i>	<i>c, c, c</i>	<i>c, c, c</i>

^aChemical shifts in ppm relative to the residual solvent peak of CHD_2CN (^1H , 1.94 (quintet) ppm). ^bLine widths are full width at a half-maximum. ^cCould not be determined.

Complexes **4** and **5** were investigated using single crystal X-ray crystallography. Details of the X-ray data collection are given in Table 3-2. Selected bond distances and angles for the complexes are shown in Table 3-3. Both **4** and **5** exhibit a pseudo-octahedral geometry with the longest Ni-N bond distance being for the phenyl-appended pyridyl donor. As is evident by comparison of the ^1H NMR spectra shown in Figure 3-1(b)-(e), complexes having a six-membered ring enolate ligand (Figure 3-1(b) and (c); **3** and **4**) exhibit generally similar ^1H NMR features that are clearly distinct from those exhibited by solvent (Figure 3-1(d), **5**) or benzoate-coordinated (Figure 3-1(e), **6**) compounds (Table 3-1). That being said, we note that all of the complexes exhibit a pattern of isotropically shifted resonances for the pyridyl ring protons with chemical shifts in the order $\alpha\text{-H} > \beta\text{-H} > \gamma\text{-H}$.¹¹

Having the family of complexes **3-6** fully characterized has enabled us to use ^1H NMR to examine the mixture of Ni(II) complexes in the “wet” reaction conditions, wherein a significant amount of ester is generated. As shown in Figure 3-1(a) it is evident that the desired Ni(II) enolate complex **2** is present, as resonances at 44.5, 41.6, 34.8, and 13.3 ppm are present. It is also clear that a Ni(II) solvent-coordinated complex, such as [(6-PhTPA)Ni(CH₃CN)(CH₃OH)](ClO₄)₂ (**5**), if present, is a very minor species. This suggests that all of the 6-PhTPA-ligated Ni(II) species in solution have one or more coordinated non-solvent ligands. A small amount of the Ni(II)-benzoate complex **6** may be present in the reaction mixture, as evidenced by signals at the 49.3 and 36.2 ppm. We note that preliminary O₂ reactivity studies indicate that complex **3** undergoes oxidative carbon-carbon bond cleavage upon exposure to oxygen to give products similar to those

Table 3-2. Summary of X-ray Data Collection and Refinement.

	3-CH₂Cl₂	4-Et₂O	5	8-0.5CH₃CN	10
Empirical formula	C ₄₀ H ₃₅ Cl ₃ N ₄ NiO ₇	C ₄₃ H ₄₃ ClN ₄ NiO ₇	C ₂₇ H ₂₉ Cl ₂ N ₅ NiO ₉	C ₄₆ H _{38.5} ClCoN _{4.5} O ₄	C ₃₇ H ₃₁ ClCoN ₄ O ₆
Formula weight	848.78	821.97	697.16	844.69	722.04
Crystal system	Monoclinic	Orthorhombic	Orthorhombic	Tetragonal	Monoclinic
Space group	Cc	Pcab	P2 ₁ 2 ₁ 2 ₁	I-4	P2 ₁ /c
a/ Å	23.2096(5)	16.0204(3)	9.8884(2)	34.4730(5)	11.0736(2)
b/ Å	15.9822(4)	19.2924(6)	10.8891(2)	34.4730(5)	24.5657(5)
c/ Å	11.9687(2)	25.0918(7)	28.1201(4)	13.5221(3)	12.18640(10)
α /°	90	90	90	90	90
β /°	117.2760(12)	90	90	90	100.8097(10)
γ /°	90	90	90	90	90
V /Å ³	3946.02(15)	7755.2(4)	3027.85(9)	16069.5(5)	3256.25(9)
Z	4	8	4	16	4
Dc / Mg m ⁻³	1.429	1.408	1.529	1.397	1.473
T / K	150(1)	150(1)	150(1)	150(1)	150(1)
Color	Orange	Orange	Purple	Red-Brown	Green
Crystal habit	Prism	Plate	Prism	Plate	Plate
Crystal size/ mm	0.25 x 0.23 x 0.20	0.38 x 0.38 x 0.10	0.33 x 0.25 x 0.20	0.35 x 0.35 x 0.13	0.35 x 0.23 x 0.10
Diffractionmeter	Nonius KappaCCD	Nonius KappaCCD	Nonius KappaCCD	Nonius KappaCCD	Nonius KappaCCD
μ / (mm ⁻¹)	0.749	0.627	0.878	0.550	0.664
2θ max /°	54.94	54.98	54.96	54.96	54.96
Reflections collected	8111	16226	6591	15365	14646
Independent reflections	8104	8868	6591	15360	7451
R _{int}	0.0445	0.0767	0.0000	0.0395	0.0374
Variable parameters	498	677	400	1060	566
R1 / wR2 (I > 0.0539 / 0.1320 2σ(I)) ^b	0.0539 / 0.1320	0.0552 / 0.1015	0.0654 / 0.1377	0.0638 / 0.1236	0.0385 / 0.0811
Goodness-of-fit (F2)	1.066	1.015	1.040	1.072	1.023
Δρ max/min / e Å ⁻³	0.972 / -0.684	0.452 / -0.465	0.699 / -0.976	0.475 / -0.586	0.337 / -0.512
Flack parameter	0.510(5)		-0.01(3)	0.371(16)	

^aRadiation used: Mo Kα (λ = 0.71073 Å). ^bR1 = $\sum ||F_o| - |F_c|| / \sum |F_o|$; wR2 = $[\sum [w(F_o^2 - F_c^2)^2] / [\sum (F_o^2)^2]]^{1/2}$ where w = 1/[σ²(F_o²) + (aP)² + bP].

Table 3-3. Selected bond lengths (Å) and angles (°).^a

	3-CH₂Cl₂	4-Et₂O	5	8-0.5CH₃CN	10
M-N(1)	2.048(4)	2.077(3)	2.089(5)	2.134(5)	2.1117(17)
M-N(2)	2.084(3)	2.101(3)	2.097(5)	2.135(5)	2.1773(17)
M-N(3)	2.122(4)	2.110(3)	2.090(5)	2.291(5)	2.1192(18)
M-N(4)	2.202(4)	2.149(2)	2.170(5)	2.285(5)	2.1437(17)
M-N(5)			2.055(5)		
M-O(1)	1.986(3)	1.997(2)	2.077(5)	2.029(4)	1.9695(14)
M-O(2)	1.998(3)	1.995(2)		1.989(4)	
O(1)-M-N(1)	92.31(13)	172.53(10)	171.61(18)	175.44(15)	100.38(6)
O(1)-M-N(2)	169.33(14)	90.38(9)	91.86(18)	95.84(16)	173.83(7)
O(1)-M-N(3)	92.78(13)	91.33(9)	88.37(19)	82.06(16)	108.72(6)
O(1)-M-N(4)	108.01(13)	85.18(9)	83.81(18)	96.88(16)	102.48(6)
O(1)-M-N(5)			90.4(2)		
O(1)-M-O(2)	90.84(12)	91.77(9)		90.30(15)	
O(2)-M-N(1)	173.30(14)	94.96(9)		93.99(17)	
O(2)-M-N(2)	94.72(14)	172.17(9)		171.34(17)	
O(2)-M-N(3)	89.15(13)	91.69(9)		99.88(17)	
O(2)-M-N(4)	89.34(14)	106.72(9)		105.54(16)	
N(1)-M-N(2)	83.13(15)	82.53(10)	82.77(18)	80.06(18)	77.04(7)
N(1)-M-N(3)	96.59(15)	85.24(10)	84.5(2)	98.68(18)	108.75(6)
N(1)-M-N(4)	84.06(15)	95.97(10)	101.40(18)	80.50(17)	127.56(7)
N(1)-M-N(5)			94.8(2)		
N(2)-M-N(3)	78.23(14)	80.73(10)	81.92(19)	75.03(18)	77.45(7)
N(2)-M-N(4)	81.20(15)	80.97(10)	79.13(19)		75.25(6)
N(2)-M-N(5)			177.2(2)		
N(3)-M-N(4)	159.18(14)	161.33(10)	159.22(19)		107.42(6)
N(3)-M-N(5)			96.43(19)		
N(4)-M-N(5)			102.82(19)		

^aEstimated standard deviations in the last significant figure are given in parentheses.

of [(6-Ph₂TPA)Ni(PhC(O)C(OH)C(O)Ph)]ClO₄ (**1**),^{2b} specifically the Ni(II) monobenzoate complex **6**, along with benzoic acid and benzil. Thus, the Ni(II)-benzoate

complex in the reaction mixture for the preparation of **3** could be due to oxidative decomposition of the sample. Alternatively, the 6-PhTPA-supported Ni(II) benzoate complex **6** might be formed via hydrolysis of the 2-oxo-2-phenylethylbenzoate ester generated in the reaction mixture. This hypothesis was evaluated via treatment of the solvent complex **5** with 2-oxo-2-phenylethylbenzoate in the presence of one equivalent of $\text{Me}_4\text{NOH}\cdot 5\text{H}_2\text{O}$ in CH_3CN . The outcome of this reaction indicated the formation of new Ni(II) species (as determined by ^1H NMR), but no ester hydrolysis (95% recovery of unaltered ester). Interestingly, performing the same reaction in the absence of the Ni(II) complex results in ester hydrolysis to give $\text{Me}_4\text{NO}_2\text{CPh}$ and $\text{PhC(O)CH}_2\text{OH}$. Thus, in the Ni(II)-containing reaction, hydroxide anion is unavailable for ester hydrolysis, presumably due to the formation of Ni-OH species, which apparently does not promote ester hydrolysis. Overall, this means that any Ni(II) benzoate complex **6** present in the reaction mixture shown in Figure 3-1(a) would be due to oxidative decomposition. Finally, we note that at this point we cannot identify species associated with resonances at 32.4 and 33.7 ppm in the “wet” reaction mixture (Figure 3-1(a)).

Co(II) Chemistry: The challenges in preparing [(6-Ph₂TPA)Co(PhC(O)C(OH)C(O)Ph)]ClO₄ (7). We were interested in preparing the Co(II) analog of **1** as it has been reported that reconstitution of *apo*-ARD with Co(II) produces an enzyme having >90% Ni(II)-ARD-type reactivity (cleavage to give CO and carboxylate products, Scheme 3-1(top)).¹³ Additionally, the ARD enzyme isolated from *K. pneumoniae* contains ~20% Co(II) (with Ni(II) being present in ~70% and Fe(II) ~10%).¹⁴ Our initial attempt to prepare [(6-Ph₂TPA)Co(PhC(O)C(OH)C(O)Ph)] ClO₄ (**7**)

involved following a procedure identical to that employed for the preparation of [(6-Ph₂TPA)Ni(PhC(O)C(OH)C(O)Ph)]ClO₄ (**1**) using the “wet” conditions. Specifically, equimolar amounts of 6-Ph₂TPA and Co(ClO₄)₂·6H₂O were combined with a slight stoichiometric excess of Me₄NOH·5H₂O and 2-hydroxy-1,3-diphenylpropane-1,3-dione in CH₃CN (~3000 ppm H₂O; Karl-Fischer titration) and the reaction mixture was stirred under N₂ for 16.5 h. We noted the rapid formation of a green color in this reaction mixture, which is significantly different from the orange-brown color that is found for [(6-Ph₂TPA)Ni(PhC(O)C(OH)C(O)Ph)]ClO₄ (**1**) and [(6-PhTPA)Ni(PhC(O)C(OH)C(O)Ph)]ClO₄ (**3**). The ¹H NMR spectral features of the green mixture are shown in Figure 3-4(a). To interpret this ¹H NMR data, we prepared and fully characterized (including assignment of ¹H NMR resonances) two new Co(II) complexes, the dibenzoylmethane derivative [(6-Ph₂TPA)Co(PhC(O)CHC(O)Ph)]ClO₄ (**8**) and the benzoate complex [(6-Ph₂TPA)Co(O₂CPh)]ClO₄ (**10**). Additionally, we investigated the ¹H NMR features of the previously reported [(6-Ph₂TPA)Co(CH₃CN)](ClO₄)₂·CH₃CN (**9**).

The cationic portions of **8** and **10** are shown in Figure 3-5. Details of the X-ray data collection are given in Table 3-2. Selected bond distances and angles for the complexes are shown in Table 3-3. The Co(II) center in **8** exhibits a distorted octahedral geometry. The bond distances involving the phenyl-appended pyridyl donors (N(3) and N(4)) are ~0.16 Å longer than the other Co-N distances. The Co(II)-O distances involving the enolate ligand differ by about ~0.03 Å, with the Co-O bond trans to the unsubstituted pyridyl donor being slightly longer. Similar to [(6-Ph₂TPA)Co(ONHC(O)CH₃)]ClO₄,¹⁵

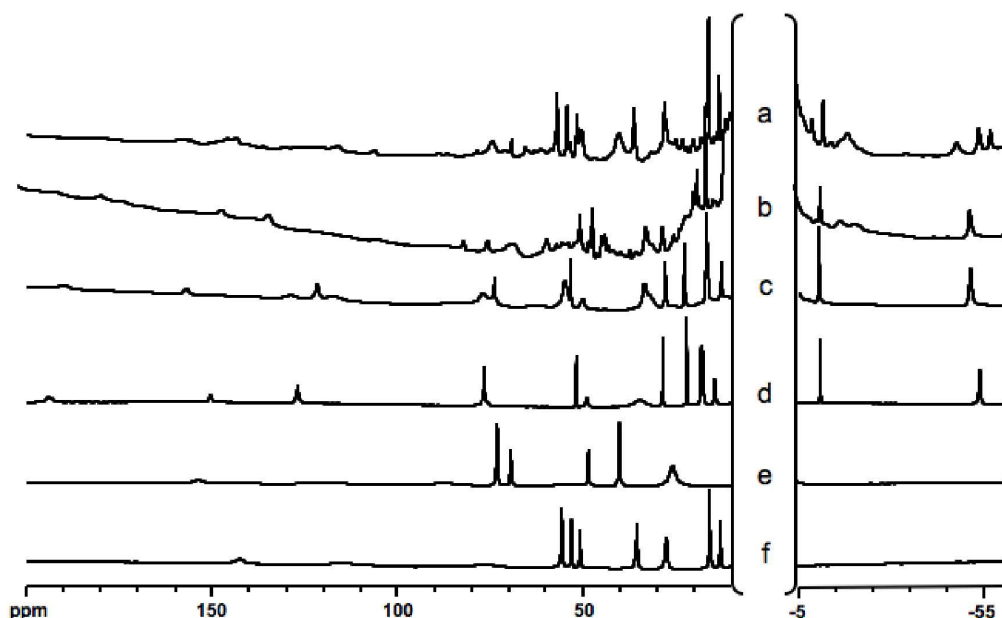


Figure 3-4. Regions of the ^1H NMR spectra of (a) the reaction mixture produced upon treatment of 6- Ph_2TPA with an equimolar amount of $\text{Co(II)(ClO}_4)_2 \cdot 6\text{H}_2\text{O}$ and slight stoichiometric excesses of $\text{Me}_4\text{NOH} \cdot 5\text{H}_2\text{O}$ and 2-hydroxy-1,3-diphenylpropan-1,3-dione in CH_3CN (~ 3000 ppm H_2O); (b) the reaction mixture generated using conditions identical to those employed for the preparation of **3** (predrying of base and solvent); (c) the reaction mixture produced upon predrying of base and solvent and shorter reaction time; (d) $[(6\text{-Ph}_2\text{TPA})\text{Co}(\text{PhC}(\text{O})\text{CHC}(\text{O})\text{Ph})]\text{ClO}_4$ (**8**); (e) $[(6\text{-Ph}_2\text{TPA})\text{Co}(\text{CH}_3\text{CN})](\text{ClO}_4)_2 \cdot \text{ClO}_4 \cdot \text{CH}_3\text{CN}$ (**9**); (f) $[(6\text{-Ph}_2\text{TPA})\text{Co}(\text{O}_2\text{CPh})]\text{ClO}_4$ (**10**). Spectra d-f are for analytically pure compounds. The ^1H NMR spectra were collected in CD_3CN at ambient temperature and were referenced to the ^1H NMR signal of CD_2HCN (1.94 ppm). The diamagnetic region of each spectrum is omitted to improve the clarity of the spectral comparison.

the bidentate anion is positioned in a hydrophobic sandwich between the phenyl appendages of the 6- Ph_2TPA ligand. The benzoate complex **10** exhibits monodentate coordination of the carboxylate ($\Delta_{\text{d}} = 0.8 \text{ \AA}$; $\Delta_{\theta} = 36.6^\circ$).¹⁶ The overall geometry of the Co(II) center is distorted trigonal bipyramial ($\tau = 0.77$; for a perfect trigonal bipyramid τ

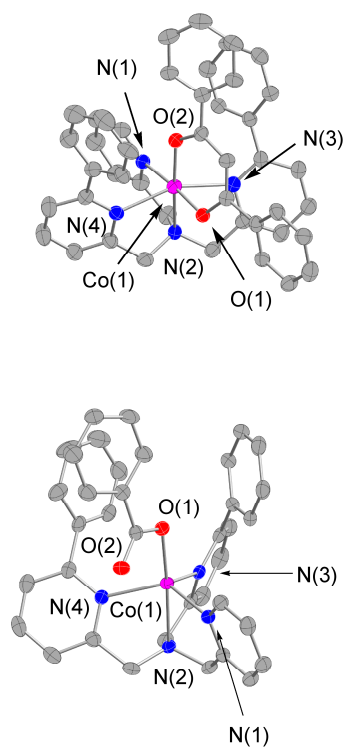


Figure 3-5. Thermal ellipsoid drawings of the cationic portions of **8** and **10**. Ellipsoids are drawn at the 50% probability level. Hydrogen atoms are not shown for clarity. Only one of two cations present in the asymmetric unit of **8** is shown.

$= 1$),¹⁷ with the carboxylate ligand in an axial position. A similar geometry was found for [(6-Ph₂TPA)Co(CH₃CN)](ClO₄)₂·CH₃CN (**9**) ($\tau = 0.89$). The solution magnetic moments for **8** and **10** were measured in CH₃CN at 298 K using the Evans method.¹⁸ The μ_{eff} values obtained for these complexes, 4.72 and 4.32 μB , respectively, are within the expected experimental range for high-spin Co(II) complexes.¹⁹ High-spin Co(II) complexes generally exhibit a ligand field transition in the range of 500-600 ppm. The intensity of this transition varies with the coordination number of the Co(II) center, with six-coordinate Co(II) complexes generally having $\epsilon < 50 \text{ M}^{-1}\text{cm}^{-1}$.²⁰

The absorption spectrum of the red-orange dibenzoylmethane complex **8** contains a band at 564 nm ($\epsilon = 77 \text{ M}^{-1}\text{cm}^{-1}$). Though the molar absorptivity value for the 564 nm band exceeds the threshold of $\epsilon < 50 \text{ M}^{-1}\text{cm}^{-1}$, ^1H NMR data for the complex (*vide infra*) suggest that the solution form of the complex has a six-coordinate Co(II) center. For the green benzoate complex **10** a ligand field transition is present at 590 nm ($49 \text{ M}^{-1}\text{cm}^{-1}$). This suggests an overall coordination number of six for the benzoate complex in CH_3CN . Assignments for the ^1H NMR resonances of **8-10** are given in Table 3-4.

Initial assignments were made on the basis of integrated intensity and T_1 values. Signals associated with the aryl and methylene hydrogens of the 6- Ph_2TPA ligand were confirmed using analog complexes prepared with the deuterated ligand analogs 6-($d_5\text{-Ph}$) $_2\text{TPA}$ and (6- Ph) $_2\text{-}d_6\text{-TPA}$ and complementary ^2H NMR spectroscopy.¹¹ For each complex the overall number of signals is consistent with an effective plane of symmetry in the cation to give equivalent phenyl-appended pyridyl donors. This is also consistent with the identification of three methylene proton resonances. Selected regions of the spectra of **8-10** are shown in Figure 3-4(d-f).

Similar to the ^1H NMR features of 6- Ph_2TPA -supported Ni(II) complexes,¹¹ each Co(II) complex exhibits a pattern of isotropically shifted resonances for the pyridyl ring protons with chemical shifts in the order $\alpha\text{-H} > \beta\text{-H} > \gamma\text{-H}$. Resonances in the region of ~80-20 ppm clearly distinguish the complexes. Within this region are signals associated with the β and β' hydrogens of the pyridyl rings (Figure 3-6). A characteristic feature of the ^1H NMR spectrum of [(6- Ph_2TPA)Co(PhC(O)CHC(O)Ph)]ClO₄ (**8**) is a signal at -49 ppm, which has been assigned as a phenyl ring proton resonance of the 6- Ph_2TPA ligand.

Table 3-4. ^1H NMR chemical shifts for **8-10** in CD_3CN at 298 K.

assignment	chem. shift (ppm) ^a	$\Delta\nu_{1/2}(\text{Hz})^b$	$T_{1\text{exp}}(\text{ms})^c$	rel. area
[(6-Ph ₂ TPA)Co(PhC(O)CHC(O)Ph)]ClO ₄ (8)				
α	151.21	247	2	1
β	77.42, 52.47	104, 49	10, 33	<i>d, d</i>
β'	27.12, 22.59	71, 62	20, 52	2, 2
γ	18.42	<i>d</i>	<i>d</i>	<i>d</i>
γ'	-10.06	69	74	2
CH ₂	193.14, 125.99, 75.82	632, 242, 104	2, 2, 10	2, 2, <i>d</i>
Ph	8.04, 3.87, -48.69	38, 42, 184	85, 41, 5	<i>d, d, d</i>
[(6-Ph ₂ TPA)Co(CH ₃ CN)](ClO ₄) ₂ (9)				
α	153.68	963	<i>d</i>	1
β	69.32, 48.34	141, 141	<i>d, 35</i>	1, 1
β'	73.05, 40.07	141, 141	48, 180	2, 2
γ	-4.28	65	150	2
γ'	-0.91	72	480	1
CH ₂	119.1, 87.60, 53.1	<i>d, 2190, d</i>	<i>d</i>	2, 2, <i>d</i>
Ph	25.68, 5.46, 2.96	751, 69, <i>d</i>	<i>d, 160, 230</i>	4, 2, <i>d</i>
[(6-Ph ₂ TPA)Co(O ₂ CPh)]ClO ₄ (10)				
α	142.22	867	< 1	1
β	52.99, 50.61	103, 153	11, 5	1, 1
β'	55.62, 35.43	153, 217	8, 4	2, 2
γ	0.64	72	9	1
γ'	-0.36	72	11	2
CH ₂	117.2, 76.35, <i>d</i>	<i>d, 2190, d</i>	< 1	<i>d, d, d</i>
Ph	8.59, 4.19, <i>d</i>	65, 88, <i>d</i>	14, 7, <i>d</i>	2, 4, <i>d</i>
Benzoate	27.45, 15.73, 12.92	286, 103, 84	2, 23, 47	2, 2, 1

^aChemical shifts in ppm relative to the residual solvent peak of CHD_2CN (1H, 1.94 (quintet) ppm). ^bLine widths are full width at a half-maximum. ^c T_1 values were obtained on 300 MHz. ^dCould not be determined.

An additional distinct resonance for this compound is found at -10 ppm and is for the γ' hydrogen. The spectrum of the benzoate complex is unique in a clustering of three of the four β/β' resonances in chemical shift range of 50-56 ppm.

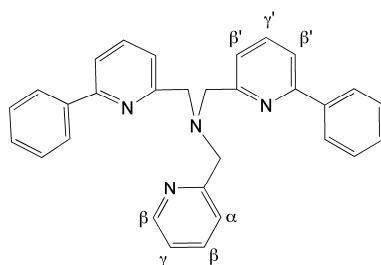


Figure 3-6. Labeling scheme for the 6-Ph₂TPA ligand.

Having fully characterized **8-10** and assigned the ¹H NMR signals of these complexes, we were positioned to evaluate the “wet” reaction mixture (Figure 3-4(a)) generated upon treatment of 6-Ph₂TPA and Co(ClO₄)₂·6H₂O with a slight stoichiometric excess of Me₄NOH·5H₂O and 2-hydroxy-1,3-diphenylpropane-1,3-dione in “wet” acetonitrile under the conditions used to isolate [(6-Ph₂TPA)Ni(PhC(O)C(OH)C(O)Ph)]ClO₄ (**1**).^{2a} It is clearly evident by the ¹H NMR features shown in Figure 3-4(a) that the Co(II) benzoate complex **10** is present with β/β'-H signals at ~55.6, 53.0, 50.6, and 35.5 ppm. Additionally, it is noteworthy that several signals are present upfield of 0 ppm. This suggests that multiple enolate-type complexes are also present (via comparison to the spectral features with those of the dibenzoylmethane complex **8** (Figure 3-4(d)). Work-up of the “wet” reaction mixture resulted in the isolation of the ester 2-oxo-2-phenylethylbenzoate in ~50% yield based on the initial amount of 2-hydroxy-1,3-diphenylpropane-1,3-dione employed. Thus, similar to the chemistry of 6-PhTPA-supported Ni(II), ester formation occurs in the Co(II) system under the “wet” reaction conditions. Additionally, we isolated ~21 mg (58% recovery) of unaltered 6-Ph₂TPA from the reaction mixture.

Rationalizing that removal of water might enable the preparation of the desired enolate complex [(6-Ph₂TPA)Co(PhC(O)C(OH)C(O)Ph)]ClO₄ (**7**), we next attempted a synthesis using the dry conditions involving predried Me₄NOH and CH₃CN that enabled the isolation of [(6-PhTPA)Ni(PhC(O)C(OH)C(O)Ph)]ClO₄ (**3**). Admixture of the reagents followed by stirring for 3 h under N₂ and workup resulted in the isolation of an orange solid with features in the ¹H NMR spectrum as shown in Figure 3-4(b). Notably, this spectrum does not indicate the presence of Co(II) benzoate complex (**8**), and suggests the formation of a single Co(II) enolate complex as evidenced by signals at ~-10 and -49 ppm. Based on the ¹H NMR features of **8**, these could be signals for the γ' and phenyl ring protons of the desired complex **7**. Unfortunately, other signals are present indicating that the isolated product is not pure. Evaluation of the organic products from the reaction once again revealed the presence of a mixture of the ester 2-oxo-2-phenylethylbenzoate and 6-Ph₂TPA in a ~1:1 ratio. Thus, unlike the (6-PhTPA)Ni(II) system, reducing the amount of water in the reaction mixture did not significantly reduce the amount of ester generated. However, removal of water does prevent formation of the benzoate complex **10**.

We next explored a variety of reaction conditions in attempts to prepare pure [(6-Ph₂TPA)Co(PhC(O)C(OH)C(O)Ph)]ClO₄ (**7**) and have found that the best results are obtained using dry conditions akin to those described herein for the preparation of [(6-PhTPA)Ni(PhC(O)C(OH)C(O)Ph)]ClO₄ (**3**) but with a shorter reaction time. Specifically, admixture of equimolar amounts of [(6-Ph₂TPA)Co(CH₃CN)](ClO₄)₂·CH₃CN (**9**), 2-hydroxy-1,3-diphenylpropane-1,3-dione, and predried Me₄NOH in CH₃CN (<10 ppm

H₂O) and stirring for 15 min results in the formation of a deep orange solution with λ_{\max} = 397 nm. We note that this is the same wavelength that was identified for the $\pi \rightarrow \pi^*$ transition of the enolate ligand in [(6-Ph₂TPA)Ni(PhC(O)C(OH)C(O)Ph)]ClO₄ (**1**)^{2b} and [(6-PhTPA)Ni(PhC(O)C(OH)C(O)Ph)]ClO₄ (**3**). Immediate removal of the solvent under vacuum, followed by workup, yielded a dark orange solid with the ¹H NMR properties as shown in Figure 3-4(c). The complex generated has many similar features to the dibenzoylmethane complex **8**, suggesting that both likely contain a six-membered ring enolate ligand. These ¹H NMR similarities, combined with the absorption maximum at 397 nm, suggest that [(6-Ph₂TPA)Co(PhC(O)C(OH)C(O)Ph)]ClO₄ (**7**), has been formed. However, like all of the reaction mixtures targeting this complex, the ester 2-oxo-2-phenylethylbenzoate and free 6-Ph₂TPA are also generated. The presence of these byproducts has prevented our obtaining elemental analysis data for **7**. That being said, evaluation of the O₂ reactivity properties of this complex are underway. Preliminary studies indicate that exposure of a CH₃CN solution of **7** to air results in a rapid color change from orange brown to green. The ¹H NMR features of the reaction mixture are consistent with formation of the benzoate complex [(6-Ph₂TPA)Co(O₂CPh)]ClO₄ (**10**). This reaction is akin to that previously reported for [(6-Ph₂TPA)Ni(PhC(O)CH(OH)CPh)]ClO₄ (**1**).^{2b} The generation of 2-oxo-2-phenylethylbenzoate in the initial “wet” reaction mixture directed at the preparation of the Co(II) enolate complex **7** (Figure 3-4(a)), and the disappearance of the benzoate complex [(6-Ph₂TPA)Co(O₂CPh)]ClO₄ (**10**) once the reagents (base and solvent) were predried, led us to hypothesize that the presence of water promotes ester hydrolysis to provide the

benzoate ligand in **10**. In an independent experiment admixture of the ester with [(6-Ph₂TPA)Co(CH₃CN)](ClO₄)₂·CH₃CN (**9**) and Me₄NOH·5H₂O resulted in the formation of the Co(II) benzoate complex [(6-Ph₂TPA)Co(O₂CPh)]ClO₄ (**10**) thus confirming our notion. As noted above, an independent experiment involving [(6-PhTPA)Ni(CH₃CN)(CH₃OH)](ClO₄)₂ (**5**), 2-oxo-2-phenylethyl benzoate, and Me₄NOH·5H₂O showed no ester hydrolysis reactivity. Thus the two different metal/ligand combinations (6-PhTPANi and 6-Ph₂TPACo) exhibit different ester hydrolysis reactivity.

Conclusions

The coordination chemistry of acireductone-type ligands reported to date is quite limited.^{2,3,5,6} In our laboratory we have pursued synthetic studies directed at the preparation of metal complexes of relevance to the ES adduct in Ni(II)-ARD, which catalyzes a CO-producing reaction. As the Ni(II) center in this enzyme can be replaced with Co(II) with almost full retention of enzyme activity,¹⁴ we are also interested in examining the chemistry of Co(II) complexes of acireductone-type ligands.

The research described herein outlines our discovery that the presence of water influences the preparation of a Ni(II) enolate complex of an acireductone-type ligand. Reducing the amount of water present in the reaction mixture via predrying of the base and solvent significantly reduced the amount of isomerization of 2-hydroxy-1,3-diphenylpropane-1,3-dione to the ester 2-oxo-2-phenylethylbenzoate and increases the yield of the desired Ni(II) enolate complex, [(6-PhTPA)Ni(PhC(O)CH(OH)CPh)]ClO₄

(3). We propose that water is involved in the acid/base chemistry necessary to promote isomerization the reaction (Scheme 3-3). It is known that isomerization of 2-hydroxy-1,3-diphenylpropane-1,3-dione to ester will occur in aqueous NaHCO_3 /methanol solution.¹⁰ In our system, a combination of a Ni(II)-OH moiety and H_2O may be necessary to promote isomerization reactivity in a general base/general acid type reaction sequence.

The 6- Ph_2TPA -supported Co(II) system exhibits a more multifaceted water-dependent chemistry. Like the (6- PhTPA)Ni-containing system, isomerization of 2-hydroxy-1,3-diphenylpropane-1,3-dione to 2-oxo-2-phenylethylbenzoate occurs in reaction mixtures containing water. However, predrying of the base and solvent in this system does not significantly reduce the amount of ester generated. Instead, a dryer reaction environment reduces the amount of a 6- Ph_2TPA -supported Co(II) benzoate complex generated relative to the “wet” reaction mixture. Independent studies of ester hydrolysis reactivity showed that the combination of [(6- Ph_2TPA)Co(CH_3CN)](ClO_4)₂· CH_3CN (**9**), $\text{Me}_4\text{NOH}\cdot 5\text{H}_2\text{O}$ and 2-oxo-2-phenylethylbenzoate in CH_3CN results in ester hydrolysis and the liberation of benzoate anion. Notably, a similar type of ester hydrolysis reactivity does not occur for a reaction mixture containing [(6- PhTPA)Ni(CH_3CN)(CH_3OH)](ClO_4)₂ (**5**), $\text{Me}_4\text{NOH}\cdot 5\text{H}_2\text{O}$, and 2-oxo-2-phenylethylbenzoate in CH_3CN . This provides a rationale for why little, if any, Ni(II) benzoate complex is generated in the “wet” reaction mixture.

Overall, our results have provided insight into the conditions required to prepare two new complexes of relevance to the ES adduct in acireductone dioxygenases. The differing effects of water on the reactions involving (6- PhTPA)Ni- and (6- Ph_2TPA)Co-

supported complexes (isomerization and/or ester hydrolysis) cannot be fully explained at this point, but may relate to differences in M-OH/H₂O chemistry for the two metal/ligand combinations. As our group also has a strong interest in metal-promoted hydrolysis reactions²¹, this area is under further investigation.

Experiments

General comments

All reagents and solvents were obtained from commercial sources and were used as received unless otherwise noted. Solvents were dried according to published procedures²² and were distilled under N₂ prior to use. Air-sensitive reactions were performed in a MBraun Unilab or Vacuum Atmospheres glovebox under an N₂ atmosphere. The acireductone analog 2-hydroxy-1,3-diphenylpropan-1,3-dione,^{2a} the Ni(II) enolate complex [(6-Ph₂TPA)Ni(PhC(O)C(OH)C(O)Ph)]ClO₄ (**1**),^{2a} and the Co(II) complex [(6-Ph₂TPA)Co(CH₃CN)]ClO₄ (**9**)¹⁵ were prepared as previously described.

Physical methods

UV-vis spectra were recorded on a Hewlett-Packard 8453 diode array spectrophotometer. IR spectra were recorded on a Shimadzu FTIR-8400 spectrometer as KBr pellets. ¹H NMR spectra of diamagnetic species were recorded on a Bruker ARX-400 spectrometer and the chemical shifts (in ppm) are referenced to the residual solvent peak(s) in CHD₂CN (¹H, 1.94 (quintet) ppm). GC-MS data was obtained using a Shimadzu QP5000 with an Alltech EC-5 column and ultra high purity helium as the carrier gas. FAB-MS data was obtained at the Mass Spectrometry Facility, Department of

Chemistry, University of California, Riverside. Elemental analyses were performed by Atlantic Microlabs Inc., Norcross, GA or Canadian Microanalytical, Service, Inc., British Columbia, Canada.

NMR methods for paramagnetic Ni(II) and Co(II) complexes

A typical one-dimensional ^1H NMR spectrum consisted of 16 K data points, 300 scans, and a 250 ms relaxation delay. An exponential weighting function ($\text{lb} = 30$ Hz) was used during processing. The 90° pulse (14.1 μs) was calibrated at 298 K. Longitudinal relaxation times (T_1) were measured using the inversion-recovery pulse sequence ($180^\circ\text{-}\tau\text{-}90^\circ$) method on a JEOL ECX-300. ^2H NMR spectra were obtained at 298 K on a Bruker ARX-400 operating at 61.43 MHz using an unlocked system. Overall, methods of data collection and processing for paramagnetic complexes followed closely from those previously described.¹¹

6-N-(6-phenyl-2-pyridyl)methyl)-N,N-((2-pyridyl)methyl)-amine (6-PhTPA).

This ligand has been previously reported⁸, however, the preparative method employed herein is an alternative route. A round bottomed flask was charged with an acetonitrile slurry of 2-(chloromethyl)-6-phenylpyridine hydrochloride (6.0 g, 0.025 mol), di-(2-picolyl)-amine (5.0 g, 0.025 mol), sodium bicarbonate (13.3 g, 0.125 mol), and a catalytic amount of tetrabutylammonium bromide. The reaction was then purged with N_2 and refluxed for 24 h. After this time, the mixture was cooled to room temperature and 0.1 M NaOH was added until the $\text{pH} > 11$. The resulting mixture was extracted with methylene chloride (3 x 200 mL). The organic fractions were combined, dried over anhydrous

Na₂SO₄, and the solvent was removed under reduced pressure. The resulting brown oil was purified using column chromatography using ethyl acetate:methanol (1:1) as the eluent. Yield: 8.56 g (93%). ¹H NMR (CDCl₃, 400 MHz): δ 8.54 (d, *J* = 4.8 Hz, 2 H), 8.00 (d, *J* = 7.4 Hz, 2 H), 7.72 (t, *J* = 7.8 Hz, 1 H), 7.68-7.65 (m, 3 H), 7.58 (d, *J* = 7.8 Hz, 2H), 7.50 (d, *J* = 7.8 Hz, 1H), 7.46 (t, *J* = 7.7 Hz, 2 H), 7.39 (dt, *J* = 7.3 Hz, *J* = 2.3 Hz, 1 H), 7.14 (dd, *J* = 7.8 Hz, *J* = 4.7 Hz, 2 H), 3.97 (s, 2 H), 3.95 (s, 4 H). These ¹H NMR features match those previously reported.⁸

Caution! Perchlorate salts of metal complexes with organic ligands are potentially explosive. Only small amounts of material should be prepared, and these should be handled with great care.²³

Attempted preparation of [(6-PhTPA)Ni(PhC(O)C(OH)C(O)Ph]ClO₄ (3) under the conditions used to prepare 1. Isolation of isomerization product. In a glovebox, equimolar amounts of 6-PhTPA (30 mg, 8.2 x 10⁻⁵ mol) and Ni(ClO₄)₂·6H₂O (30 mg, 8.2 x 10⁻⁵ mol) were combined in ~3 mL of acetonitrile (dried from CaH₂; ~3000 ppm water determined via Karl-Fischer titration) and stirred until everything had dissolved. This resulted in the formation of a purple-brown solution. This solution was then added to solid Me₄NOH·5H₂O (16 mg, 9.0 x 10⁻⁵ mol) and the mixture was stirred for an additional ~1 min. At this time, 2-hydroxy-1,3-diphenylpropane-1,3-dione (22 mg, 9.0 x 10⁻⁵ mol), dissolved in ~1 mL of acetonitrile, was added and the deep orange solution was stirred overnight at ambient temperature. The solvent was then removed

under vacuum and the remaining solid was dissolved in ~5 mL of dichloromethane. This solution was passed through a celite/glass wool plug and the filtrate was then reduced in volume to ~1 mL. Addition of excess hexanes (~20 mL) resulted in the deposition of an orange powder, which was dried under vacuum. ^1H NMR analysis indicated the presence of the desired enolate complex $[(6\text{-PhTPA})\text{Ni}(\text{PhC}(\text{O})\text{C}(\text{OH})\text{C}(\text{O})\text{Ph})]\text{ClO}_4$ (**3**) and other (6-PhTPA)Ni(II) containing products. To identify the organic products in the reaction mixture, the CH_2Cl_2 /hexanes solution from which the metal complexes were precipitated was filtered through a celite/glass wool plug. The filtrate was then dried under vacuum leaving a white solid (10 mg). ^1H NMR and GC-MS analysis of the white solid confirmed its identity as a 2-oxo-2-phenylethylbenzoate via comparison with independently synthesized sample. The amount of solid recovered is consistent with a 46% yield starting from 2-hydroxy-1,3-diphenylpropane-1,3-dione.

Evaluation of ester formation in the reaction leading to the formation of [(6-Ph₂TPA)]Ni(PhC(O)C(OH)C(O)Ph]ClO₄ (1**).** In the glovebox, equimolar amounts of 6-Ph₂TPA (34 mg, 7.6×10^{-5} mol) and Ni(ClO₄)₂·6H₂O (28 mg, 7.6×10^{-5} mol) were mixed in ~3 mL of acetonitrile and stirred until everything had dissolved, which gave a purple solution. This solution was then combined with solid Me₄NOH·5H₂O (15 mg, 8.3×10^{-5} mol) and the mixture was stirred for ~1 min. At this time, a CH₃CN solution (~1 mL) of 2-hydroxy-1,3-diphenylpropane-1,3-dione (20 mg, 8.3×10^{-5} mol) was added and the mixture was stirred overnight at ambient temperature to give a deep orange solution. After removal of the solvent under vacuum, the residue was dissolved dichloromethane (~5 mL) and the solution was filtered through a celite/glass wool plug. The filtrate was

collected and the solvent volume was reduced to ~1 mL under vacuum. Addition of excess hexanes (~20 mL) resulted in the deposition of **1** as an orange-brown solid which was dried under vacuum. (48.2 mg, 76% yield). The formulation of the complex was confirmed by ^1H NMR. The solution from which the precipitate was obtained was then filtered through a celite/glass wool plug to remove any residual metal complex and the filtrate was brought to dryness under vacuum yielding a white solid (11 mg). ^1H NMR analysis of this solid indicated the presence of 2-oxo-2-phenylethylbenzoate and 6- Ph_2TPA in a 2:1 ratio.

Isolation of analytically pure [(6-PhTPA)Ni(PhC(O)C(OH)C(O)Ph)]ClO₄ (3**) using predried base and solvent.** In this entire procedure extra dry CH_3CN purchased from ACROS Organics (<10 ppm H_2O) was used. Under a N_2 atmosphere, $\text{Me}_4\text{NOH}\cdot 5\text{H}_2\text{O}$ (16 mg, 9.0×10^{-5} mol) was dissolved in methanol in a Schlenk flask and the mixture was dried under vacuum for >24 h. To the remaining solid was added an acetonitrile solution (~2 mL) containing 6-PhTPA (30 mg, 8.2×10^{-5} mol) and $\text{Ni}(\text{ClO}_4)_2\cdot 6\text{H}_2\text{O}$ (30 mg, 8.2×10^{-5} mol). The resulting mixture was stirred for ~1 min. At this time, a CH_3CN solution (~1 mL) of 2-hydroxy-1,3-diphenylpropane-1,3-dione (22 mg, 9.0×10^{-5} mol) was added and the reaction mixture was immediately put under vacuum. Upon stirring for ~3 h at ambient temperature, the solution became deep orange/brown. After removal of the solvent under reduced pressure, the remaining orange/brown solid was dissolved in CH_2Cl_2 (~5 mL) and the solution was filtered through a celite/glass wool plug. The filtrate was concentrated under reduced pressure to a volume of ~1 mL, which was then added to excess hexanes (~20 mL). This resulted in

the deposition of an orange/brown solid which was dried for ~ 2 h under vacuum. Yield: 59 mg (94%). X-ray quality crystals were obtained from CH₂Cl₂/n-pentane. Anal. Calcd for: C₃₉H₃₃ClN₄NiO₇·1/6CH₂Cl₂: C, 60.56; H, 4.33; N, 7.22. Found: C, 60.48; H, 4.02; N, 7.29. The presence of trace CH₂Cl₂ in the elemental analysis sample was confirmed by ¹H NMR. FTIR: 3439 (ν_{O-H}), 1095 (ν_{ClO₄}), 621 (ν_{ClO₄}); UV-vis (CH₃CN) nm (ε, M⁻¹cm⁻¹) 393 (10600).

[(6-PhTPA)Ni(PhC(O)CHC(O)Ph)]ClO₄ (4). A solution of Ni(ClO₄)₂·6H₂O (35 mg, 1.0 x 10⁻⁴ mol) in acetonitrile (~3 mL) was added to solid 6-PhTPA (37 mg, 1.0 x 10⁻⁴ mol) and the resulting mixture was stirred until all of the solids had dissolved. An acetonitrile solution (~2 mL) containing dibenzoylmethane (21 mg, 1.0 x 10⁻⁴ mol) and Me₄NOH·5H₂O (17 mg, 1.0 x 10⁻⁴ mol) was then added and the mixture was stirred overnight at ambient temperature. The solvent was removed under reduced pressure and the remaining solid was dissolved in CH₂Cl₂. The solution was filtered through a celite/glass wool plug and the solvent was subsequently removed from the filtrate under vacuum. The remaining solid was dissolved in a small amount of acetonitrile and excess diethyl ether (~20 mL) was added to precipitate the desired product. Yield: 40 mg (54%). X-ray quality crystals were obtained by diethyl ether diffusion into an acetonitrile solution of the complex. Anal. Calcd for: C₃₉H₃₃ClN₄NiO₆·0.95C₄H₁₀O: C, 62.82; H, 5.23; N, 6.85. Found: C, 62.98; H, 5.27; N, 7.00. FTIR (KBr, cm⁻¹) 1092 (ν_{ClO₄}), 621 (ν_{ClO₄}). UV-vis (CH₃CN) nm (ε, M⁻¹cm⁻¹) 543 (26), 793 (22), 907 (30); FAB-MS *m/z* (relative intensity) 647 ([M-ClO₄]⁺, 100%).

[(6-PhTPA)Ni(CH₃CN)(CH₃OH)](ClO₄)₂ (5). A solution of 6-Ph₂TPA (48 mg, 1.3×10^{-4} mol) and Ni(ClO₄)₂·6H₂O (45 mg, 1.3×10^{-4} mol) in acetonitrile (~3 mL) was prepared and stirred until all solids had dissolved. The solution was then brought to dryness under vacuum and the residue was dissolved in MeOH. Crystals were grown by Et₂O diffusion into the methanol solution. Yield: 72 mg (84%). Anal. Calcd for: C₂₇H₂₉Cl₂N₅NiO₉: C, 46.52; H, 4.19; N, 10.05. Found: C, 46.17; H, 4.30; N, 10.00. FTIR (KBr, cm⁻¹) 1092 (ν_{ClO₄}), 623 (ν_{ClO₄}). UV-vis (CH₃CN) nm (ε, M⁻¹cm⁻¹) 541 (20), 793 (17), 913 (23); FAB-MS *m/z* (relative intensity) 424 ([M-2(ClO₄)-CH₃CN-CH₃OH-H⁺]⁺, 9%).

[(6-PhTPA)Ni(O₂CPh)]ClO₄ (6). An acetonitrile solution (~3 mL) containing 6-PhTPA (33 mg, 8.9×10^{-5} mol) and Ni(ClO₄)₂·6H₂O (32 mg, 8.9×10^{-5} mol) was prepared and stirred until all solids had dissolved. This solution was then combined with solid sodium benzoate (13 mg, 8.9×10^{-5} mol) and ~1 mL of MeOH was added. This mixture was stirred for ~1 h at ambient temperature and the solvent was then removed under reduced pressure. The remaining solid was dissolved in CH₂Cl₂ and the solution was passed through a celite/glass wool plug. The solvent was removed from the filtrate under reduced pressure. The desired complex was obtained by dissolving the solid in minimal CH₂Cl₂ followed by addition of excess n-pentane. The process was repeated three times to obtain analytically pure complex Yield: 30 mg (53% yield). X-ray quality crystals were obtained by diffusion of a CH₂Cl₂/i-PrOH/AcOEt solution of the complex into n-pentane. Anal. Calcd for: C₃₁H₂₇ClN₄NiO₆·1/3CH₂Cl₂: C, 55.85; H, 4.14; N, 8.32. Found: C, 55.59; H, 4.31; N, 8.31. The presence of CH₂Cl₂ in the elemental analysis

sample was confirmed by ^1H NMR. FTIR (KBr, cm^{-1}) 1092 (ν_{ClO_4}), 623 (ν_{ClO_4}); UV-vis (CH_3CN) nm (ϵ , $\text{M}^{-1}\text{cm}^{-1}$) 543 (14), 802 (7), 953 (15); FAB-MS m/z (relative intensity) 545 ($[\text{M}-\text{ClO}_4]^+$, 75%).

Evaluation of 2-oxo-2-phenylethylbenzoate hydrolysis in the presence of [(6-PhTPA)Ni(CH₃CN)(CH₃OH)](ClO₄)₂ (9) and Me₄NOH·5H₂O. In a glovebox, [(6-PhTPA)Ni(CH₃CN)(MeOH)](ClO₄)₂ (5) (23 mg, 3.3×10^{-5} mol), was dissolved in acetonitrile and combined with equimolar amounts Me₄NOH·6H₂O (6.0 mg, 3.29×10^{-5} mol) and PhC(O)OCH₂C(O)Ph (7.9 mg, 3.29×10^{-5} mol) and the mixture was stirred for 16.5 h. The solvent was then removed under reduced pressure and the remaining solid was dissolved in CH₂Cl₂, and the solution was filtered through a celite/glass wool plug. The filtrate was concentrated under vacuum and precipitation of the metal complex(es) was induced by the addition of excess hexane. The ^1H NMR of this solid indicated the presence of multiple Ni(II) complexes, as evidenced by several overlapping signals in the region of 80-20 ppm. These complexes are likely one or more Ni-OH species. The solution from the precipitate was isolated was filtered through a celite/glass wool plug and the filtrate was brought to dryness leaving a white solid (7.5 mg). ^1H NMR of this solid indicated the presence of unaltered ester PhC(O)OCH₂C(O)Ph in 95% yield. No other organic products were detected.

Attempted preparation of [(6-Ph₂TPA)Co(PhC(O)C(OH)C(O)Ph]ClO₄ (7) under the conditions used to prepare 1. In a N₂-filled glovebox, 6-Ph₂TPA (36 mg, 8.2×10^{-5} mol) and Co(ClO₄)₂·6H₂O (30 mg, 8.2×10^{-5} mol) were mixed in ~3 mL of acetonitrile (~3000 ppm H₂O via Karl-Fischer titration) and the solution was stirred until

everything had dissolved. This purple solution was then combined with solid $\text{Me}_4\text{NOH}\cdot 5\text{H}_2\text{O}$ (16 mg, 9.0×10^{-5} mol) and the mixture was stirred for ~1 min. To this solution was added a CH_3CN solution (1 mL) of 2-hydroxy-1,3-diphenylpropane-1,3-dione (22 mg, 9.0×10^{-5} mol). The deep orange solution was then stirred overnight at ambient temperature during which time the color changed to green. The solvent was removed under vacuum and the remaining solid was dissolved in CH_2Cl_2 (~5 mL). This solution was passed through a celite/glass wool plug and the filtrate was reduced to ~1 mL under vacuum. Addition of excess hexanes (~20 mL) resulted in the deposition of a brown solid (40 mg). ^1H NMR analysis indicates the presence of $[(6\text{-Ph}_2\text{TPA})\text{Co}(\text{O}_2\text{CPh})]\text{ClO}_4$ (**10**) and other Co(II) compounds (Figure 4-3(a)). The solution remaining after the isolation of the metal complexes was filtered through a celite/glass wool plug and the filtrate was brought to dryness under vacuum leaving a white solid (32 mg). ^1H NMR (in CD_3CN) and GC-MS analysis of this solid confirmed the presence of the ester 2-oxo-2-phenylethylbenzoate (~11 mg, 50% based on 2-hydroxy-1,3-diphenylpropane-1,3-dione) and the 6- Ph_2TPA (~21 mg, ~58% recovery).

Attempted preparation of $[(6\text{-Ph}_2\text{TPA})\text{Co}(\text{PhC}(\text{O})\text{C}(\text{OH})\text{C}(\text{O})\text{Ph})]\text{ClO}_4$ (7**) under conditions used to isolate **3**.** In this entire procedure extra dry CH_3CN purchased from ACROS Organics (<10 ppm H_2O) was used. Prior to the synthesis, $\text{Me}_4\text{NOH}\cdot 5\text{H}_2\text{O}$ was dissolved in ~2 mL methanol, transferred to a Schlenk flask, and dried under vacuum for >24 h. In the glovebox, $[(6\text{-Ph}_2\text{TPA})\text{Co}(\text{CH}_3\text{CN})](\text{ClO}_4)_2$ (**9**) (64 mg, 8.2×10^{-5} mol) was dissolved in acetonitrile and stirred until everything had dissolved, yielding a purple solution. Next, 2-hydroxy-1,3-diphenylpropane-1,3-dione (22 mg, 9.0×10^{-5} mol)

dissolved in ~1 mL of acetonitrile was added to the solid, pre-dried $\text{Me}_4\text{NOH}\cdot 5\text{H}_2\text{O}$ (16 mg; 9.0×10^{-5} mol). This mixture was immediately combined with the solution of $[(6\text{-Ph}_2\text{TPA})\text{Co}(\text{CH}_3\text{CN})](\text{ClO}_4)_2$ and the mixture was stirred for 3 h, under vacuum, yielding a deep orange/red solution. The solvent was then removed under reduced pressure. The remaining orange solid was dissolved in ~5 mL of dichloromethane, and the solution was filtered through a celite/glass wool plug. The filtrate was concentrated to ~1 mL under vacuum and the Co(II)-containing products were precipitated by the addition of excess hexanes (~20 mL). This resulted in the isolation of 54 mg of an orange solid. The ^1H NMR features of this solid are shown in Figure 4-3(b). The hexane layer was filtered through a celite/glass wool plug and the filtrate was brought to dryness under vacuum. A white solid was obtained (22 mg). ^1H NMR analysis of this solid showed the presence of 2-oxo-2-phenylethylbenzoate and 6- Ph_2TPA in ~1:1 ratio.

Attempted preparation of $[(6\text{-Ph}_2\text{TPA})\text{Co}(\text{PhC}(\text{O})\text{C}(\text{OH})\text{C}(\text{O})\text{Ph})\text{ClO}_4$ (7) under dry conditions and using a short reaction time. In this entire procedure extra dry CH_3CN purchased from ACROS Organics (<10 ppm H_2O) was used. $\text{Me}_4\text{NOH}\cdot 5\text{H}_2\text{O}$ (5.9 mg, 3.3×10^{-5} mol) was dissolved in ~3 mL acetonitrile. This solution was brought to dryness and the remaining solid was dried under vacuum for 2 h. This step was repeated twice. Next, $[(6\text{-Ph}_2\text{TPA})\text{Co}(\text{CH}_3\text{CN})](\text{ClO}_4)_2$ (**9**) (26 mg, 3.3×10^{-5} mol) and 2-hydroxy-1,3-diphenylpropane-1,3-dione (7.8 mg, 3.3×10^{-5} mol) were independently dissolved in CH_3CN (2 mL). The solution of 2-hydroxy-1,3-diphenylpropane-1,3-dione was added to the solid Me_4NOH and the CH_3CN solution of $[(6\text{-Ph}_2\text{TPA})\text{Co}(\text{CH}_3\text{CN})](\text{ClO}_4)_2$ (**9**) was subsequently added. The reaction immediately

turned dark orange (λ_{max} 397 nm). It was stirred for 15 min and then the solvent was removed under reduced pressure. The remaining dark orange solid was dissolved in dichloromethane (~3 mL) and the solution was filtered through a celite/glass wool plug. The filtrate was reduced in volume to ~1 mL and the Co(II) product was precipitated via the addition of excess of hexanes (~20 mL). The ^1H NMR features of this solid are shown in Figure 4-3(c). UV-vis (CH_3CN) $\lambda_{\text{max}} = 397$ nm. The hexane layer was filtered through a celite/glass wool plug and the filtrate was brought to dryness under vacuum. A white solid was obtained (12 mg). ^1H NMR analysis of this solid indicated the presence of the ester 2-oxo-2-phenylethylbenzoate and 6- Ph_2TPA in a ratio of 3:1.

[(6- Ph_2TPA)Co($\text{PhC}(\text{O})\text{CHC}(\text{O})\text{Ph})\text{ClO}_4$ (8**).** A mixture of 6- Ph_2TPA (18 mg, 4.1×10^{-5} mol) and $\text{Co}(\text{ClO}_4)_2 \cdot 6\text{H}_2\text{O}$ (14 mg, 3.7×10^{-5} mol) in acetonitrile (~3 mL) was prepared and stirred until everything had dissolved. To this solution was added dibenzoylmethane (10 mg, 4.6×10^{-5} mol) as a solution in acetonitrile (~1 mL). The resulting mixture was stirred for 10 min at which point it was transferred to a glass vial containing solid $\text{Me}_4\text{NOH} \cdot 5\text{H}_2\text{O}$ (7.5 mg, 4.1×10^{-5} mol). This mixture was then stirred overnight at ambient temperature. After removal of the solvent under reduced pressure, the remaining dark orange-red solid was dissolved in CH_2Cl_2 and filtered through a celite/glass wool plug. The solvent was removed from the filtrate under vacuum and the remaining solid was recrystallized by Et_2O diffusion into the acetonitrile solution. Yield: 24 mg (79%). Anal. Calcd for: $\text{C}_{45}\text{H}_{37}\text{ClCoN}_4\text{O}_6$: C, 65.60; H, 4.52; N, 6.80. Found: C, 65.46; H, 4.39; N, 7.15. FTIR (KBr, cm^{-1}) 1094 (ν_{ClO_4}), 623 (ν_{ClO_4}). UV-vis (CH_3CN) nm

(ϵ , $M^{-1}cm^{-1}$) 350 (7500), 564 (77); FAB-MS m/z (relative intensity) 724 ($[M-ClO_4]^+$, 45%).

[(6-Ph₂TPA)Co(O₂CPh)]ClO₄ (10). A mixture of 6-Ph₂TPA (36 mg, 8.1×10^{-5} mol) and Co(ClO₄)₂·6H₂O (27 mg, 7.3×10^{-5} mol) in acetonitrile (~3 mL) was prepared and stirred until everything had dissolved. This solution was then added to solid sodium benzoate (13 mg, 8.9×10^{-5} mol) and the resulting mixture was stirred overnight at room temperature. The solvent was then removed under reduced pressure. The remaining green solid was dissolved in CH₂Cl₂ and filtered through a celite/glass wool plug. The filtrate was brought to dryness under reduced pressure and the remaining solid was recrystallized by Et₂O diffusion into an acetonitrile solution. Yield: 51 mg (98%). Anal. Calcd for: C₃₇H₃₁ClCoN₄O₆: C, 61.55; H, 4.33; N, 7.76. Found: C, 61.39; H, 4.34; N, 7.86. FTIR (KBr, cm^{-1}) 1097 (ν_{ClO_4}), 621 (ν_{ClO_4}); UV-vis (CH₃CN) nm (ϵ , $M^{-1}cm^{-1}$) 462 (103), 619 (66); FAB-MS m/z (relative intensity) 622 ($[M-ClO_4]^+$, 14 %).

Preparation of deuterated analogs of 8-10 of either the 6-(d₅-Ph)₂TPA or (6-Ph)₂-d₆-TPA ligand. These analogs were prepared using 6-(d₅-Ph)₂TPA and (6-Ph)₂-d₆-TPA¹¹ and following the procedures for their protio analogs. ²H NMR spectra of these complexes were obtained as previously described. We note that a d₅-analog of **10**, [(6-Ph₂TPA)Co(O₂C-d₅-Ph)]ClO₄, was also prepared to enable the identification of the benzoate phenyl resonances.

Evaluation of 2-oxo-2-phenylethylbenzoate hydrolysis in the presence of [(6-Ph₂TPA)Co(CH₃CN)](ClO₄)₂·CH₃CN (9) and Me₄NOH·5H₂O. Under a nitrogen atmosphere, a solution of [(Ph₂TPA)Co(CH₃CN)](ClO₄)₂·CH₃CN (**9**) (26 mg, 3.3×10^{-5}

mol) in acetonitrile (~3 mL) was added to solid $\text{Me}_4\text{NOH}\cdot 5\text{H}_2\text{O}$ (6.0 mg, 3.3×10^{-5} mol) and 2-oxo-2-phenylethylbenzoate (7.9 mg, 3.3×10^{-5} mol) and the mixture was stirred for 16.5 h at ambient temperature. The color of the solution changed from purple to green. The solvent was removed under reduced pressure and the remaining solid was dissolved in CH_2Cl_2 . The solution was filtered through a glass wool/celite plug. The filtrate was then concentrated to ~1 mL under reduced pressure and excess hexanes (~20 mL) was added to induce precipitation of a green solid. Yield: 22 mg. ^1H NMR analysis confirmed the presence of $[(\text{Ph}_2\text{TPA})\text{Co}(\text{O}_2\text{CPh})]\text{ClO}_4$ (**10**, major species) and $[(\text{Ph}_2\text{TPA})\text{Co}(\text{CH}_3\text{CN})](\text{ClO}_4)_2\cdot\text{CH}_3\text{CN}$ (**9**, minor species). The solution remaining following the isolation of the solid was passed through a celite/glass wool plug and the filtrate was brought to dryness under reduced pressure. A white solid was isolated (5.7 mg). By ^1H NMR this solid is a mixture of unaltered ester (minor) and 6- Ph_2TPA (major).

X-ray crystallography. A single crystal of each complex was mounted on a glass fiber with viscous oil and then transferred to a Nonius Kappa CCD diffractometer (Mo $\text{K}\alpha$, $\lambda = 0.71073 \text{ \AA}$) for data collection at 150(1) K. For each compound an initial set of cell constants was obtained from 10 frames of data that were collected with an oscillation range of $1^\circ/\text{frame}$ and an exposure time of 20s/frame. Indexing and unit cell refinement based on all observed reflections from those ten frames indicated monoclinic lattices for **3**· CH_2Cl_2 and **10**, orthorhombic lattices for **4**· Et_2O and **5**, and a tetragonal lattice for **8**· $0.5\text{CH}_3\text{CN}$. Final cell constants for each complex were determined from a set of strong reflections from the actual data collection. For each data set, these reflections were indexed, integrated, and corrected for Lorentz, polarization, and absorption effects using

DENZO-SMN and SCALEPAC.²⁴ The structures were solved by a combination of direct methods and heavy atom using SIR97. All non-hydrogen atoms were refined with anisotropic displacement coefficients. Unless otherwise noted, hydrogen atoms were assigned isotropic displacement coefficients ($U(\text{H}) = 1.2 U(\text{C})$ or $1.5U(\text{C}_{\text{methyl}})$) and their coordinates were allowed to ride on their respective carbons using SHELXL97.²⁵

The Ni(II) enolate complex **3**·CH₂Cl₂ crystallizes in the monoclinic crystal system in the space group *Cc* with one molecule of methylene chloride per formula unit. The Ni(II) dibenzoylmethane complex **4**·Et₂O crystallizes in the space group *Pcab* with one molecule of diethyl ether per formula unit. All hydrogen atoms in this structure were located and refined independently. The Ni(II) solvent-coordinated complex **5** crystallizes in the space group *P2₁2₁2₁*. The Co(II) dibenzoylmethane complex **8**·0.5CH₃CN crystallizes in the space group *I-4*. There are two independent formula units per asymmetric unit, with the second being denoted by “A”. One molecule of acetonitrile is present per asymmetric unit. The perchlorate anion exhibits disorder. The Co(II) benzoate complex **10** crystallizes in the space group *P2₁/c*. All hydrogen atoms in this structure were located and refined independently.

References

1. Pochapsky, T. C.; Ju, T.; Dang, R.; Beaulieu, R.; Pagani, G. M.; OuYang, B. In *Metal Ions in Life Sciences*; Sigel, A.; Sigel, H.; Sigel, R. K. O. Eds.; Wiley-VCH: Weinheim, Germany, 2007; pp 473-498.
2. Szajna, E.; Arif, A. M.; Berreau, L. M. *J. Am. Chem. Soc.* **2005**, *127*, 17186-17187. (b) Szajna-Fuller, E.; Rudzka, K.; Arif, A. M.; Berreau, L. M. *Inorg.*

- Chem.* **2007**, *46*, 5499-5507. (c) Grubel, K.; Fuller, A. L.; Chambers, B. M.; Arif, A. M.; Berreau, L. M. *Inorg. Chem.* **2010**, *49*, 1071-1081.
3. Berreau, L. M.; Borowski, T.; Grubel, K.; Allpress, C. J.; Wikstrom, J. P.; Germain, M. E.; Rybak-Akimova, E. V.; Tierney, D. L. *Inorg. Chem.* **2011**, *50*, 1047-1057.
 4. Borowski, T.; Bassan, A.; Siegbahn, P. E. M. *THEOCHEM* **2006**, *772*, 89-92.
 5. Jeffrey, J. C.; Liard, D. J.; Ward, M. D. *Inorg. Chim. Acta* **1996**, *251*, 9-12.
 6. Rudzka, K.; Arif, A. M.; Berreau, L. M. *Inorg. Chem.* **2008**, *47*, 10832-10840. (b)
Rudzka, K.; Grubel, K.; Arif, A. M.; Berreau, L. M. *Inorg. Chem.* **2010**, *49*, 7623-7625.
 7. The neutral form of acireductone-type compounds are known to form both five- and six-membered rings involving hydrogen-bonding between adjacent C-O(H) units. Schank, K. *Synthesis* **1972**, 176-190.
 8. Chuang, C. L.; Lim, K.; Canary, J. W. *Supramolecular Chemistry* **1995**, *5*, 39-43.
 9. Keto-form of the C(1)-phenyl acireductone analog shown in Scheme 1-3 (middle).
 10. Karrer, P.; Kebrle, J.; Thakkar R. M. *Helv. Chim. Acta* **1950**, *33*, 1711-1724.
 11. Szajna, E.; Dobrowolski, P.; Fuller, A. L.; Arif, A. M.; Berreau, L. M. *Inorg. Chem.* **2004**, *43*, 3988-3997.
 12. Methylene proton resonances of the chelate ligand can also appear in this region.¹¹
 13. Dai, Y.; Wensink, P. C.; Abeles, R. H. *J. Biol. Chem.* **1999**, *274*, 1193-1195. (b)
Ju, T.; Goldsmith, R. B.; Chai, S. C.; Maroney, M. J.; Pochapsky, S. S.; Pochapsky, T. C. *J. Mol. Biol.* **2006**, *363*, 823-824.

14. Dai, Y.; Pochapsky, T. C.; Abeles, R. H. *Biochemistry* **2001**, *40*, 6379-6387.
15. Makowska-Grzyska, M. M.; Szajna, E.; Shipley, C.; Arif, A. M.; Mitchell, M. H.; Halfen, J. A.; Berreau, L. M. *Inorg. Chem.* **2003**, *42*, 7472-7478.
16. Monodentate: $\Delta d > 0.6 \text{ \AA}$, $\Delta\theta > 28^\circ$. Kleywegt, G. J.; Wiesmeijer, W. G. R.; van Driel, G. J.; Driessen, W. L.; Reedijk, J.; Noordik, J. H. *J. Chem. Soc., Dalton Trans.* **1985**, 2177-2184.
17. Addison, W.; Rao, T. N.; Reedijk, J.; van Rijn, J.; Vershcoor, G. C. *J. Chem. Soc., Dalton Trans.* **1984**, 1349-1356.
18. Evans, D. F. *J. Chem. Soc.* **1959**, 2003-2005.
19. Huheey, J. E.; Keiter, E. A.; Keiter, R. L. *Inorganic Chemistry: Principles of Structure and Reactivity*; Harper Collins: New York, NY, 1993.
20. McMillin, D. R. *Electronic Absorption Spectroscopy*. In *Physical Methods in Bioinorganic Chemistry: Spectroscopy and Magnetism*; L. Que, Jr.; University Science Books: Sausalito, CA, 2000; pp 1-58.
21. Berreau, L. M. *Adv. Phys. Org. Chem.* **2006**, *41*, 79-181.
22. Armarego W. L. F.; Perrin, D. D. *Purification of Laboratory Chemicals*, 4th ed.; Butterworth-Heinemann: Boston, MA, 1996.
23. Wolsey, W. C. *J. Chem. Educ.* **1973**, *50*, A335-A337.
24. Otwinowski, Z.; Minor W. *Methods Enzymol.* **1997**, *276*, 307-326.
25. Sheldrick, G. M. *SHELXL-97 Program for the Refinement of Crystal Structures*; University of Göttingen, Germany, 1997.

CHAPTER 4
SYNTHESIS, CHARACTERIZATION, AND LIGAND EXCHANGE REACTIVITY OF
A SERIES OF FIRST ROW DIVALENT METAL 3-HYDROXYFLAVONOLATE
COMPLEXES¹

Abstract

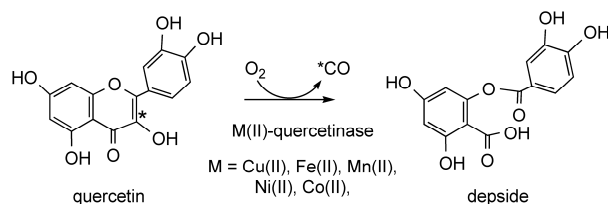
A series of divalent metal flavonolate complexes of the general formula [(6-Ph₂TPA)M(3-Hfl)]X (**1-5-X**; X = OTf⁻ or ClO₄⁻; 6-Ph₂TPA = N,N-bis((6-phenyl-2-pyridyl)methyl)-N-((2-pyridyl)methyl)amine; M = Mn(II), Co(II), Ni(II), Cu(II), Zn(II); 3-Hfl = 3-hydroxyflavonolate) was prepared and characterized by X-ray crystallography, elemental analysis, FTIR, UV-vis, ¹H NMR or EPR, and cyclic voltammetry. All of the complexes have a bidentate coordinated flavonolate ligand. The difference in M-O distances (Δ_{M-O}) involving this ligand varies through the series, with the asymmetry of flavonolate coordination increasing in the order Mn(II) ~ Ni(II) < Cu(II) < Zn(II) < Co(II). The hypsochromic shift of the absorption band I ($\pi \rightarrow \pi^*$) of the coordinated flavonolate ligand in **1-5-OTf** (relative to that in free anion) increases in the order Ni(II) < Mn(II) < Cu(II) < Zn(II), Co(II). Previously reported 3-Hfl complexes of divalent metals fit well with this ordering. ¹H NMR studies indicate that the 3-Hfl complexes of Co(II), Ni(II),

¹Coauthored by Katarzyna Grubel, Katarzyna Rudzka, Atta M. Arif, Katie L. Klotz, Jason A. Halfen, and Lisa M. Berreau. Reproduced with permission from *Inorganic Chemistry* **2010**, 49, 82-96. Copyright 2010 American Chemical Society.

and Zn(II) exhibit a pseudo-octahedral geometry in solution. EPR studies suggest that the Mn(II) complex **1-OTf** may form binuclear structures in solution. The mononuclear Cu(II) complex **4-OTf** has a distorted square pyramidal geometry. The oxidation potential of the flavonolate ligand depends on the metal ion present and/or the solution structure of the complex, with the Mn(II) complex **1-OTf** exhibiting the lowest potential, followed by the pseudo-octahedral Ni(II) and Zn(II) 3-Hfl complexes, and the distorted square pyramidal Cu(II) complex **4-OTf**. The Mn(II) complex [(6-Ph₂TPA)Mn(3-Hfl)]OTf (**1-OTf**) is unique in the series in undergoing ligand exchange reactions in the presence of M(ClO₄)₂·6H₂O (M = Co, Ni, Zn) in CD₃CN to produce [(6-Ph₂TPA)M(CD₃CN)_n](X)₂, [Mn(3-Hfl)₂·0.5H₂O], and MnX₂ (X = OTf or ClO₄⁻). Under similar conditions, the 3-Hfl complexes of Co(II), Ni(II), and Cu(II) undergo flavonolate ligand exchange to produce [(6-Ph₂TPA)M(CD₃CN)_n](X)₂ (M = Co, Ni, Cu; n = 1 or 2) and [Zn(3-Hfl)₂·2H₂O]. An Fe(II) complex of 3-Hfl, [(6-Ph₂TPA)Fe(3-Hfl)]ClO₄ (**8**), was isolated and characterized by elemental analysis, FTIR, UV-vis, ¹H NMR, cyclic voltammetry, and a magnetic moment measurement. This complex reacts with O₂ to produce the diiron(III) μ-oxo compound [(6-Ph₂TPAFe(3-Hfl))₂(μ-O)](ClO₄)₂ (**6**).

Introduction

Flavonoids are polyphenolic compounds that are produced in plants.¹ One of these compounds, quercetin (Scheme 4-1), is found in many fruits and vegetables, and is of considerable current interest for its antioxidant and antimicrobial properties.^{2,3} In the soil



Scheme 4-1.

environment, fungal and bacterial quercetin dioxygenases catalyze oxidative carbon-carbon bond cleavage and CO release from a metal-coordinated quercetin in a 2,4-dioxygenolytic ring cleavage reaction. Fungal quercetinases are known to contain a mononuclear Cu(II) center and have been extensively investigated.⁴⁻⁹ Studies of a bacterial quercetinase from *Bacillus subtilis* (YxaG) showed that when this enzyme is produced in *E. coli* it will bind a variety of divalent metals, with the highest level of reactivity being found for Mn(II).^{10,11} Recent investigations of a quercetinase from *Streptomyces* sp. FLA expressed in *E. coli* revealed that this enzyme is most active in the presence of Ni(II), with the next highest level of activity being found with Co(II).¹²

The quercetinase enzymes from *Aspergillus japonicus* and *B. subtilis* have been characterized by X-ray crystallography.^{9,10} Both are members of the cupin superfamily of proteins (bicupins), with two well-separated active site metal centers, each having a ligand donor set comprised of three histidine donors and a glutamate ligand. In the structure of the copper-containing enzyme from *Aspergillus japonicus*, the copper centers exhibit two different geometries. One is a distorted tetrahedron comprised of three histidine donors and a water molecule, and in the other, a glutamate ligand (Glu73) is also coordinated in an axial position to give an overall distorted trigonal bipyramidal copper

center. These geometries are present in a ~70:30 ratio. EPR studies of the protein are consistent with this mixture of geometries also being present in solution. In the tetrahedral geometry, Glu73 acts as a hydrogen bond acceptor for the metal-bound water molecule. Coordination of quercetin to the copper center occurs in a monodentate fashion via the deprotonated C(3)-OH moiety, with Glu73 possibly acting as the active site base for substrate deprotonation.¹³ The overall geometry of the copper center in the enzyme/substrate adduct is distorted trigonal bipyramidal. A key feature of the coordinated quercetin is pyramidalization of the C(2) atom indicating increased sp^3 character that may stabilize radical formation in a reaction involving O_2 .

The *B. subtilis* enzyme was initially reported to be an Fe(II)-containing quercetin 2,3-dioxygenase,^{14,15} and was crystallized with Fe(II) present in both active sites of this bicupin enzyme.¹⁰ Both metal centers exhibit a coordination number of five, with three histidine donors, a glutamate, and a water molecule. The overall geometry of the Fe(II) center is distorted trigonal bipyramidal in the *N*-terminal active site and distorted square pyramidal in the C-terminal domain of the protein. Metal ion replacement studies of the *B. subtilis* enzyme (via reconstitution of the *apo* enzyme) indicated increased levels of activity for Mn(II)- and Co(II)-containing enzyme (35- and 24-fold, respectively) relative to that found for Fe(II). Based on this data, it has been suggested that Mn(II) may be the preferred metal cofactor for the *B. subtilis* enzyme. EPR studies of the Mn(II)-containing enzyme from *B. subtilis* suggest octahedral coordination of the metal center.¹¹

The quercetinase QueD from *Streptomyces* sp. FLA is a monocupin dioxygenase.¹⁶ When overexpressed in *E. coli*, this enzyme exhibited the highest level of

activity when Ni(II) and Co(II) salts were added to the LB medium.^{12,17} An increase in activity was not observed when Mn(II), Fe(II), Cu(II) or Zn(II) was added. EPR studies of the cobalt-containing enzyme indicate a high-spin ($S = 3/2$) Co(II) center in a trigonal bipyramidal or tetrahedral geometry in the resting state. EPR experiments performed in the presence of quercetin and O₂ revealed no evidence of a change in valency of the cobalt ion during substrate turnover.¹²

Different mechanistic pathways have been proposed for the spin-forbidden, O₂-dependent quercetin oxidation reaction depending on whether a redox active metal center is present in the active site of the enzyme. For Cu(II)-containing quercetinase enzymes, it is unlikely that O₂ will coordinate to the type II oxidized metal center, and the reaction is suggested to involve valence tautomerism between the Cu(II)-quercetin adduct and a Cu(I)-flavonoxy radical species, the latter of which can act as a one-electron reductant toward O₂. The pyramidalization of the C(2) center identified in the X-ray structure of the ES adduct of the *A. japonicus* enzyme suggests possible stabilization of the radical at this atom.¹³ For redox-active metal ions such as Mn(II), the metal center may serve as an electron conduit in an adduct wherein both the flavonolate and O₂ coordinate to the metal center prior to oxygen activation. Specifically, electron transfer from the metal center to coordinated O₂, with subsequent electron transfer from the coordinated quercetin monoanion to the oxidized metal center, would generate a quercetin radical-M(II)-O₂-species, from which C-C bond cleavage and CO release could proceed. This proposed mechanism is similar to the reaction pathway suggested for Fe(II)- and Mn(II)-containing extradiol catechol dioxygenases.¹⁸

Overall, from studies of the *A. japonicus*, *B. subtilis*, and *Streptomyces* sp. FLA quercetinases, possible roles for the divalent metal center in substrate oxidation have been suggested to include: (1) reduction of the pK_a of quercetin to enable substrate deprotonation, (2) stabilization of the flavonolate intermediate, (3) influence on the coordination mode (mono- versus bidentate) and redox potential of the bound flavonolate, (4) facilitation of the formation of radical character on the coordinated flavonolate via valence tautomerism, and (5) acting as a redox conduit for structures wherein both flavonolate and O_2 are coordinated to the metal center.

Model studies of copper-containing forms of quercetinases have demonstrated that both Cu(I) and Cu(II) flavonolate complexes undergo reaction with O_2 to produce CO and the deposite.¹⁹ Kinetic studies of the reaction involving the Cu(II) complex $[Cu(3-Hfl)_2]$ (3-Hfl = 3-hydroxyflavonolate) with O_2 in DMF indicate a rate law that is second-order overall ($-d[Cu(3-Hfl)_2]/dt = k_{obs}[Cu(3-Hfl)_2][O_2]$). In the presence of pyridine, the observed rate increases by ~ 2.5 -fold, which has been attributed to a change in the coordination mode of the flavonolate ligand from bidentate to monodentate. Model studies involving other divalent metal ions are considerably fewer in number. Catalytic oxygenation of 3-hydroxyflavone derivatives by bis(salicylidene)ethylenediaminatocobalt(II) ($[Co(salen)]$) at room temperature has been reported.²⁰ This catalysis occurs in the presence of DMSO and DMF, but not in methanol, THF, or CH_2Cl_2 . The involvement of a Co- O_2 complex in the reaction has been proposed. A Co(III) complex, $[Co(III)(salen)(4'MeOflaH)]$, was found to be susceptible to oxygenation in pyridine and DMF, but was found to be stable to oxygen in non-

coordinating solvents. This O₂ reactivity correlates with dissociation of the flavonolate ligand from the Co(III) center.^{21,22} Two recent studies outlined the structural and O₂ reactivity properties of Fe(III) and Mn(II) flavonolate complexes.^{23,24} Fe(III)(4'MeOflaH)₃ and Mn(II)(3-Hfl)₂(py)₂ were found to undergo reaction with O₂ at 100 °C in DMF with second-order rate constants of 0.50 M⁻¹s⁻¹ and 0.08 M⁻¹s⁻¹, respectively. On the basis of comparison of rate constants at 100 °C, these complexes are more reactive than the copper analogs Cu(3-Hfl)₂ (k = 0.0087 M⁻¹s⁻¹) and Cu(3-Hfl)₂(py)₂ (0.04 M⁻¹s⁻¹), suggesting a metal dependent reactivity order of Fe(III) > Mn(II) > Cu(II).²³ The Fe(III) complex Fe(III)(salen)(3-Hfl) contains a bidentate flavonolate ligand and undergoes reaction with O₂ at elevated temperatures (100-120 °C).²⁴ In the presence of excess carboxylate anion, the rate of reaction with O₂ increases, with bulky carboxylates (e.g. triphenyl acetate) producing the greatest rate enhancement (~two orders of magnitude at 100 °C). This is attributed to the formation of a more reactive monodentate flavonolatoiron(III) complex. Evidence for direct electron transfer from the flavonolate ligand to O₂ to form O₂⁻ was found in the reaction via the use of the superoxide scavenger nitroblue tetrazolium (NBT).

From the studies described above and investigations of the O₂ reactivity of non-coordinated flavonolate anions, it is clear that enhancing the electron density within the flavonolate anion through deprotonation and limiting its coordination mode to monodentate, are key factors in enhancing the rate of oxygenation. What it is currently unclear is how differences in the divalent metal ion present in quercetinase enzymes produce differing rates of oxygenation, as has been found for the *B. subtilis* and *Streptomyces* sp. FLA enzymes. Such differences may result from modulation of the

coordination mode and/or the redox potential of the flavonolate, or may relate to the ability of the metal center to serve as a redox conduit. As an approach toward systematically examining the influence of the divalent metal ion, we report the preparation and characterization of the first extensive series of structurally-related divalent metal flavonolate complexes. Our initial goal in this research was to examine how differences in the divalent metal center (Mn(II), Fe(II), Co(II), Ni(II), Cu(II), and Zn(II)) influence flavonolate coordination, and spectroscopic and redox properties. The choice of the tetradentate 6-Ph₂TPA ligand as the supporting scaffold was based on its relevance to the coordination environment in enzymes of the cupin superfamily.²⁵ We have previously used this ligand to study chemistry of relevance to Ni(II)-acireductone dioxygenase,²⁶⁻²⁹ another dioxygenase of the cupin superfamily that produces CO upon substrate oxygenation. The results presented herein indicate that the nature of the divalent metal ion influences the coordination mode and redox potential of a 3-hydroxyflavonolate ligand in complexes of the general formula [(6-Ph₂TPA)M(3-Hfl)]X (M = Mn(II), Co(II), Ni(II), Cu(II), Zn(II); X = OTf⁻ or ClO₄⁻). In the course of characterizing the Mn(II) complex, we found evidence for ligand exchange reactions, which were subsequently further explored. The Fe(II) flavonolate complex [(6-Ph₂TPA)Fe(3-Hfl)]ClO₄ was prepared and characterized, albeit an X-ray structure was not obtained. This is due to the fact that the complex is very O₂ sensitive and quickly undergoes reaction to produce a diiron(III) μ -oxo compound, wherein each iron center has a coordinated flavonolate ligand. The structure of this diiron(III) complex was determined by X-ray crystallography.

Experimental

General and Physical Methods. All chemicals were purchased from commercial sources and used as received unless otherwise noted. Synthetic reactions were performed in a MBraun Unilab glovebox under a N₂ atmosphere. Solvents for glovebox use were dried according to published methods and distilled under N₂ prior to use.³⁰ The 6-Ph₂TPA ligand was prepared as previously described.²⁵

¹H NMR spectra of **2-5** were obtained in CD₃CN solution on a Bruker ARX-400 spectrometer. Data was collected for paramagnetic complexes as previously described.²⁶ Chemical shifts (in ppm) are referenced to the residual solvent peak(s) in CHD₂CN (¹H, 1.94 (quintet) ppm). FTIR spectra were collected using KBr pellets on a Shimadzu FTIR-8400 spectrometer. UV-vis spectra were recorded at ambient temperature using a Hewlett-Packard 8453 diode array spectrophotometer. Cyclic voltammetry data was collected using a BAS-Epsilon system.²⁵ Conditions for the CV experiments are listed in a footnote of Table 4-5 and in the text. EPR spectra were collected on a Bruker EMX-Plus spectrometer fitted with a liquid helium cooled probe. ESI/APCI and MALDI mass spectral data for complexes was collected at the Mass Spectrometry Facility, University of California, Riverside. Room temperature magnetic susceptibilities were determined by the Evans method.³¹ Elemental analyses were performed by Atlantic Microlab, Inc., Norcross, GA.

*Caution! Perchlorate salts of metal complexes with organic ligands are potentially explosive. Only small amounts of material should be prepared, and these should be handled with great care.*³²

General Procedure for the Synthesis of [(6-Ph₂TPA)M(3-Hfl)]OTf

Complexes: (a) M = Mn (1-OTf), Cu (4-OTf), or Zn (5-OTf). In a N₂-filled glovebox, a methanol solution (2 mL) of M(OTf)₂ (1.37 x 10⁻⁴ mol) was added to solid 6-Ph₂TPA (1.37 x 10⁻⁴ mol) and the mixture was stirred until all of the chelate ligand had dissolved. The resulting solution was added to a methanol solution (2 mL) containing 3-Hfl (1.37 x 10⁻⁴ mol) and Me₄NOH·5H₂O (1.37 x 10⁻⁴ mol). The mixture was then allowed to stir overnight at ambient temperature. The reaction mixture was taken out of the glovebox and the solvent was removed under reduced pressure. The residual solid was suspended on the top of a celite plug and washed several times with distilled water. The wet solid was then dissolved in CH₂Cl₂ and the filtrate was collected and brought to dryness under reduced pressure. The residue was dissolved in CH₂Cl₂ and the analytically pure microcrystalline flavonolate complex was precipitated via the addition of excess Et₂O and cooling of the mixture at -30 °C for 12 h.

Note regarding experimental data: Extensive characterization data (FTIR, UV-vis, mass spectrometry, magnetic moment, cyclic voltammetry) for the triflate compounds **1-5-OTf** is provided in Table 4-5. Selected data for the perchlorate analogs **1-5-ClO₄**, which were primarily prepared for X-ray crystallographic studies, is given below.

[(6-Ph₂TPA)Mn(3-Hfl)]OTf (1-OTf). Yield: 73% (green crystals).

[(6-Ph₂TPA)Cu(3-Hfl)]OTf (4-OTf). Yield: 74% (dark green crystals).

[(6-Ph₂TPA)Zn(3-Hfl)]OTf (5-OTf). Yield: 98% (yellow crystals). ¹H NMR (CD₃CN, 400 MHz): δ 8.53 (d, *J* = 5.2 Hz, 1 H), 8.18 (dt, *J* = 7.3 Hz, *J* = 1.5 Hz, 2 H), 7.92 (td, *J* = 7.8 Hz, *J* = 7.7 Hz, *J* = 1.7 Hz, 1 H), 7.78 (t, *J* = 7.7 Hz, 2 H), 7.65 (m, 5 H), 7.39 (m, 11 H), 7.13 (dt, *J* = 6.8 Hz, *J* = 1.5 Hz, 4 H), 7.03 (tt, *J* = 7.4 Hz, *J* = 1.2 Hz, 2 H), 6.94 (tt, *J* = 8.0 Hz, *J* = 1.5 Hz, 4 H), 4.85 (d, *J* = 14.7 Hz, 2 H), 4.51 (d, *J* = 14.8 Hz, 2 H), 4.39 (s, 2 H); ¹³C{¹H} NMR (CD₃CN, 400 MHz): δ 187.7, 168.1, 164.0, 163.8, 162.9, 156.5, 154.6, 148.8, 147.6, 146.3, 141.1, 140.5, 137.4, 136.8, 136.1, 135.7, 135.6, 135.1, 134.8, 132.2, 131.9, 131.3, 130.9, 130.2, 130.1, 125.8, 125.2, 64.6, 61.5 (29 signals expected for equivalent phenyl-appended pyridyl donors; 29 observed).

(b) M = Co (2-OTf) or Ni (3-OTf). Under a nitrogen atmosphere, a methanol (~2 mL) solution of MCl₂·5H₂O (1.37 x 10⁻⁴ mol) was added to solid 6-Ph₂TPA (1.37 x 10⁻⁴ mol) and the mixture was stirred until all of the chelate ligand had dissolved. Two equivalents of silver triflate (AgOTf; 2.74 x 10⁻⁴ mol) was then added to the mixture. After stirring for 30 min, the solution was filtered through a celite/glass wool plug. The filtrate was added to a methanol solution (~2 mL) containing 3-Hfl (1.37 x 10⁻⁴ mol) and Me₄NOH·5H₂O (1.37 x 10⁻⁴ mol). The resulting solution was stirred overnight at ambient temperature. At this time, the reaction was taken out of the glovebox and the solvent was removed under reduced pressure. Using a work-up procedure identical to that described above for **1-OTf**, analytically pure microcrystalline products were obtained.

[(6-Ph₂TPA)Co(3-Hfl)]OTf (2-OTf). Yield: 54% (dark red crystals).

[(6-Ph₂TPA)Ni(3-Hfl)]OTf·0.25CH₂Cl₂ (3-OTf). Yield: 82% (green crystals).

The presence of dichloromethane in the elemental analysis sample was confirmed using ¹H NMR spectroscopy.

General Procedure for the Synthesis of [(6-Ph₂TPA)M(3-Hfl)]ClO₄ Complexes (1-5-ClO₄). In a glovebox, a acetonitrile solution (~2 mL) of M(ClO₄)₂·6H₂O (M = Mn, Co, Ni, Cu, Zn; 1.37 x 10⁻⁴ mol) was added to solid 6-Ph₂TPA (1.37 x 10⁻⁴ mol) and the resulting mixture was stirred until all of the chelate ligand had dissolved. An acetonitrile slurry (~2 mL) of tetramethylammonium hydroxide pentahydrate (Me₄NOH·5H₂O; 1.37 x 10⁻⁴ mol) and 3-hydroxyflavone (3-Hfl; 1.37 x 10⁻⁴ mol) was then added and the resulting mixture was stirred overnight at ambient temperature. After removal of the solvent under reduced pressure, the remaining solid was dissolved in CH₂Cl₂ and the solution was filtered through a glass wool/celite plug. The filtrate was then brought to dryness under reduced pressure. Crystals suitable for single crystal X-ray crystallography were obtained using the following approaches at ambient temperature: **1-ClO₄** (green crystals), diethyl ether diffusion into a dichloromethane solution; **2-ClO₄** (dark red crystals) and **3-ClO₄** (green crystals), diethyl ether diffusion into a acetonitrile solution; and **4-ClO₄** (green crystals), diethyl ether diffusion into dichloromethane:isopropanol:methanol (1:0.1:1) solution. For **5-ClO₄**, yellow crystals were obtained from dichloromethane/diethyl ether solution at 4 °C.

The ¹H NMR features of **2-ClO₄**, **3-ClO₄**, and **5-ClO₄** match those found for the triflate analogs. **1-ClO₄**: Anal. Calcd for C₄₅H₃₅ClMnN₄O₇·1/4CH₂Cl₂: C, 63.54; H, 4.18; N, 6.55. Found: C, 63.47; H, 4.11; N, 6.45. **2-ClO₄**: Anal. Calcd for C₄₅H₃₅ClCoN₄O₇

$\cdot 1/4\text{CH}_2\text{Cl}_2$: C, 63.77; H, 4.18; N, 6.59. Found: C, 4.03; H, 4.19; N, 6.54. **3-ClO₄**: Anal. Calcd for $\text{C}_{45}\text{H}_{35}\text{ClNi}_4\text{N}_4\text{O}_7$: C, 64.50; H, 4.21; N, 6.69. Found: C, 64.18; H, 3.92; N, 6.55. **4-ClO₄**: Anal. Calcd for $\text{C}_{45}\text{H}_{35}\text{ClCu}_4\text{N}_4\text{O}_7 \cdot 1/5\text{CH}_2\text{Cl}_2$: C, 63.14; H, 4.30; N, 6.52. Found: C, 63.45; H, 4.15; N, 6.31. **5-ClO₄**: Anal. Calcd for $\text{C}_{45}\text{H}_{35}\text{ClZn}_4\text{N}_4\text{O}_7 \cdot 1/5\text{CH}_2\text{Cl}_2$: C, 63.01; H, 4.14; N, 6.50. Found: C, 63.15; H, 4.31; N, 6.33.

[(6-Ph₂TPA)Fe(NCCH₃)](ClO₄)₂ (7). A CH₃CN solution (~ 2mL) of Fe(ClO₄)₂·6H₂O (0.030 g, 0.083 mmol) was added to solid 6-Ph₂TPA. The resulting solution was stirred for 1 h at room temperature under a N₂ atmosphere. The solvent was then removed under reduced pressure and the remaining solid product was recrystallized via Et₂O diffusion into a CH₃CN solution. Yellow crystals suitable for single crystal X-ray analysis and yellow powder were isolated from a blue solution. Yield: 73%. Anal Calcd. for $\text{C}_{32}\text{H}_{29}\text{N}_5\text{FeCl}_2\text{O}_8 \cdot \text{H}_2\text{O}$: C, 50.81; H, 4.13; N, 9.26. Found: C, 51.03; H, 3.99; N, 9.35. FTIR (KBr, cm⁻¹) 1092 (ν_{ClO₄}), 623 (ν_{ClO₄}); UV-vis (CH₃CN, nm) 509, 892. LRFAB-MS (CH₂Cl₂/NBA), *m/z* (relative intensity), 597 ([[(6-Ph₂TPA)Fe(ClO₄)]⁺ 15%).

Table 4-1. Summary of ¹H NMR of **7** in CD₃CN:

α, CH ₂	β	β'	Ph	γ	γ'
112	61.1	59.8	10.2	-8.5	-11.8
99.4	60.2	44.1	4.7		
82.4			2.5		
60					

Ligand Exchange Reactions. (a) To a solution of [(6-Ph₂TPA)Mn(3-Hfl)]OTf (9.0 x 10⁻⁶ mol) in CD₃CN (0.8 mL) solid M(ClO₄)₂·6H₂O (M = Co, Ni, or Zn; 9.0 x 10⁻⁶ mol) was added. Each reaction mixture was then capped, shaken vigorously, and a ¹H

NMR spectrum was recorded within 15 min. For each metal perchlorate salt, the NMR spectrum is consistent with the formation of $[(6\text{-Ph}_2\text{TPA})\text{M}(\text{CD}_3\text{CN})_n](\text{ClO}_4)_2$ ($\text{M} = \text{Co}$ ($n = 1$), Ni ($n = 2$), or Zn ($n = 1$)). The product $[\text{Mn}(3\text{-Hfl})_2 \cdot 0.5\text{H}_2\text{O}]$ is formed in each reaction, and was isolated from the Ni(II)-containing reaction mixture and characterized by elemental analysis, FTIR, and UV-vis.

(b) In a NMR tube, a CD_3CN solution (0.8 mL) of $[(6\text{-Ph}_2\text{TPA})\text{M}(3\text{-Hfl})]\text{OTf}$ ($\text{M} = \text{Co}$, Ni , and Cu ; **2-4-OTf**; 7.7×10^{-6} mol) was treated with solid 0.5 eq $\text{Zn}(\text{ClO}_4)_2 \cdot 6\text{H}_2\text{O}$ (3.9×10^{-6} mol). Each reaction mixture was then capped, shaken vigorously, and a ^1H NMR spectrum was recorded within 15 min. For the reactions involving the Co(II) and Ni(II) derivatives, the ^1H NMR spectroscopic features are consistent with the formation of $[(6\text{-Ph}_2\text{TPA})\text{M}(\text{CD}_3\text{CN})_n](\text{X})_2$ ($\text{M} = \text{Ni}$, $n = 2$; $\text{M} = \text{Co}$, $n = 1$; $\text{X} = \text{OTf}^-$ or ClO_4^-). A poorly soluble, yellow precipitate is also formed in each reaction mixture. Spectroscopic analysis (^1H NMR (CD_3OD) and FTIR (KBr)) of this solid suggested the formation of $[\text{Zn}(3\text{-Hfl})_2]$. This compound was independently synthesized via treatment of $\text{Zn}(\text{ClO}_4)_2 \cdot 6\text{H}_2\text{O}$ with two equivalents each of 3-Hfl and $\text{Me}_4\text{NOH} \cdot 5\text{H}_2\text{O}$ in methanol, which yielded a yellow precipitate. Analysis of this material by ^1H NMR (CD_3OD), UV-vis, and elemental analysis indicated the formulation $[\text{Zn}(3\text{-Hfl})_2 \cdot 2\text{H}_2\text{O}]$. The UV-vis and ^1H NMR spectroscopic features of this material match that of the yellow precipitate generated in the ligand exchange reaction.

Synthesis of $[(6\text{-Ph}_2\text{TPA})\text{Fe}(3\text{-Hfl})]\text{ClO}_4$ (8). Under a nitrogen atmosphere, a methanol solution (~ 2 mL) of $\text{Fe}(\text{ClO}_4)_2 \cdot 6\text{H}_2\text{O}$ (1.37×10^{-4} mol) was added to solid 6- Ph_2TPA (1.37×10^{-4} mol) and the resulting mixture was stirred for 2 h at ambient

temperature. The solvent was then removed under reduced pressure, and the solid was dissolved in a small amount of methanol (~1 mL). Addition of Et₂O produced a yellow-orange precipitate, which was dried under vacuum. A ¹H NMR spectrum of the complex in CD₃CN was obtained. This spectrum matched that of [(6-Ph₂TPA)Fe(CH₃CN)](ClO₄)₂, which has been independently generated and characterized. A methanol solution (~2 mL) of [(6-Ph₂TPA)Fe(CH₃CN)](ClO₄)₂ (1.37 x 10⁻⁴ mol) was treated with 3-Hfl (1.37 x 10⁻⁴ mol) and Me₄NOH·5H₂O (1.37 x 10⁻⁴ mol) dissolved in methanol (~2 mL). The resulting mixture was stirred for 15 minutes and the solvent was then removed under vacuum. The remaining green-yellow solid was dissolved in CH₂Cl₂ (~2 mL) and passed through a celite/glass wool plug. The filtrate was brought to dryness under reduced pressure, and the resulting solid (yield: 96%) was analyzed by ¹H NMR, FTIR, UV-vis, a magnetic moment measurement, and elemental analysis. FTIR (KBr, cm⁻¹) 1558 (ν_{C=O}); UV-vis (CH₃CN) nm (ε, M⁻¹cm⁻¹) 415 (14700); μ_{eff} = 4.7 μB. Anal. Calcd for C₄₅H₃₅ClFeN₄O₇: C, 64.72; H, 4.22; N, 6.71. Found: C, 65.23; H, 4.22; N, 6.71.

Reactivity of [(6-Ph₂TPA)Fe(3-Hfl)]ClO₄ in Air; Isolation of [(6-Ph₂TPA)Fe(3-Hfl)₂(μ-O)](ClO₄)₂ (6). A methanol solution (~2 mL) of [(6-Ph₂TPA)Fe(3-Hfl)]ClO₄ was prepared by mixing equimolar amounts (1.37 x 10⁻⁴ mol) of 6-Ph₂TPA, Fe(ClO₄)₂·6H₂O, Me₄NOH·5H₂O and 3-Hfl and stirring under a nitrogen atmosphere for 2 h. The solvent was then removed under reduced pressure and the remaining solid was dissolved in CH₂Cl₂ (~2 mL) and filtered through a celite/glass wool plug. The filtrate was then brought to dryness. A portion of the solid (8.45 x 10⁻⁵ mol) was dissolved in CH₃CN (~5 mL) and this solution was exposed to air for 24 h. Diethyl ether was then

diffused into the CH₃CN solution, resulting in the deposition of dark-brown crystals suitable for single crystal X-ray crystallography. Yield: 58%. UV-vis (MeOH), nm (ϵ , M⁻¹cm⁻¹) 388 (24400), 490 (7300); ESI/APCI-MS, m/z (relative intensity) 743.2 ([M-2ClO₄]²⁺, 30%). Anal. Calcd for: C₉₀H₇₀Cl₂Fe₂N₈O₁₅·2H₂O: C, 62.77; H, 4.33; N, 6.51. Found: C, 62.96; H, 4.19; N, 6.70.

X-ray Crystallography. For each compound, **1-5-ClO₄** and **6**, a single crystal was mounted on a glass fiber with traces of viscous oil and then transferred to a Nonius KappaCCD diffractometer equipped with Mo K α radiation ($\lambda = 0.71073 \text{ \AA}$) for data collection. For unit cell determination, ten frames of data were collected at 150(1) K with an oscillation range of 1 deg/frame and an exposure time of 20 sec/frame. Final cell constants were determined from a set of strong reflections from the actual data collection. Reflections were indexed, integrated, and corrected for Lorentz, polarization, and absorption effects using DENZO-SMN and SCALEPAC.³³ The structures were solved by a combination of direct and heavy-atom methods using SIR 97.³⁴ All of the non-hydrogen atoms were refined with anisotropic displacement coefficients. Unless otherwise stated, all hydrogen atoms were assigned isotropic displacement coefficients $U(\text{H}) = 1.2U(\text{C})$ or $1.5U(\text{C}_{\text{methyl}})$, and their coordinates were allowed to ride on their respective carbons using SHELXL97.³⁵

Structure Solution and Refinement. Complex **1-ClO₄** crystallizes in the space group $P2_1/n$, with a disordered ClO₄⁻ molecule in the asymmetric unit. Complex **2-ClO₄** crystallizes in the space group $C2/c$ with two cation/anion pairs per asymmetric unit along with two molecules of CH₃CN. The differences in the cations (with the second being

labeled with (A)) are subtle, with the most noticeable differences being in one Co-NPhPy bond distance and in O-Co-N bond angles involving the O(1) atom of the flavonolate and nitrogen atoms of the chelate ligand. One of the two CH₃CN solvate molecules is comprised of two 50% occupied positions for all heavy atoms. Complex **3-ClO₄** crystallizes in the space group *P2₁/a*. Two oxygen atoms of the perchlorate anion exhibit disorder (80:20) over two positions. Complex **4-ClO₄** crystallizes in the space group *P2₁/c*. One molecule of diethyl ether is also present in the asymmetric unit. Complex **5-ClO₄** crystallizes in the space group *P-1*. Two independent cation/anion pairs and two CH₂Cl₂ solvent molecules are found in the asymmetric unit. The two cations (with the second being labeled with (A)) have very minor differences in bond lengths/angles involving the Zn(II) center and both exhibit a distorted square pyramidal geometry ($\tau = 0.35$).³⁶ One CH₂Cl₂ solvate exhibits disorder over two positions (50:50) for each heavy atom. Complex **6** crystallizes in the space group *P-1* with 2.5 CH₃CN solvate molecules per asymmetric unit. Two oxygen atoms and the chlorine atom of a perchlorate anion are disordered over two positions (90:10).

Results

The goal of this investigation was to prepare and comprehensively characterize a structurally similar set of divalent metal flavonolate complexes as a prelude to O₂ reactivity studies of these complexes. The metal ions employed are those of relevance to bacterial and fungal quercetin dioxygenases (Mn(II), Fe(II), Co(II), Ni(II), Cu(II)). For

spectroscopic and redox behavior comparisons, the d^{10} Zn(II) flavonolate analog complex was also prepared.

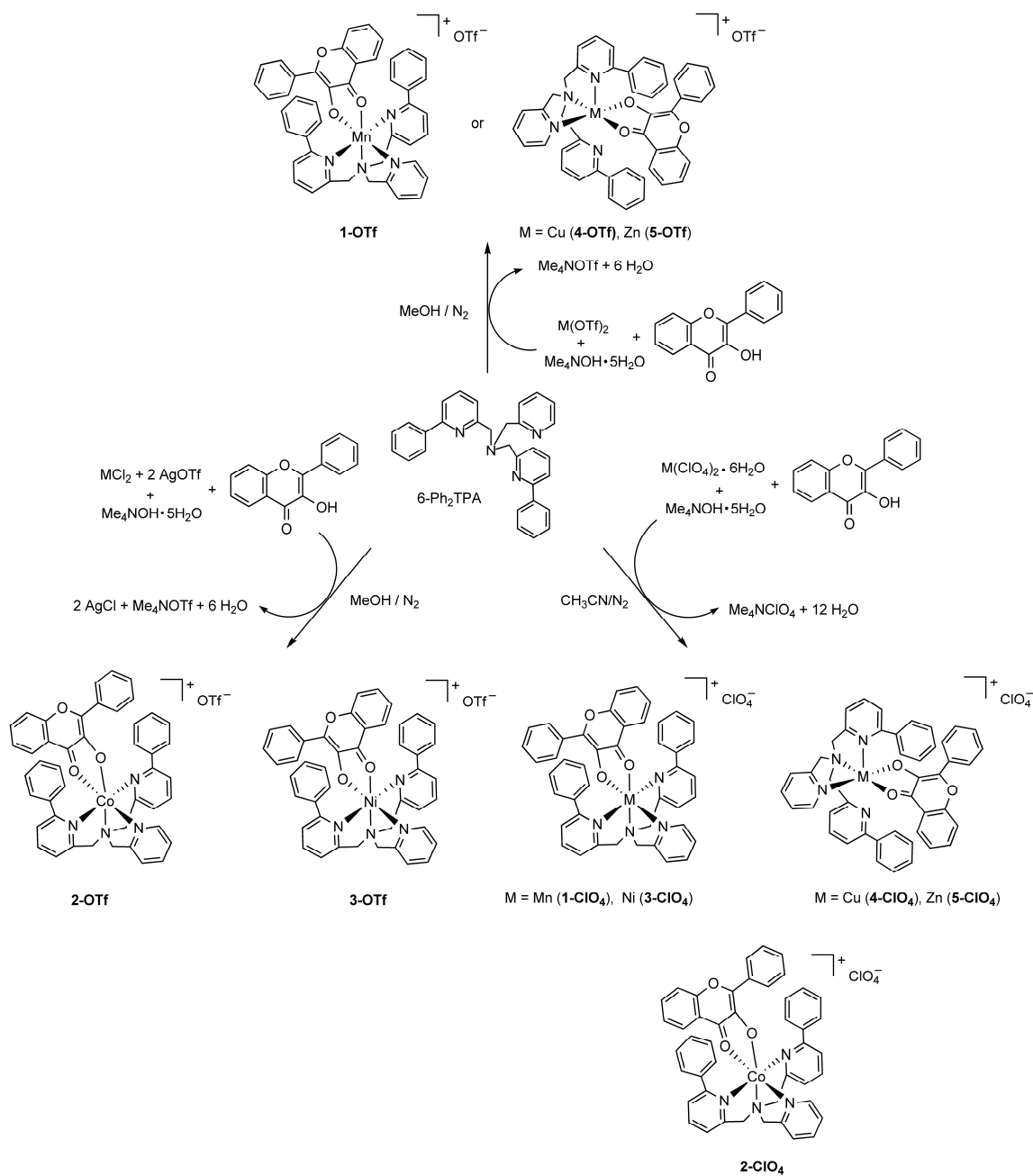
Synthesis. Divalent metal flavonolate complexes of the general formula [(6-Ph₂TPA)M(3-Hfl)]X were prepared by the synthetic routes outlined in Scheme 4-2. Triflate derivatives were isolated as analytically pure polycrystalline materials. Perchlorate analogs were found to be highly crystalline materials suitable for single crystal X-ray crystallography. All syntheses were performed under a N₂ atmosphere.

X-ray Crystallography. The perchlorate analogs **1-5-ClO₄** were characterized by single crystal X-ray crystallography. A summary of the data acquisition and refinement parameters are given in Table 4-2. Selected bond distances and angles are given in Tables 4-3 and 4-4, respectively.

Thermal ellipsoid drawings of the Mn(II) (**1-ClO₄**) and Ni(II) (**3-ClO₄**) complexes are shown in Figure 4-1. Each metal center exhibits a pseudo-octahedral geometry with the ketone oxygen (O(2)) of the flavonolate positioned *trans* to the tertiary amine nitrogen of the chelate ligand. In both complexes, the flavonolate ligand is located between the two hydrophobic phenyl appendages of the chelate ligand.

To our knowledge, complex **1-ClO₄** is the first Mn(II) complex of the 6-Ph₂TPA ligand to exhibit coordination of both phenyl-appended pyridyl donors. Complexes having an additional bidentate ligand, such as the hydroxamate complex [(κ^3 -6-Ph₂TPAMn)₂(μ -ONHC(O)CH₃)₂](ClO₄)₂²⁵ and the oxalate derivative [(κ^3 -6-Ph₂TPAMn)₂(μ -C₂O₄)](ClO₄)₂,³⁷ have previously been found to exhibit κ^3 -coordination (facial and meridional, respectively) of the chelate ligand, with one non-coordinated phenylpyridyl

appendage. In **1-ClO₄**, the Mn(1)-O(1) and Mn(1)-O(2) distances (2.121(3) Å and 2.143(3) Å, respectively) are similar.



Scheme 4-2.

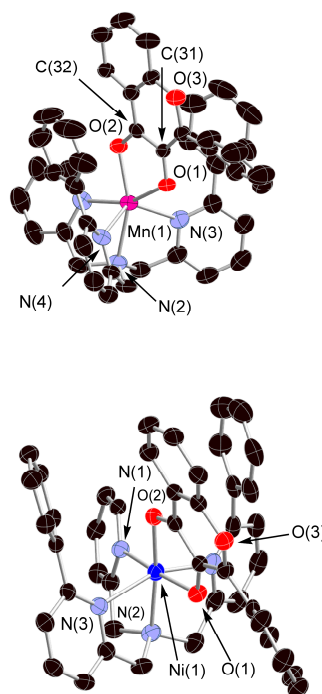


Figure 4-1. Thermal ellipsoid drawings (50% probability) of the cationic portions of **1-ClO₄** (top) and **3-ClO₄** (bottom). Hydrogen atoms have been omitted for clarity.

In the only other Mn(II) complex of 3-hydroxyflavonolate reported to date, [(Mn(3-Hfl)₂(py)₂],²³ the Mn-O distances differ by ~0.06 Å, with the bond involving the ketone oxygen being longer. The average Mn-O distance in **1-ClO₄** (2.13 Å) is shorter than that found in [(Mn(3-Hfl)₂(py)₂] (2.16 Å).²³ The average Mn-N distance in **1-ClO₄** is ~2.33 Å, which is similar to that found in [(κ³-6-Ph₂TPAMn)₂(μ-ONHC(O)CH₃)₂](ClO₄)₂²⁵ and [(κ³-6-Ph₂TPAMn)₂(μ-C₂O₄)](ClO₄)₂.³⁷

The mononuclear **3-ClO₄** is structurally similar to Ni(II) acetohydroxamate and enolate complexes of the 6-Ph₂TPA ligand.^{25,28} For example, the average Ni-O and Ni-N_{PhPy}, as well as the N_{Py} and N_{Amine} distances (Table 4-3) are similar in these complexes.

The Ni(1)-O(1) distance (1.996(2) Å) is slightly shorter than the distance involving the ketone oxygen atom (Ni(1)-O(2), 2.010(3) Å). In the only other Ni complex of 3-hydroxyflavonolate reported to date, [(Ni(3-Hfl)₂(py)₂]³⁸, the Ni-O distances are slightly longer (2.023(2) and 2.067(2) Å). The structure of the Co(II) complex [(6-Ph₂TPA)Co(3-Hfl)]ClO₄ (**2-ClO₄·2CH₃CN**) contains two independent cation/anion pairs per asymmetric unit (the second labeled with an “A” designation). The two cations are structurally similar, each having a pseudo-octahedral geometry (Figure 4-2). Unlike the Mn(II) and Ni(II) analogs (**1-ClO₄** and **3-ClO₄**), this complex has the deprotonated oxygen atom of the 3-Hfl ligand positioned *trans* to the tertiary amine nitrogen atom of the chelate ligand and exhibits notably different Co-O distances (Co(1)-O(1) 1.956(2) Å; Co(1)-O(2), 2.172(2) Å). This is similar to the bidentate ligand coordination present in the Co(II) acetohydroxamate complex [(6-Ph₂TPA)Co(ONHC(O)CH₃)]ClO₄, which exhibits Co-O bond lengths of 1.935(2) and 2.142(2) Å.²⁵

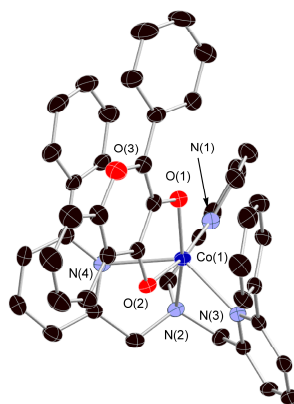


Figure 4-2. Thermal ellipsoid drawing (50% probability) of the cationic portion of one of the two cations present in the asymmetric unit of **2-ClO₄·2CH₃CN**. Hydrogen atoms have been omitted for clarity.

Table 4-2. Summary of X-ray Data Collection and Refinement.

	1-ClO ₄	2-ClO ₄ ·2CH ₃ CN	3-ClO ₄	4-ClO ₄ ·Et ₂ O	5-ClO ₄ ·2CH ₂ Cl ₂
Empirical formula	C ₄₅ H ₃₅ ClMnN ₄ O ₇	C ₉₄ H ₇₆ Cl ₂ Co ₂ N ₁₀ O ₁₄	C ₄₅ H ₃₅ ClN ₄ NiO ₇	C ₄₉ H ₄₅ ClCuN ₄ O ₈	C ₉₄ H ₇₄ Cl ₆ N ₈ O ₁₄ Zn ₂
M _r	834.16	1758.41	837.93	916.88	1859.04
Crystal system	Monoclinic	Monoclinic	Monoclinic	Monoclinic	Triclinic
Space group	<i>P</i> 2 ₁ / <i>n</i>	<i>C</i> 2/ <i>c</i>	<i>P</i> 2 ₁ / <i>a</i>	<i>P</i> 2 ₁ / <i>c</i>	<i>P</i> -1
<i>a</i> / Å	11.6175(8)	43.8551(6)	18.5881(4)	17.7565(6)	11.6633(2)
<i>b</i> / Å	16.3708(14)	18.27219(2)	19.6427(4)	12.6011(2)	18.3461(3)
<i>c</i> / Å	20.6689	21.2336(3)	10.4897	19.0305(6)	20.3958(3)
α / °	90	90	90	90	103.0861(8)
β / °	94.219(5)	101.7509(8)	90.4537(11)	90.0709(12)	90.5675(9)
γ / °	90	90	90	90	98.3257(9)
<i>V</i> / Å ³	3920.3(5)	16658.4(4)	3829.88(13)	4258.1(2)	4201.95(12)
<i>Z</i>	4	8	4	4	2
<i>D_c</i> / Mg m ⁻³	1.413	1.402	1.453	1.430	1.469
<i>T</i> / K	150(1)	150(1)	150(1)	150(1)	150(1)
Color	Yellow	Brown	Yellow/Green	Green	Yellow
Crystal habit	Prism	Plate	Dichroic Prism	Prism	Prism
Crystal size/ mm	0.38 × 0.13 × 0.13	0.38 × 0.38 × 0.20	0.35 × 0.18 × 0.10	0.25 x 0.23 x 0.05	0.28 x 0.28 x 0.15
Diffractometer	Nonius KappaCCD	Nonius KappaCCD	Nonius KappaCCD	Nonius KappaCCD	Nonius KappaCCD
μ / (mm ⁻¹)	0.464	0.536	0.636	0.638	0.833
2 θ max / °	50.02	54.96	54.98	50.74	52
Completeness to θ (%)	97.8	99.9	99.2	98.8	99.2
Reflections collected	10543	36402	15907	14181	30941
Independent reflections	6770	19074	8729	7731	16397
<i>R</i> _{int}	0.0623	0.0519	0.0410	0.0377	0.0519
Variable parameters	552	1084	532	568	1127
<i>R</i> 1 / <i>wR</i> 2 ^b	0.0640/0.1367	0.0562/0.1411	0.0576/0.1087	0.0646/0.1564	0.0458/0.1011
Goodness-of-fit (F2)	1.043	1.027	1.036	1.029	1.027
$\Delta\rho_{\max/\min}$ / e Å ⁻³	0.415/-0.304	1.181/-0.760	0.744/-0.672	1.093/-0.772	0.709/-0.726

^aRadiation used: Mo K α ($\lambda = 0.71073$ Å) ^b $R1 = \sum ||F_o| - |F_c|| / \sum |F_o|$; $wR2 = [\sum [w(F_o^2 - F_c^2)^2] / [\sum (F_o^2)^2]]^{1/2}$, where $w = 1 / [\sigma^2(F_o^2) + (aP)^2 + bP]$.

Table 4-3. Selected Bond Distances (Å) for Complexes **1-5-ClO₄**.

	1-ClO₄	2-ClO₄ ·2CH₃CN^a	3-ClO₄	4-ClO₄·Et₂O	5-ClO₄ ·2CH₂Cl₂^a
M–N(1)	2.284(4)	2.111(3)	2.061(2)	1.993(3)	2.085(2)
M–N(2)	2.340(3)	2.175(2)	2.067(3)	2.029(3)	2.144(2)
M–N(3)	2.390(3)	2.244(2)	2.278(2)	2.340(3)	2.107(2)
M–N(4)	2.338(3)	2.331(3)	2.231(2)		
M–O(1)	2.121(3)	1.956(2)	1.996(2)	1.921(3)	1.951(2)
M–O(2)	2.143(3)	2.172(2)	2.031(2)	2.010(3)	2.1175(19)
Δ _{M-o}	0.022	0.22	0.035	0.089	0.17
C(31)–O(1)	1.313(4)	1.317(4)	1.315(3)	1.349(5)	1.315(3)
C(32)–O(2)	1.262(5)	1.260(4)	1.267(3)	1.252(5)	1.255(3)

^aData for one of two cations present in the asymmetric unit.**Table 4-4.** Selected Bond Angles (deg) for Complexes **1-5-ClO₄**.

	1-ClO₄	2-ClO₄·2CH₃CN^a	3-ClO₄	4-ClO₄·Et₂O	5-ClO₄·2CH₂Cl₂^a
O(1)–M–O(2)	75.15(10)	79.81(8)	82.95(8)	84.27(13)	81.73(8)
N(1)–M–O(1)	159.22(12)	91.14(9)	172.29(9)	98.47(14)	102.36(9)
N(1)–M–O(2)	82.14(12)	169.84(9)	99.77(9)	166.64(13)	147.28(8)
N(1)–M–N(2)	72.07(13)	76.66(10)	83.05(10)	84.17(14)	81.18(9)
N(1)–M–N(3)	103.35(12)	105.45(10)	98.73(9)	102.15(13)	108.81(9)
N(1)–M–N(4)	99.40(13)	101.11(9)	81.10(9)		
N(2)–M–N(3)	74.56(13)	77.37(9)	77.36(9)	77.24(12)	79.91(9)
N(2)–M–N(4)	69.16(12)	71.48(9)	80.88(10)		
N(2)–M–O(1)	128.54(11)	161.56(9)	95.33(9)	172.93(14)	164.64(9)
N(2)–M–O(2)	154.14(12)	110.92(9)	171.21(9)	91.68(13)	87.35(8)
N(3)–M–N(4)	128.10(12)	132.59(9)	158.08(9)		
N(3)–M–O(1)	86.95(11)	119.73(9)	88.22(8)	108.43(12)	112.38(8)
N(3)–M(1)–O(2)	114.42(12)	83.24(8)	93.95(8)	89.24(12)	99.07(8)
N(4)–M(1)–O(1)	87.74(11)	97.96(9)	91.21(9)		
N(4)–M(1)–O(2)	114.48(11)	75.85(8)	107.73(9)		

^aData for one of two cations present in the asymmetric unit.

The average Co-N_{PhPy} distance is notably longer in **2-ClO₄·2CH₃CN** (av 2.39 Å) versus the hydroxamate complex (av 2.27 Å), while the Co-N_{Amine} and Co-N_{Py} distances are similar. A search of the Cambridge Crystallographic Database (version 5.30 (November)) revealed that **2-ClO₄** is the first structurally characterized Co(II) flavonolate complex. One Co(III) flavonolate complex has been previously characterized by X-ray crystallography.³⁹

The cationic portions of the Cu(II) and Zn(II) analogs **4-ClO₄·Et₂O** and **5-ClO₄·2CH₂Cl₂** are shown in Figure 4-3. The Cu(II) center in **4-ClO₄·Et₂O** is distorted

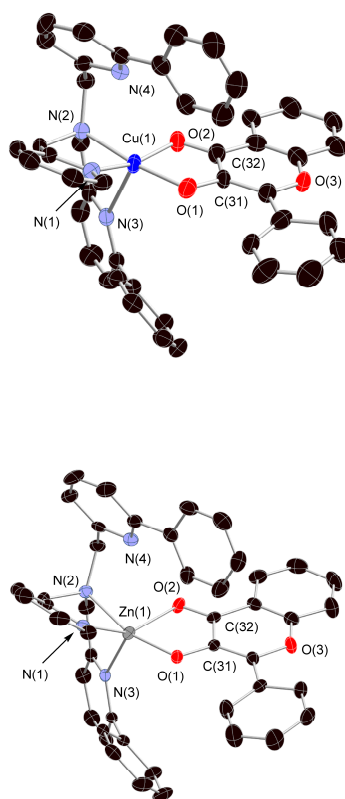


Figure 4-3. Thermal ellipsoid drawings (50% probability) of the cationic portions of **4-ClO₄·Et₂O** (top) and **5-ClO₄·2CH₂Cl₂** (bottom). Hydrogen atoms have been omitted for clarity.

square pyramidal ($\tau = 0.11$).³⁶ For the Zn(II) complex, there are two cation/anion pairs per asymmetric unit. The cations have only minor differences in bond lengths/angles involving the Zn(II) center and both exhibit a distorted square pyramidal geometry ($\tau = 0.35$).³⁶ The overall features of 6-Ph₂TPA chelate ligand coordination in the cationic portions of **4-ClO₄·Et₂O** and **5-ClO₄·2CH₂Cl₂** differ in terms of the M-N_{PhPy} distance, which is ~0.24 Å longer in the Cu(II) complex, and the M-N_{Py} and M-N_{Amine} distances which are > 0.05 Å longer in the Zn(II) complex. In both **4-ClO₄·Et₂O** and **5-ClO₄·2CH₂Cl₂** the coordination of the flavonolate ligand involves a shorter bonding interaction between the metal and the deprotonated hydroxyl donor (1.921(3) and 1.951(2) Å, respectively) and a longer bond with the ketone oxygen (2.010(3) and 2.1175(19) Å, respectively). Several Cu(II) complexes having a 3-hydroxyflavonolate ligand have been previously characterized by X-ray crystallography.⁴⁰⁻⁴⁶ A portion of these compounds have a bidentate or tridentate supporting chelate ligand,⁴⁰⁻⁴³ whereas others are species such as [Cu(3-Hfl)₂(py)₂] and [Cu(3-Hfl)₂]. In these two types of complexes, the Cu-O bond distances are generally in the range of 1.90-2.21 Å, and the Δ_{M-O} varies from 0.04 to 0.29 Å.⁴⁷ For Zn(II), three 3-Hfl complexes, having either a bidentate or tridentate supporting chelate ligand, have been previously reported.⁴⁸⁻⁵⁰ These complexes exhibit a range of Zn-O distances of 1.98-2.24 Å and Δ_{M-O} values of 0.16-0.26 Å. The bond lengths and Δ_{M-O} values for **4-ClO₄·Et₂O** and **5-ClO₄·2CH₂Cl₂** fall within the noted ranges.

Considering the entire series of 6-Ph₂TPA-supported complexes, the asymmetry in terms of the M-O interactions in **5-ClO₄·2CH₂Cl₂** ($\Delta_{M-O} \sim 0.17 \text{ \AA}$) is slightly less than that found in the Co(II) derivative **2-ClO₄** ($\Delta_{M-O} \sim 0.21 \text{ \AA}$), considerably greater than that found in the Mn(II) and Ni(II) analogs ($\Delta_{M-O} < 0.04 \text{ \AA}$), and approximately double that found in the Cu(II) complex ($\Delta_{M-O} \sim 0.09 \text{ \AA}$). Hence, in the series of 6-Ph₂TPA supported complexes, the asymmetry of flavonolate coordination increases in the order Mn (II) ~ Ni(II) < Cu(II) < Zn(II) < Co(II). Examination of the bond lengths within the coordinated flavonolate ligands of **1-5-ClO₄** revealed that the Mn(II), Co(II), Ni(II), and Zn(II) complexes exhibit only a slight elongation (0.02-0.03 \AA) of the C(32)-O(2) bond involving the ketone moiety, and a slight contraction ($\sim 0.04 \text{ \AA}$) of the C(31)-O(1) bond of the hydroxyl donor, relative to the distances found in uncoordinated flavonol (1.232(3) and 1.357(3) \AA , respectively).⁵¹ The Cu(II) analog **4-ClO₄·Et₂O** exhibits C-O distances (C(32)-O(2) 1.252(5) \AA ; C(31)-O(1), 1.349(5) \AA) that are quite close to those of the free flavonol.⁵¹ Notably, the Cu(II) complex exhibits a short C(31)-C(32) bond (1.399(6) \AA) relative to that found in the other 6-Ph₂TPA-supported complexes (av 1.45 \AA). A similar short C-C bond length was found in [Cu(II)(bpy)(3-Hfl)(2-HOC₆H₄COCO₂)] (1.369(14) \AA),⁴¹ but other known Cu(II) flavonolate derivatives exhibit a distance of $\sim 1.44 \text{ \AA}$.⁴²⁻⁴⁶ Overall, the bond lengths within the flavonolate ligands of **1-5-ClO₄** are minimally affected by the identity of the metal ion present.

Spectroscopic, Magnetic, and Redox Properties of 1-5-OTf. Presented in Table 4-5 are selected spectroscopic features of **1-5-OTf**. Also given are magnetic moments, which indicate that each complex has a high-spin divalent metal center, and redox

features identified in the range of +1.4 V to -1.0 V. ^1H NMR spectra were also collected for the Co(II), Ni(II), and Zn(II) complexes.

Infrared Spectroscopy. In the solid state, each complex exhibits a $\nu_{\text{C=O}}$ vibration for the coordinated flavonolate ketone moiety. The highest energy $\nu_{\text{C=O}}$ is found for the cobalt complex **2-OTf**, which is consistent with the fact that the perchlorate analog has the longest M(1)-O(2) distance of the series of complexes and therefore should polarize the carbonyl to the weakest extent. That being said, we note that the C(32)-O(2) bond lengths throughout the series **1-5-ClO₄** are the same within experimental error. The Cu(II) complex **4-OTf** exhibits the lowest energy $\nu_{\text{C=O}}$ vibration, which is consistent with the structural data for **4-ClO₄**, which has the shortest M(1)-O(2) distance of the series of complexes.

Table 4-5. Analytical, Spectroscopic, Magnetic, and Cyclic Voltammetry Data for **1-5-OTf**.

Complex	1-OTf	2-OTf	3-OTf -0.25CH ₂ Cl ₂	4-OTf	5-OTf
Anal. Calcd. (found):	62.51 (62.05)	62.23 (61.94)	61.11 (61.06)	61.91 (62.02)	61.78 (61.74)
C:	3.99 (4.06)	3.97 (3.89)	3.97 (4.04)	3.95 (3.98)	3.94 (4.01)
H:	6.34 (6.16)	6.31 (6.11)	6.31 (5.86)	6.28 (6.21)	6.28 (6.30)
N:					
UV-vis, nm	431 (17600)	422 (17100)	443 (20000)	428 (22200)	420 (20100)
(ϵ , M ⁻¹ cm ⁻¹) ^a					
ESI-MS m/z (rel intensity)	734.2059 (100) ^b	738.2037 (16)	737.2064 (15)	742.2002 (16)	743.1984 (2)
[M-OTf] ⁺					
FTIR ^c , cm ⁻¹ $\nu_{\text{C=O}}$	1550	1557	1548	1542	1552
μ_{eff} , μB^d	5.90	4.38	3.34	1.93	^e
E_{p}^f versus Fc/Fc ⁺	+365	^g	+506	+660 ^h	+534

^aSpectra collected in dry CH₃CN. ^bObtained by MALDI. ^cSpectra collected as dilute KBr pellets. ^dDetermined by Evans method (Evans D. F. J. Chem. Soc. **1959**, 115, 2003). ^eDiamagnetic. ^fAll cyclic voltammetry data was obtained under argon in CH₂Cl₂ with a complex concentration of 1 mM and Bu₄NClO₄ (0.1 M) as the supporting electrolyte. The scan rate was 50-100 mV/s. The experimental set-up consisted of a platinum button working electrode, a silver wire reference electrode, and a platinum wire auxiliary electrode. All potentials are reported relative to an internal Fc/Fc⁺ standard. Under these conditions, the Fc/Fc⁺ couple is at +460 mV versus silver wire. ^gNo electrochemical behavior between +1.4 V and -1.0 V. ^hA quasi-reversible reduction peak at -1088 mV vs. Fc/Fc⁺ has been tentatively assigned to the Cu(II)/Cu(I) couple as no other compound of the group has waves at potentials lower than Fc/Fc⁺.

UV-vis Spectroscopy. Neutral flavonol compounds exhibit an absorption feature in the range of 350-380 nm, which is termed band I and is assigned to the $\pi \rightarrow \pi^*$ transition.⁵² When dissolved in CH₃CN under anaerobic conditions, each complex **1-5-OTf** exhibits an intense absorption feature in the range of 420–443 nm. For comparison, we have measured the absorption features of a flavonolate salt ([Me₄N⁺][3Hfl⁻]) in CH₃CN (band I, $\lambda_{\text{max}} = 458$ nm).⁵³ For each metal complex, a hypsochromic shift of the absorption band is found relative to the 3-Hfl salt, with the exact shift being influenced by the nature of the metal ion. For example, the Mn(II) complex **1-OTf** exhibits band I at 431 nm. This matches well with the band I reported for Mn(3-Hfl)₂(py)₂ (432 nm).²³ To our knowledge, absorption spectra of an enzyme/substrate complex a Mn(II)-containing quercetinase enzyme have not been reported.¹¹ Notably, the Ni(II) complex **3-OTf** exhibits the smallest shift with band I at 443 nm, and the zinc and cobalt complexes **5-OTf** and **2-OTf** exhibit the largest shifts, with band I at 420 and 422 nm, respectively. For the Ni(II)-containing form of QueD from *Streptomyces* sp. FLA, under anaerobic conditions, addition of quercetin at pH = 8 produces an absorption feature at 385 nm, which represents a hypsochromic shift relative to the absorption feature of free quercetin at pH = 8 ($\lambda_{\text{max}} = 391$ nm). Similarly, addition of quercetin to anaerobic cobalt-containing QueD produces a band I absorption at 378 nm.¹² Thus, in both the synthetic and enzyme systems, the presence of Co(II) produces a more significant hypsochromic shift in band I. The absorption maximum found for the Cu(II) complex **4-OTf** (428 nm) is within the reported range for Cu(II) flavonolate complexes (416-434 nm).¹⁹ The band I absorption of [Zn(3-Hfl)(idpa)]ClO₄ (idpa = 3,3'-iminobis(N,N-dimethylpropylamine) has been

reported as 419 nm, which matches well with that found for **5-CIO4**.⁵⁴ Overall, from the limited set of well-characterized divalent metal 3-hydroxyflavonolate complexes reported in the literature to date (including those reported herein), the hypsochromic shift of the band I $\pi \rightarrow \pi^*$ transition (relative to the free 3-Hfl anion) generally increases in the order Ni(II) < Mn(II) < Cu(II) < Zn(II), Co(II).

EPR Spectroscopy. EPR spectra were obtained for the Mn(II) and Cu(II) complexes of the series (**1-OTf** and **4-OTf**) and are shown in Figure 4-4. The spectrum collected for **1-OTf** is similar to the spectrum collected for the hydroxamate-bridged dimanganese complex $[(6\text{-Ph}_2\text{TPAMn})(\mu\text{-ONHC(O)CH}_3)_2](\text{ClO}_4)_2$.²⁵ No hyperfine coupling is discernable in the spectrum of either **1-OTf** or the Mn(II) hydroxamate complex. The similarity of these spectra suggested to us the possible formation of a flavonolate-bridged dimanganese complex in solution. Reactivity studies outlined below provide additional evidence for the chemical similarities of **1-OTf** and the hydroxamate complex in CH₃CN. We note that the Mn(II)-containing form of the *B. subtilis* quercetin dioxygenase in the presence of quercetin under anaerobic conditions exhibits a six-line EPR signal at $g = 2$, with a hyperfine coupling constant of approximately 93 G.¹¹ A second, less intense six-line signal is also present at $g = 9$ and exhibits a similar hyperfine coupling constant. This data is consistent with the enzyme containing a mononuclear pseudooctahedral Mn(II) center having oxygen/nitrogen ligands.⁵⁵ The axial EPR spectrum of **4-OTf** is consistent with the distorted square pyramidal geometry of the Cu(II) center and a dx^2-y^2 ground state ($g_{\parallel} \sim 2.24$; $g_{\perp} \sim 2.06$; $A_{\parallel} \sim 180$ G). The

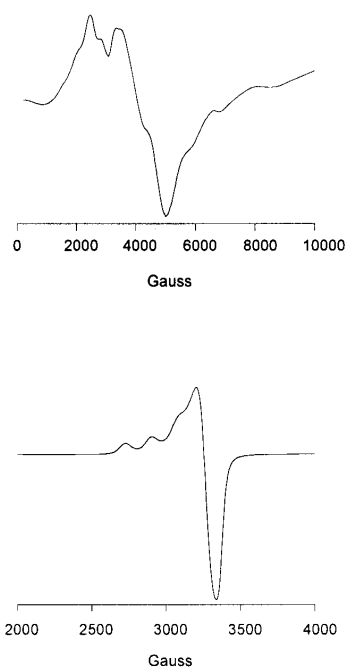


Figure 4-4. EPR spectra of **1-OTf** and **4-OTf**. Spectra were recorded at 4.7 K, 1.002 mW microwave power, and 9.39 GHz. The samples were ≤ 1 mM in CH_3CN .

anaerobic enzyme/substrate complex of the quercetinase enzyme from *Aspergillus japonicus* exhibits an EPR signal with $g// = 2.366$ and $A// \sim 110$ G.⁵⁶

^1H NMR Spectroscopy. The ^1H NMR spectra of analytically pure **2-OTf**, **3-OTf**, and **5-OTf** were measured in CD_3CN at ambient temperature. The spectra for the paramagnetic Co(II) and Ni(II) complexes are shown in Figure 4-5. While full assignment of the resonances of **2-OTf** and **3-OTf** have not been made, the spectra are clearly distinct from those of other complexes of bidentate ligands (e.g. hydroxamate derivatives) and can be used to evaluate complex purity and reactivity.²⁵ There are no concentration dependent changes in these NMR spectra. Attempts were made to collect two-dimensional COSY

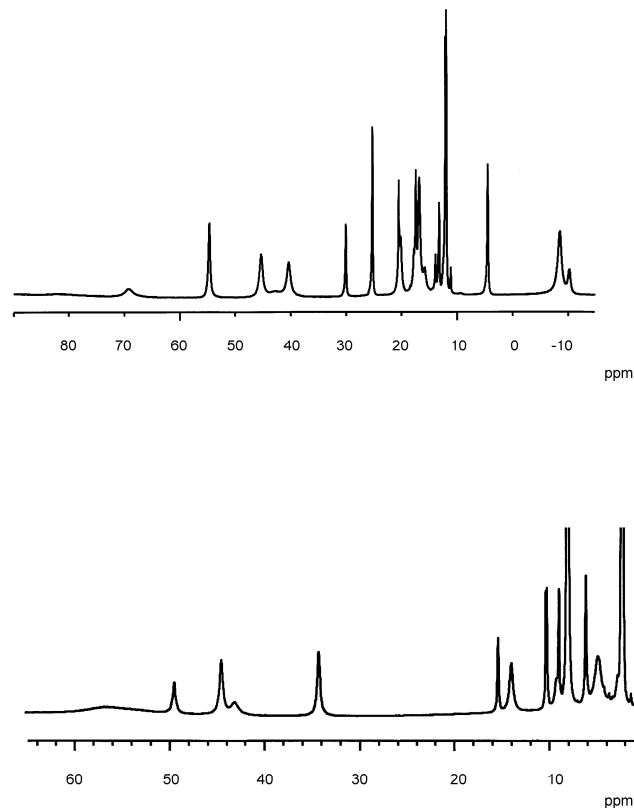


Figure 4-5. ^1H NMR spectra of **2-OTf** (top) and **3-OTf** (bottom) in CD_3CN at ambient temperature.

spectra to assign the pyridyl ring proton resonances of the 6- Ph_2TPA ligands in **2-OTf** and **3-OTf**.²⁶ Unfortunately, these experiments did not reveal any crosspeaks. It is important to note that the total number of paramagnetically shifted resonances in the spectra of **2-OTf** and **3-OTf** is consistent with the presence of an effective plane of symmetry containing the pyridyl donor, which gives equivalent phenyl-appended pyridyl donors. This indicates that the solution structure of these compounds is generally similar to that found in the solid state. The features of the ^1H and ^{13}C NMR spectra of **5-OTf** (see experimental section) are consistent the formation of a six-coordinate $\text{Zn}(\text{II})$ center in

solution via coordination of all donors of the supporting 6-Ph₂TPA ligand. Most notably, the total number of carbon signals is consistent with the presence of an effective plane of symmetry that makes the phenyl-appended pyridyl donors equivalent.

Cyclic Voltammetry. The redox properties of **1-5-OTf** were examined by cyclic voltammetry. An irreversible oxidation wave was identified for **1-OTf** and **3-5-OTf** and the E_{p_a} values are given in Table 4-3. The Co(II) complex **2-OTf** did not show any electrochemical behavior in the range examined. A quasi-reversible reduction peak at -1088 mV vs. Fc/Fc⁺ (Figure 4-6) for **4-OTf** has been tentatively assigned to the Cu(II)/Cu(I) couple, as no other compound of the group has waves at potentials lower than Fc/Fc⁺. These data for **1-5-OTf** indicate that the nature of the divalent metal influences the redox potential of the coordinated flavonolate over a range of ~300 mV. The differences in oxidation potential found for this series of complexes depends on the metal and/or the solution structure of the metal complex. The Mn(II) derivative **1-OTf**,

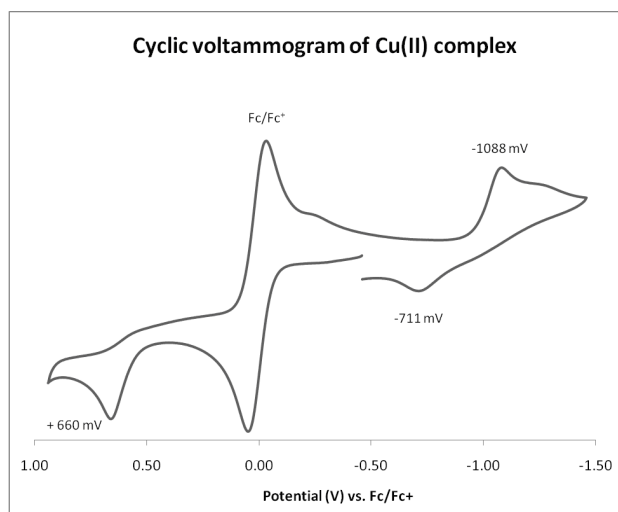


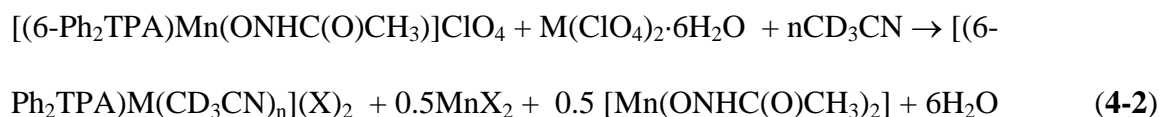
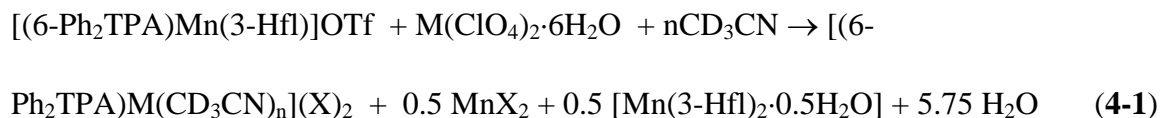
Figure 4-6. Cyclic voltammogram for the Cu(II) complex **4-OTf**.

which based on EPR, may form binuclear species in solution, has the lowest potential, indicating that the flavonolate is a better reductant toward O_2 than the same ligand in the Ni(II), Cu(II), and Zn(II) analog complexes. For the Ni(II) and Zn(II) complexes **3-ClO₄** and **5-ClO₄**, irreversible oxidation of the flavonolate ligand occurs at +0.506 and +0.536 V vs. Fc/Fc^+ , respectively. For the Cu(II) complex, which is distorted square pyramidal in acetonitrile, the potential is more positive (+0.660 V). Potentials previously reported for 3-hydroxyflavonolate complexes of the general formula $[M(3-Hfl)(H_2O)_n]Cl$ ($M = Cu, n = 2$; $M = Fe, n = 4$) are in the same range as those reported herein.⁵⁷

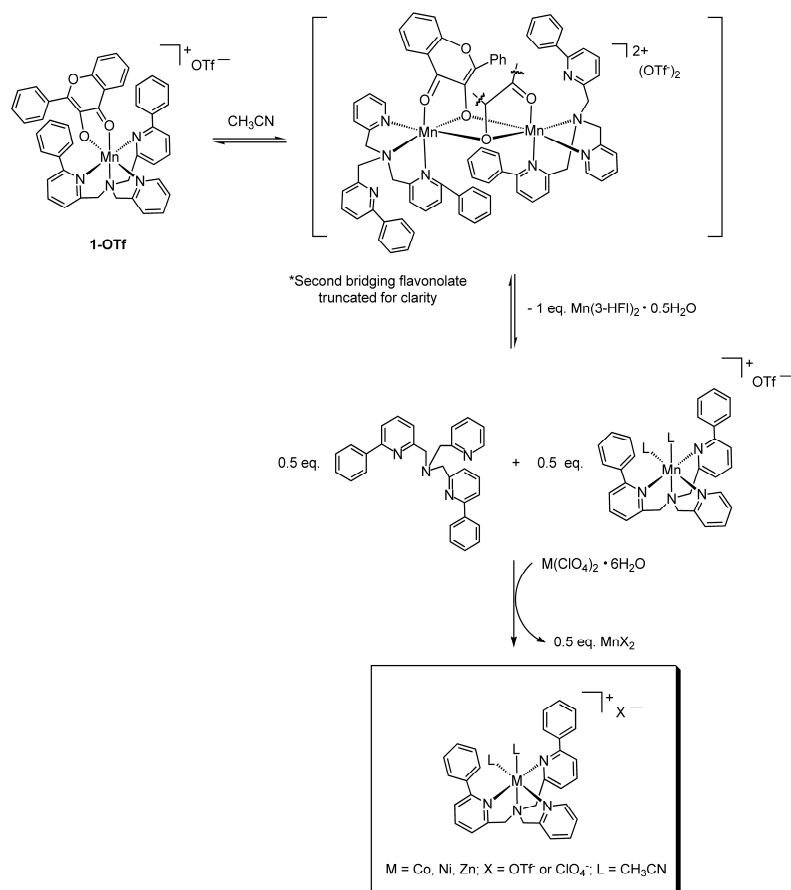
Ligand Exchange Reactivity. The results of initial electrospray ionization mass spectrometry experiments suggested that the Mn(II) flavonolate complex **1-OTf** would undergo reaction with available Zn(II) ion to produce a ligand exchange product, $[(6-Ph_2TPA)Zn(OTf)]^+$. To examine this reactivity, in independent NMR tube experiments, $[(6-Ph_2TPA)Mn(3-Hfl)]OTf$ was treated with an equimolar amount of $M(ClO_4)_2 \cdot 6H_2O$ ($M = Co(II), Ni(II), \text{ and } Zn(II)$) in CD_3CN . For each reaction, well resolved 1H NMR spectra consistent with the quantitative formation of a divalent metal solvate complex of the added metal, $[(6-Ph_2TPA)M(CD_3CN)_n](X)_2$ ($n = 1$ or 2 ; $X = OTf^-$ or ClO_4^-) were obtained.^{25,26} A yellow-green precipitate formed in each reaction mixture and was identified as $[Mn(3-Hfl)_2 \cdot 0.5H_2O]$ by elemental analysis. This compound was isolated from the reaction mixture involving Ni(II) by selective crystallization in 39% yield (for 0.5 equivalent). In addition to the stoichiometric formation of $[(6-Ph_2TPA)M(CD_3CN)_n](X)_2$ and 0.5 eq. of $[Mn(3-Hfl)_2 \cdot 0.5H_2O]$, mass balance requires the formation of 0.5 eq. of MnX_2 salt (equation 4-1), which could not be isolated from the

reaction mixture. Notably, we found that the Mn(II) hydroxamate complex [(6-Ph₂TPAMn)(μ-ONHC(O)CH₃)₂](ClO₄)₂²⁵ also reacts with M(ClO₄)₂·6H₂O to produce [(6-Ph₂TPA)M(CD₃CN)](X)₂ (M = Co, Ni, Zn; X = OTf⁻ or ClO₄⁻; equation 4-2), as determined by ¹H NMR. The similarity in EPR spectral features (vide supra) and reactivity of [(6-Ph₂TPA)Mn(3-Hfl)]OTf and [(6-Ph₂TPAMn)(μ-ONHC(O)CH₃)₂](ClO₄)₂ suggest that the compounds may have similar solution structures. We propose that these structures include μ-η¹:η²-coordination of the chelate anion (3-Hfl or acetohydroxamate) as is found in the X-ray structure of [(6-Ph₂TPAMn)(μ-ONHC(O)CH₃)₂](ClO₄)₂.²⁵

M = Co, Ni, Zn; X = OTf⁻ or ClO₄⁻:



In this coordination motif, each Mn(II) center coordinates the anionic oxygen of each bridging ligand. We propose that from this structure an equilibrium mixture is formed, and is comprised of 0.5 eq. [Mn(3-Hfl)₂·0.5H₂O], 0.5 eq. free chelate ligand, and 0.5 eq. of [(6-Ph₂TPA)Mn(CD₃CN)₂](X)₂ (Scheme 4-3). Formation of the final product mixture, including one equivalent of [(6-Ph₂TPA)M(CD₃CN)_n](X)₂ (M = Co, Ni, Zn), could result



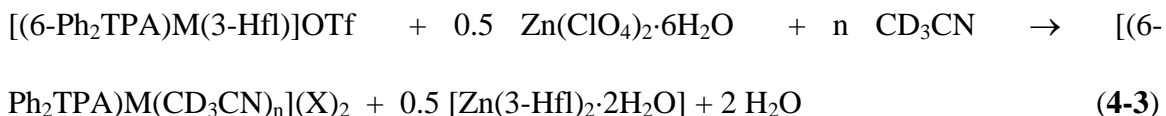
Scheme 4-3. Proposed reaction pathway for ligand exchange in the reaction of **1-OTf** with divalent metal perchlorate salts.

from coordination of the free divalent metal ion to the free chelate ligand, and displacement of Mn(II) (as MnX₂) from [(6-Ph₂TPA)Mn(CD₃CN)₂](X)₂. The latter reaction has been independently investigated by ¹H NMR and found to occur rapidly in CD₃CN for M = Co(II), Ni(II), and Zn(II).

In another type of ligand exchange reaction, we found that treatment of the non-manganese flavonolate complexes [(6-Ph₂TPA)M(3-Hfl)]OTf (M = Co (**2-OTf**), Ni (**3-OTf**), and Cu (**4-OTf**)) with 0.5 eq Zn(ClO₄)₂·6H₂O in CD₃CN results in the formation of

[(6-Ph₂TPA)M(CD₃CN)_n](X)₂ (n = 1 or 2; X = OTf⁻ or ClO₄⁻) species as indicated by ¹H NMR. Hence, in these reactions flavonolate ligand exchange occurs, but no change in the metal bound by the 6-Ph₂TPA ligand takes place. The other product in the reaction is [Zn(3-Hfl)₂·2H₂O] (equation 4-3), which is a poorly soluble yellow precipitate. This material was identified by independent synthesis and characterization, followed by comparison of UV-vis and ¹H NMR properties between the reaction product and the independently generated material.

M = Co, Ni, Cu; X = OTf⁻ or ClO₄⁻



What about Fe(II)? The quercetinase enzyme from *B. subtilis* was originally described as a non-heme iron enzyme.¹⁰ However, the turnover number for this enzyme was reported to be two orders of magnitude lower than for the Cu(II)-containing *A. flavus*, which led researchers to suggest that Fe(II) might not be the correct cofactor for the enzyme. Follow-up studies suggested that Mn(II) was probably the correct cofactor for the *B. subtilis* enzyme.¹¹ To date, only two iron flavonolate complexes, both Fe(III) derivatives, have been crystallographically characterized.^{23,24}

To gauge the chemistry of Fe(II) relative to the other 3d metal ions investigated herein, we initiated attempts to prepare a Fe(II) flavonolate complex supported by the 6-Ph₂TPA ligand. In our first approach, treatment of 6-Ph₂TPA with equimolar amounts of

$\text{Fe}(\text{ClO}_4)_2 \cdot 6\text{H}_2\text{O}$, 3-hydroxyflavonol, and $\text{Me}_4\text{NOH} \cdot 5\text{H}_2\text{O}$ under a N_2 atmosphere, followed by stirring overnight, work-up, and crystallization from $\text{CH}_3\text{CN}/\text{Et}_2\text{O}$ resulted in the deposition of dark brown single crystals. X-ray crystallographic analysis of these crystals revealed the formation of the diiron(III) μ -oxo compound $[(6\text{-Ph}_2\text{TPAFe}(3\text{-Hfl}))_2(\mu\text{-O})](\text{ClO}_4)_2$ (**6**·**2.5CH**₃CN, Figure 4-7). The structural and spectroscopic properties of this complex are discussed in detail below. However, as an approach toward understanding the reaction pathway leading to the formation of **6**, we further explored the synthetic conditions.

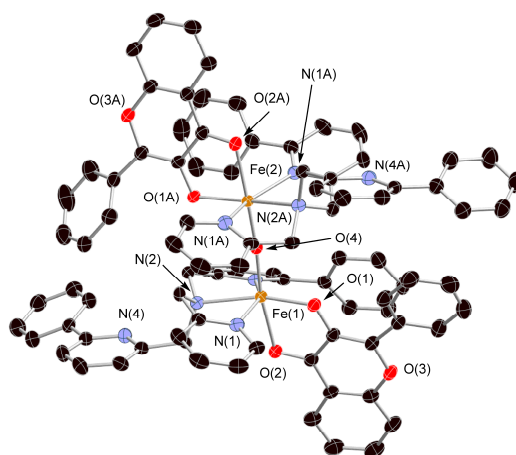


Figure 4-7. Thermal ellipsoid drawings (50% probability) of the cationic portions of **6**·**2.5CH**₃CN. Hydrogen atoms have been omitted for clarity.

Treatment of 6-Ph₂TPA with $\text{Fe}(\text{ClO}_4)_2 \cdot 6\text{H}_2\text{O}$ in CH_3CN , followed by recrystallization from $\text{CH}_3\text{CN}/\text{Et}_2\text{O}$, yielded $[(6\text{-Ph}_2\text{TPA})\text{Fe}(\text{CH}_3\text{CN})](\text{ClO}_4)_2$ (**7**) as pale yellow crystals. Characterization details for this Fe(II) complex are given in the supporting information.

Treatment of **7** with equimolar amounts of 3-hydroxyflavonol and $\text{Me}_4\text{NOH}\cdot 5\text{H}_2\text{O}$ in methanol, and stirring for 15 minutes under a freshly purged N_2 atmosphere, gave a green-yellow solution from which, after work-up, a green-yellow precipitate was isolated. The analytical and spectroscopic properties of this complex are consistent with the formulation $[(6\text{-Ph}_2\text{TPA})\text{Fe}(3\text{-Hfl})]\text{ClO}_4$ (**8**). For this complex, the flavonolate $\nu_{\text{C=O}}$ vibration is at 1558 cm^{-1} , and the band I $\pi \rightarrow \pi^*$ transition is at 415 nm ($\epsilon \sim 14700\text{ M}^{-1}\text{cm}^{-1}$). These features are similar to those found for the Co(II) derivative **2-OTf**, suggesting that the flavonolate ligand may be coordinated with a $\Delta_{\text{M-O}}$ similar to that found in the cobalt complex. The magnetic moment for **8** ($\mu_{\text{eff}} = 4.7\ \mu\text{B}$) is consistent with the presence of a high-spin Fe(II) center.⁵⁸ The ^1H NMR spectrum of **8** contains several paramagnetically shifted resonances over a range of $\sim 110\text{ ppm}$ (Figure 4-8). Investigation of the redox properties of **8** by cyclic voltammetry (CH_2Cl_2 , $[\text{8}] = 1\text{ mM}$, Bu_4NClO_4 (0.1 M) supporting electrolyte, scan rate 50-100 mV/s) revealed a quasi-reversible couple at $\sim -0.05\text{ V}$ versus ferrocene/ferrocenium, which is assigned as the Fe(II)/Fe(III) couple. No redox activity was found at more positive potentials, indicating that upon oxidation of the iron center, the redox potential for the coordinated flavonolate is shifted from that observed for the other divalent metal 3-Hfl complexes. This redox behavior is consistent with the observed metal-centered O_2 reactivity described below.

Complex **8** is very air sensitive, which complicated our efforts to characterize it, especially in solution. Exposure of a CH_3CN solution of **8** to air results in a rapid darkening of the color, which corresponds to the formation of the μ -oxo compound **6**

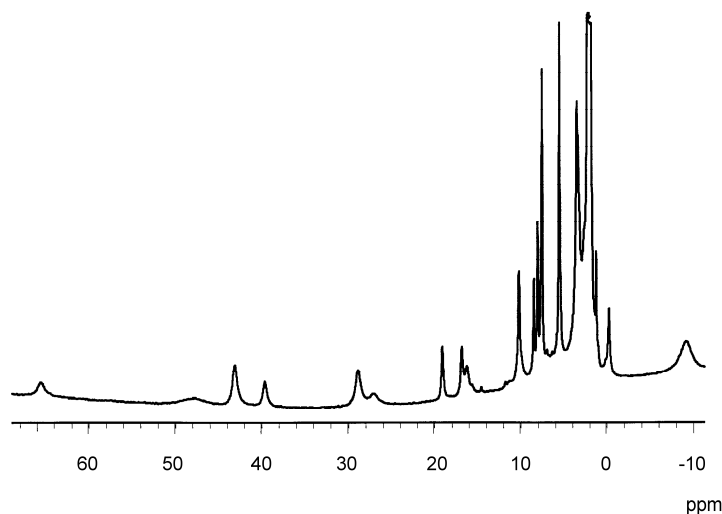


Figure 4-8. ^1H NMR spectrum of $[(6\text{-Ph}_2\text{TPA})\text{Fe}(3\text{-Hfl})]\text{ClO}_4$ (**8**) in CD_3CN at ambient temperature. In addition to the resonances shown, broad peaks are also present at 112 and 92 ppm.

This complex was characterized by X-ray crystallography, elemental analysis, UV-vis, FTIR, and mass spectrometry. A summary of the iron coordination chemistry is shown in Scheme 4-4.

The cationic portion of $\mathbf{6}\cdot\mathbf{2.5CH}_3\text{CN}$ is shown in Figure 4-7. Details of the X-ray data collection of this complex are given in Table 4-6. Selected bond distances and angles are given in Tables 4-7 and 4-8, respectively. Each Fe(III) center has a $\kappa^3\text{-6-Ph}_2\text{TPA}$ ligand, a bidentate flavonolate ligand, and the $\mu\text{-oxo}$ bridge. The flavonolate ligands are coordinated to Fe(1) and Fe(2) with $\Delta_{\text{M-O}} = 0.17$ and 0.14 \AA , respectively. This is similar to the coordination found in the Co(II) and Zn(II) flavonolate complexes $\mathbf{2}\text{-ClO}_4$ and $\mathbf{5}\text{-ClO}_4\cdot\text{CH}_2\text{Cl}_2$. Similarly, the Fe(III) complexes $[(\text{salen})\text{Fe}(\text{III})(3\text{-Hfl})]$ and $[\text{Fe}(4'\text{-MeOflaH})_3]$ have $\Delta_{\text{M-O}} = 0.18$ and 0.15 \AA , respectively.^{23,24} Thus, all of the Fe(III)

flavonolate complexes that have been structurally characterized to date exhibit very similar levels of asymmetry with respect to flavonolate coordination.

The Fe-O(flavonolate) bond distances are also very similar in all three compounds. We note that the flavonolate ketone oxygen donor is positioned *trans* to the μ -oxo bridge in **6**·**2.5**CH₃CN, whereas the deprotonated oxygen donor is *trans* to the tertiary amine nitrogen. This results in a meridional donor array from the κ^3 -bound chelate ligand. The Fe-O bond distances involving the oxo bridge in **6**·**2.5**CH₃CN are within experimental error identical to those found in [(6-C₆H₄O-TPAFe)₂(μ -O)](BPh₄)₂.⁵⁹ The average Fe-N distance in **6**·**2.5**CH₃CN (~2.20 Å) is slightly longer than what is found in [(6-C₆H₄-TPAFe)₂(μ -O)](BPh₄)₂ (~2.18 Å). However, both distances are consistent with a high-spin ($S = 5/2$) state for each iron center.⁶⁰

A vibration at 1549 cm⁻¹ in the solid state infrared spectrum of **6** is assigned as the $\nu_{C=O}$ vibration of the flavonolate, based on comparison to the spectral features of [(salen)Fe(III)(3-Hfl)] (1549 cm⁻¹).²⁴ Compound **6** is slightly soluble in methanol and exhibits absorption bands at 388 and 490 nm (Figure 4-9). Unlike its Fe(II) flavonolate precursor **8**, an absorption feature for the flavonolate ligand in the region of 400-450 nm could not be readily identified. The absorption features of **6** and **8** are compared in Figure 4-9. For [(salen)Fe(III)(3-Hfl)], an absorption maximum at 407 nm was reported.²⁴ The ¹H NMR spectrum of **6** in *d*₄-methanol consists of broad resonances in the range of 0 to ~40 ppm (Figure 4-10).

Table 4-6. Summary of X-ray Data Collection and Refinement for **6-2.5CH₃CN**.

Empirical formula	C ₉₇ H _{77.5} Cl ₂ Fe ₂ N _{10.5} O ₁₅
<i>M_r</i>	1788.78
Crystal system	Triclinic
Space group	<i>P</i> -1
<i>a</i> / Å	14.02370(10)
<i>b</i> / Å	15.2054(2)
<i>c</i> / Å	21.6638(3)
α /°	70.1168(7)
β /°	74.8473(7)
γ /°	81.5826(8)
<i>V</i> / Å ³	4184.67(9)
<i>Z</i>	2
<i>D_c</i> / Mg m ⁻³	1.420
<i>T</i> / K	150(1)
Color	Red
Crystal habit	Prism
Crystal size/ mm	0.28 x 0.18 x 0.15
Diffractometer	Nonius KappaCCD
μ / (mm ⁻¹)	0.486
2 θ max /°	54.92
Completeness to θ (%)	99.0
Reflections collected	35639
Independent reflections	18968
<i>R</i> _{int}	0.0393
Variable parameters	1151
<i>R</i> ₁ / <i>wR</i> ₂	0.0460/0.1010
Goodness-of-fit (<i>F</i> ₂)	1.019
$\Delta\rho$ _{max} /min / e Å ⁻³	0.397/-0.487

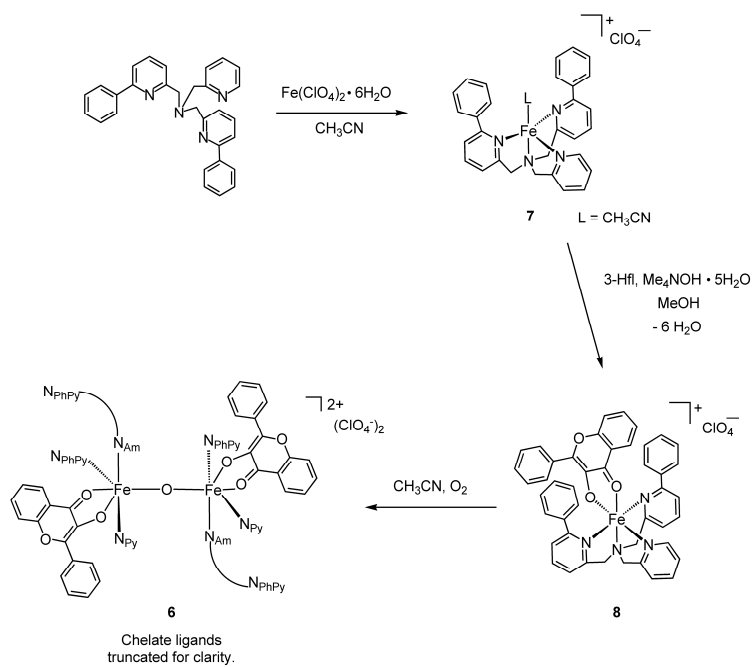
^aRadiation used: Mo K α (λ = 0.71073 Å) *bR*₁ = $\sum | |F_o| - |F_c| | / \sum |F_o|$; *wR*₂ = $[\sum [w(F_o^2 - F_c^2)^2] / \sum (F_o^2)]^{1/2}$, where $w = 1/[\sigma^2(F_o^2) + (aP)^2 + bP]$.

Table 4-7. Selected Bond Distances (Å) for **6·2.5CH₃CN**.

Fe(1)-O(1)	1.9712(14)	Fe(2)-O(1A)	1.9655(14)
Fe(1)-O(2)	2.1460(15)	Fe(2)-O(2A)	2.1054(15)
Fe(1)-O(4)	1.7890(14)	Fe(2)-O(4)	1.7992(14)
Fe(1)-N(1)	2.1679(17)	Fe(2)-N(1A)	2.1822(18)
Fe(1)-N(2)	2.2489(17)	Fe(2)-N(2A)	2.2180(18)
Fe(1)-N(3)	2.2241(17)	Fe(2)-N(3A)	2.2109(18)
O(1)-C(31)	1.330(3)	O(1A)-C(31A)	1.326(3)
O(2)-C(32)	1.271(3)	O(2A)-C(32A)	1.274(2)

Table 4-8. Selected Bond Angles (deg) for **6·2.5CH₃CN**.

O(4)-Fe(1)-O(1)	96.02(6)	O(4)-Fe(2)-O(1A)	95.13(6)
O(4)-Fe(1)-O(2)	170.00(6)	O(4)-Fe(2)-O(2A)	169.80(6)
O(1)-Fe(1)-O(2)	78.51(6)	O(1A)-Fe(2)-O(2A)	79.72(6)
O(4)-Fe(1)-N(1)	97.29(7)	O(4)-Fe(2)-N(1A)	96.62(7)
O(1)-Fe(1)-N(1)	90.11(6)	O(1A)-Fe(2)-N(1A)	88.98(6)
O(2)-Fe(1)-N(1)	91.13(6)	O(2A)-Fe(2)-N(1A)	92.12(6)
O(4)-Fe(1)-N(3)	93.65(6)	O(4)-Fe(2)-N(3A)	93.35(6)
O(1)-Fe(1)-N(3)	117.63(6)	O(1A)-Fe(2)-N(3A)	118.27(6)
O(2)-Fe(1)-N(3)	81.72(6)	O(2A)-Fe(2)-N(3A)	81.55(6)
N(1)-Fe(1)-N(3)	148.90(7)	N(1A)-Fe(2)-N(3A)	149.99(7)
O(4)-Fe(1)-N(2)	93.62(6)	O(4)-Fe(2)-N(2A)	93.42(6)
O(1)-Fe(1)-N(2)	162.47(6)	O(1A)-Fe(2)-N(2A)	161.88(6)
O(2)-Fe(1)-N(2)	93.87(6)	O(2A)-Fe(2)-N(2A)	94.03(6)
N(1)-Fe(1)-N(2)	74.13(6)	N(1A)-Fe(2)-N(2A)	74.17(7)
N(3)-Fe(1)-N(2)	76.19(6)	N(3A)-Fe(2)-N(2A)	77.04(7)



Scheme 4-4.

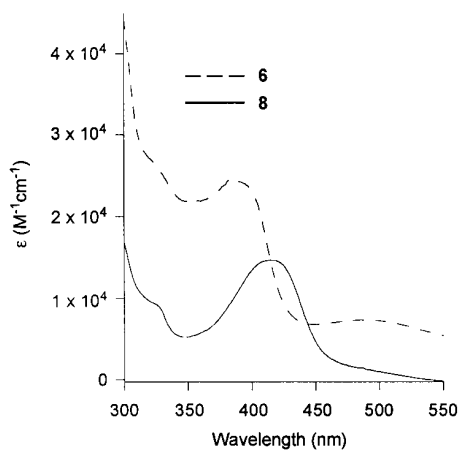


Figure 4-9. UV-vis absorption features of $[(6\text{-Ph}_2\text{TPAFe}(3\text{-Hfl}))_2(\mu\text{-O})](\text{ClO}_4)_2$ (**6**) and $[(6\text{-Ph}_2\text{TPA})\text{Fe}(3\text{-Hfl})]\text{ClO}_4$ (**8**).

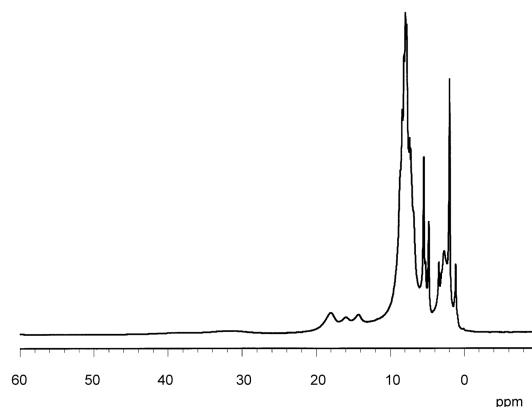


Figure 4-10. ^1H NMR spectrum of **6** in CD_3CN .

Several features of this spectrum are significantly overlapped in the aromatic range (-10 to 40 ppm), consistent with the presence of several types of aryl protons. The dramatically different features of this spectrum versus that found for $[(6\text{-Ph}_2\text{TPA})\text{Fe}(3\text{-Hfl})]\text{ClO}_4$ (**8**, Figure 4-8) is likely due to antiferromagnetic coupling of the $S = 5/2$ metal centers via the oxo bridge.^{59,61,62}

Final Comments

The chemistry of metal complexes of flavonolate ligands is of significant current interest. Metal flavonolate complexes have been prepared and investigated for their antioxidant and DNA cleavage reactivity.⁶³⁻⁷⁴ Because of their biological relevance, metal flavonolate complexes have also been the subject of several recent computational investigations.⁷⁵⁻⁷⁸ As noted in the introduction, fungal and bacterial quercetinase enzymes have been shown to exhibit varying levels of activity as a function of the divalent metal ion present. While a few initial investigations directed at evaluating the effect of the metal ion on flavonolate/ O_2 chemistry of relevance to quercetin dioxygenase

enzymes have been reported,^{23,24} these studies lack a systematic approach. Specifically, the studies reported to date have included comparisons between complexes having different supporting chelate ligands and/or metal oxidation states. The research described herein is the first detailed systematic mapping of how metal ion content influences the structural, spectroscopic, redox properties, and ligand exchange reactivity of structurally-related flavonolate complexes. These complexes are relevant to the metal/flavonolate adducts proposed to form in quercetinase enzymes of varying metal ion content. The results presented herein lay the groundwork for detailed O₂ reactivity studies as a function of the divalent metal ion present. These investigations are currently in progress.

References

1. Iwashina, T. *J. Plant Res.* **2000**, *113*, 287-299.
2. Pietta, P.-G. *J. Nat. Prod.* **2000**, *63*, 1035-1042.
3. Cushine, T. P. T.; Lamb, A. *J. Int. J. Antimicrob. Agents* **2005**, *26*, 343-356.
4. Oka, T.; Simpson, F. J. *Biochem. Biophys. Res. Commun.* **1971**, *43*, 1-5.
5. Oka, T.; Simpson, F. J.; Krishnamurty, H. G. *Can. J. Microbiol.* **1972**, *18*, 493-508.
6. Hund, H. K.; Breuer, J.; Lingens, F.; Huttermann, J.; Kappl, R.; Fetzner, S. *Eur. J. Biochem.* **1999**, *263*, 871-878.
7. Tranchimand, S.; Ertel, G.; Gaydou, V.; Gaudin, C.; Tron, T.; Iacazio, G. *Biochimie* **2008**, *90*, 781-789.
8. Kooter, I. M.; Steiner, R. A.; Dijkstra, B. W.; van Noort, P. I.; Egmond, M. R.; Huber, M. *Eur. J. Biochem.* **2002**, *269*, 2971-2979.

9. Fusetti, F.; Schroter, K. H.; Steiner, R. A.; van Noort, P. I.; Pijning, T.; Rozeboom, H. J.; Kalk, K. H.; Egmond, M. R.; Dijkstra, B. W. *Structure* **2002**, *10*, 259-268.
10. Gopal, B.; Madan, L. L.; Betz, S. F.; Kossiakoff, A. A. *Biochemistry* **2005**, *44*, 193-201.
11. Schaab, M. R.; Barney, B. M.; Francisco, W. A. *Biochemistry* **2006**, *45*, 1009-1016.
12. Merkens, H.; Kappl, R.; Jakob, R. P.; Schmid, F. X.; Fetzner, S. *Biochemistry* **2008**, *47*, 12185-12196.
13. Steiner, R. A.; Kalk, K. H.; Dijkstra, B. W. *Proc. Natl. Acad. Sci.* **2002**, *99*, 16625-16630.
14. Bowater, L.; Fairhurst, S. A.; Just, V. J.; Bornemann, S. *FEBS Lett.* **2004**, *557*, 45-48.
15. Barney, B. M.; Schaab, M. R.; LoBrutto, R.; Francisco, W. *Protein Expression Purif.* **2004**, *35*, 131-141.
16. Merkens, H. Sielker, S.; Rose, K.; Fetzner, S. *Arch. Microbiol.* **2007**, *187*, 475-487.
17. Based on comparison of k_{cat} and K_M values with those of Fe(II)-containing enzyme.
18. Emerson, J. P.; Kovaleva, E. G.; Farquhar, E. R.; Lipscomb, J. D.; Que, L. Jr. *Proc. Natl. Acad. Sci.* **2008**, *105*, 7347-7352 and references cited therein.

19. Kaizer, J.; Balogh-Hergovich, E.; Czaun, M.; Csay, T.; Speier, G. *Coord. Chem. Rev.* **2006**, *250*, 2222-2233.
20. Nishinaga, A.; Tojo, T.; Matsuura, T. *J. Chem. Soc., Chem. Commun.* **1974**, 896-897.
21. Nishinaga, A.; Numada, N.; Maruyama, K. *Tetrahedron Lett.* **1989**, *30*, 2257-2258.
22. Nishinaga, A.; Kuwashige, T.; Tsutsui, T.; Mashino, T.; Maruyama, K. *J. Chem. Soc., Dalton Trans.* **1994**, 805-810.
23. Kaizer, J.; Baráth, G.; Pap, J.; Speier, G.; Giorgi, M.; Réglie, M. *Chem. Commun.* **2007**, 5235-5237.
24. Baráth, G.; Kaizer, J.; Speier, G.; Párkányi, L. Kuzmann, E.; Vértes, A. *Chem. Commun.* **2009**, 3630-3632.
25. Makowska-Grzyska, M. M.; Szajna, E.; Shipley, C.; Arif, A. M.; Mitchell, M. H.; Halfen, J. A.; Berreau, L. M. *Inorg. Chem.* **2003**, *42*, 7472-7488.
26. Szajna, E.; Dobrowolski, P.; Fuller, A. L.; Arif, A. M.; Berreau, L. M. *Inorg. Chem.* **2004**, *43*, 3988-3997.
27. Szajna, E.; Arif, A. M.; Berreau, L. M. *J. Am. Chem. Soc.* **2005**, *127*, 17186-17187.
28. Szajna-Fuller, E.; Rudzka, K.; Arif, A. M.; Berreau, L. M. *Inorg. Chem.* **2007**, *46*, 5499-5507.
29. Szajna-Fuller, E.; Chambers, B. M.; Arif, A. M.; Berreau, L. M. *Inorg. Chem.* **2007**, *46*, 5486-5498.

30. Armarego, W. L. F.; Perrin, D. D. *Purification of Laboratory Chemicals*, 4th ed.; Butterworth-Heinemann: Boston, MA, 1996.
31. Evans, D. F. *J. Chem. Soc.* **1959**, 2003-2005.
32. Wolsey, W. C. *J. Chem. Educ.* **1973**, 50, A335-A337.
33. Otwinowski, Z.; Minor, W. *Methods Enzymol.* **1997**, 276, 307-326.
34. Altomare, A.; Burla, M. C.; Camalli, M.; Cascarano, G. L.; Giacovazzo, C.; Guagliardi, A.; Moliterni, A. G. G.; Polidori, G.; Spagna, R. *J. Appl. Cryst.* **1999**, 32, 115-119.
35. Sheldrick, G. M. *SHELXL-97 Program for the Refinement of Crystal Structures*; University of Göttingen, Germany, 1997.
36. Addison, A. W.; Rao, T. N.; Reedijk, J.; van Rijn, J.; Verschoor, G. C. *J. Chem. Soc., Dalton Trans.* **1984**, 1349-1356.
37. Fuller, A. L.; Arif, A. M.; Berreau, L. M. Unpublished result.
38. Farina, Y.; Yamin, B. M.; Fun, H-K.; Yip, B-C.; Teoh, S-G. *Acta Cryst.* **1995**, C51, 1537-1540.
39. One Co(III) flavonolate complex supported by a salen ligand is listed in the Cambridge Crystallographic Database. Hiller, W.; Nishinaga, A.; Rieker, A. Z. *Naturforsch., B: Chem. Sci.* **1992**, 47, 1185.
40. Kaizer, J.; Pap, J.; Speier, G.; Parkanyi, L. *Eur. J. Inorg. Chem.* **2004**, 2253-2259.
41. Lippai, I.; Speier, G.; Huttner G.; Zsolnai, L. *Chem. Commun.* **1997**, 741-742.
42. Balogh-Hergovich, Kaizer, J.; Speier, G.; Huttner, G.; Zsolnai, L. *Inorg. Chim. Acta* **2000**, 304, 72-77.

43. Balogh-Hergovich, E.; Kaizer, J.; Speier, G.; Huttner, G.; Jacobi, A. *Inorg. Chem.* **2000**, *39*, 4224-4229.
44. Okabe, N.; Yamamoto, E.; Yasunori, M. *Acta Crystallogr., Sect. E: Struct. Rep. Online* **2003**, *59*, m715-m716.
45. Balogh-Hergovich, E.; Speier, G.; Argay, G. *J. Chem. Soc., Chem. Commun.* **1991**, 551-552.
46. Balogh-Hergovich, E.; Kaizer, J.; Speier, G.; Argay, G.; Párkányi, L. *J. Chem. Soc., Dalton Trans.* **1999**, 3847-3854.
47. The Cu(II) complex [Cu(II)(bpy)(fla)(2-HOC₆H₄COCO₂)] has been reported to have Cu-O bond lengths of 2.190(9) and 1.760(11) Å and $\Delta_{M-O} = 0.43$ Å.⁴¹
48. Balogh-Hergovich, E.; Kaizer, J.; Speier, G.; Huttner, G.; Rutsch, P. *Acta Crystallogr., Sect. C: Cryst. Struct. Commun.* **1999**, *55*, 557-558.
49. Annan, T. A.; Peppe, C.; Tuck, D. G. *Can. J. Chem.* **1990**, *68*, 423-430.
50. Kaizer, J.; Kupán, A.; Pap, J.; Speier, G.; Réglíer, M.; Michel, G. *Z. Kristallogr.-New Cryst. Struct.* **2000**, *215*, 571-572.
51. Etter, M. C.; Urbanczyk-Lipkowska, Z.; Baer, S.; Barbara, P. F. *J. Mol. Struct.* **1986**, *144*, 155-167.
52. Jurd, L.; Geissman, T. X. *J. Org. Chem.* **1956**, *21*, 1395-1401.
53. Barhács, et. al. report the absorption maximum of [K][3-Hfl] to be 465 nm. Barhács, L.; Kaizer, J.; Speier, G. *J. Org. Chem.* **2000**, *65*, 3449-3452.
54. Barhács, L.; Kaizer, J.; Speier, G. *J. Mol. Catal. A* **2001**, *172*, 117-125.

55. Reed, G. H.; Markham, G. D. *Biological Magnetic Resonance*; Berliner, L. J. and Rueben, J., Eds.; Plenum: New York, NY, Vol. 6, pp 73-142.
56. Spectrum obtained at 77K.
57. de Souza, R. F. V.; Sussuchi, E. M.; De Giovani, W. F. *Synth. React. Inorg. Met-Org. Chem.* **2003**, *33*, 1125-1144.
58. Huheey, J. E.; Keiter, E. A.; Keiter, R. L. *Inorganic Chemistry: Principles of Structure and Reactivity*; Harper Collins: New York, NY, 1993.
59. Jensen, M. P.; Lange, S. J.; Mehn, M. P.; Que, E. L.; Que, L., Jr. *J. Am. Chem. Soc.* **2003**, *125*, 2113-2128.
60. Zang, Y.; Kim, J.; Dong, Y.; Wilkinson, E. C.; Appelman, E. H.; Que, L., Jr. *J. Am. Chem. Soc.* **1997**, *119*, 4197-4205.
61. Wu, F.-J.; Kurtz, D. M., Jr. *J. Am. Chem. Soc.* **1989**, *111*, 6563-6572.
62. Norman, R. E.; Yan, S.; Que, L., Jr.; Backes, G.; Ling, J.; Sanders-Loehr, J.; Zhang, J. H.; O'Connor, C. J. *J. Am. Chem. Soc.* **1990**, *112*, 1554-1562.
63. Ryan, P.; Hynes, M. J. *J. Inorg. Biochem.* **2008**, *102*, 127-136.
64. Kazazic, S. P.; Butkovic, V.; Srzic, D.; Klasinc, L. *J. Agric. Food Chem.* **2006**, *54*, 8391-8396.
65. de Souza, R. F. V.; De Giovani, W. F. *Spectrochim Acta A* **2005**, *61*, 1985-1990.
66. Bukhari, S. B.; Memon, S.; Mahroof-Tahir, M.; Bhangar, M. I. *Spectrochim. Acta A* **2009**, *71*, 1901-1906.
67. Guo, M.; Perez, C.; Wei, Y.; Rapoza, E.; Su, G.; Bou-Abdallah, F.; Chasteen, N. D. *Dalton Trans.* **2007**, 4951-4961.

68. El Hajji, H.; Nkhili, E.; Tomao, V.; Dangles, O. *Free Radic. Res.* **2006**, *40*, 303-320.
69. de Souza, R. F. V.; De Giovani, W. F. *Redox Rep.* **2004**, *9*, 97-104.
70. Mira, L.; Fernandez, M. T.; Santos, M.; Rocha, R.; Florencio, M. H.; Jennings, K. R. *Free Radic. Res.* **2002**, *36*, 1199-1208.
71. Tan, J.; Wang, B.; Zhu, L. *J. Biol. Inorg. Chem.* **2009**, *14*, 727-739.
72. Tan, J.; Wang, B.; Zhu, L. *Bioorg. Med. Chem.* **2009**, *17*, 614-620.
73. Tan, J.; Zhu, L.; Wang, B. *Dalton Trans.* **2009**, 4722-4728.
74. El Amrani, F. B. A.; Perrelló, L.; Real, J. A.; Gozález-Álvarez, M.; Alzuet, G.; Borrás, J.; Garcia-Granda, S.; Montejo-Bernardo, J. *J. Inorg. Biochem.* **2006**, *100*, 1208-1218.
75. Lekka, C. E.; Ren, J.; Meng, S.; Kaxiras, E. *J. Phys. Chem. B* **2009**, *113*, 6478-6483.
76. Ren, J.; Meng, S.; Lekka, C. E.; Kaxiras, E. *J. Phys. Chem. B* **2008**, *112*, 1845-1850.
77. Leopoldini, M.; Russo, N.; Chiodo, S.; Toscano, M. *J. Agric. Food Chem.* **2006**, *54*, 6343-6351.
78. Cornard, J. P.; Dangleterre, L.; Lapouge, C. *Chem. Phys. Lett.* **2006**, *419*, 304-308.

CHAPTER 5

PHOTOCHEMICALLY-INDUCED DIOXYGENASE-TYPE CO-RELEASE OF
GROUP 12 FLAVONOLATE COMPLEXES¹**Abstract**

Exposure of 3-hydroxyflavonolate complexes of the group 12 metals to UV light under aerobic conditions results in oxidative carbon-carbon bond cleavage and CO release. This reactivity is novel in that it occurs under mild reaction conditions and suggests that light-induced CO-release reactivity involving metal flavonolate species may be possible in biological systems.

Introduction

Flavonoids are a class of a naturally occurring, polyphenolic substances produced in plants. They are of current interest as potential therapeutic agents due to their anti-microbial, anti-oxidative, and UV-protective activity.¹ A prominent member of this family of compounds is quercetin (Figure 5-1), a natural compound that is being investigated to prevent or treat a variety of diseases.^{1a,2} Quercetin is found in an assortment of foods including black and green tea, red onions, and many other fruits and vegetables that are widely touted for their beneficial health effects.

¹ Coauthored by Katarzyna Grubel, Brynna Laughlin, Thora R. Maltais, Rhett C. Smith, Atta M. Arif, and Lisa M. Berreau. Reproduced with permission from *Chemical Communications* **2011**. Copyright 2011 The Royal Society of Chemistry.

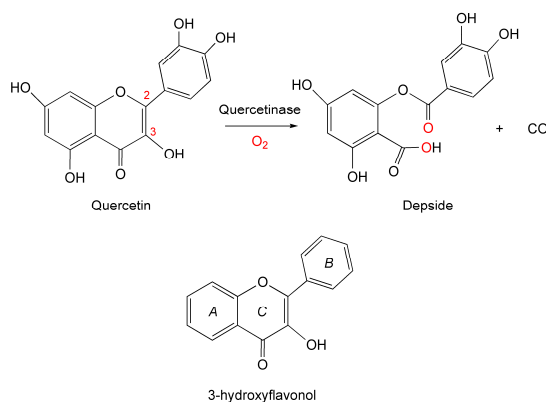


Figure 5-1. Top: Structure of quercetin (including numbering of C-C bond that undergoes oxidative cleavage) and the reaction catalyzed by quercetinase enzymes. Bottom: Structure of 3-hydroxyflavonol (3-Hfl) and labeling of rings.

Studies of the interactions of flavonoids with metal ions are essential toward understanding how complexation modulates the reactivity properties of the flavonoid.³ Investigations of metal-flavonoid species are relevant toward understanding the active site chemistry of quercetinases from fungi and bacteria that catalyze oxidative cleavage of the C(2)-C(3) bond (a dioxygenase-type reaction; Figure 5-1) and CO release.^{4,5} In another area of research, metal complexes of 3-hydroxyflavonol (3-Hfl, Figure 5-1 (bottom)) are being used as model systems to evaluate interactions between components of soil organic matter and bioavailable or contaminating heavy metal ions.⁶ To adequately address these areas, systematic studies of structure/reactivity relationships of metal flavonolate complexes are needed, including studies involving environmentally toxic metals ions such as Cd(II) and Hg(II). However, to date such systematic studies are lacking, and while the chemistry of copper flavonolate species has been significantly advanced in recent years,⁷ far fewer X-ray crystallographically characterized flavonolate

complexes of other metal ions have been reported.⁸ To address this deficiency, we recently prepared and characterized the first series of 3-Hfl complexes of the 3d metals, including a Zn(II) derivative, [(6-Ph₂TPA)Zn(3-Hfl)]ClO₄ (**1**; 6-Ph₂TPA, *N,N*-bis((6-phenyl-2-pyridil)methyl)-*N*-((2-pyridil)methyl)amine).⁹

Discussion

Outlined herein is the first systematic study of the structural, spectroscopic, and aerobic photochemical reactivity properties of Group 12 metal 3-Hfl complexes. Our results demonstrate that all three group 12 metal ions form isolable flavonolate complexes that can be characterized by X-ray crystallography, and that each complex undergoes an aerobic photochemically-induced dioxygenase-type reaction to release CO and form a metal-depside complex. These results are novel for a number of reasons. First, aerobic photoinduced flavonoid ring-opening and CO release has not been previously reported for any metal flavonolate complex and is relevant to plant and soil chemistry involving metal-flavonoid interactions. Second, the observed dioxygenase reactivity for the complexes contrasts with prior reports of Zn(II)-flavonolate species that exhibit photoisomerization reactivity akin to that found for free 3-hydroxyflavonol.¹⁰

The Cd(II) and Hg(II) flavonolate complexes [(6-Ph₂TPA)M(3-Hfl)]ClO₄ (M = Cd(II), **2**; M = Hg(II), **3**) were prepared in a similar manner to the Zn(II) analog.⁹ Each complex was characterized by X-ray crystallography, elemental analysis, IR, multinuclear NMR, UV-vis, and fluorescence. While the Zn(II) center of **1** has a coordination number of five in the solid state, the Cd(II) and Hg(II) analogs **2** and **3** exhibit a distorted octahedral geometry (Figure 5-2).¹¹ In both complexes the ketone oxygen of the C ring is

coordinated trans to the tertiary amine nitrogen of the chelate ligand. The average M-O distance involving the flavonolate oxygen atoms increases down the group (**1**: 2.03 Å; **2**: 2.25 Å; **3**: 2.30 Å),¹² and the asymmetry of the flavonolate coordination (Δ_{M-O}) is largest for the Zn(II) and Hg(II) derivatives (0.17 and 0.21 Å, respectively). The flavonolate moiety in **2** and **3** is positioned between the phenyl appendages of the 6-Ph₂TPA ligand (Figure 5-2). The average distance between the centroid of ring C of the flavonolate and the centroids of the aryl rings of the chelate ligand is ~4.0 Å.

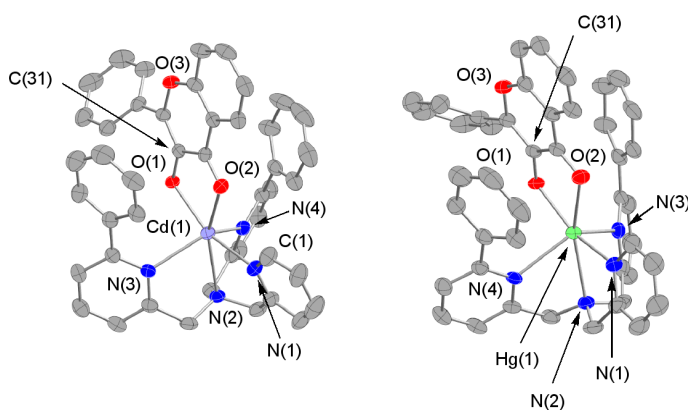


Figure 5-2. Thermal ellipsoid drawings of the cationic portions of **2** and **3**. Ellipsoids are plotted at the 50% probability level. Hydrogen atoms are omitted for clarity.

Comparison of the ¹H NMR spectra of **1-3** (Figure 5-3) shows that each complex has effective C_s symmetry in solution with equivalent phenyl-appended pyridyl appendages. There are interesting differences in the ¹H NMR spectra of this series of complexes in terms of the chemical shifts of proton resonances associated with the phenyl appendages of the 6-Ph₂TPA ligand. Namely, in **2** and **3** the resonances of the meta and

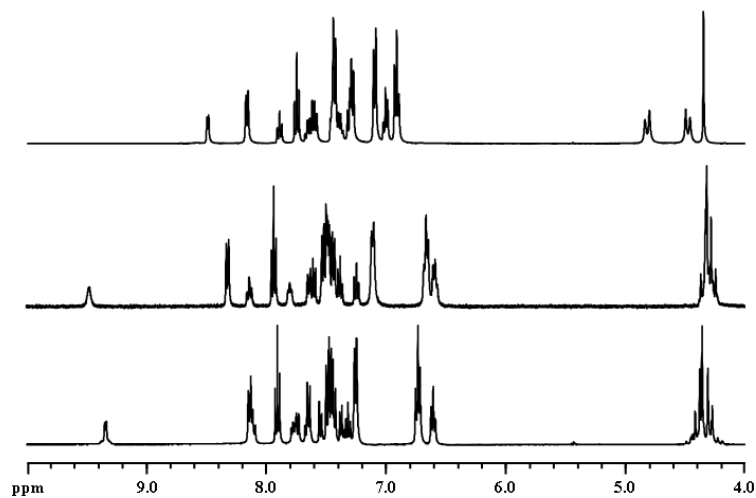


Figure 5-3. ^1H NMR spectra of $[(6\text{-Ph}_2\text{TPA})\text{Zn}(3\text{-Hfl})]\text{ClO}_4$ (**1**, top), $[(6\text{-Ph}_2\text{TPA})\text{Cd}(3\text{-Hfl})]\text{ClO}_4$ (**2**, middle), and $[(6\text{-Ph}_2\text{TPA})\text{Hg}(3\text{-Hfl})]\text{ClO}_4$ (**3**, bottom).

para protons of the phenyl appendages are shifted upfield, which is consistent with π -stacking involving the C ring of the flavonolate. Additionally, the signal for the C(1)-H of the unsubstituted pyridyl ring in **2** and **3** is shifted downfield by ~ 0.9 ppm relative to the same signal in **1**. We attribute this deshielding to the presence of close contact between C(1) of the unsubstituted pyridyl ring and the carbonyl O(2) atom of the coordinated flavonolate (for both complexes **2** and **3** C(1)...O(2) distance is ~ 3.0 Å).

The $\pi \rightarrow \pi^*$ transition of the flavonolate moiety of **2** is found at 430 nm and is red-shifted relative to that of **1** (420 nm) and **3** (415 nm). Fluorescence emission spectra of the complexes show a Stokes shift of 60 nm for **1** and **3**, and 46 nm for **2** (Figures 5-4, 5-5, and 5-6). The excited states associated with these emissions have lifetimes of ~ 2.0 ns (**1**: 2.0(1); **2**: 1.7(1) ns; **3**: 2.0(1) ns). The fluorescence quantum yields are **1-3** 0.18, 0.06, and 0.02, respectively. We note that the complexes presented herein have lower

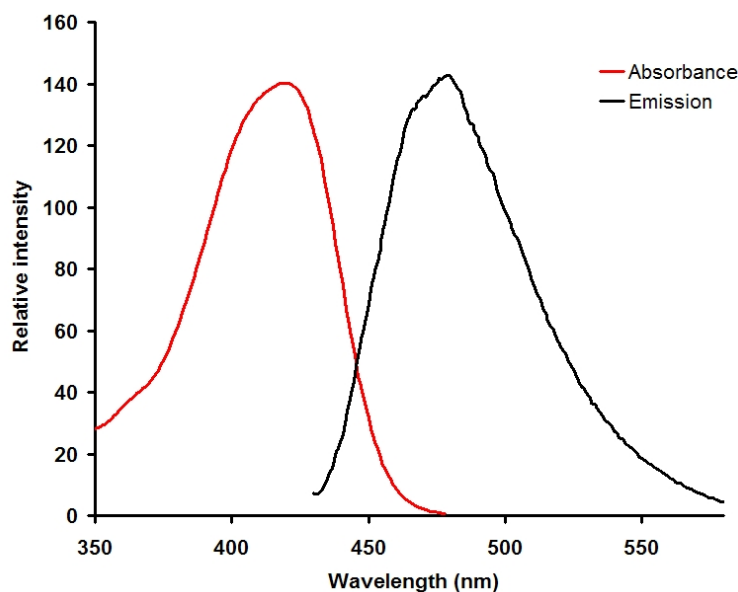


Figure 5-4. Absorption and emission spectra of **1**.

fluorescence quantum yields than that previously reported for $[\text{Zn}(\text{3-Hfl})]^+$ (0.38), albeit the structure of this species has not been determined.¹⁰ The divalent metal flavonolate complexes **1-3** are stable with respect to exposure to oxygen in the solid state under room light for >90 days. However, exposure of aerobic CH_3CN solutions of **1-3** to UV light (Rayonet, 300 nm irradiation) results in clean, high-yield dioxygenase-type reactivity to give the depside complexes $[(6\text{-Ph}_2\text{TPA})\text{M}(\text{O-bs})]\text{ClO}_4$ ($\text{M} = \text{Zn}$ (**4**), Cd (**5**), Hg (**6**); $\text{O-bs} = \text{O-benzoylsalicylate}$; Scheme 5-1) and CO .¹³ Each reaction proceeds with a high quantum yield at 300 nm: **1** ($\phi = 0.9$), **2** ($\phi = 1.0$), and **3** ($\phi = 0.8$).

The shorter excited state lifetime and lower reaction quantum yield of the $\text{Hg}(\text{II})$ complex is due to enhanced spin-orbit coupling.¹⁴ Use of $^{18}\text{O}_2$ in the reactions of **1** and **2** resulted in quantitative incorporation (>98% as determined by mass spectrometry and FTIR) of two labeled oxygen atoms into the depside ligand. Comparison of the fully

assigned ^{13}C NMR spectra of **2**, **5**, and $[(6\text{-Ph}_2\text{TPA})\text{Cd}(\text{CH}_3\text{CN})](\text{ClO}_4)_2$ (**7**, Figures 7-9) clearly show that the carbon lost as CO is derived from the C(31)-O(1) unit (Figure 5-7).

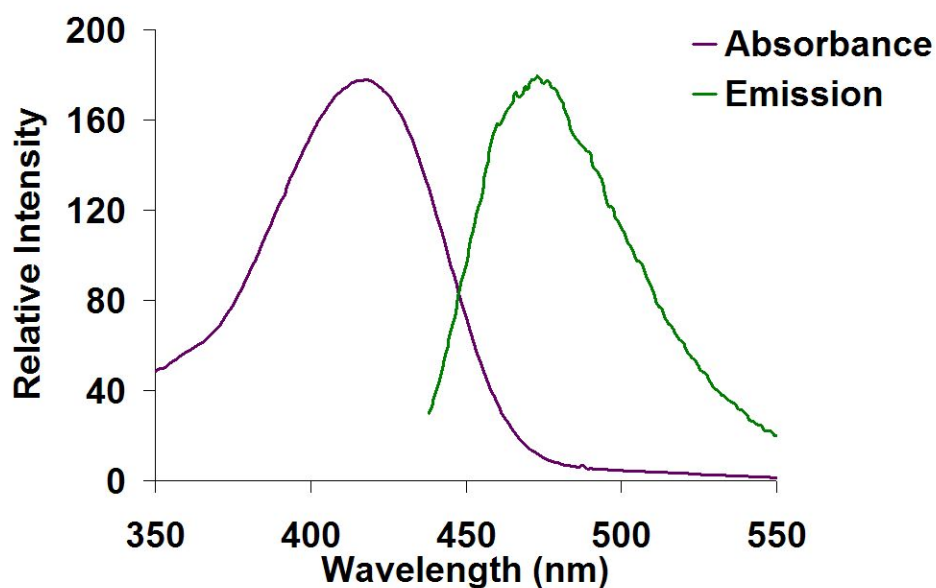


Figure 5-6. Absorption and emission spectra of **3**.

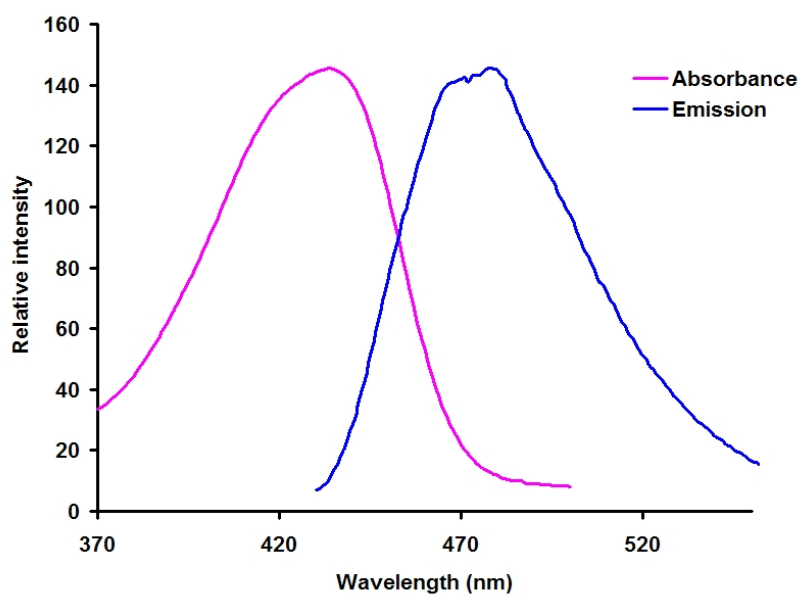
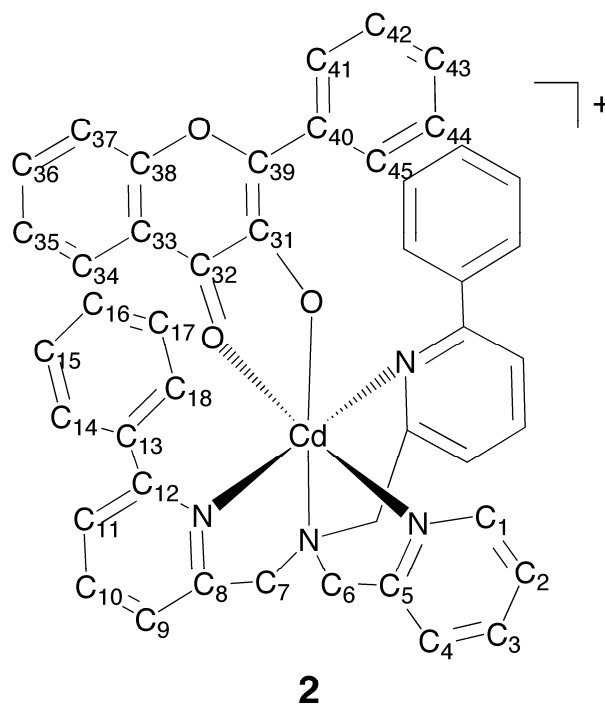


Figure 5-5. Absorption and emission spectra of **2**.

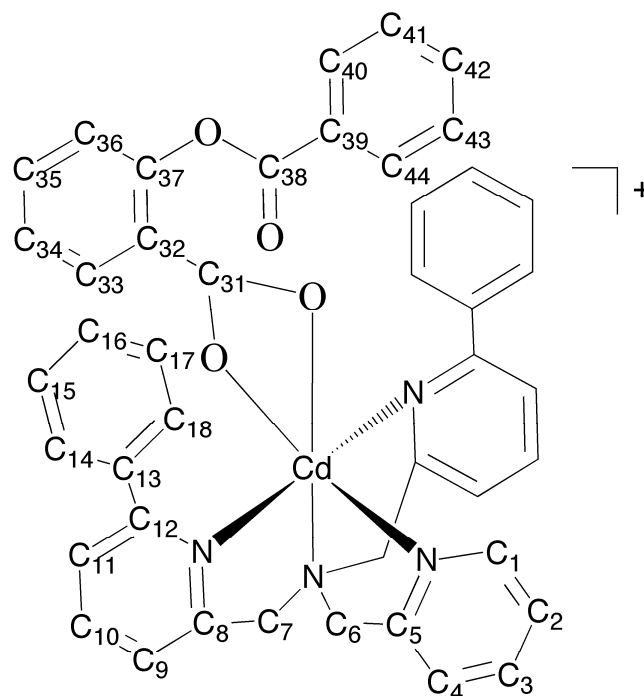
Complexes **4** and **5** were characterized by X-ray crystallography, elemental analysis, NMR spectroscopy, IR spectroscopy, and mass spectrometry. Complex **6** was characterized by NMR spectroscopy, IR spectroscopy, and mass spectrometry. The cationic portions of **4** and **5** are shown in Figure 3. In **4**¹⁵ the zinc center has a nearly trigonal bipyramidal geometry,¹⁶ with the *O*-bs ligand coordinated in a monodentate fashion in an axial position.¹⁷ In **5**, the deposite is coordinated as a bidentate ligand.^{17,18} The spectroscopic properties of the deposite complexes **4** and **5** are as expected (Figure 5-10). We note that ¹H NMR spectra of **6** give evidence for a small amount of loss of the 6-Ph₂TPA ligand in CD₃CN solutions of this complex.¹⁹

The results presented herein are novel when considered in the context of the previously reported photochemistry of 3-Hfl. Irradiation of a pyridine solution of 3-Hfl using a 300 W tungsten lamp, in the presence of a photosensitizer (Bengal rose), has been reported to result in the formation of the photooxygenation products deposite (*O*-bs) and CO.²⁰ This reaction involves the generation of ¹O₂ which reacts with ground state 3-Hfl. Struder *et al.* reported that photooxygenation of 3-Hfl occurs in O₂-saturated nonpolar solvents in the absence of a photosensitizer.²¹



C1	150.9	C31	148.5
C2	126.1	C32	177.7
C3	141.0	C33	121.0
C4	125.8	C34	125.6
C5	155.5	C35	123.7
C6	58.3	C36	132.4
C7	58.4	C37	118.5
C8	156.5	C38	154.3
C9	124.3	C39	146.3
C10	140.7	C40	135.2
C11	124.6	C41	127.9
C12	160.8	C42	128.8
C13	139.5	C43	128.6
C14	128.3	C44	128.8
C15	129.2	C45	127.8
C16	129.3		

Figure 5-7. $^{13}\text{C}\{^1\text{H}\}$ NMR chemical shift assignments (in ppm) for **2**. The resonances were assigned on the basis of HMQC and COSY data.



5

C1	149.7	C31	166.1
C2	125.9	C32	<i>a</i>
C3	141.1	C33	<i>a</i>
C4	124.8	C34	<i>a</i>
C5	155.3	C35	<i>a</i>
C6	58.2	C36	<i>a</i>
C7	58.5	C37	151.6
C8	156.2	C38	171.9
C9	<i>a</i>	C39	131.4
C10	141.1	C40	<i>a</i>
C11	<i>a</i>	C41	<i>a</i>
C12	160.6	C42	<i>a</i>
C13	140.0	C43	<i>a</i>
C14	<i>a</i>	C44	<i>a</i>
C15	<i>a</i>		
C16	<i>a</i>		

Figure 5-8. $^{13}\text{C}\{^1\text{H}\}$ NMR chemical shift assignments (in ppm) for **5**. The resonances were assigned on the basis of HMQC and COSY data. ^aThirteen signals could not be definitively assigned. These are found at: 134.0, 133.8, 132.7, 130.7, 130.4, 130.0, 129.4, 128.6, 127.1, 125.9, 126.7, 124.3, 123.0.

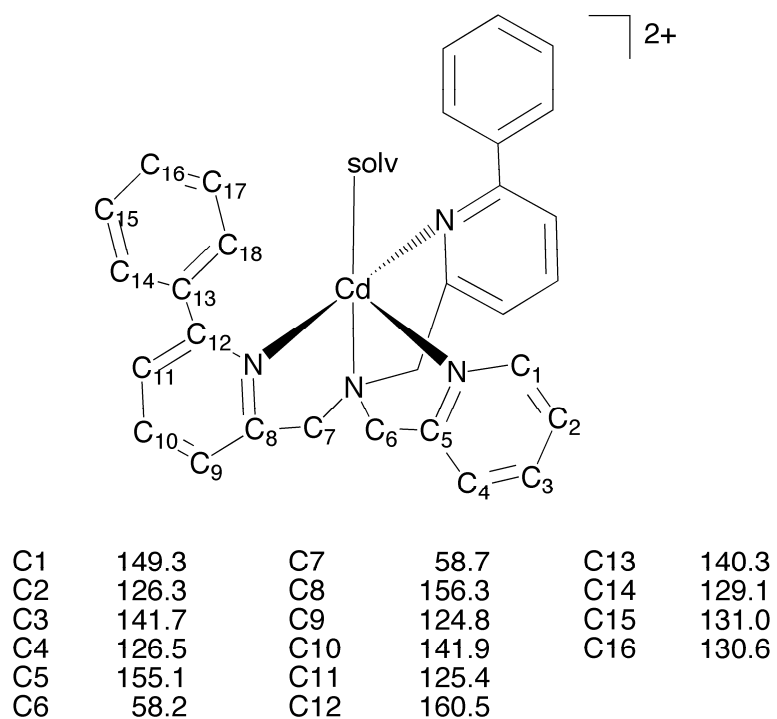


Figure 5-9. $^{13}\text{C}\{^1\text{H}\}$ NMR chemical shift assignments (in ppm) for $[(6\text{-Ph}_2\text{TPA})\text{Cd}(\text{CH}_3\text{CN})](\text{ClO}_4)_2$ (**7**). The resonances were assigned on the basis of HMQC and COSY data.

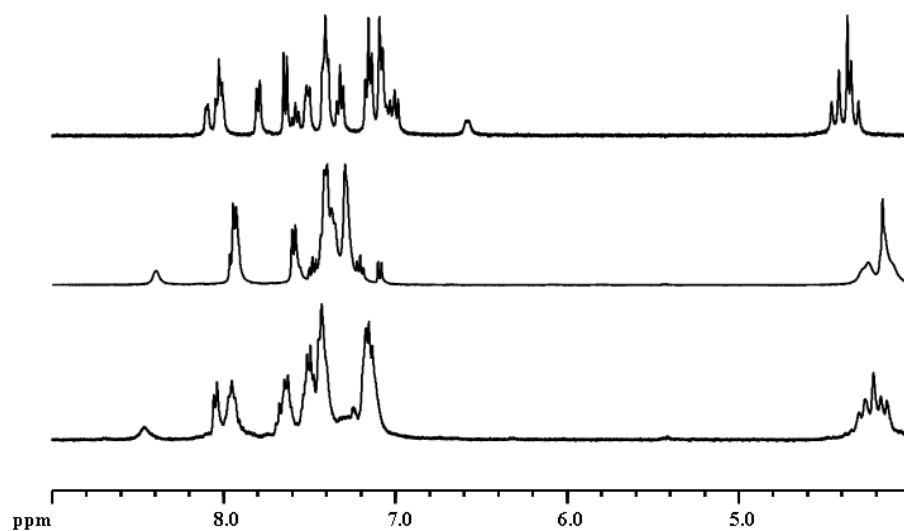


Figure 5-10. ^1H NMR spectra of $[(6\text{-Ph}_2\text{TPA})\text{Zn}(\text{O-bs})]\text{ClO}_4$ (**4**, top), $[(6\text{-Ph}_2\text{TPA})\text{Cd}(\text{O-bs})]\text{ClO}_4$ (**5**, middle), and $[(6\text{-Ph}_2\text{TPA})\text{Hg}(\text{O-bs})]\text{ClO}_4$ (**6**, bottom).

In this case, photooxygenation was suggested to result from reaction between a triplet tautomer state, wherein the C(3) hydroxyl proton has been transferred to the C(4)-carbonyl moiety in a zwitterionic structure, and ground state $^3\text{O}_2$. We note that this chemistry is solvent dependent, as in CH_3OH , CH_3CN , or CH_2Cl_2 photooxygenation does not happen and instead photorearrangement to give 3-phenyl-3-hydroxy-1,2-inandione occurs.

Previously, the presence of metal ions was reported to prevent the photoinduced rearrangement of neutral 3-Hfl, or have no effect on the photochemical reaction.^{10,22a} However, the results presented herein show that metal 3-hydroxyflavonolate complexes can undergo photoinduced dioxygenase type CO-release reactivity when irradiated with UV light. In these complexes the coordinated flavonolate anion is akin to the triplet tautomeric structure of 3-Hf²³, thereby enabling photoinduced photooxygenation and CO-release reactivity. Notably, this reactivity occurs under conditions that are considerably milder than those reported for thermal dioxygenase-type reactions of Cu(3-Hfl) complexes.⁷ Overall, the results presented herein suggest that the formation of metal-flavonolate species in nature may enable light-induced dioxygenase-type CO-release reactivity under mild conditions.

Experimental

General Methods. All reagents and solvents were obtained from commercial sources and were used as received unless otherwise noted. Anaerobic procedures were performed in a VAC atmospheres glovebox. Solvents for glovebox use were dried according to published methods and distilled under N_2 .²⁴ The zinc complexes [(6-

$\text{Ph}_2\text{TPA})\text{Zn}(\text{3-Hfl})\text{]X}$ (**1-X**, X = OTf⁻ or ClO₄⁻) were prepared as previously described.⁹

Physical Methods. UV-vis spectra were collected using a HP8453A spectrometer. FTIR spectra were recorded on a Shimadzu FTIR-8400 spectrometer as KBr pellets. ¹H, ¹³C, and ¹¹³Cd NMR spectra were obtained using a Bruker ARX-400. Chemical shifts are referenced to the residual solvent peak(s) in *d*₃-acetonitrile (¹H: 1.94 (quintet) ppm; ¹³C{¹H} 1.39 (heptet)). ¹¹³Cd NMR spectra were recorded at 88.9 MHz using CD₃CN as the solvent and were referenced to an external standard of 0.5 M Cd(ClO₄)₂·5H₂O in D₂O (0.00 ppm). Additional details regarding the acquisition of ¹¹³Cd NMR spectra have been previously reported.²⁵ CO formation was determined qualitatively via the PdCl₂ method¹⁴ or using an Agilent 3000A Micro GC. Mass spectral data was collected at the Mass Spectrometry Facility, University of California, Riverside. Elemental analyses were performed by Atlantic Microlabs Inc., Norcross, GA.

Acetonitrile solutions of **1–3** (6.70×10^{-5} M) for fluorescence measurements were prepared under anaerobic conditions. Each solution was transferred to a quartz cell sealed with a septum-containing screw cap (VWR Spectrosil). Anaerobic emission spectra were obtained using Shimadzu RF-530XPC in the range of 250-900 nm with excitation wavelength corresponding to the absorption maximum of the complex above 400 nm. The excitation slit width was set at 5 nm and the emission slit width was set at 5 nm for all fluorescence experiments.

Quantum Yield Measurements. In a 100 mL volumetric flask complex **1**, **2**, or **3** (7.1×10^{-6} mol; 6.0 mg, 6.3 mg, and 7.0 mg, respectively) was dissolved in acetonitrile and filled to the mark. Three samples (3 mL each) were prepared for each complex and

put into an air-free quartz cuvettes. Each cuvette was then inserted into an UV reactor and exposed to 300 nm radiation for 60 s. After this time, reaction progress was evaluated using UV-vis spectroscopy, by measuring the intensity of the band I absorption of the metal-bound flavonolate.⁹ The lamp output was measured using standard actinometry.²⁶

*Caution! Perchlorate salts of metal complexes with organic ligands are potentially explosive. Only small amounts of material should be prepared, and these should be handled with great care.*²⁷

Synthesis of [(6-Ph₂TPA)Cd(3-Hfl)]ClO₄ (2). In a glovebox, a methanol solution (~2 mL) of Cd(ClO₄)₂·6H₂O (50.0 mg, 1.19 x 10⁻⁴ mol) was added to solid 6-Ph₂TPA (52.8 mg, 1.19 x 10⁻⁴ mol) and the mixture was stirred until all of the ligand had dissolved. The colorless solution was added to a methanol solution (~2 mL) of 3-Hfl (28.4 mg, 1.19 x 10⁻⁴ mol) and Me₄NOH·5H₂O (21.6 mg, 1.19 x 10⁻⁴ mol). The mixture was then allowed to stir for 3 h at ambient temperature. After this time, the solvent was removed under reduced pressure. The residual bright yellow solid dissolved in CH₂Cl₂ and filtered through a glass wool/celite plug. Precipitation of the product was induced by the addition of excess hexanes. The solid that deposited was then brought to dryness under reduced pressure. Yield: 91 mg, 94%. X-ray quality crystals were obtained by diethyl ether diffusion into an acetonitrile solution. Elemental analysis: found: C, 59.42; H, 3.97; N, 6.06. Calcd for C₄₅H₃₅CdN₄O₇·0.25CH₂Cl₂: C, 59.54; H, 3.92; N, 6.14 (the presence of CH₂Cl₂ was confirmed by a ¹H NMR measurement); UV-vis

$\lambda_{\max}(\text{CH}_3\text{CN})/\text{nm}$ ($\epsilon/\text{M}^{-1}\text{cm}^{-1}$) 430 (13500); FTIR (KBr, cm^{-1}) 1549 ($\nu_{\text{C=O}}$); ^1H NMR (CD_3CN , 400 MHz): δ 9.47 (s, 1H), 8.32 (d, $J = 7.6$ Hz, 2H), 8.14 (t, $J = 8.4$ Hz, 1H), 7.93 (t, $J = 7.7$ Hz, 2H), 7.80 (t, 1H), 7.66-7.30 (m, 10H), 7.24 (dt, $J_1 = 7.9$ Hz, $J_2 = 1.1$ Hz, 1H), 7.11 (d, $J = 7.1$ Hz, 3H), 6.66 (t, $J = 7.4$ Hz, 3H), 6.58 (t, $J = 6.9$ Hz, 1H), 4.38-4.22 (m, 6H); $^{13}\text{C}\{^1\text{H}\}$ NMR (CD_3CN , 100 MHz): δ 177.7, 160.8, 156.2, 155.6, 154.3, 150.9, 148.5, 146.3, 141.0, 140.7, 139.5, 135.2, 132.4, 129.3, 129.2, 128.8, 128.6, 128.3, 127.8, 126.2, 125.8, 125.6, 124.6, 124.3, 123.8, 121.0, 118.5, 58.4, 58.3 (29 signals expected for equivalent phenyl-appended pyridyl donors; 29 observed).; $^{113}\text{Cd}\{^1\text{H}\}$ NMR (CD_3CN , 88.9 MHz): δ 186.8; ESI-APCI, m/z (relative intensity) 793.1732 ($[\text{M}-\text{ClO}_4]^+$, 3%).

The ^{13}C NMR spectral features of **2** are given in Figure 5-7. In order to make signal assignments for this complex a related compound lacking the 3-Hfl ligand [(6-Ph₂TPA)Cd(CH₃CN)](ClO₄)₂ (**7**) was prepared and characterized (see below).

Synthesis of [(6-Ph₂TPA)Hg(3-Hfl)]ClO₄ (3**).** A methanol solution (~2 mL) of Hg(ClO₄)₂·6H₂O (50.0 mg, 9.85 x 10⁻⁵ mol) was added to solid 6-Ph₂TPA (43.6 mg, 9.85 x 10⁻⁵ mol) and the mixture was stirred until all of the ligand had dissolved. The colorless solution was added to a methanol solution (~2 mL) of 3-Hfl (23.5 mg; 9.85 x 10⁻⁵ mol) and Me₄NOH·5H₂O (17.9 mg; 9.85 x 10⁻⁵ mol). The mixture was then allowed to stir for 3 h at ambient temperature. After this time, the solvent was removed under reduced pressure. The residual bright-yellow solid dissolved in CH₂Cl₂ and filtered through a glass wool/celite plug. Precipitation of the product was induced by the addition of excess hexanes. The solid that deposited was then brought to dryness under reduced pressure.

Yield: 94 mg, 97%. X-ray quality crystals were obtained by ether diffusion into a dichloromethane solution. Elemental analysis: found: C, 54.80; H, 3.63; N, 5.56. Calcd for $C_{45}H_{35}HgN_4O_7$: C, 55.16; H, 3.60; N, 5.72; UV-vis λ_{max} (CH_3CN)/nm ($\epsilon/M^{-1}cm^{-1}$) 415 (14000); FTIR (KBr, cm^{-1}) 1566 ($\nu_{C=O}$); 1H NMR (CD_3CN , 400 MHz): δ 9.34 (d, $J = 4.7$ Hz, 1H), 8.15-8.05 (m, 3 H), 7.91 (t, $J = 7.8$ Hz, 2H), 7.80-7.60 (m, 4 H), 7.58-7.20 (m, 13 H), 6.74 (t, $J = 7.5$ Hz, 4H), 6.61 (t, $J = 7.4$ Hz, 2H), 4.50-4.20 (m, 6H); $^{13}C\{^1H\}$ NMR (CD_3CN , 100 MHz): δ 175.2, 160.1, 155.0, 154.3, 154.1, 151.1, 146.5, 145.8, 141.2, 140.4, 139.4, 134.7, 132.7, 129.3, 129.1, 129.1, 128.8, 128.3, 128.0, 127.1, 126.3, 125.9, 124.5, 124.3, 124.1, 121.3, 118.7, 58.9, 58.2 (29 signals expected for equivalent phenyl-appended pyridyl donors; 29 observed); ESI-APCI, m/z (relative intensity) 881.2434 ($[M-ClO_4]^+$, 1.8%).

Photoinduced dioxygenase-type reactivity of 1-3: Isolation of [(6-Ph₂TPA)Zn(*O*-bs)]OTf (4), [(6-Ph₂TPA)Cd(*O*-bs)]ClO₄ (5), and [(6-Ph₂TPA)Hg(*O*-bs)]ClO₄ (6) (bs = *O*-benzoylsalicylate). Aerobic CH_3CN solutions of **1-3** were irradiated using a Rayonet Photoreactor equipped with 300 nm Hg lamps. The progress of each reaction was monitored by UV-vis. After each reaction reached completion, the solvent was removed under reduced pressure. Complexes **3-6** were precipitated from acetonitrile via the addition of excess diethyl ether. Each isolated solid was dried under vacuum. X-ray quality crystals for **4** and **5** were obtained by diethyl ether diffusion into an acetonitrile solution.

[(6-Ph₂TPA)Zn(*O*-bs)]ClO₄ (4). Yield: 88%. Elemental analysis: found: C, 59.13; H, 3.81; N, 6.29. Calcd for $C_{45}H_{35}F_3N_4O_7SZn \cdot 0.75H_2O$: C, 59.28; H, 4.04; N, 6.14

(the presence of H₂O was also confirmed by a ¹H NMR measurement); FTIR (KBr, cm⁻¹): 1736 (ν_{C=O}); ¹H NMR (CD₃CN, 400 MHz): δ 8.0 (d, *J* = 4.3 Hz, 1H), 8.02 (dt, *J* = 7.7 Hz, 3H), 7.80 (dd, *J*₁ = 8.3 Hz, *J*₂ = 1.2 Hz, 2H), 7.28-7.65 (m, 12H), 6.96-7.20 (m, 10H), 6.65 (m, 1H), 4.20-4.50 (m, 6H); ¹³C{¹H} NMR (CD₃CN, 100 MHz): δ 169.6, 166.0, 160.6, 156.4, 155.2, 151.2, 149.1, 141.8, 141.6, 139.4, 134.1, 133.9, 132.4, 131.2, 130.6, 130.2, 129.4, 129.3, 129.0, 126.0, 125.7, 125.5, 125.1, 123.6, 123.3, 57.7, 57.5 (26 signals observed); MALDI-MS, *m/z* (relative intensity) 747.1933 ([M-OTf]⁺, 100%).

[(6-Ph₂TPA)Cd(*O*-bs)]ClO₄ (5). Yield: 96%. Elemental analysis: found: C, 58.74; H, 3.98; N, 6.75. Calcd for C₄₅H₃₅CdN₄O₇·0.4CH₃CN: C, 59.00; H, 4.00; N, 6.76 (the presence of CH₃CN was also confirmed by a ¹H NMR measurement); FTIR (KBr, cm⁻¹): 1736 (ν_{C=O}). ¹H NMR (CD₃CN, 400 MHz): δ 8.3 (s, 1H), 8.00-7.85 (m, 4H), 7.65-7.00 (m, 21H), 4.26-4.00 (m, 6H); ¹³C{¹H} NMR (CD₃CN, 100 MHz): δ 171.9, 165.1, 160.6, 156.2, 155.3, 151.6, 149.7, 141.1, 140.0, 134.0, 133.8, 132.7, 131.4, 130.7, 130.4, 130.0, 129.4, 128.6, 125.9, 125.9, 125.7, 124.8, 124.3, 124.0, 58.5, 58.2 (26 signals observed). ¹¹³Cd{¹H} NMR (CD₃CN, 88.9 MHz): δ 134.3; ESI-APCI, *m/z* (relative intensity) 797.1700 ([M-ClO₄]⁺, 9%).

[(6-Ph₂TPA)Hg(*O*-bs)]ClO₄ (6). FTIR (KBr, cm⁻¹): 1734 (ν_{C=O}); ESI-APCI, *m/z* (relative intensity) 885.2381 ([M-ClO₄]⁺, 10%).

¹⁸O₂ Labeling of Photooxygenation Reactions 1 and 2. In the glovebox **1-ClO₄** (2.24 x 10⁻⁵ mol) or **2** (1.12 x 10⁻⁵ mol) was dissolved in ~10 mL of acetonitrile and the solution was then transferred to a solvent transfer flask from which was promptly degassed by three freeze-pump-thaw cycles. After the third thawing, ~25 cm³ of ¹⁸O₂

(99%; ICON Isotopes) was introduced and the reaction was put into a Rayonet Photoreactor equipped with 300 nm Hg lamps until the color of the reaction bleached from bright yellow to colorless. Upon completion of each reaction, the solvent was removed under reduced pressure. Mass spectral analysis of the products (**4** and **5**) indicated quantitative (>98%) ^{18}O incorporation into two oxygen atoms of the *O*-benzoysalicylato (*O*-bs) ligand.

Synthesis of [(6-Ph₂TPA)Cd(CH₃CN)](ClO₄)₂ (7**).** An acetonitrile solution (~2 mL) of Cd(ClO₄)₂·6H₂O (50.0 mg, 1.19 x 10⁻⁴ mol) was added to solid 6-Ph₂TPA (52.8 mg, 1.19 x 10⁻⁴ mol) and stirred until all of the ligand had dissolved. Crystals were obtained by diethyl ether diffusion into an acetonitrile solution. Yield: 95 mg, 92%; Elemental analysis: found: C, 48.08; H, 3.66; N, 8.80. Calcd for C₃₂H₂₉CdCl₂N₅O₈: C, 48.35; H, 3.68; N, 8.81; FTIR (KBr, cm⁻¹) 1092 (ν_{ClO_4}), 621 (ν_{ClO_4}). ¹H NMR (CD₃CN, 400 MHz): δ 8.41 (d, J = 4.8 Hz, 1H), 8.09-8.02 (m, 3H), 7.65-7.37 (m, 16H), 4.45-4.23 (m, 6H); δ 160.5, 156.3 (J ($^{13}\text{C}^{113}\text{Cd}$) = 67.2 Hz), 155.1 (J ($^{13}\text{C}^{113}\text{Cd}$) = 93.2 Hz), 149.3, 141.9, 141.7, 140.3, 131.0, 130.6, 129.1, 126.5 (J ($^{13}\text{C}^{113}\text{Cd}$) = 42.4 Hz), 126.3 (J ($^{13}\text{C}^{113}\text{Cd}$) = 33.6 Hz), 125.4, 124.8, 58.7, 58.2 (16 signals expected for equivalent phenyl-appended pyridyl donors; 16 observed). ¹¹³Cd{¹H} NMR (CD₃CN, 88.9 MHz): δ 187.02.

X-ray Crystallography. A single crystal of **2-5** was mounted on a glass fiber with traces of viscous oil and then transferred to a Nonius KappaCCD diffractometer equipped with Mo K α radiation (λ = 0.71073 Å). For unit cell determination, ten frames of data were collected at 150(1) K with an oscillation range of 1 deg/frame and an

exposure time of 20 sec/frame. Final cell constants were determined from a set of strong reflections from the actual data collection. All reflections were indexed, integrated, and corrected for Lorentz polarization and absorption effects using DENZO-SMN and SCALEPAC.²⁸ Structures were solved by a combination of direct and heavy-atom methods using SIR 97.²⁹ All of the non-hydrogen atoms were refined with anisotropic displacement coefficients. For complexes **2**, **3**, and **4** the hydrogen atoms were assigned isotropic displacement coefficients (U)_H = 1.2 U (C) or 1.5 U (C_{methyl}), and their coordinates were allowed to ride on their respective carbons using SHELXL97.³⁰ Hydrogen atoms in **4** were located and refined independently using SHELXL97.³⁰

Structure Solution and Refinement. Complex **2** crystallizes in the space group $P2_1/n$. Three out of four oxygen atoms in the perchlorate anion are disordered. Complex **3** crystallizes in the space group $P2_1/n$. Complex **4** crystallizes in the space group $P2_1/c$. Complex **5** crystallizes in $P-1$ space group with one molecule of acetonitrile in the crystal lattice. Two out of four oxygen atoms in the perchlorate anion of **5** are disordered.

Details of the X-ray data collection and refinement are given in Table 5-1. Selected bond distances and angles are given in Tables 5-2 and 5-3.

Table 5-1. Summary of X-ray Data Collection and Refinement for **2-5**.

	2	3	4	5
Empirical formula	C ₄₅ H ₃₅ CdClN ₄ O ₇	C ₄₅ H ₃₅ ClHgN ₄ O ₇	C ₄₅ H ₃₅ F ₃ N ₄ O ₇ SZn	C ₄₆ H ₃₈ CdClN ₅ O ₈
M _r	891.62	979.81	898.20	936.66
Crystal system	Monoclinic	Monoclinic	Monoclinic	Triclinic
Space group	P2 ₁ /n	P2 ₁ /n	P2 ₁ /c	P-1
a/ Å	11.4616(2)	11.4117(2)	10.1785(2)	14.2066(2)
b/ Å	16.3861(3)	16.3761(2)	16.3337(5)	13.24300(10)
c/ Å	20.8770(4)	20.9794(3)	24.1620(5)	14.3060(2)
α/°	90	90	90	102.5400(9)
β/°	95.0205(11)	95.0070(9)	91.0370(14)	116.8087(6)
γ/°	90	90	90	99.7178(9)
V / Å ³	3905.89(12)	3905.65(10)	4016.34(17)	2075.18(5)
Z	4	4	4	2
D _c / Mg m ⁻³	1.516	1.666	1.485	1.499
T / K	150(1)	150(1)	150(1)	150(1)
Color	Yellow	Yellow	Colorless	Colorless
Crystal habit	Prism	Prism	Prism	Prism
Crystal size/ mm	0.28 x 0.23 x 0.13	0.20 x 0.15 x 0.10	0.25 x 0.20 x 0.13	0.23 x 0.20 x 0.13
Diffractionmeter	Nonius Kappa CCD	Nonius Kappa CCD	Nonius Kappa CCD	Nonius Kappa CCD
μ / (mm ⁻¹)	0.686	4.068	0.736	0.652
2θ _{max} /°	54.96	54.98	54.92	54.94
Completeness to θ (%)	99.9	99.8	99.5	99.7
Reflections collected	15965	16904	15119	17877
Independent reflections	8943	8946	9139	9483
R _{int}	0.0303	0.0366	0.0342	0.0202
Variable parameters	552	552	690	571
R1 / wR2 ^b	0.0631/0.0859	0.0565/0.0674	0.0829/0.1034	0.0469/0.0803
Goodness-of-fit (F ²)	1.019	1.039	1.016	1.037
Δρ _{max/min} / e Å ⁻³	0.840/-0.573	1.486/-0.784	0.332/-0.482	0.907/-1.184

^aRadiation used: Mo Kα (λ = 0.71073 Å) ^bR1 = $\sum ||F_o| - |F_c|| / \sum |F_o|$; wR2 = $[\sum [w(F_o^2 - F_c^2)^2] / [\sum (F_o^2)^2]]^{1/2}$, where $w = 1/[\sigma^2(F_o^2) + (aP)^2 + bP]$.

Table 5-2. Selected Bond Distances (Å) for Complexes 2-5.

	2	3	4	5
M-N(1)	2.337(2)	2.324(3)	2.115(2)	2.3328(19)
M-N(2)	2.430(2)	2.470(3)	2.1913(18)	2.3762(18)
M-N(3)	2.4636(19)	2.563(3)	2.155(2)	2.4592(18)
M-N(4)	2.420(2)	2.494(3)	2.132(2)	2.4172(17)
M-O(1)	2.2134(17)	2.194(2)	1.9387(15)	2.4062(16)
M-O(2)	2.2792(16)	2.408(2)		2.2439(16)
Δ_{M-o}	0.07	0.21		0.16
C(31)-O(1)	1.316(3)	1.317(4)		
C(32)-O(2)	1.256(3)	1.248(4)		

Table 5-3. Selected Bond Angles (deg) for Complexes 2-5.

	2	3	4	5
O(1) – M – O(2)	74.74(6)	73.37(8)		56.42(6)
N(1) – M – O(1)	156.95(7)	155.23(10)	99.53(7)	84.18(6)
N(1) – M – O(2)	82.45(7)	82.05(10)		140.59(6)
N(1) – M – N(2)	71.13(7)	71.10(11)	77.34(7)	72.65(7)
N(1) – M – N(3)	103.81(7)	103.23(10)	121.81(8)	99.30(7)
N(1) – M – N(4)	98.09(7)	97.57(10)	117.93(8)	105.14(6)
N(2) – M – N(3)	72.82(7)	71.72(10)	75.42(7)	73.96(6)
N(2) – M – N(4)	67.65(7)	66.12(9)	78.53(7)	70.54(6)
N(2) – M – O(1)	131.54(7)	133.43(9)	176.79(8)	156.65(6)
N(2) – M – O(2)	153.56(7)	153.15(9)		146.73(6)
N(3) – M – N(4)	124.990(7)	123.03(10)	105.51(8)	127.72(6)
N(3) – M – O(1)	89.41(6)	90.47(9)	105.88(7)	107.88(6)
N(3) – M – O(2)	116.00(7)	115.92(9)		94.16(6)
N(4) – M – O(1)	89.28(7)	91.84(9)	103.78(7)	119.88(6)
N(4) – M – O(2)	116.60(6)	119.16(9)		95.08(6)

References

1. (a) Bischoff, S. C. *Curr. Opin. Clin. Nutr. Metab. Care* **2008**, *11*, 733-740; (b) Cazarolli, L. H.; Zanatta, L.; Alberton, E. H.; Figueiredo, M. S. R. B.; Folador, P.; Damazio, R. G.; Pizzolatti M. G.; Silva, F. R. M. B. *Mini-Rev. Med. Chem.* **2008**, *8*, 1429-1440; (c) Boots, A. W.; Haenen G. R. M. M.; Bast, A. *Eur. J. Pharmacol.* **2008**, *585*, 325-337; (d) Friedman, M. *Mol. Nutr. Food Res.* **2007**, *51*, 116-134; (e) Amic, D.; Davidovic-Amic, D.; Beslo, D.; Rastija, V.; Lucic, B.; Trinajstic, N. *Curr. Med. Chem.* **2007**, *14*, 827-845; (f) Cushnie T. P. T.; Lamb, A. J. *Int. J. Antimicrob. Agents* **2005**, *26*, 343-356.
2. (a) Yao, H.; Xu, W.; Shi, X.; Zhang, Z. *J. Environ. Sci. Health, Part C: Environ. Carcinog. Ecotoxicol. Rev.* **2011**, *29*, 1-31; (b) Jagtap, S.; Meganathan, K.; Wagh, V.; Winkler, J.; Hescheler, J.; Sachinidis, A. *Curr. Med. Chem.* **2009**, *16*, 1451-1462.
3. (a) de Souza, R. F. V.; De Giovani, W. F. *Spectrochim. Acta, Part A* **2005**, *61*, 1985-1990; (b) de Souza, R. F. V.; Sussuchi, E. M.; De Giovani, W. F. *Synth. React. Inorg. Met-Org. Chem.* **2003**, *33*, 1125-1144.
4. Steiner, R. A.; Kalk, K. H.; Dijkstra, B. W. *Proc. Natl. Acad. Sci* **2002**, *99*, 16625-16630.
5. (a) Merkens, H.; Kappl, R.; Jakob, R. P.; Schmid, F. X.; Fetzner, S. *Biochemistry* **2008**, *47*, 12185-12196; (b) Schaab, M. R.; Barney, B. M.; Francisco, W. A. *Biochemistry* **2006**, *45*, 1009-1016; (c) Gopal, B.; Madan, L. L.; Betz, S. F.; Kossiakoff, A. A. *Biochemistry* **2005**, *44*, 193-201.

6. (a) Dangleterre, L.; Cornard, J. P. *Polyhedron* **2005**, *24*, 1593-1598; (b) Lapouge, C.; Cornard, J. P. *J. Phys. Chem. A* **2005**, *109*, 6752-6761.
7. (a) Pap, J. S.; Kaizer, J.; Speier, G. *Coord. Chem. Rev.* **2010**, *254*, 781-793; (b) Kaizer, J.; Balogh-Hergovich, É.; Czaun, M.; Csay, T.; Speier, G. *Coord. Chem. Rev.* **2006**, *250*, 2222-2233.
8. (a) Barath, G.; Kaizer, J.; Speier, G.; Parkanyi, L.; Kuzmann, E.; Vertes, A. *Chem. Commun.* **2009**, 3630-3632; (b) Kaizer, J.; Barath, G.; Pap, J.; Speier, G.; Giorgi, M.; Reglier, M. *Chem. Commun.* **2007**, 5235-5237.
9. Grubel, K.; Rudzka, K.; Arif, A. M.; Klotz, K.; Halfen, J. A.; Berreau, L. M. *Inorg. Chem.* **2010**, *49*, 82-96.
10. Protti, S. ; Mezzetti, A. ; Lapouge, C. ; Cornard, J. P. *Photochem. Photobiol. Sci.* **2008**, *7*, 109-119.
11. **2:** C₄₅H₃₅CdClN₄O₇, *M* = 891.62, monoclinic, *a* = 11.4616(2), *b* = 16.3861(3), *c* = 20.8770(4) Å, *U* = 3905.89(12) Å³, *T* = 151(1) K, space group *P*2₁/*n*, *Z* = 4, 15965 reflections measured, 8943 unique (*R*_{int} = 0.0303) which were used in all calculations. The final *R* values (*I* > 2σ(*I*)) are *R*1 = 0.0364 and *wR*2 = 0.0765.
3: C₄₅H₃₅HgClN₄O₇, *M* = 979.81, monoclinic, *a* = 11.4117(2), *b* = 16.3761(2), *c* = 20.9794(3) Å, *U* = 3905.65(10) Å³, *T* = 151(1) K, space group *P*2₁/*n*, *Z* = 4, 16904 reflections measured, 8946 unique (*R*_{int} = 0.0366) which were used in all calculations. The final *R* values (*I* > 2σ(*I*)) are *R*1 = 0.0364 and *wR*2 = 0.0883.

12. The average M-N distance involving the chelate ligand increases by ≥ 0.3 Å for the Cd(II) and Hg(II) derivatives relative to **1** (avg. M-N: **1**: 2.11 Å; **2**: 2.41 Å; **3**: 2.46 Å).
13. CO formation was detected via GC and the PdCl₂ method. Allen, T. H.; Root, W. S. *J. Biol. Chem.* **1955**, *215*, 309-317. CO₂ formation was minimal and the error range of the GC analysis.
14. (a) Tamayo, A.; Pedras, B.; Lodeiro, L.; Escriche, L.; Casabó, J.; Capelo, J. L.; Covelo, B.; Kivekäs, R.; Silanpää, R. *Inorg. Chem.* **2007**, *46*, 7818-7826; (b) Burrell, C. N.; Bodine, M. I.; Elbjeirami, O.; Reibenspies, J. H.; Omary, M. A.; Gabbai, F. P. *Inorg. Chem.* **2007**, *46*, 1388-1395.
15. **4**: C₄₅H₃₅F₃N₄O₇SZn, *M* = 898.20, monoclinic, *a* = 10.1785(2), *b* = 16.3337(5), *c* = 24.1620(5) Å, *U* = 4016.34(17) Å³, *T* = 151(1) K, space group *P*2₁/*c*, *Z* = 4, 15119 reflections measured, 9139 unique (*R*_{int} = 0.0342) which were used in all calculations. The final *R* values (*I* > 2σ(*I*)) are *R*1 = 0.0432 and *wR*2 = 0.0883.
16. **4**: $\tau^5 = 0.92$; τ^5 is a parameter that describes the geometry of a five-coordinate metal center. A trigonal bipyramidal geometry correlates with $\tau^5 = 1$, whereas a square pyramidal geometry has $\tau^5 = 0$. Addison, A. W.; Rao, T. N.; Reedijk, J.; van Rijn, J.; Verschoor, G. C. *J. Chem. Soc., Dalton Trans.* **1984**, 1349-1356.
17. Monodentate: $\Delta d > 0.6$ Å, $\Delta\theta > 28^\circ$; bidentate: $\Delta d < 0.3$ Å, $\Delta\theta < 14^\circ$. Kleywegt, G. J.; Wiesmeijer, W. G. R.; van Driel, G. J.; Driessen, W. L.; Reedijk, J.; Noordik, J. H. *J. Chem. Soc., Dalton Trans.* **1985**, 2177-2184.

18. **5**: C₄₆H₃₈CdClN₅O₈, $M = 936.66$, triclinic, $a = 14.2066(2)$, $b = 13.24300(10)$, $c = 14.3060(2)$ Å, $U = 2075.18(5)$ Å³, $T = 151(1)$ K, space group $P-1$, $Z = 4$, 17877 reflections measured, 9483 unique ($R_{\text{int}} = 0.0202$) which were used in all calculations. The final R values ($I > 2\sigma(I)$) are $R1 = 0.0348$ and $wR2 = 0.0749$.
19. Additional studies of the solution NMR properties of **6** are currently in progress.
20. (a) Matsuura, T.; Matsushima, H.; Sakamoto, H. *J. Am. Chem. Soc.* **1967**, *89*, 6370-6371; (b) Matsuura, T.; Matsushima, H.; Nakashima, R. *Tetrahedron* **1970**, *26*, 435-443.
21. Studer, S. L.; Brewer, W. E.; Martinez, M. L.; Chou, P.-T. *J. Am. Chem. Soc.* **1989**, *111*, 7643-7644.
22. (a) Sisa, M.; Bonnet, S. L.; Ferreira, D.; Van der Westhuizen, J. H. *Molecules* **2010**, *15*, 5196-5245; (b) Matsuura, T.; Takemoto, T.; Nakashima, R. *Tetrahedron* **1971**, *19*, 1539-1540; (c) Matsuura, T.; Takemoto, T.; Nakashima, R. *Tetrahedron* **1973**, *29*, 3337-3340; (d) Ficarra, R.; Ficarra, P.; Tommasini, S.; Campagna, S.; Guglielmo, G. *Boll. Chim. Farm.* **1994**, *133*, 665-669.
23. Yokoe, I.; Higushi, K.; Shirataki, Y.; Komatsu, M. *Chem. Pharm. Bull.* **1981**, *29*, 894-898.
24. Armarego, W. L. F.; Perrin, D. D. *Purification of Laboratory Chemicals*, 4th ed.; Butterworth-Heinemann: Boston, MA, 1996.
25. Allred, R. A.; McAlexander, H. L.; Arif, A. M.; Berreau, L. M. *Inorg. Chem.* **2002**, *41*, 6790-6801.

26. (a) Hatchard, C. G.; Parker, C. A. *Proceedings of the Royal Society, London A* **1956**, 518-536; (b) Kuhn, H. J.; Braslavsky, S. E.; Schmidt, R. *Chemical Actinometry, IUPAC Technical Report*, **2004**, 1-47.
27. Wolsey, W. C. *J. Chem. Educ.* **1973**, 50, A335-A337.
28. Otwinowski, Z.; Minor, W.; *Methods Enzymol.* **1997**, 276, 307-326.
29. Altomare, M. C.; Burla, M.; Camalli, G. L.; Cascarano, C.; Giacovazzo, A.; Guagliardi, A. G. G.; Moliterni, G.; Polidori, R.; Spagna, *J. Appl. Cryst.* **1999**, 32, 115-119.
30. Sheldrick, G. M. *SHELXL-97 Program for the Refinement of Crystal Structures*; University of Göttingen, Germany, 1997.

CHAPTER 6

PHOTOCHEMICAL CO RELEASE REACTIVITY OF OPEN-SHELL 3d
DIVALENT FLAVONOLATE COMPLEXES**Abstract**

Irradiation of 3-hydroxyflavonolate complexes of Mn(II), Co(II), Ni(II), and Cu(II) supported by the 6-Ph₂TPA ligand (**1-4**) at 300 nm results in CO release and the formation of the corresponding depside complexes (**8-11**) which were isolated and characterized. These reactions proceed considerably slower than those involving closed-shell metal ions due to quenching of the excited state by the open-shell metal ion. Each depside complex reacts with 3-Hfl, with the Ni(II) and Cu(II) depside complexes undergoing reaction to regenerate the flavonolate complex to the greatest extent. This suggests that all of the flavonolate complexes should exhibit catalytic CO-release reactivity under photochemical conditions. Higher conversion is anticipated for the systems containing Ni(II) and Cu(II).

Introduction

Flavonoids are naturally occurring compounds found in plants. Due to their anti-microbial, anti-oxidative, and UV-protective properties the chemistry of this class of molecules is of considerable current interest.¹ 3-hydroxyflavonol (3-Hfl, Figure 6-1(top)) is a flavonoid, albeit it is not found naturally in plants. This molecule has been used as an analog for the flavonoid quercetin (Figure 6-1(bottom)) in model studies of relevance to quercetin dioxygenases.^{2,3} These enzymes, which are found in bacteria

and fungi, catalyze the oxidative ring-opening of the *C* ring of quercetin, a reaction which results in the release of one equivalent of CO (Figure 6-1(bottom)).^{4,5} Notably, quercetinase has been found to utilize different 3*d* metal ions depending on the source.^{4,5} Specifically, quercetinases found in fungi are Cu(II) enzymes, while the bacterial enzyme from *Streptomyces* sp. FLA was shown to exhibit the highest activity with Ni(II) or Co(II) as the active site metal, with other metal ions, such as Mn(II), yielding lower activity.

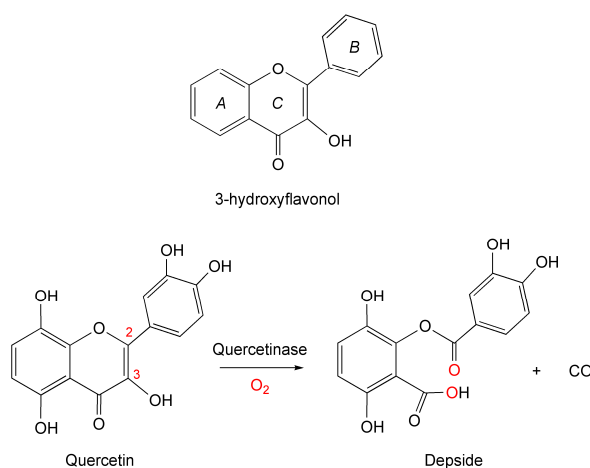


Figure 6-1. Top: Structure of 3-hydroxyflavonol. Bottom: Structure of quercetin and reaction catalyzed by quercetinase enzymes.

Several investigations of the thermally-induced oxidative cleavage reactivity of copper-flavonolate complexes have been reported.^{2,3} Recently, similar studies have been described for mononuclear Mn(II) and Fe(III) flavonolate species.³ However, it should be noted that to date, no series of structurally-similar 3-Hfl complexes has been examined in terms of oxidative carbon-carbon bond cleavage reactivity. Thus,

the influence of the metal ion cannot be clearly evaluated. To begin to address this issue, we recently reported the first series of structurally-related flavonolate complexes of 3d metals (**1-5**, Figure 6-2).⁶ We have also prepared a structurally similar series for the Group 12 metal ions (**5-7**, Figure 6-2).⁷

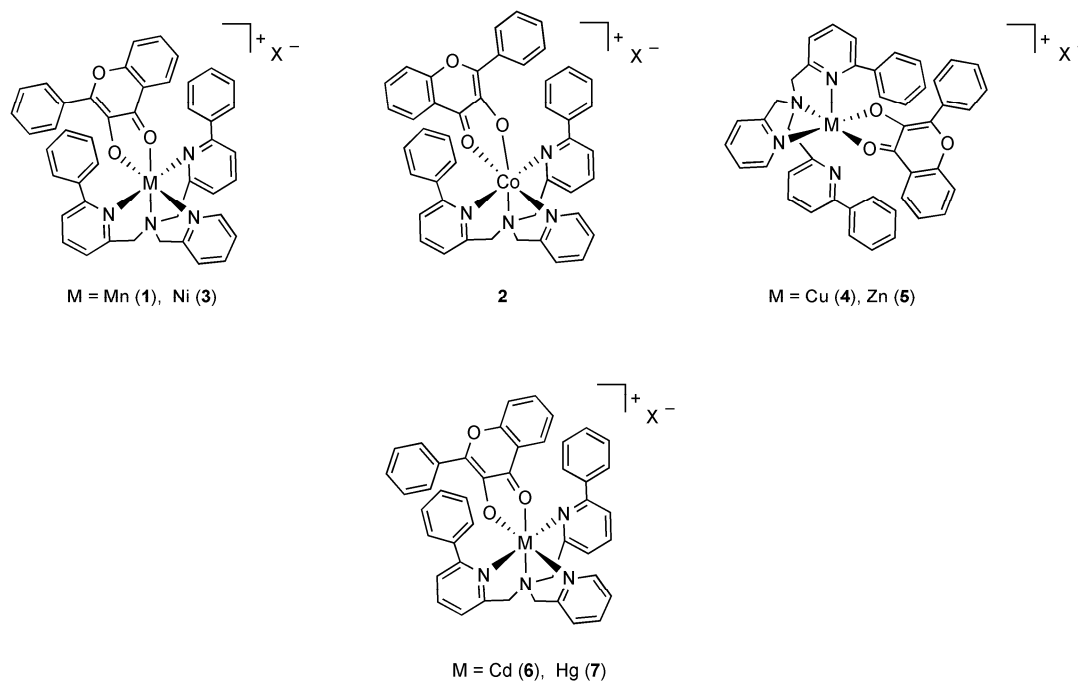


Figure 6-2. Structural features of **1-7**. X = ClO₄⁻ or OTf⁻.

We discovered that the latter series of complexes undergo clean photoinduced dioxygenase-type reactivity with release of CO when irradiated at 300 nm. These complexes exhibit high reaction quantum yields ($\phi > 0.8$) resulting in short reaction times. This chemistry is novel in that photoinduced CO-release had not been previously reported for divalent metal-flavonolate complexes. We are interested in examining such chemistry as it may be used toward the development of new CO-

releasing molecules (CORMs).⁸ Such molecules are of current interest for potential therapeutic applications, as the administration of small quantities of CO has been shown to enhance blood vessel dilation and exhibits antimicrobial and anti-inflammatory activity.⁹

Herein we report studies of the photoinduced CO-release reactivity of the 3-Hfl complexes **1-4** (Figure 6-2). While undergoing reactions similar to those found for **5-7**, low quantum yields from quenching of the flavonolate excited state result in slower CO-release for these compounds relative to that exhibited by **5-7**. The divalent deprotonated complexes generated upon irradiation of **1-4** (labeled as **8-11**) react with 3-Hfl to differing extents, suggesting that under photochemical conditions catalytic flavonolate conversion and CO release should be possible. However, we anticipate that such reactions will exhibit variable turnovers depending on the divalent metal ion present.

Results and Discussion

Spectroscopic properties and UV reactivity of 1-4. Complexes **1-4** were investigated in terms of their fluorescent emission properties. Irradiation of each complex at 285-300 nm produces an emission at ~475 nm. The intensity of the emission band increases when the irradiation is performed at 420 nm into the $\pi \rightarrow \pi^*$ band I of the flavonolate. Representative absorption and emission ($\lambda_{\text{ex}} = 420 \text{ nm}$) spectra of **1** collected under anaerobic conditions are shown in Figure 6-3. Similar spectra were found for **2-4**. Notably, the emission intensity of these complexes is

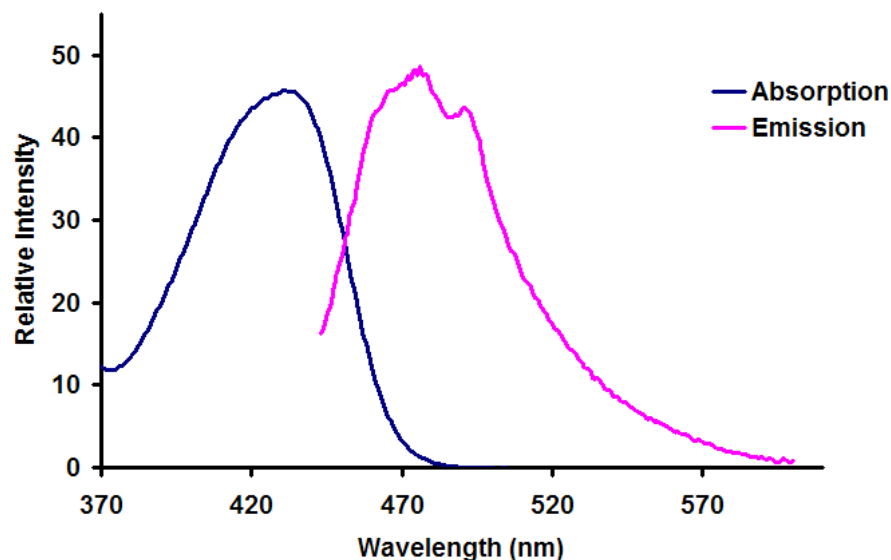


Figure 6-3. Absorption and emission spectra of **1**.

similar and significantly lower than that exhibited by **5-7**. This is a result of quenching of the excited state by the open shell $3d$ metal center in **1-4**.¹⁰

Irradiation of O_2 -purged solutions of **1-4** at 300 nm using a Rayonet photoreactor resulted in the gradual loss of the $\pi \rightarrow \pi^*$ absorption band of the flavonolate. The total reaction time needed for reaction completion ranged from hours for the Ni(II) complex **3** to more than 8 days of continuous irradiation for the Cu(II) analog **4**. The quantum yield for each reaction was determined by actinometry using ferrioxalate as a standard to measure photon flux. The values obtained (**1**, **2**, and **4**: $\phi = 0.05$; **3**: $\phi = 0.08$) are much lower than that found for **5-7** and are consistent with the significantly longer reaction times required completion of the reactions involving the open-shell complexes. Sampling of the headspace gas of each reaction by GC and via the $PdCl_2$

method¹¹ indicated the formation of CO. Following work-up, the depside complexes **8-11** (Scheme 6-1) were characterized by elemental analysis, ¹H NMR (only **9** and **10**), FTIR, mass spectrometry, and in one case (**9·0.5CH₃CN**) by X-ray crystallography.

The cationic portion of **9·0.5CH₃CN** is shown in Figure 6-4. A summary of the X-ray data collection is given in Table 6-1, selected bond distances and angles are given in Table 6-2. The geometry surrounding the Co(II) center is a distorted trigonal bipyramid ($\tau = 0.80$)¹² with the depside coordinated monodentate in an axial position. The Co(II)-N_{PhPy} and Co-N_{Py} bonds are similar to those found in the Co(II) flavonolate complex **2**.

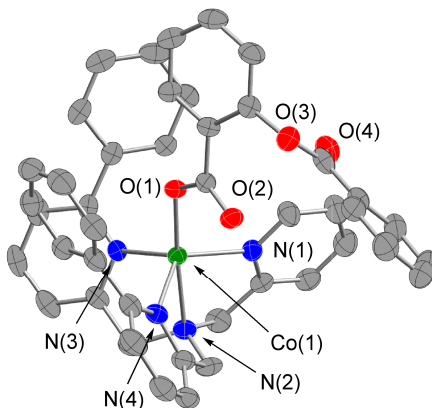


Figure 6-4. Thermal ellipsoid drawing of the cationic portion of **9·0.5CH₃CN**. Ellipsoids are drawn at the 50% probability level. Hydrogen atoms are omitted for clarity.

Table 6-1. Summary of X-ray data collection and parameters for **9**.

9·0.5CH₃CN	
Empirical formula	C ₄₅ H _{36.50} ClCoN _{4.50} O ₈
<i>M_r</i>	862.67
Crystal system	Monoclinic
Space group	<i>C2/c</i>
<i>a</i> / Å	31.0219(6)
<i>b</i> / Å	11.0735(2)
<i>c</i> / Å	23.9944(5)
α / °	90
β / °	106.9654(10)
γ / °	90
<i>V</i> / Å ³	7883.9(3)
<i>Z</i>	8
<i>D_c</i> / Mg m ⁻³	1.454
<i>T</i> / K	150(1)
Color	Green
Crystal habit	Prism
Crystal size / mm	0.30 x 0.28 x 0.15
Diffractometer	Nonius KappaCCD
μ / (mm ⁻¹)	0.566
2 θ max / °	55.00
Completeness to θ (%)	99.5
Reflections collected	16568
Independent reflections	9028
<i>R</i> _{int}	0.0417
Variable parameters	544
<i>R</i> 1 / <i>wR</i> 2 ^b	0.0894/0.1330
Goodness-of-fit (<i>F</i> 2)	1.036
$\Delta\rho$ max/min / e Å ⁻³	0.675/-0.624

^aRadiation used: Mo K α (λ = 0.71073 Å) ^b*R*1 = $\sum | |F_o| - |F_c| | / \sum |F_o|$; *wR*2 = $[\sum [w(F_o^2 - F_c^2)^2] / \sum (F_o^2)^2]^{1/2}$, where $w = 1/[\sigma^2(F_o^2) + (aP)^2 + bP]$.

Table 6-2. Selected Bond Distances (Å) and Angles (°) for **9**.

Co – N(1)	2.105(2)
Co – N(2)	2.177(2)
Co – N(3)	2.120(2)
Co – N(4)	2.110(2)
Co – O(1)	1.9460(17)
N(1) – Co – O(1)	100.35(8)
N(1) – Co – N(2)	76.53(9)
N(1) – Co – N(3)	110.42(9)
N(1) – Co – N(4)	123.49(9)
N(2) – Co – N(3)	76.91(9)
N(2) – Co – N(4)	74.92(9)
N(2) – Co – O(1)	176.42(8)
N(3) – Co – N(4)	109.07(9)
N(3) – Co – O(1)	106.01(8)
(4) – Co – O(1)	105.73(8)

Complexes **9** and **10** are amenable to investigation by ^1H NMR using paramagnetic parameters. The spectral features of analytically pure **9** are shown in Figure 6-5 (middle), along with the spectral features of [(6-Ph₂TPA)Co(3-Hfl)]ClO₄ (**2**, Figure 6-5 (top)). Assignment of ligand-based resonances in the spectra of **2** and **9** will require additional studies using deuterated versions of the 6-Ph₂TPA ligand. However, the pattern of resonances exhibited by the compounds is sufficiently different to indicate that ^1H NMR will be useful in examining interconversions of these compounds (*vide infra*). The ^1H NMR spectrum of the Ni(II) flavonolate and depside complexes (**3** and **10**) are shown in the top and middle portions of Figure 6-6, respectively. Based on prior ^1H NMR studies of Ni(II) complexes supported by the 6-Ph₂TPA ligand, assignment of the β , β' , and γ protons of the pyridyl rings can be

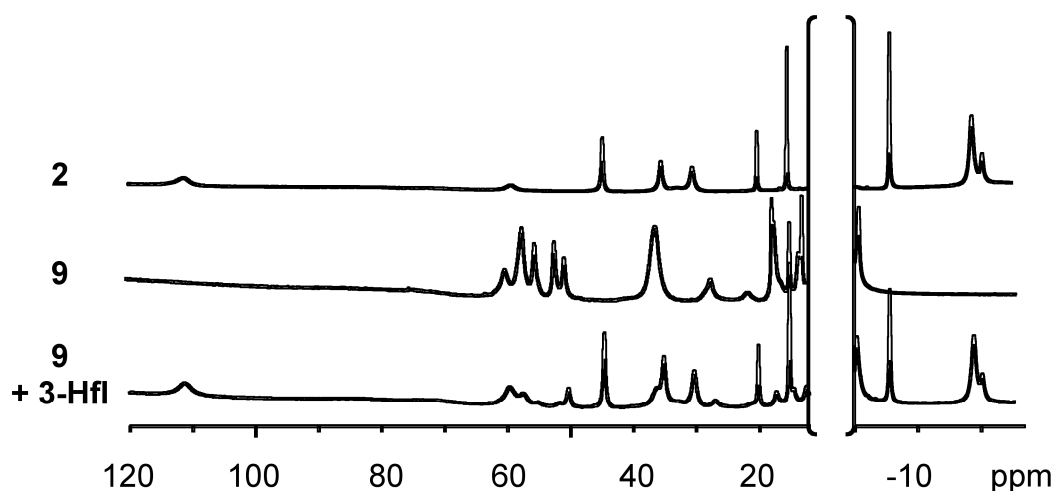


Figure 6-5. Features of the ^1H NMR spectra of $[(6\text{-Ph}_2\text{TPA})\text{Co}(3\text{-Hfl})]\text{ClO}_4$ (**2**, top), $[(6\text{-Ph}_2\text{TPA})\text{Co}(O\text{-bs})]\text{ClO}_4$ (**9**, middle), and **9** upon treatment with one equivalent of 3-Hfl in CD_3CN (bottom).

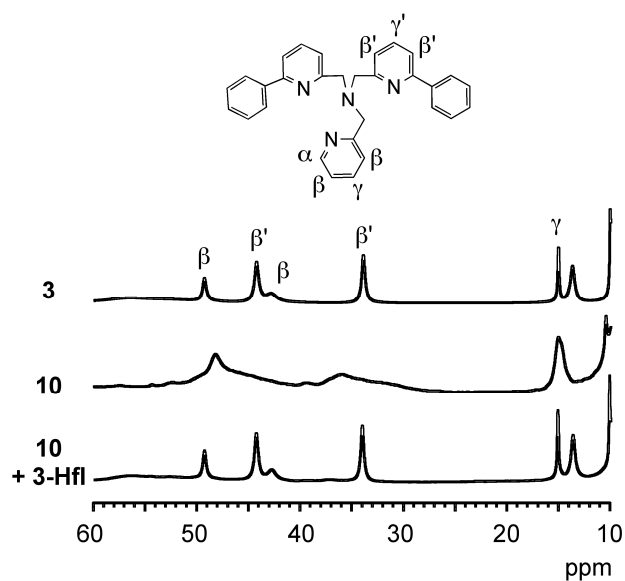


Figure 6-6. Features of the ^1H NMR spectra of $[(6\text{-Ph}_2\text{TPA})\text{Ni}(3\text{-Hfl})]\text{ClO}_4$ (**3**, top), $[(6\text{-Ph}_2\text{TPA})\text{Ni}(O\text{-bs})]\text{ClO}_4$ (**10**, middle), and **10** upon treatment with one equivalent of 3-Hfl in CD_3CN (bottom).

made on the basis of chemical shift and integrated intensity.¹³ The features of the deprotonated complex **10** in the region of 30-55 ppm are generally similar to those

exhibited by the benzoate complex $[(6\text{-Ph}_2\text{TPA})\text{Ni}(\text{O}_2\text{CPh})]\text{ClO}_4$, the structure of which contains a bidentate benzoate ligand in the absence of water.¹⁴

Evaluation of reactivity of depside complexes with 3-Hfl. Speier *et al.* have previously reported that various Cu(II) 3-Hfl complexes can serve as catalysts for the oxidative degradation of the flavonol under thermal conditions.¹⁵ We are interested in determining whether catalytic activity is possible under photochemical conditions with various metal 3-Hfl complexes. As a prelude to catalytic studies, we have examined the reactivity of the depside complexes **8-11** with 3-Hfl using UV-vis, and in two cases ($[(6\text{-Ph}_2\text{TPA})\text{Co}(\text{O-bs})]\text{ClO}_4$ (**9**) and $[(6\text{-Ph}_2\text{TPA})\text{Ni}(\text{O-bs})]\text{ClO}_4$ (**10**), using ^1H NMR. The UV-vis spectra of the reactions of **8-11** with one equivalent of 3-Hfl are shown in Figures 6-7 thru 6-10.

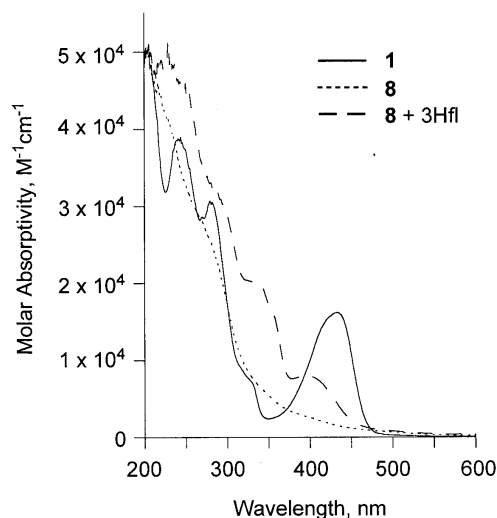


Figure 6-7. Features of the UV-vis spectra of **1**, **8**, and the reaction of **8** with one equivalent of 3-Hfl in CH₃CN.

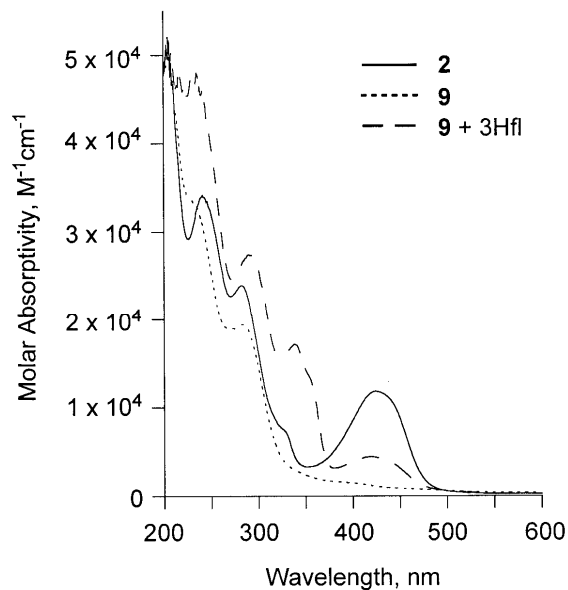


Figure 6-8. Features of the UV-vis spectra of **2**, **9**, and the reaction of **9** with one equivalent of 3-Hfl in CH₃CN.

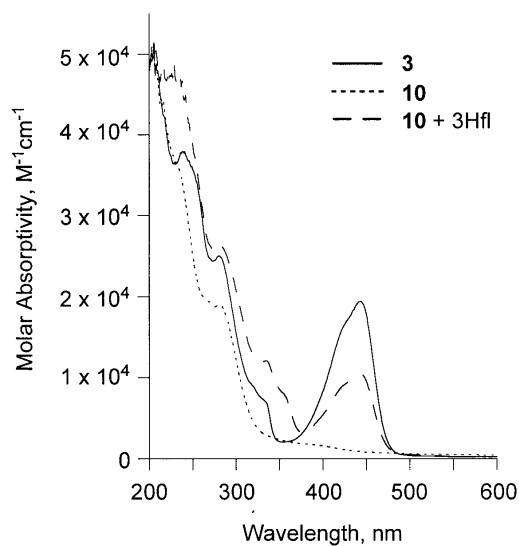


Figure 6-9. Features of the UV-vis spectra of **3**, **10**, and the reaction of **10** with one equivalent of 3-Hfl in CH₃CN.

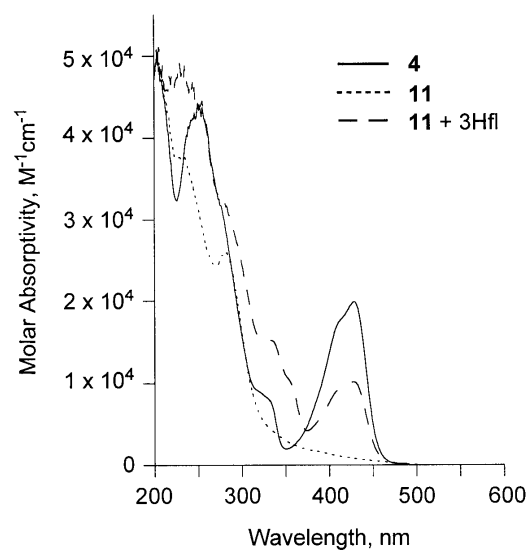


Figure 6-10. Features of the UV-vis spectra of **4**, **11**, and the reaction of **11** with one equivalent of 3-Hfl in CH₃CN.

Comparison of the spectra reveals that all of the complexes show some regeneration of the flavonolate complex, as determined by comparison of the absorption bands at ~420-440 nm. The Ni(II) and Cu(II) systems regenerate the flavonolate complexes to the greatest extent, whereas the Mn(II) and Co(II) systems exhibit spectra suggesting the presence of a significant amount of free 3-Hfl ($\lambda_{\text{max}} \sim 340$ nm). The substantial regeneration of the Ni(II) flavonolate complex **3** is also supported by ¹H NMR data (Figure 6-6(bottom)) wherein the spectral features generated match those exhibited by analytically pure **3**. In contrast, the ¹H NMR data for the reaction involving the Co(II) depside complex and 3-Hfl shows multiple species, which suggests that only partial regeneration of **2** has been accomplished (Figure 6-5 (bottom)).

Conclusions

Irradiation of 3-hydroxyflavonolate complexes of Mn(II), Co(II), Ni(II), and Cu(II) supported by the 6-Ph₂TPA ligand (**1-4**) at 300 nm results in CO release and the formation of the corresponding depside complexes (**8-11**). Complexes **8-11** were isolated and characterized by multiple methods, including X-ray crystallography in case of complex **9**. Due to quenching of the excited state by the open-shell metal ion, the photooxidation reactions of complexes **1-4** proceed considerably slower than those involving closed-shell metal ions. The depside complexes **8-11** were shown to react with neutral 3-Hfl to regenerate **1-4**, with complexes **3** and **4** undergoing this regeneration to the greatest extent. This suggests that these flavonolate complexes should exhibit catalytic CO-release reactivity under photochemical conditions, with the highest conversion anticipated for the Ni(II)- and Cu(II)-containing systems.

Experiments

General comments. All reagents and solvents were obtained from commercial sources and were used as received unless otherwise noted. Solvents were dried according to published procedures and were distilled under N₂ prior to use.¹⁶ Air-sensitive reactions were performed in a MBraun Unilab or Vacuum Atmospheres glovebox under an N₂ atmosphere. The flavonolate complexes **1-4** were prepared as previously described.⁶

Physical methods. UV-vis spectra were recorded on a Hewlett-Packard 8453 diode array spectrophotometer. Fluorescence emission spectra were obtained using a Shimadzu RF-530XPC spectrometer in the range of 250-900 nm with excitation

wavelength corresponding to the absorption maximum of the complex above 400 nm. The excitation and emission slit widths were set at 5 nm for all experiments. Reaction quantum yield measurements were determined using actinometry with ferrioxalate as a standard to measure photon flux.¹⁷ IR spectra were recorded on a Shimadzu FTIR-8400 spectrometer as KBr pellets. ¹H NMR spectra of paramagnetic species were recorded on a Bruker ARX-400 spectrometer as previously described and the chemical shifts (in ppm) are referenced to the residual solvent peak(s) in *CHD*₂CN (¹H, 1.94 (quintet) ppm).¹² Elemental analyses were performed by Atlantic Microlabs Inc., Norcross, GA.

*Caution! Perchlorate salts of metal complexes with organic ligands are potentially explosive. Only small amounts of material should be prepared, and these should be handled with great care.*¹⁸

Irradiation of 1-4 with UV light. Isolation and characterization of 8-11. A solution of each complex (**1-4**, ~5 x 10⁻³ M) was dissolved in 10 mL of acetonitrile and transferred to a round-bottomed flask. The flask was purged with O₂ for 40 s and then inserted into a UV reactor. The reaction progress was periodically evaluated using UV-vis spectroscopy by measuring the intensity of the absorption of the metal-bound flavonolate at λ_{max} ~420-440 nm. After each reaction reached completion, the solvent was evaporated under reduced pressure. The remaining residue was then dissolved in a minimal amount of acetonitrile. Addition of excess diethyl ether

resulted in the deposition of powders of **8-11**. Each powdered sample was subsequently dried under vacuum. Crystals of **9** suitable for a single crystal X-ray diffraction study were obtained via diffusion of diethyl ether into a dilute solution of the complex at room temperature.

[(6-Ph₂TPA)Mn(O-bs)]OTf·0.25CH₂Cl₂ (8). Green/beige powder. Yield: 74%. Anal. Calcd for C₄₅H₃₅F₃MnN₄O₇S·0.25CH₂Cl₂: C, 55.36; H, 3.78; N, 5.57. Found: C, 55.48; H, 4.00; N, 5.76. FTIR (KBr, cm⁻¹): 1736 (ν_{C=O}). ESI/APCI-MS, *m/z* (relative intensity) 738.2049 ([M-OTf]⁺, 1.8%).

[(6-Ph₂TPA)Co(O-bs)]ClO₄·0.2H₂O (9). Green crystals. Yield: 88%. Anal. Calcd for C₄₄H₃₅ClCoN₄O₈·0.2H₂O: C, 60.18; H, 4.48; N, 6.38. Found: C, 60.45; H, 4.22; N, 6.26. FTIR (KBr, cm⁻¹): 1736 (ν_{C=O}). ESI/APCI-MS, *m/z* (relative intensity) 742.1982 ([M-ClO₄]⁺, 100%).

[(6-Ph₂TPA)Ni(O-bs)]ClO₄·2H₂O·0.6ACN (10). Beige/pink powder. Yield: 78%. Anal. Calcd for C₄₄H₃₅ClN₄NiO₈·2H₂O·0.6ACN: C, 60.15; H, 4.56; N, 7.14. Found: C, 60.57; H, 4.34; N, 7.46. FTIR (KBr, cm⁻¹): 1736 (ν_{C=O}). ESI/APCI-MS, *m/z* (relative intensity) 741.1995 ([M-ClO₄]⁺, 100%).

[(6-Ph₂TPA)Cu(O-bs)]ClO₄·3H₂O·0.9ACN (11). Blue crystals. Yield: 85%. Anal. Calcd for C₄₄H₃₅ClCuN₄O₈·3H₂O·0.9ACN: C, 58.66; H, 4.70; N, 7.32. Found: C, 58.71; H, 4.07; N, 7.32. FTIR (KBr, cm⁻¹): 1736 (ν_{C=O}). ESI/APCI-MS, *m/z* (relative intensity) 746.1952 ([M-ClO₄]⁺, 48%).

X-ray Crystallography. A single crystal of **9·0.5CH₃CN** was mounted on a glass fiber using a viscous oil and then was transferred to a Nonius Kappa CCD for

data collection at 150(1) K. Methods for determination of cell constants and unit cell refinement have been previously reported.¹⁹ The structure was solved using a combination of direct methods and heavy atom using SIR 97. All non-hydrogen atoms were refined with anisotropic displacement coefficients.

Structure Solution and Refinement. Complex **9·0.5CH₃CN** crystallizes in the space group *C2/c* with three oxygen atoms of the perchlorate anion exhibiting disorder.

References

1. (a) Bischoff, S. C. *Curr. Opin. Clin. Nutr. Metab. Care* **2008**, *11*, 733-740; (b) Cazarolli, L. H.; Zanatta, L.; Alberton, E. H.; Figueiredo, M. S. R. B.; Folador, P.; Damazio, R. G.; Pizzolatti M. G.; Silva, F. R. M. B. *Mini-Rev. Med. Chem.* **2008**, *8*, 1429-1440; (c) Boots, A. W.; Haenen G. R. M. M.; Bast, A. *Eur. J. Pharmacol.* **2008**, *585*, 325-337; (d) Friedman, M. *Mol. Nutr. Food Res.* **2007**, *51*, 116-134; (e) Amic, D.; Davidovic-Amic, D.; Beslo, D.; Rastija, V.; Lucic, B.; Trinajstic, N. *Curr. Med. Chem.* **2007**, *14*, 827-845; (f) Cushnie, T. P. T. Lamb, A. J. *Int. J. Antimicrob. Agents* **2005**, *26*, 343-356.
2. (a) Pap, J. S.; Kaizer, J.; Speier, G. *Coord. Chem. Rev.* **2010**, *254*, 781-793; (b) Kaizer, J.; Balogh-Hergovich, É.; Czaun, M.; Csay, T.; Speier, G. *Coord. Chem. Rev.* **2006**, *250*, 2222-2233; (c) Malkhasian, A. Y.; Finch, M. E.; Nikolovski, B.; Menon, A.; Kucera, B. E.; Chavez, F. A. *Inorg. Chem.* **2007**, *46*, 2950-2952.

3. (a) Barath, G.; Kaizer, J.; Speier, G.; Parkanyi, L.; Kuzmann, E.; Vertes, A. *Chem. Commun.* **2009**, 3630-3632; (b) Kaizer, J.; Barath, G.; Pap, J.; Speier, G.; Giorgi, M.; Relier, M. *Chem. Commun.* **2007**, 5235-5237.
4. Steiner, R. A.; Kalk, K. H.; Dijkstra, B. W. *Proc. Natl. Acad. Sci.* **2002**, *99*, 16625-16630.
5. (a) Merkens, H.; Kappl, R.; Jakob, R. P.; Schmid, F. X.; Fetzner, S. *Biochemistry* **2008**, *47*, 12185-12196; (b) Schaab, M. R.; Barney, B. M.; Francisco, W. A. *Biochemistry* **2006**, *45*, 1009-1016; (c) Gopal, B.; Madan, L. L.; Betz, S. F.; Kossiakoff, A. A. *Biochemistry* **2005**, *44*, 193-201.
6. Grubel, K.; Rudzka, K.; Arif, A. M.; Klotz, K.; Halfen, J. A.; Berreau, L. M. *Inorg. Chem.* **2010**, *49*, 82-96.
7. Grubel, K.; Maltais, T. R.; Smith, R. C.; Arif, A. M.; Berreau, L. M. *Chem. Commun.* **2011**, to be submitted.
8. Mann, B. E. *Top. Organomet. Chem.* **2010**, *32*, 247-285.
9. Mann, B. E.; Motterlini, R. *Chem. Commun.* **2007**, 4197-4208.
10. Lakowicz, J. R. *Principles of Fluorescence Spectroscopy*, 3rd ed.; Kluwer Academic/Plenum Publishers, New York, NY, 2006.
11. Allen, T. H.; Root, W. S. *J. Biol. Chem.* **1955**, *215*, 309-317.
12. Addison, A. W.; Rao, T. N.; Reedijk, J.; van Rijn, J.; Verschoor, G. C. *J. Chem. Soc., Dalton Trans.* **1984**, 1349-1356.
13. Szajna, E.; Dobrowolski, P.; Fuller, A. L.; Arif, A. M.; Berreau, L. M. *Inorg. Chem.* **2004**, *43*, 3988-3997.

14. (a) Szajna-Fuller, E.; Rudzka, K.; Arif, A. M.; Berreau, L. M. *Inorg. Chem.* **2007**, *46*, 5499-5507; (b) Szajna-Fuller, E.; Chambers, B. M.; Arif, A. M.; Berreau, L. M. *Inorg. Chem.* **2007**, *46*, 5486-5498.
15. (a) Kaizer, ; Goger, S.; Speier, G.; Reglier, M.; Giorgi, M. *Inorg. Chem. Commun.* **2006**, *9*, 251-254; (b) Balogh-Hergovich, É.; Kaizer, J.; Pap, J.; Speier, G.; Huttner, G.; Zsolnai, L. *Eur. J. Inorg. Chem.* **2002**, 2287-2295; (c) Barhacs, L.; Kaizer, J.; Pap, J.; Speier, G. *Inorg. Chim. Acta* **2001**, *320*, 83-91; (d) Balogh-Hergovich, É.; Kaizer, J.; Speier, G. *Inorg. Chim. Acta* **1997**, *256*, 9-14; (e) Balogh-Hergovich, É.; Kaizer, J.; Speier, G. *J. Mol. Catal. A: Chem.* **2000**, *159*, 215-224.
16. Armarego, W. L. F.; Perrin, D. D. *Purification of Laboratory Chemicals*, 4th ed.; Butterworth-Heinemann, Boston, MA, 1996.
17. Kuhn, H. J.; Braslavsky, S. E.; Schmidt, R. *Pure Applied. Chem.* **2004**, *76*, 2105-2146.
18. Wolsey, W. C. *J. Chem. Educ.* **1973**, *50*, A335.
19. Szajna, E.; Makowska-Grzyska, M. M.; Wasden, C. C.; Arif, A. M.; Berreau, L. M. *Inorg. Chem.* **2005**, *44*, 7595-7605.

CHAPTER 7

SUMMARY

Since their first introduction in 2002, CO-releasing molecules (CORMs) have attracted a significant amount of attention as potential therapeutic agents. However, the vast majority of known CORMs involve carbonyl groups coordinated on toxic metal centers. Moreover, currently, there is little or no control over the time and dosage of carbon monoxide released from existing CORMs. In the Berreau group, we are interested in elucidating factors influencing CO release from bioinspired and biofriendly molecules. The work described in this dissertation presented our contribution to understanding multiple aspects affecting the coordination and stabilization of acireductone and flavonolate anions on metal centers, as well as subsequent CO release from these moieties.

We have shown that both secondary coordination sphere alterations and the identity of the metal ion influence the coordination of the enolate acireductone-type moiety to a metal center. Even though the influence of the secondary environment on the coordination and reactivity of exogenous ligands is widely recognized, our laboratory is the first to determine how alterations in the supporting ligand affect the formation of Ni(II)-enolate species of relevance to acireductone dioxygenases. Notably, the identity of the metal center plays a crucial role in the chemistry of the ARD enzyme. Although *apo*-ARD can be reconstituted with either Ni(II) or Co(II) to yield the same type of reactivity, we have shown that synthetic model complexes of these forms of the enzyme show considerable metal-dependence in their ability to

stabilize the enolate anion. Our research has also highlighted the influence of water on the aforementioned process. These results will benefit the design of new structural and functional models of the acireductone dioxygenase enzyme, which is one of only a few enzymes known to release CO.

In another study we have synthesized the first series of divalent metal-flavonolate complexes supported by the same chelate ligand 6-Ph₂TPA. This has allowed us to evaluate the influence of the metal center on the coordination properties and spectroscopic features of a metal-coordinated flavonolate moiety. We have shown that these complexes exhibit photo-induced CO-release reactivity that is highly dependent on the metal electron configuration, with d^{10} metals such as the Zn(II)-containing complex exhibiting in the most rapid CO release. This result is interesting for several reasons. First, we have shown that the photo-induced CO release can be accomplished from metal-bound flavonolate anion. Second, use of a bio-relevant CO-release molecule (flavonol) and a bio-friendly metal such as Zn(II), is a significant step toward developing a new class of biofriendly CO-releasing molecules.

The next stage of the research will need to involve the generation of analogs of [(6-Ph₂TPA)Zn(3-Hfl)]X wherein modulation in the supporting chelate ligand and flavonolate improve the biological-relevant features (e.g. solubility, absorption properties) of the complex. CO generated from each of these new complexes will need to be quantified, and the half-life of each CO-release reaction determined. This will enable comparison of CO-release reactivity with previously reported CORMs. Additionally, collaborations with other laboratories should be established to perform

tests with the synthetic zinc flavonolate complexes that are pertinent to living subjects. Such tests include examining the effect of irradiation of the complex (to induce CO release) on the: 1) modification of K^+ -channels, 2) vasodilation of mouse aorta, and 3) photoinduced cytotoxicity against cancer cells, to name a few. The results of these tests will provide insight into the feasibility of the use of zinc flavonolate complexes as CORMs.

APPENDICES

American Chemical Society's Policy on Theses and Dissertations

If your university requires you to obtain permission, you must use the RightsLink permission system. See RightsLink instructions at <http://pubs.acs.org/page/copyright/permissions.html>.

This is regarding request for permission to include **your** paper(s) or portions of text from **your** paper(s) in your thesis. Permission is now automatically granted; please pay special attention to the **implications** paragraph below. The Copyright Subcommittee of the Joint Board/Council Committees on Publications approved the following:

Copyright permission for published and submitted material from theses and dissertations

ACS extends blanket permission to students to include in their theses and dissertations their own articles, or portions thereof, that have been published in ACS journals or submitted to ACS journals for publication, provided that the ACS copyright credit line is noted on the appropriate page(s).

Publishing implications of electronic publication of theses and dissertation material

Students and their mentors should be aware that posting of theses and dissertation material on the Web prior to submission of material from that thesis or dissertation to an ACS journal may affect publication in that journal. Whether Web posting is considered prior publication may be evaluated on a case-by-case basis by the journal's editor. If an ACS journal editor considers Web posting to be "prior publication", the paper will not be accepted for publication in that journal. If you intend to submit your unpublished paper to ACS for publication, check with the appropriate editor prior to posting your manuscript electronically.

Reuse/Republishing of the Entire Work in Theses or Collections: Authors may reuse all or part of the Submitted, Accepted or Published Work in a thesis or dissertation that the author writes and is required to submit to satisfy the criteria of degree-granting institutions. Such reuse is permitted subject to the ACS' "Ethical Guidelines to Publication of Chemical Research" (<http://pubs.acs.org/page/policy/ethics/index.html>); the author should secure written confirmation (via letter or email) from the respective ACS journal editor(s) to avoid potential conflicts with journal prior publication*/embargo policies. Appropriate citation of the Published Work must be made. If the thesis or dissertation to be published is in electronic format, a direct link to the Published Work must also be included using the ACS Articles on Request author-directed link – see <http://pubs.acs.org/page/policy/articlesonrequest/index.html>

* Prior publication policies of ACS journals are posted on the ACS website at <http://pubs.acs.org/page/policy/prior/index.html>

If your paper has not yet been published by ACS, please print the following credit line on the first page of your article: "Reproduced (or 'Reproduced in part') with permission from [JOURNAL NAME], in press (or 'submitted for publication'). Unpublished work copyright [CURRENT YEAR] American Chemical Society." Include appropriate information.

If your paper has already been published by ACS and you want to include the text or portions of the text in your thesis/dissertation, please print the ACS copyright credit line on the first page of your article: "Reproduced (or 'Reproduced in part') with permission from [FULL REFERENCE CITATION.] Copyright [YEAR] American Chemical Society." Include appropriate information.

Submission to a Dissertation Distributor: If you plan to submit your thesis to UMI or to another dissertation distributor, you should not include the unpublished ACS paper in your thesis if the thesis will be disseminated electronically, until ACS has published your paper. After publication of the paper by ACS, you may release the entire thesis (**not the individual ACS article by itself**) for electronic dissemination through the distributor; ACS's copyright credit line should be printed on the first page of the ACS paper.

Permission Request Form for RSC Material

To request permission to use material from a publication published by The Royal Society of Chemistry (RSC), please complete and return this form.

To: Contracts & Copyright Department
The Royal Society of Chemistry
Thomas Graham House
Science Park
Milton Road
Cambridge CB4 0WF
UK

From: Name KATARZYNA GRUBEL
Address 160 E, 900 N, # 21
LOGAN, UT 84301
USA
Tel (435) 512-9309
Fax
Email GRUBELK@GMAIL.COM

Tel +44 (0)1223 432134
Fax +44 (0)1223 423623
Email contracts-copyright@rsc.org

I am preparing the following work for publication:

Article/Chapter Title DISSERTATION
Journal/Book Title _____
Editor/Author(s) _____
Publisher _____

I would very much appreciate your permission to use the following material:

Journal/Book Title Chemical Communications
Editor/Author(s) Grubel, K.; Laugel, B.; Mallat, T.; Smith, R.; Arif, A.; Berreau, L.
Volume Number N/A
Year of Publication N/A
Description of Material Manuscript submitted, pending revisions (ID CC-COM
Page(s) N/A -07-2011-018961

I will acknowledge the original source as follows (to be supplied by the RSC on signature) and in each electronic version of my publication I will include a hyperlink to the article on the Royal Society of Chemistry website:

see email

Signed: _____

Date: 21st July 2011

The Royal Society of Chemistry hereby grants permission for the use of the material specified above in the work described and in all subsequent editions of the work for distribution throughout the world, in all media including electronic and microfilm. You may use the material in conjunction with computer-based electronic and information retrieval systems, grant permissions for photocopying, reproductions and reprints, translate the material and to publish the translation, and authorise document delivery and abstracting and indexing services. Please note that if the material specified above or any part of it appears with credit or acknowledgement to a third party then you must also secure permission from that third party before reproducing that material. The Royal Society of Chemistry is a signatory to the STM Guidelines on Permissions (available on request).

Signed: _____

Date: 22/7/11

Permission Request Form for RSC Material

To request permission to use material from a publication published by The Royal Society of Chemistry (RSC), please complete and return this form.

To: Contracts & Copyright Department
The Royal Society of Chemistry
Thomas Graham House
Science Park
Milton Road
Cambridge. CB4 0WF
UK

From: Name KATARYNA GRUBEL
Address 160E, 900N, # 21
LOGAN, UT 84301
USA
Tel (435) 512-9308
Fax _____
Email GRUBELK@GMAIL.COM

I am preparing the following work for publication:

Article/Chapter Title DISSERTATION
Journal/Book Title _____
Editor/Author(s) _____
Publisher _____

I would very much appreciate your permission to use the following material:

Journal/Book Title DALTON TRANSACTION
Editor/Author(s) Grubel, K; Ingle, G; Fuller, A; Arif, A; Berreau, L,
Volume Number 40
Year of Publication 2011
Description of Material Manuscript ID: DT-ART-04-2011-01058.F.R1
Page(s) N/A

I will acknowledge the original source as follows (to be supplied by the RSC on signature) and in each electronic version of my publication I will include a hyperlink to the article on the Royal Society of Chemistry website:

see email

Signed: _____

Date: 21st July 2011

The Royal Society of Chemistry hereby grants permission for the use of the material specified above in the work described and in all subsequent editions of the work for distribution throughout the world, in all media including electronic and microfilm. You may use the material in conjunction with computer-based electronic and information retrieval systems, grant permissions for photocopying, reproductions and reprints, translate the material and to publish the translation, and authorise document delivery and abstracting and indexing services. Please note that if the material specified above or any part of it appears with credit or acknowledgement to a third party then you must also secure permission from that third party before reproducing that material. The Royal Society of Chemistry is a signatory to the STM Guidelines on Permissions (available on request).

Signed: _____

Date: 22/7/11

25 April 2011

Dr. Amy L. Fuller
George L. Clark X-Ray Facility
& 3M Materials Laboratory
67 Noyes Lab
505 South Mathews Ave.
Urbana, IL 61801

Katarzyna Grubel
Dept. of Chemistry and Biochemistry
Utah State University
0300 Old Main Hill
Logan, UT 84322-0300
Phone (435) 797-0365
Fax (435) 797-3390

Dear Dr. Fuller,

I am in the process of preparing my dissertation in Chemistry and Biochemistry Department at Utah State University.

I am requesting your permission to include the following manuscripts in their entirety as a chapter in my dissertation:

1. Grubel K.; Ingle, G. K.; Fuller, A. L.; Arif, A. M.; Berreau, L. M.* "Influence of Water on the Formation of O₂-Reactive Divalent Metal Enolate Complexes of Relevance to Acireductne Dioxygenases" Manuscript accepted to 40th birthday edition of *Dalton Transactions*.
2. Grubel, K.; Fuller, A. L.; Chambers; B. M., Arif, A. M; Berreau, L. M. "O₂-dependent Aliphatic Carbon-Carbon Bond Cleavage Reactivity in a Ni(II) Enolate Complex Having a Hydrogen Bond Donor Microenvironment; Comparison with a Hydrophobic Analog" *Inorganic Chemistry* **2010**, *49*, 1071-1081.

I will acknowledge your contribution to this part of my dissertation by the inclusion of a footnote on the title page for that chapter. Additionally, a copy of this letter will become an Appendix to the dissertation. Please, advise me of any changes you require.

Please, indicate your approval of this request by signing the endorsement below. If you have any questions, please call me at the number above.

If possible, please provide your reply immediately. Thank you very much for your consideration,
Katarzyna Grubel

I hereby give permission to Katarzyna Grubel to reprint the manuscripts listed above in her dissertation.

Signed _____

Date July 21, 2011

'22 July 2011

Bonnie Chambers
Logan, UT 84322

Katarzyna Grubel
Dept. of Chemistry and Biochemistry
Utah State University
0300 Old Main Hill
Logan, UT 84322-0300
Phone (435) 797-0365
Fax (435) 797-3390

Dear Bonnie Chambers,

I am in the process of preparing my dissertation in Chemistry and Biochemistry Department at Utah State University.

I am requesting your permission to include the following manuscripts in their entirety as a chapter in my dissertation:

1. Grubel, K.; Fuller, A. L.; Chambers; B. M., Arif, A. M; Berreau, L. M. "O₂-dependent Aliphatic Carbon-Carbon Bond Cleavage Reactivity in a Ni(II) Enolate Complex Having a Hydrogen Bond Donor Microenvironment; Comparison with a Hydrophobic Analog" *Inorganic Chemistry* **2010**, *49*, 1071-1081.

I will acknowledge your contribution to this part of my dissertation by the inclusion of a footnote on the title page for that chapter. Additionally, a copy of this letter will become an Appendix to the dissertation. Please, advise me of any changes you require.

Please, indicate your approval of this request by signing the endorsement below. If you have any questions, please call me at the number above.

If possible, please provide your reply immediately. Thank you very much for your consideration,
Katarzyna Grubel

I hereby give permission to Katarzyna Grubel to reprint the manuscripts listed above in her dissertation.

Signed _____

Date 7/25/2011

21 July 2011

Gajendrasingh K. Ingle
University of South Florida
4202 E. Fowler Avenue
Tampa, FL 33620

Katarzyna Grubel
Dept. of Chemistry and Biochemistry
Utah State University
0300 Old Main Hill
Logan, UT 84322-0300
Phone (435) 797-0365
Fax (435) 797-3390

Dear Gajendrasingh Ingle,

I am in the process of preparing my dissertation in Chemistry and Biochemistry Department at Utah State University.

I am requesting your permission to include the following manuscripts in their entirety as a chapter in my dissertation:

1. Grubel K.; Ingle, G. K.; Fuller, A. L.; Arif, A. M.; Berreau, L. M.* "Influence of Water on the Formation of O₂-Reactive Divalent Metal Enolate Complexes of Relevance to Acireductne Dioxygenases" Manuscript accepted to 40th birthday edition of *Dalton Transactions*.

I will acknowledge your contribution to this part of my dissertation by the inclusion of a footnote on the title page for that chapter. Additionally, a copy of this letter will become an Appendix to the dissertation. Please, advise me of any changes you require.

Please, indicate your approval of this request by signing the endorsement below. If you have any questions, please call me at the number above.

If possible, please provide your reply immediately. Thank you very much for your consideration,
Katarzyna Grubel

25 April 2011

Dr. Katarzyna Rudzka
Dept. of Biophysics and Biophysical Chemistry
Johns Hopkins University, School of Medicine
Baltimore, Maryland 21205 USA

Katarzyna Grubel
Dept. of Chemistry and Biochemistry
Utah State University
0300 Old Main Hill
Logan, UT 84322-0300
Phone (435) 797-0365
Fax (435) 797-3390

Dear Dr. Rudzka,

I am in the process of preparing my dissertation in Chemistry and Biochemistry Department at Utah State University.

I am requesting your permission to include the following manuscripts in their entirety as a chapter in my dissertation:

1. Grubel K.; Rudzka, K.; Arif, A. M.; Klotz, K. L.; Halfen, J. A.; Berreau, L. M. "Synthesis, Characterization, and Ligand Exchange Reactivity of a Series of First Row Divalent Metal 3-Hydroxyflavonolate Complexes" *Inorganic Chemistry* 2010, 49, 82-96.

I will acknowledge your contribution to this part of my dissertation by the inclusion of a footnote on the title page for that chapter. Additionally, a copy of this letter will become an Appendix to the dissertation. Please, advise me of any changes you require.

Please, indicate your approval of this request by signing the endorsement below. If you have any questions, please call me at the number above.

If possible, please provide your reply immediately. Thank you very much for your consideration.

Katarzyna Grubel

I hereby give permission to Katarzyna Grubel to reprint the manuscripts listed above in her dissertation.

Signed _____

Date 7/22/2011

1 August 2011

Katie Klotz
Department of Chemistry,
University of Wisconsin-Eau Claire,
Eau Claire, Wisconsin 54702

Katarzyna Grubel
Dept. of Chemistry and Biochemistry
Utah State University
0300 Old Main Hill
Logan, UT 84322-0300
Phone (435) 797-0365
Fax (435) 797-3390

Dear Katie Klotz,

I am in the process of preparing my dissertation in Chemistry and Biochemistry Department at Utah State University.

I am requesting your permission to include the following manuscript in its entirety as a chapter in my dissertation:

1. Grubel K.; Rudzka, K.; Arif, A. M.; Klotz, K. L.; Halfen, J. A.; Berreau, L. M. "Synthesis, Characterization, and Ligand Exchange Reactivity of a Series of First Row Divalent Metal 3-Hydroxyflavonolate Complexes" *Inorganic Chemistry* **2010**, *49*, 82-96.

I will acknowledge your contribution to this part of my dissertation by the inclusion of a footnote on the title page for that chapter. Additionally, a copy of this letter will become an Appendix to the dissertation. Please, advise me of any changes you require.

Please, indicate your approval of this request by signing the endorsement below. If you have any questions, please call me at the number above.

If possible, please provide your reply immediately. Thank you very much for your consideration.

Katarzyna Grubel

I hereby give permission to Katarzyna Grubel to reprint the manuscripts listed above in her dissertation.

Signed _____

Date 8/8/2011

25 April 2011

Dr. Jason A. Halfen
University of Wisconsin-Eau Claire
105 Garfield Avenue
443 Phillips Hall
Eau Claire, WI 54702-4004

Katarzyna Grubel
Dept. of Chemistry and Biochemistry
Utah State University
0300 Old Main Hill
Logan, UT 84322-0300
Phone (435) 797-0365
Fax (435) 797-3390

Dear Dr. Halfen,

I am in the process of preparing my dissertation in Chemistry and Biochemistry Department at Utah State University.

I am requesting your permission to include the following manuscript in its entirety as a chapter in my dissertation:

1. Grubel K.; Rudzka, K.; Arif, A. M.; Klotz, K. L.; Halfen, J. A.; Berreau, L. M.* "Synthesis, Characterization, and Ligand Exchange Reactivity of a Series of First Row Divalent Metal 3-Hydroxyflavonolate Complexes" *Inorganic Chemistry* **2010**, *49*, 82-96.

I will acknowledge your contribution to this part of my dissertation by the inclusion of a footnote on the title page for that chapter. Additionally, a copy of this letter will become an Appendix to the dissertation. Please, advise me of any changes you require.

Please, indicate your approval of this request by signing the endorsement below. If you have any questions, please call me at the number above.

If possible, please provide your reply immediately. Thank you very much for your consideration.

Katarzyna Grubel

I hereby give permission to Katarzyna Grubel to reprint the manuscripts listed above in her dissertation.

Signed _____

Date 8.31.11

21 July 2011

Bryinna Laughlin
Clemson University
Department of Chemistry
Center for Optical Materials Science and Engineering Technologies
479 Hunter Laboratories
Clemson, SC 29634

Katarzyna Grubel
Dept. of Chemistry and Biochemistry
Utah State University
0300 Old Main Hill
Logan, UT 84322-0300
Phone (435) 797-0365
Fax (435) 797-3390

Prof. Smith,

I am in the process of preparing my dissertation in Chemistry and Biochemistry Department at Utah State University.

I am requesting your permission to include the following manuscripts in their entirety as a chapter in my dissertation:

1. Grubel, K.; Laughlin, B.; Maltais, T. R.; Smith, R. C.; Arif, A. M.; Berreau, L. M. "Photochemically-induced Dioxygenase-type CO-release of Group 12 Flavonolate Complexes" Manuscript submitted to *Chemical Communications* **2011**, pending revisions.

I will acknowledge your contribution to this part of my dissertation by the inclusion of a footnote on the title page for that chapter. Additionally, a copy of this letter will become an Appendix to the dissertation. Please, advise me of any changes you require.

Please, indicate your approval of this request by signing the endorsement below. If you have any questions, please call me at the number above.

If possible, please provide your reply immediately. Thank you very much for your consideration,
Katarzyna Grubel

I hereby give permission to Katarzyna Grubel to reprint the manuscripts listed above in her dissertation.

Signed _____ D, re 7/28/11

21 July 2011

Thora R. Maltais
Purdue University,
West Lafayette, IN 47907

Katarzyna Grubel
Dept. of Chemistry and Biochemistry
Utah State University
0300 Old Main Hill
Logan, UT 84322-0300
Phone (435) 797-0365
Fax (435) 797-3390

Dear Thora Maltais,

I am in the process of preparing my dissertation in Chemistry and Biochemistry Department at Utah State University.

I am requesting your permission to include the following manuscripts in their entirety as a chapter in my dissertation:

1. Grubel, K.; Maltais, T. R.; Smith, R. C.; Arif, A. M.; Berreau, L. M. "Photochemically-induced Dioxygenase-type CO-release of Group 12 Flavonolate Complexes" Manuscript submitted to *Chemical Communications* **2011**, pending revisions.

I will acknowledge your contribution to this part of my dissertation by the inclusion of a footnote on the title page for that chapter. Additionally, a copy of this letter will become an Appendix to the dissertation. Please, advise me of any changes you require.

Please, indicate your approval of this request by signing the endorsement below. If you have any questions, please call me at the number above.

If possible, please provide your reply immediately. Thank you very much for your consideration,
Katarzyna Grubel

I hereby give permission to Katarzyna Grubel to reprint the manuscripts listed above in her dissertation.

Signed _____ Date 7/21/11

21 July 2011

Prof. Rhett C. Smith
Clemson University
Department of Chemistry
Center for Optical Materials Science and Engineering Technologies
479 Hunter Laboratories
Clemson, SC 29634

Katarzyna Grubel
Dept. of Chemistry and Biochemistry
Utah State University
0300 Old Main Hill
Logan, UT 84322-0300
Phone (435) 797-0365
Fax (435) 797-3390

Prof. Smith,

I am in the process of preparing my dissertation in Chemistry and Biochemistry Department at Utah State University.

I am requesting your permission to include the following manuscripts in their entirety as a chapter in my dissertation:

1. Grubel, K.; Laughlin, B.; Maltais, T. R.; Smith, R. C.; Arif, A. M.; Berreau, L. M. "Photochemically-induced Dioxygenase-type CO-release of Group 12 Flavonolate Complexes" Manuscript submitted to *Chemical Communications* **2011**, pending revisions.

I will acknowledge your contribution to this part of my dissertation by the inclusion of a footnote on the title page for that chapter. Additionally, a copy of this letter will become an Appendix to the dissertation. Please, advise me of any changes you require.

Please, indicate your approval of this request by signing the endorsement below. If you have any questions, please call me at the number above.

If possible, please provide your reply immediately. Thank you very much for your consideration,
Katarzyna Grubel

I hereby give permission to Katarzyna Grubel to reprint the manuscripts listed above in her dissertation.

Signed _____

Date

7-28-11

25 April 2011

Dr. Atta M. Arif
Department of Chemistry,
University of Utah,
Salt Lake City, Utah 84112-0850

Katarzyna Grubel
Dept. of Chemistry and Biochemistry
Utah State University
0300 Old Main Hill
Logan, UT 84322-0300
Phone (435) 797-0365
Fax (435) 797-3390

Dear Dr. Arif,

I am in the process of preparing my dissertation in Chemistry and Biochemistry Department at Utah State University.

I am requesting your permission to include the following manuscripts in their entirety as a chapter in my dissertation:

1. Grubel, K.; Maltais, T. R.; Smith, R. C.; Arif, A. M.; Berreau, L. M. "Photochemically-induced Dioxygenase-type CO-release of Group 12 Flavonolate Complexes" Manuscript submitted to *Chemical Communications* **2011**, pending revisions.
2. Grubel K.; Ingle, G. K.; Fuller, A. L.; Arif, A. M.; Berreau, L. M. "Influence of Water on the Formation of O₂-Reactive Divalent Metal Enolate Complexes of Relevance to Acireductne Dioxygenases" Manuscript submitted to 40th birthday edition of *Dalton Transactions*.
3. Grubel, K.; Fuller, A. L.; Chambers; B. M., Arif, A. M; Berreau, L. M. "O₂-dependent Aliphatic Carbon-Carbon Bond Cleavage Reactivity in a Ni(II) Enolate Complex Having a Hydrogen Bond Donor Microenvironment; Comparison with a Hydrophobic Analog" *Inorganic Chemistry* **2010**, *49*, 1071-1081.
4. Grubel K.; Rudzka, K.; Arif, A. M.; Klotz, K. L.; Halfen, J. A.; Berreau, L. M. "Synthesis, Characterization, and Ligand Exchange Reactivity of a Series of First Row Divalent Metal 3-Hydroxyflavonolate Complexes" *Inorganic Chemistry* **2010**, *49*, 82-96.

I will acknowledge your contribution to this part of my dissertation by the inclusion of a footnote on the title page for that chapter. Additionally, a copy of this letter will become an Appendix to the dissertation. Please, advise me of any changes you require.

Please, indicate your approval of this request by signing the endorsement below. If you have any questions, please call me at the number above.

If possible, please provide your reply immediately. Thank you very much for your consideration,
Katarzyna Grubel

I hereby give permission to Katarzyna Grubel to reprint the manuscripts listed above in her dissertation.

Signed _____

Date

7/22/2011

CURRICULUM VITAE

Katarzyna Grubel
grubelk@gmail.com

Current Address

760E, 900N #21
Logan, UT 84321
(435) 512-9309

Permanent Address

ul. Warszawska 33B/2
44-100 Gliwice, Poland

EDUCATION

September 2006 –
August 2011

Utah State University

Department of Chemistry and Biochemistry; Logan, UT
PhD program in Inorganic Chemistry

Advisor: Prof. Lisa M. Berreau

Dissertation Title: “Ligand and Metal Effects on the CO-release
Reactivity of Metal Acireductone and Flavonolate Complexes”

October 2005 –
July 2006

Silesian University of Technology

Faculty of Chemistry, Department of Inorganic Chemistry and
Technology; Gliwice, Poland

Entered PhD program in Inorganic Chemistry

Advisor: Dr. Marek Smolik

October 2000 –
September 2005

Silesian University of Technology

Faculty of Chemistry, Department of Organic Chemistry,
Biochemistry, and Biotechnology; Gliwice, Poland

MS. in Organic Chemistry

Advisor: Dr. Gabriela Pastuch-Gawołek

Thesis Title: “Synthesis of Potential Glycotransferase Inhibitors”

ADDITIONAL COURSES

January 2011

Physical Science Responsible Conduct of Research Course

A course by Collaborative Institutional Training Initiative (CITI)

PUBLICATIONS

1. Grubel, K.; Maltais, T. R.; Smith, R. C.; Arif, A. M.; Berreau, L. M.* “Photochemical CO release Reactivity of Open-Shell 3d Divalent Flavonolate” Manuscript in preparation.
2. Grubel, K.; Laughlin, B.; Maltais, T. R.; Smith, R. C.; Arif, A. M.; Berreau, L. M. “Photochemically-induced Dioxygenase-type CO-release of Group 12 Flavonolate Complexes” Manuscript accepted to *Chemical Communications* **2011**.
3. Grubel K.; Ingle, G. K.; Fuller, A. L.; Arif, A. M.; Berreau, L. M.* “Influence of Water on the Formation of O₂-Reactive Divalent Metal Enolate Complexes of Relevance to Acireductne Dioxygenases” Manuscript accepted to 40th birthday edition of *Dalton Transactions*.
4. Berreau, L. M.*; Borowski, T.; Grubel, K.; Allpress, C. J.; Wikstrom, J. P.; Germain, M. E.; Rybak-Akimova, E. V.; Tierney, D. L. “Mechanistic Studies of the O₂-dependent Aliphatic Carbon-Carbon Bond Cleavage Reaction of a Nickel Enolate Complex” *Inorganic Chemistry* **2011**, *50*, 1047-1057.
5. Rudzka, K.; Grubel, K.; Arif, A. M.; Berreau, L. M.* “Hexanickel Enediolate Cluster Generated in a Acireductone Dioxygenase Model Reaction” *Inorganic Chemistry* **2010**, *49*, 7623–7625.
6. Grubel, K.; Fuller, A. L.; Chambers; B. M., Arif, A. M; Berreau, L. M.* “O₂-dependent Aliphatic Carbon-Carbon Bond Cleavage Reactivity in a Ni(II) Enolate Complex Having a Hydrogen Bond Donor Microenvironment; Comparison with a Hydrophobic Analog” *Inorganic Chemistry* **2010**, *49*, 1071-1081.
7. Grubel K.; Rudzka, K.; Arif, A. M.; Klotz, K. L.; Halfen, J. A.; Berreau, L. M.* “Synthesis, Characterization, and Ligand Exchange Reactivity of a Series of First Row Divalent Metal 3-Hydroxyflavonolate Complexes” *Inorganic Chemistry* **2010**, *49*, 82-96.

ORAL PRESENTATIONS

1. Grubel, K.; Maltais, T. R.; Smith, R. C.; Arif, A. M.; Berreau, L. M.* “CO-release Chemistry of Zinc-Containing Complexes” Invited Oral Presentation at the DataBlitz, Bioinorganic Chemistry Gordon Research Seminar, Ventura, CA, February **2011**.
2. Grubel K.; Rudzka, K.; Ingle, G.; Read, C.; Fuller, A. L.; Arif, A. M.; Berreau, L. M.* “Ligand and Metal Effects on the Formation of O₂-Reactive Divalent Metal Enolate Complexes: Evaluation of the Influence of Water ” Oral Presentation at the 240th National American Chemical Society Meeting, Boston, MA, August **2010**.

POSTER PRESENTATIONS

1. Grubel, K.; Maltais, T. R.; Smith, R. C.; Arif, A. M.; Berreau, L. M.* “CO-Release Chemistry of Metal-Flavonolate Complexes” Poster Presentation at the Gordon Research Seminar, Ventura, CA, February **2011**.
2. Grubel K.; Arif, A. M.; Berreau, L. M.* “UV- and Heat-Induced O₂ Reactivity of Divalent Metal Flavonolate Complexes” Poster Presentation at the Intermountain Graduate Research Symposium, Logan, UT, March **2010**.
3. Grubel K.; Arif, A. M.; Berreau, L. M.* “UV- and Heat-Induced O₂ Reactivity of Divalent Metal Flavonolate Complexes” Poster Presentation at the 239th National American Chemical Society Meeting, San Francisco, CA, March **2010**.
4. Grubel K.; Rudzka, K.; Arif, A. M.; Berreau, L. M.* “Synthesis and Characterization of Divalent Metal Flavonolate Complexes” Poster Presentation at the 237th National American Chemical Society Meeting, Salt Lake City, UT, March **2009**.
5. Grubel, K.; Fuller, A. L.; Arif, A. M.; Berreau, L. M.* “Effect of the Secondary Environment on the Chemistry of Ni(II) Complexes: Relevance to Acireductone Dioxygenases” Poster Presentation at the 63rd Northwest/21st Rocky Mountain Regional American Chemical Society Meeting, Park City, UT, June **2008**.
6. Grubel, K.; Fuller, A. L.; Arif, A. M.; Berreau, L. M.* “Effect of the Secondary Environment on the Chemistry of Ni(II) Complexes: Relevance to Acireductone Dioxygenases” Poster Presentation at the 235th National American Chemical Society Meeting, New Orleans, LA, April **2008**.

PATENTS

U.S. patent application 61454902: CO-Releasing Zinc Flavonolate Complexes

AWARDS

- 2011** College of Science Graduate Researcher of the Year – Utah State University
- 2010** Claude E. ZoBell Scholarship – Utah State University, College of Science Award

TEACHING EXPERIENCE

September 2006 – **Teaching Assistant at Utah State University**
 May 2011 1210 General Chemistry I Recitations
 1220 General Chemistry II Recitations

1215 General Chemistry Laboratory
1225 General Chemistry Laboratory
3520 Inorganic Chemistry Laboratory
Undergraduate Tutoring Resource Room

October 2005 –
July 2006 **Teaching Assistant at Silesian University of Technology**
General Chemistry I Recitations
General Chemistry II Recitations
Basic Inorganic Chemistry I Laboratory
Basic Inorganic Chemistry II Laboratory

INTERNSHIPS

August 2004 **ZM „BUMAR” Łabędy, Poland**
Laboratory Technician
I was given training in fields of European Quality Certificates and Measurement.

July 2004 **Police Dept. in Katowice, Poland**
Laboratory Technician in the Drugs and Alcohol Department
My duties involved analysis of drugs, alcohol, and burnt materials.
I was trained in using GC-MS, IR and specific drugs tests.

AFFILIATIONS

- Member of the American Chemical Society
- Member of the Collaborative Institutional Training Initiative

LANGUAGE SKILLS

Fluent in Polish and English